

**SPACE SHUTTLE
ORBITAL MANEUVERING ENGINE
PLATELET INJECTOR PROGRAM
NAS 9-13133**

FINAL REPORT

JM6

CR 151442

Rec'd ✓

(NASA-CR-151442) SPACE SHUTTLE ORBITAL
MANEUVERING ENGINE PLATELET INJECTOR PROGRAM
Final Report (Aerojet Liquid Rocket Co.)
322 p LC A14/MF A01

N77-27179

CSCI 21H

Unclass

G3/20

36718

REPORT NO. 13133-F-1
1 DECEMBER 1975



Aerojet
Liquid Rocket
Company

SACRAMENTO
CALIFORNIA 95813

SPACE SHUTTLE
ORBITAL MANEUVERING ENGINE
PLATELET INJECTOR PROGRAM

Final Report
13133-F-1

Prepared by
Aerojet Liquid Rocket Company
A Division of Aerojet-General Corporation
Sacramento, California 95813

Contract NAS 9-13133

Prepared For
National Aeronautics and Space Administration
Lyndon B. Johnson Space Center
Primary Propulsion Branch
Houston, Texas 72058

Report 13133-F-1

FOREWORD

Aerojet Liquid Rocket Company submits this Final Report as part of the OME Platelet Injector Program, Contract NAS 9-13133.

The work was conducted under the cognizance of Mr. R. C. Kahl of NASA/JSC who is the contract monitor. Aerojet personnel include L. B. Bassham, program manager, Dr. R. J. LaBotz, operations project manager, and R. W. Michel, project engineer.

Report 13133-F-1

ABSTRACT

The OME Platelet Injector Program, Contract NAS 9-13133, was undertaken to evaluate a platelet-face injector for the Orbit Maneuvering Engine (OME) on the Space Shuttle as a means of obtaining additional design margin and lower cost. This final report documents the entire program exclusive of testing done at NASA/WSTF in 1973 and 1974, which is reported separately.

The program was conducted in three phases. The first phase evaluated single injection elements, or unelements; it involved visual flow studies, mixing experiments using propellant simulants, and hot firings to assess combustion efficiency, chamber wall compatibility, and injector face temperatures. In the second phase, subscale units producing 600 lbf thrust were used to further evaluate the orifice patterns chosen on the basis of unelement testing. In addition to combustion efficiency, chamber and injector heat transfer, the subscale testing provided a preliminary indication of injector stability. Full scale testing of the selected patterns at 6000 lbf thrust was performed in the third phase. Performance, heat transfer, and combustion stability were evaluated over the anticipated range of OMS operating conditions. The effects on combustion stability of acoustic cavity configuration, including cavity depth, open area, inlet contour, and other parameters, were investigated.

Report 13133-F-1

TABLE OF CONTENTS

<u>No.</u>		<u>Page</u>
I.	Introduction	1
II.	Summary	4
	A. Unielement Testing	6
	B. Subscale Testing	6
	C. Full Scale Testing	7
III.	Results and Conclusions	9
	A. Unielement Testing	10
	B. Subscale Testing	10
	C. Full Scale	11
IV.	Recommendations	17
	A. Based on Unielement, Subscale, and ALRC Full Scale Testing	18
	B. Based on WSTF Testing	19
V.	Application of Results	23
VI.	Contributions of OME to OMS	26
	A. Injector	27
	B. Chamber	27
	C. Acoustic Cavity	28
	D. Engine Operation	28
VII.	Unielement Program	30
	A. Introduction	31
	B. Unielement Design	31
	C. Spray Tests	41
	D. Mixing Tests	41
	E. Hot Fire Tests	58
	F. Conclusions	72
VIII.	Subscale Program	73
	A. Objective and Approach	74
	B. Design	74
	C. Cold Flow	88
	D. Hot Testing	94
	E. Results	99

Report 13133-F-1

TABLE OF CONTENTS (cont.)

<u>No.</u>		<u>Page</u>
IX.	Full Scale Testing and Demonstration Program	117
	A. Introduction	118
	B. Facility	118
	C. Chambers	122
	D. Cavity Configuration	125
	E. Injectors	133
	F. Test Series Description	157
	G. Test Summary	178
	H. Conclusions	179
X.	Full Scale Performance	194
	A. Introduction	195
	B. Data Analysis Results	196
	C. Performance Comparison	208
	D. Analysis and Extrapolation Techniques	212
XI.	Full Scale Heat Transfer	242
	A. Introduction	243
	B. Chamber Heat Fluxes	243
	C. Chamber Heat Transfer Correlating Coefficient	258
	D. Mini-Skirt Heat Fluxes	260
	E. Cavity Environment	265
	F. Injector Face Environment	267
	G. Baffle Heat Transfer	267
XII.	Full Scale Combustion Stability	271
	A. Introduction	272
	B. Hardware Description	273
	C. X-Doublet Injectors	274
	D. X-Doublet Testing	274
	E. Description of Resurging	275
	F. Factors Influencing Resurging	280
	G. Mechanism of Resurging	300
	H. Summary	302
	Bibliography	305

Report 13133-F-1

LIST OF FIGURES

<u>Figure</u>		<u>Page</u>
1	XD-2B Unielement Injector	32
2	X-Doublet Element	33
3	Unlike 90° Doublet Element	34
4	Splash Plate Element	35
5	Like Doublet Element	37
6	V-Doublet Element	38
7	Vortex Element	39
8	OME Platelet Injector Unielement Cold Flow Characterization	42
9	OME Platelet Injector Unielement Cold Flow Characterization	43
10	Advanced Injector Cold Flow Collection Apparatus	44
11	Unielement Propellant Flow Distribution, XD-0 Pattern	46
12	Unielement Propellant Flow Distribution, XD-2 Pattern	47
13	Unielement Propellant Flow Distribution, XD-4 Pattern	48
14	Unielement Propellant Flow Distribution, XDI-1 Pattern	49
15	Unielement Propellant Flow Distribution, XDI-2 Pattern	50
16	Unielement Propellant Flow Distribution, UD-1 Pattern	51
17	Unielement Propellant Flow Distribution, UD-2 Pattern	52
18	Unielement Propellant Flow Distribution, UD-3 Pattern	53
19	Unielement Propellant Flow Distribution, SP-1 Pattern	54
20	Unielement Propellant Flow Distribution, LD-B Pattern	55
21	Unielement Propellant Flow Distribution, LD-FWD Pattern	56
22	2 in. and 4 in. Chambers Used in Unielement Testing	59
23	Energy Release Efficiency vs Mixture Ratio	63
24	Energy Release Efficiency vs Mixture Ratio	64
25	Energy Release Efficiency vs Fuel Temperature	66
26	Energy Release Efficiency vs Fuel Temperature	67
27	Unielement Face Temperature Characteristics	68
28	Unielement Face Temperature Characteristics	69
29	Unielement Hot Fire Testing	70

Report 13133-F-1

LIST OF FIGURES (cont.)

<u>Figure</u>		<u>Page</u>
30	Unielement Hot Fire Testing	71
31	Preliminary Subscale Layout - Splash Plate	78
32	Preliminary Subscale Layout - X-Doublet	79
33	Preliminary Subscale Layout - Unlike Doublet	80
34	Subscale Injector Manifold	81
35	Subscale Splash Plate Injector	83
36	Subscale Splash Plate Injector	84
37	X-Doublet Injector	85
38	Subscale Hardware Components	86
39	Subscale Resonator Ring	87
40	Subscale Chamber (4.0 in.)	89
41	Subscale L* Section (3.0 in.)	90
42	Subscale Film Coolant Ring	91
43	Subscale Splash Plate Mixture Ratio Distribution	92
44	Subscale X-Doublet Mixture Ratio Distribution	93
45	OME Platelet Injector Performance, Subscale Injector	100
46	Subscale Injector, X-Doublet Performance	102
47	Film Cooled Chamber Performance Data	103
48	Splash Plate Injector Thermal Characteristics	105
49	X-Doublet Injector Thermal Characteristics	106
50	Composite Plot of Platelet Injector Heat Flux Data	107
51	Composite Plot of Film Cooled Chamber Heat Flux Data	108
52	Spectral Analysis of XDT Injector Test 121	112
53	J-4 Test Facility	120
54	Research Physics Laboratory	121
55	Thrust Chamber Assembly	123
56	Heat Sink Chamber	124
57	L* Section	126
58	Film Coolant Ring	127
59	Skirt Heat Sink Chamber	128

Report 13133-F-1

LIST OF FIGURES (cont.)

<u>Figure</u>		<u>Page</u>
60	Chamber on Test Stand	129
61	Acoustic Cavity Configurations	132
62	Comparison of XDT-1 and XDT-2 Pattern	134
63	Injector Manifold	136
64	Injector Core	137
65	Injector Core Weldment	138
66	Full Scale Injector Assembly	139
67	Full Scale Injector (Frontside)	140
68	Full Scale XDT Injector (Backside)	141
69	Demonstration Injector Design	142
70	Demonstration Injector Design	143
71	Demonstration Injector Design	144
72	Demonstration Injector Design	145
73	Demonstration Injector Design	146
74	X-Doublet Pattern	148
75	Demonstration Injector Face	149
76	Splash Plate Pattern	150
77	Integral Baffle Injector Core	152
78	Jig for Bonding Integral Baffle Injector Face	153
79	Integral Baffle Injector	154
80	Full Scale Test Chronology	155
81	Specific Impulse Obtained with the DXDT1-1 Injector with 16 in. Chamber Length Configuration	200
82	Specific Impulse Obtained with the DXDT1-2 Injector with 12 and 16 in. Length Chambers	201
83	Specific Impulse Obtained with the XDT1-A, -B, -C Injectors with 16 in. Heat Sink Chambers	202
84	Specific Impulse Obtained with the .6 XDT and .4 SP Mixed Element Injectors	204

Report 13133-F-1

LIST OF FIGURES (cont.)

<u>Figure</u>		<u>Page</u>
85	Specific Impulse of XDT2-A Injector with 12.8 and 16.4 in. Length Chambers	206
86	Specific Impulse of XDT1 Injector without Face Ring Dams	207
87	Specific Impulse of XDT1-C Injector with High Contraction Ratio Chamber	209
88	Specific Impulse Obtained with the Like-Douplet Injector with 16 in. Length Chamber	210
89	Heat Flux Data for the XDT-1 Injector	244
90	Heat Flux Data for the XDT-2 Injector	246
91	Mixed Element Injector Heat Flux Results	248
92	Heat Flux Results for the Cylindrical Combustion Chamber	249
93	Comparison of the Mixed Element and XDT Injectors	250
94	Heat Flux Data for the DXDT-1 Injector	252
95	Circumferential Heat Flux Data for DXDT1-2	254
96	Heat Flux Data for the DXDT1-2 Injector	255
97	Comparison of Demonstration Injector Heat Fluxes	256
98	Heat Flux Data for the High Contraction Ratio Chamber	257
99	Heat Transfer Correlation Coefficients - Reactive	259
100	Heat Transfer Correlation Coefficients - Non-Reactive	261
101	Gas-Side Heat Transfer Correlation, DXDT1 Injectors	262
102	Mini-Skirt Heat Flux Data	263
103	Non-Reactive Nozzle Heat Transfer Correlation Coefficients	264
104	Cavity Heat Flux	266
105	Maximum Face Temperature vs O/F Ratio	268
106	Injector Face Heat Flux Correlation	269
107	Total Baffle Heat Load, Integral Baffle Injector	270
108	Mixed Mode Characteristics	277
109	Three Phases of Resurge Instability	278
110	Injector Core	281
111	Fuel Circuit Pressure Drop Ring	284
112	Fuel Circuit Pressure Responses During Instability	285

Report 13133-F-1

LIST OF FIGURES (cont.)

<u>Figure</u>		<u>Page</u>
113	Resonator Inlet Configurations	287
114	Cavity Inlet Effect	288
115	Cavity Overlap Results	289
116	Maximum Overlap - High C_D Resonator Inlet Configuration	290
117	Stability Margin Testing	292
118	Effect of Cavity Area on Wave Form	293
119	Cavity Temperature at Shutdown	296
120	1T Resonator Temperature Data Summary	297
121	Cavity Temperature vs Mixture Ratio	298
122	Demonstration Injector Cavity Temperatures	299

Report 13133-F-1

LIST OF TABLES

<u>Table</u>		<u>Page</u>
I	Summary of Unielement Patterns Tested	40
II	Summary of Unielement Hot Firings	60
III	Subscale Design Point	75
IV	OME Platelet Injector Subscale Thruster Design Summary	77
V	Subscale Test Summary	95
VI	OME Transverse Platelet 600 lbF Test Summary, X-Doublet Injector	110
VII	OME Transverse Platelet 600 lbF Test Summary, Splash Plate Injector	113
VIII	OME Transverse Platelet 600 lbF Test Summary, Mixed Element Injector	116
IX	Injector Summary	156
X	Summary of Hardware Configurations in Full Scale Tests at ALRC	180
XI	Summary of Operating Conditions for Full Scale Tests at ALRC	184
XII	Injector Performance Summary	197
XIII	Nomenclature Used in Performance Summary	217
XIV	X-Doublet Injectors	274

ORIGINAL PAGE IS
OF POOR QUALITY

I. INTRODUCTION

Report 13133-F-1

I. INTRODUCTION

The Orbit Maneuvering Engine Platelet Injector Program, Contract NAS 9-13133, was awarded to Aerojet Liquid Rocket Company (ALRC) for the design and evaluation of a platelet injector suitable for the Space Shuttle Orbit Maneuvering System (OMS) 6000 lbf thrust engine. The contract was started September 25, 1972, and consisted of three phases involving single injector elements of 6 lbf thrust, subscale injectors of 600 lbf thrust, and finally, full scale injectors for the 6000 lbf application.

The face of a platelet injector is formed from a stack of thin metal platelets which are diffusion bonded into a single unit; propellant orifices and flow passages are photoetched into or through each platelet prior to bonding. The platelet concept was selected because of several unique features including ease of manufacture, potential high performance with reduced chamber lengths, and ease of pattern rework allowing economical and expeditious engine development. In the first phase of the program, unielement testing, single injection elements were evaluated on the basis of performance, hydraulics, and compatibility. The most promising candidate elements were evaluated further in the second phase, subscale testing, to assess the effects of multielement interaction on performance, compatibility, and stability. The third phase, full scale testing, was conducted to substantiate these characteristics for flight-sized hardware.

Full scale testing included evaluation of workhorse and preprototype regeneratively cooled chambers. For the most part, regenerative chamber testing was conducted under altitude conditions at NASA/WSTF and is completely documented elsewhere.^{1,2} Except for purposes of comparison, the WSTF results will not be presented in this report. The WSTF testing served as a demonstration of the regenerative chambers and, in addition, evaluated such factors as: film cooling, chamber length variations, effect of helium saturated propellant, ingestion of helium bubbles into the propellant circuits, start and shutdown transient

¹ WSTF Test Report, Report No. 13133-S-1, 12 December 1973

² 1974 WSTF Test Report, Report No. 13133-S-3, 1 April 1975

Report 13133-F-1

I, Introduction (cont.)

behavior, simulation of the vehicle pod feed system, chugging, restart with and without a purge, postfire propellant evacuation and heat soakback characteristics, purge definition, chamber heat transfer, and performance.

Full scale testing at ALRC, mostly with uncooled hardware, comprised some 362 firings, and was primarily concerned with combustion stability and the effects of acoustic cavity configuration. This report documents fully the ALRC testing, as well as the unielement and subscale work.

The entire program, in particular the full scale testing at WSTF, was guided in its planning and progress by the philosophy that it must provide early identification and solution of potential problems, both in regard to hardware design and fabrication, as well as to engine behavior and operating limits as determined under test conditions.

ORIGINAL PAGE IS
OF POOR QUALITY

II. SUMMARY

Report 13133-F-1

II. SUMMARY

The primary objective of the program was to demonstrate a platelet face injector for application on the OMS engine. This engine is to develop 6000 lbf thrust using nitrogen tetroxide, N_2O_4 , and monomethylhydrazine, MMH, as propellants, with a chamber pressure of 125 psia and a mixture ratio of 1.65. The program was conducted in four phases and consisted of nine tasks proceeding from a single injection element to the full scale configuration. This report summarizes these tasks topically which are addressed as follows:

Unielement Program (6 lbs_f Thrust)

Task IA - Injector Element Design and Analytical Evaluations

Subscale Program (600 lbs_f Thrust)

Task IB - Subscale Design

Task II - Injector Element Experiments Evaluation

Full Scale Program (6000 lbs_f Thrust)

Task IV - Demonstration Injector Design

Task V - Demonstration Injector Fabrication

Task VI - Demonstration Injector Test Evaluation

Demonstration Program (6000 lbs_f Thrust)

Task VII - Platelet Injector Design Update

Task XI - Regenerative Chamber Fabrication

Contractually Required Reports

Task XII - Reporting

II, Summary (cont.)

A. UNIELEMENT TESTING

0
0
Six fundamentally different injection elements were conceived and tested in the unielement phase of the program. These were selected on the basis of fabricability using platelet construction techniques plus the usual considerations of performance, compatibility, and stability. Thirty-nine geometrical variations of the six basic elements were built and tested to some degree.

Testing included: (1) spray tests with water allowing visual observation of both circuits, separately and together; (2) mixing tests involving propellant simulants to enable mapping of mixture ratio and mass flux profiles; (3) hot fire tests to provide some indication of combustion efficiency, sensitivity to propellant temperature and mixture ratio, and injector and chamber wall compatibility. Eighty-eight hot fire tests were conducted.

As a result of unielement testing, two elements were selected for subscale and full scale evaluation. One was a splash plate which showed high performance, excellent compatibility, and insensitivity to operating point and propellant temperature. The other was an X-doublet which showed lower performance and also lower heat flux levels.

B. SUBSCALE TESTING

Subscale testing consisted of eighty-seven hot fire tests and fourteen cold flow tests. The purpose of the latter was to investigate pattern, hydraulic, and propellant distribution characteristics. In the hot firings, three patterns were tested: the splash plate, the X-doublet, and a mixed element consisting of the splash plate and X-doublet patterns. Two variations of the splash plate and X-doublet elements were used.

Report 13133-F-1

II, B, Subscale Testing (cont.)

The purpose of the hot fire tests was to establish performance, heat transfer, and stability with multielement injection. The effectiveness of acoustic cavities in damping combustion instabilities was evaluated in fifty-five bombed firings, and the effect of chamber length on stability was likewise examined. Chugging tests were run. The variation in performance and chamber heat transfer with fuel film cooling was also investigated. Two series of tests each comprising 1500 thermal cycles were conducted to assess cycle life capability of platelet face injectors.

The stability of the splash plate pattern was found in subscale testing to be very sensitive to operating point and propellant temperature, so much so that the X-doublet was selected as the primary candidate pattern for full scale design and evaluation.

C. FULL SCALE TESTING

Full scale testing at ALRC was conducted primarily to identify the effects of injector pattern, cavity configuration, chamber length, film cooling, and operating point on performance, compatibility, and stability characteristics. The period of testing extended over one year and in part was tandem to the WSTF testing. Five basic injector designs were utilized, and twelve individual faces were actually fired. There were 362 firings at ALRC, 294 of which were bombed, with a total duration of 819 sec.

The primary areas of investigation related to the influences of cavity depth and area, cavity inlet contour and flow resistance, and injector overlap on stability margin. Lesser areas of investigation related to the effects of film cooling, chamber length, and bomb location; also, several tests were concerned with low and high pressure drop injectors, a high contraction ratio chamber, chugging, and the substitution of A-50 for the specified fuel, MMH.

Report 13133-F-1

II, C, Full Scale Testing (cont.)

On the basis of successful testing accomplished at WSTF in 1973, the XDT-2 pattern was chosen as the primary candidate for further altitude cell evaluation. However, because of the large body of empirical data subsequently accumulated at ALRC with the XDT-1 pattern, it was designated as the prototype. In 1974 WSTF testing, the XDT-1 pattern fully met all of the applicable flight hardware design specifications.

ORIGINAL PAGE IS
OF POOR QUALITY

III. RESULTS AND CONCLUSIONS

III. RESULTS AND CONCLUSIONS

The results and conclusions presented below derive mostly from the WSTF testing which was the principal evaluation of the demonstration injector and chamber fired under altitude conditions. Unielement and subscale testing and full scale stability testing at ALRC, while important to the development of the demonstration design, nonetheless was secondary in terms of program objectives. Discussion in these areas will consequently be limited.

A. UNIELEMENT TESTING

1. Unielement testing with propellant simulants as well as in hot firings provides an effective means of studying flow and atomization characteristics, mixture ratio and mass flux profiles. It is a useful and inexpensive screening procedure for screening different elements and likewise a useful design technique for optimizing a particular element configuration.

2. As a result of unielement testing, the splash plate element, SP-2, was selected as the primary candidate for subscale test evaluation on the basis of its high performance, excellent compatibility, and insensitivity to propellant temperature and operating point.

3. The X-doublet, XD-0 was chosen as a back-up configuration, in part because of its lower performance.

B. SUBSCALE TESTING

1. Subscale testing provided an intermediate step between unielement evaluations and full scale hardware design. It allowed a meaningful evaluation of performance, heat transfer, and stability under multielement firing conditions, and it did so at somewhat lower costs for hardware fabrication and test purposes than would obtain with full scale hardware. On the other hand, little was accomplished by the subscale tests that could not have been done as easily in full scale testing. Particularly with regard to stability results, subscale testing can be misleading.

III,B, Subscale Testing (cont.)

2. The subscale injectors twice demonstrated a cycle life capability of 1500 thermal cycles without structural damage.

3. The splash plate element chosen in the unielement testing as the primary candidate was found in subscale testing to have unstable tendencies. The X-doublet proved more acceptable and thus replaced the other as the primary candidate.

C. FULL SCALE

The full scale results discussed below are broken down into areas of particular interest, e.g., fabrication, performance, heat transfer, stability, etc. For the most part, the hot test results are based on WSTF altitude testing, except for stability results which are based primarily on ALRC sea level tests.

1. Fabrication

a. The fabricability of full scale platelet injectors was demonstrated. No significant fabrication problems were encountered with the baseline bonding procedure. When an inadvertant deviation from this procedure occurred, four injectors were fabricated which developed leaks.

b. The ease and rapidity of injector rework was an unanticipated benefit of the platelet fabrication technique. A pattern could be machined off the face and a completely new pattern made from existing artwork and installed within three days.

c. The applicability of platelet fabrication methods to baffled injectors was demonstrated. A three bladed, integral baffle injector was constructed without incident.

d. The fabricability of milled slot regenerative chambers with electroformed nickel external walls was demonstrated.

III,C, Full Scale (cont.)

2. Performance

a. Delivered specific impulse at the nominal operating point is between 314 and 317 sec for the platelet injectors; the nonplatelet like-doublet injector achieved comparable performance.

b. Performance degradation due to the use of helium-saturated propellants is negligible.

c. The use of approximately 8% of the fuel as film coolant reduces specific impulse about 1 sec with the like-doublet.

d. The performance loss due to the removal of the 4 in. L* section amounted to 2 to 3 sec for either type of injector.

e. Performance improves from 0.2 to 1.2 sec as propellant temperature is raised from 40 to 110°F.

3. Heat Transfer

a. Maximum gas-side regenerative chamber temperature at the throat is 765°F when using the prototype injector at nominal conditions. The corresponding cycle life is estimated to be 1350 cycles for the flight chamber.

b. The gas-side regenerative wall temperature increases about 18°F for a 0.1 increase in mixture ratio, and about 70°F for a 25 psi increase in chamber pressure. Helium saturation has a negligible effect on wall temperature and film cooling has only a slight effect.

c. The coolant bulk temperature rise is 164°F for the prototype hardware at nominal conditions. The rise increases 10°F for every 0.1 increase in mixture ratio. It is not a function of chamber pressure.

Report 13133-F-1

III,C, Full Scale (cont.)

0
0
d. The burnout safety factor (R_{BO}^{-1}) is estimated to be about 1.40 for the flight hardware at nominal conditions. Calculated safety factors less than 1.00 were actually tested indicating some conservatism in the analytical approach.

e. Film cooling is not necessary with the X-doublet injector.

f. Helium bubbles of length sufficient to momentarily extinguish combustion were introduced into each propellant circuit without incident. The bubble in the fuel circuit passes through the chamber somewhat preferentially on the inlet side. The oxidizer-circuit bubble caused high face temperatures (1350°F) on the like-doublet injector; whether the X-doublet platelet injector would experience comparable temperature levels is uncertain.

g. Pressure oscillations in the fuel inlet manifold of the regenerative chamber were observed under certain test conditions. The cause of these oscillations is uncertain.

h. Wall temperature excursions from one steady-state level to a higher level after several seconds of firing were observed on both chambers. Such excursions ranged from 50 to 100°F and suggest a shift from nucleate to film boiling in a very local area of the coolant channel.

4. Stability

a. A stable baseline injector-acoustic cavity configuration was established. It consisted of the X-doublet injector in conjunction with a circumferential cavity housing having eight 1-T cavities and four 3-T cavities. The 1-T cavities were 1.5 in. deep, as measured from the injector face, and had an open area equal to 18% of the injector face area; the 3-T cavities were 0.4 in. deep and had an open area equal to 9% of the face.

III,C, Full Scale (cont.)

f. The stability margin of this baseline configuration was determined to be 80%, that is, the cavity area was 80% greater than required for stable operation.

c. The primary mode of instability with the X-doublet patterns was resurging, which consists of periodic bursts of spinning 1-T mode. The frequency of these bursts is about 400 Hz.

d. The installation of dams at the three null points in each of the injector face ring manifolds was the single most effective means of eliminating resurging instability.

e. The stability of the X-doublet patterns was very sensitive to the acoustic cavity inlet geometry. This sensitivity apparently results from interference of the cavity lip with the injection spray pattern rather than any change in acoustic characteristics. The sensitivity of the like-doublet pattern to cavity configuration was not extensively tested.

f. The mixed element injector required 1-T, 2-T, and 3-T cavities to eliminate acoustic mode instabilities with a 16 in. chamber. It was unstable with this cavity configuration in a 12 in. chamber.

g. The mixed element-integral baffle injector was spontaneously unstable in a depressed 1-T mode. The three-bladed baffle was intended to provide 1-T damping and the acoustic cavities 2-T and 3-T damping.

5. Start and Shutdown Transients (Prototype Chamber)

a. In WSTF testing, thrust overshoot during the start transient averaged about 40% of steady state value but in several tests exceeded 50%. Pressure overshoot could not be established accurately because of slow-response instrumentation.

Report 13133-F-1

III,C, Full Scale (cont.)

b. Start impulse ranged from 30 to 50 lb-sec for a dry engine start or an unpurged engine restart after coasts of 30 sec or longer. Considerably higher values were experienced for unpurged engine restarts with shorter coasts.

c. Variation of the time interval from FS_1 to 90% thrust was within ± 0.1 sec of the average value.

d. Shutdown impulse varied by more than 500 lb-sec over the range of operating points tested; correction to nominal conditions appears feasible and is necessary to meet the specification.

e. Variation of the time interval from FS_2 to 10% thrust was within $\pm .150$ sec of the average value.

f. Postfire chamber pressure oscillations were characteristic of cold engine shutdowns.

g. Helium saturation has a negligible effect on start or shutdown characteristics.

6. Evacuation and Soakout Characteristics; Purge; Limits of Simulation

a. Fuel circuit evacuation times without a purge extended to 100 or 150 sec for the A-1 or workhorse chamber, depending on hardware and propellant temperature, and to 100 sec for the A-2 or demonstration chamber. Longer evacuation times are anticipated with cold propellant and cold hardware. Fuel freezing due to evaporative cooling was not experienced because cell pressures were never below the fuel triple point pressure.

Report 13133-F-1

III,C, Full Scale (cont.)

b. Oxidizer evacuation times ranged from 10 to 20 sec depending on temperature. Freezing occurred regularly without detrimental effect to restart. In one test, the oxidizer inlet line was positioned so as not to drain; temperatures 40°F below the freezing point were measured and complete sublimation of the accumulated frost required nearly 10 min.

c. The postfire chamber temperature response of the A-1 chamber closely followed the saturation temperature corresponding to the measured fuel injector manifold pressure for as long as liquid remained in the system. Thereafter, the chamber soaked out to peak temperatures ranging between 100 and 200°F in 15 to 20 min, depending on firing duration.

d. The postfire chamber temperature response of the A-2 chamber did not closely follow the fuel saturation temperature, suggesting that the chamber is largely void of liquid immediately after valve closure, except in the inlet manifold. Temperatures remained in the range of 250 to 300°F for as long as 30 sec or until bulk boiling began in the manifold at which time they showed a considerable drop. Subsequent soakout temperatures peaked between 150 and 250°F.

e. The necessity for a fuel circuit purge cannot be disproven without testing below the fuel triple point pressure so that the risk of frozen fuel accumulating on the chamber walls, viz., downstream of the injector, may be assessed. However, nothing in the testing to date indicates that a purge is necessary.

f. The fuel circuit purges tested did not appear to be totally effective in expelling the fuel. The most effective purges appear to be of low flow rate and long duration, rather than high flow rate and short duration. The purge is best initiated immediately on shutdown signal. The current OMS purge, 380 standard cubic inches of gaseous nitrogen for 5 sec, is considered adequate but not optimum.

ORIGINAL PAGE IS
OF POOR QUALITY

IV. RECOMMENDATIONS

IV. RECOMMENDATIONS

A. BASED ON UNIELEMENT, SUBSCALE, AND ALRC FULL SCALE TESTING

Primarily the recommendations being made are a result of WSTF testing of prototype hardware as discussed below. However, a number of recommendations ensue from the unielement, subscale, and ALRC stability testing.

1. Injection Elements

a. Development of the splash plate element should be pursued. This element demonstrated exceptionally high performance with reduced chamber lengths but was not stable. Stabilized, the pattern could prove a most useful innovation.

b. The vortex element should likewise be pursued. It shows promise for achieving high performance in reduced chamber length on the basis of unielement spray and mixing test results, but has never been hot-fired.

c. Additional investigation of mixed element patterns is recommended. Mixed element injectors hold the promise of combining the higher performance characteristics of one element type with the greater stability of another type.

2. Stability Testing

a. A program to evaluate the influence of the acoustic cavity lip on the outer edge of the injector pattern should be conducted. Such a program could give substantial insight into pattern-cavity interactions and what is required for stability.

b. Additional testing of the integral baffle injector should be performed with a modified pattern to establish the requirements for stability. Also, the baffled injector, in conjunction with the XDT pattern, might be used to confirm the hypothesized mechanism of resurging, in that it should eliminate the spinning 1-T mode which triggers the resurge.

Report 13133-F-1

IV,A, Based on Unielement, Subscale, and ALRC Full Scale Testing (cont.)

0
0

c. Application of unielement testing to stability investigations should be considered, perhaps by high speed photographic techniques, perhaps in conjunction with an acoustic "driver" to affect the injection, atomization, vaporization, and combustion processes in the same manner as happens in full scale hardware. Experimental techniques allowing manipulation of parameters important to each of the four processes individually without affecting the other three would be most useful in determining the driving mechanism of any type of instability.

B. BASED ON WSTF TESTING

The following recommendations are based on altitude testing of prototype hardware at WSTF.

a. Further testing at high P_c , high O/F conditions is recommended because of the limited testing done at this end of the operating "box".

b. Testing to simulate the design specification condition wherein the initial slug of both propellants is at the limiting temperature, 125°F or 30°F, while the remainder is at the nominal value, should be conducted.

c. The effects of a helium bubble froth in either propellant should be investigated.

d. Restarts after 30 to 60 sec coast periods should be investigated in greater detail.

e. Testing at call pressures below the fuel triple point is imperative to determine if a purge is necessary.

Report 13133-F-1

IV,B, Based on WSTF Testing (cont.)

f. If a purge is found necessary, more testing would be required to optimize the pertinent purge parameters. The resulting shutdown transient would have to be evaluated to ascertain compliance with the design specification.

g. More postfire heat soakback data should be acquired.

h. Hot restarts after short coasts (less than 10 sec) should be investigated further because of the several instabilities encountered under these conditions.

i. Cavity gas temperatures and heat flux profiles should be determined in greater detail than has been done.

j. Cycle life capability of the full scale hardware should be demonstrated.

2. Technical Issues

a. A simple one-degree of-freedom model of the WSTF test stand should be constructed to allow interpretation of measure start transient thrust measurements (see Specification Change #a below).

b. The chamber gas-side wall temperature excursions that were monitored warrant further investigation.

c. Additional stability testing is recommended.

d. Purging of the oxidizer circuit as well as the fuel circuit should be reassessed.

e. The effect of tolerance and tolerance stack-up on injector and chamber wall temperatures, thermal margin, injection characteristics, performance, and stability should be considered fully.

IV,B, Based on WSTF Testing (cont.)

f. The fluid dynamic model of the engine system should be improved in the area of shutdown transient simulation.

g. The thermal model of the flight system should be updated to reflect postfire behavior of the flight prototype chamber.

3. Specification Changes

a. Chamber pressure overshoot during the start transient may exceed the allowable 150% of steady-state levels. It may be necessary to raise the allowable level to 200%.

b. The shutdown impulse specification could be simplified by defining impulse as total impulse to zero thrust without specifying a time limit. It may be necessary to increase the allowable impulse value in any event.

4. Instrumentation

a. Higher response chamber pressure measurements are imperative if overshoot is to be determined accurately (see Specification Change No. a, above.)

b. More chamber gas-side thermocouples are advisable and improved installation is pertinent. The demonstration chamber, in particular, was lacking in thermal instrumentation.

c. Both flow meters and pressure transducers proved unreliable at times during the testing, and certain of the latter drifted as a result of temperature variations. Every effort should be made to eliminate this in future tests.

d. Digital data as generated at WSTF would be easier to use if the various functions were titled with the commonly accepted nomenclature, rather than the function number as was done, viz., P_C , T_{FJ} and T_{WG} rather than 4011P, 4019T, and 4025%.

Report 13133-F-1

IV,B, Based on WSTF Testing (cont.)

5. Fabrication and Inspection

a. During bonding of the platelet stack to the injector body, it is important that the body is given sufficient support to prevent creep. Corrective measures have been incorporated in the fabrication procedure.

b. Proper cleansing of the chamber surface prior to electroforming is of the utmost importance.

c. Inspection techniques for determining bond quality between the platelet stack and the injector face should be developed.

d. Inspection techniques to assess the bond between the electroformed outer shell and the inner liner of the chamber should likewise be developed.

ORIGINAL PAGE IS
OF POOR QUALITY

V. APPLICATION OF RESULTS

V. APPLICATION OF RESULTS

The primary application of the results of this program has been the baseline design definition of the Space Shuttle OMS engine. In addition, however, the technology is relevant to several other rocket engine applications.

5-10 lb Thrust Vernier Engines

The unielement program, Task I, clearly demonstrated the use of single injection elements, fabricated of platelets, at the 6 lb thrust level. These novel devices achieved high performance in minimal chamber length with minimum propellant volumes. The low cost flexibility of the concept provides a solid foundation for the application of unielements to this thrust class of rocket engine.

10-1000 lb Thrust RCS Engines

The subscale program, Task II, demonstrated the multielement flexibility of the platelet concept at the 600 lb thrust level. Various injector designs achieved high performance, good chamber compatibility, stability, and excellent cycle life. Low cost fabrication techniques coupled with the rework capability of platelet construction allow for expeditious development of engines in this thrust class. Moreover, injector thrust capability can be scaled up or down quite simply by photographic enlargement or reduction processes.

6000 lb Thrust Maneuvering Engines

The full scale demonstration programs, Tasks VI and VII, not only defined a baseline design for the OMS engine but also showed additional benefits to the platelet injector concept. Mixing of platelet elements by merging the artwork of two or more patterns allows the design emphasis to be shifted to stability,

Report 13133-F-1

V. Application of Results (cont.)

0
0
performance or cooling margin as required. The rework feature provides for injector development with an inexpensive and rapid fabrication cycle. The program also demonstrated that the platelet concept is not restricted to an unbaffled injector with the fabrication of an integral baffle unit having three separate injector compartments. These various design options clearly illustrate the inherent flexibility of the platelet injector concept as applied to engines in this higher thrust category.

ORIGINAL PAGE IS
OF POOR QUALITY

VI. CONTRIBUTIONS OF OME TO OMS

VI. CONTRIBUTIONS OF OME TO OMS

The major accomplishment of the OME Platlet Injector Program has been to establish a firm technology base for the design and development of the OMS engine, and to provide a fundamental understanding of engine behavior for a variety of conditions that may or will be encountered in actual flight operation. The most significant contributions relate to the design of the injector, chamber, and acoustic cavity, and to operation of the engine.

A. INJECTOR

1. Cycle Life - Cycle life of 1500 cycles was twice demonstrated in subscale testing.

2. Hydraulics - Hydraulic design of the full scale injector was developed and demonstrated.

3. Fabrication Sequence - A low cost fab sequence was devised and shown to be satisfactory.

4. Rework Capability - Successful refacing of injector bodies was accomplished, allowing pattern changes to be made at low cost and with minimum delay.

B. CHAMBER

1. Fabrication Technique - The techniques for fabricating the electroformed jacket/milled slot chamber were shown to be satisfactory.

2. Heat Transfer Evaluations - Heat flux, wall temperature, and coolant bulk temperature rise data acquired in full scale tests expedited the analytical thermal design of the OMS chamber.

VI, B, Chamber (cont.)

3. Cycle Life - Acceptable cycle life capability for the OMS chamber could be shown on the basis of these data.

C. ACOUSTIC CAVITY

1. Design - The OMS will use the dual tuned acoustic cavity, with essentially the same area, tune, and inlet geometry as developed in the OME program.

2. Stability Margin - The stability margin of this configuration was fully evaluated.

3. Critical Factors - Critical factors in the design, fabrication and instrumentation of acoustic cavities were identified.

4. Operating Point Sensitivity - The influence of chamber pressure, mixture ratio, and propellant temperature on cavity tune were investigated.

D. ENGINE OPERATION

1. Helium Saturation - The effect of helium saturation of the propellants on engine transients and performance was fully analyzed.

2. Helium Bubble Ingestion - Ingestion of large helium bubbles into each propellant circuit was examined.

3. Operating Point Sensitivity - The influence of chamber pressure, mixture ratio, and propellant temperature on performance, heat transfer, and engine transient behavior was evaluated.

4. Chugging - The threshold chamber pressure for chugging was established.

Report 13133-F-1

VI,D, Engine Operation (cont.)

5. Propellant Lead - Propellant lead effects were investigated.
6. Film Cooling - The need for and effect of film cooling was determined.
7. Engine Transients - Start and shutdown transients of the engine have been characterized.
8. Engine Restart - Restart of hot and cold engines, purged and unpurged, with hot and cold propellants, has been investigated.
9. Propellant Evacuation - Postfire propellant evacuation was assessed for a range of engine and propellant temperatures.
10. Postfire Heat Soakback - Postfire heat soakback characteristics and maximum coast temperatures have been determined.
11. Purge - Purge effectiveness for a variety of purge parameters was evaluated.
12. Compliance with OMS Specification - Except for minor deviations compliance with the OMS design specification has been demonstrated.
13. Future Testing - Areas that require additional test evaluation, including high temperature propellants, purge effectiveness, and reduced cell pressures, have been identified.

ORIGINAL PAGE IS
OF POOR QUALITY

VII. UNIELEMENT PROGRAM

VII. UNIELEMENT PROGRAM

A. INTRODUCTION

This section discusses the unielement testing, Task I, which preceded subscale and full scale hardware development. Unielements are the fundamental injection pattern unit of typically one oxidizer and one fuel orifice. The function of the unielement tests was to provide a simple means of determining hydraulic, spray, and mixing characteristics using water and propellant simulants in cold flow tests, and in hot fire performance tests to define pattern sensitivity to mixture ratio and propellant temperature. Several types of tests were conducted: (1) spray tests with water allowing visual observations of both injectants, separately and together; (2) mixing tests with immiscible simulants to enable mapping of mixture ratio and mass flux profiles; (3) hot fire tests in uncooled chamber to determine performance, pattern sensitivity, face and wall compatibility. Thirty-nine variations of six basic injector patterns were tested to some degree in the unielement series. These will be described in detail, as will the test results, and the conclusions drawn in this phase of the program.

B. UNIELEMENT DESIGN

Figure 1 shows a unielement injector which is 0.650 in. dia and 0.150 in. thick. The entire injector is made of platelets and incorporates the manifold as well as the elements in the platelet stack. The three basic patterns originally tested were the X-doublet, unlike-doublet, and splash plate, which are shown in Figures 2, 3, and 4, respectively. These configurations were chosen on the basis of a survey of patterns applicable to the platelet concept and represent three different atomization mechanisms. The X-doublet impinged two directly aligned like-propellant streams within the face and injected the resulting fans parallel and offset from each other (like-propellant

Report 13133-F-

ORIGINAL PAGE IS
OF POOR QUALITY

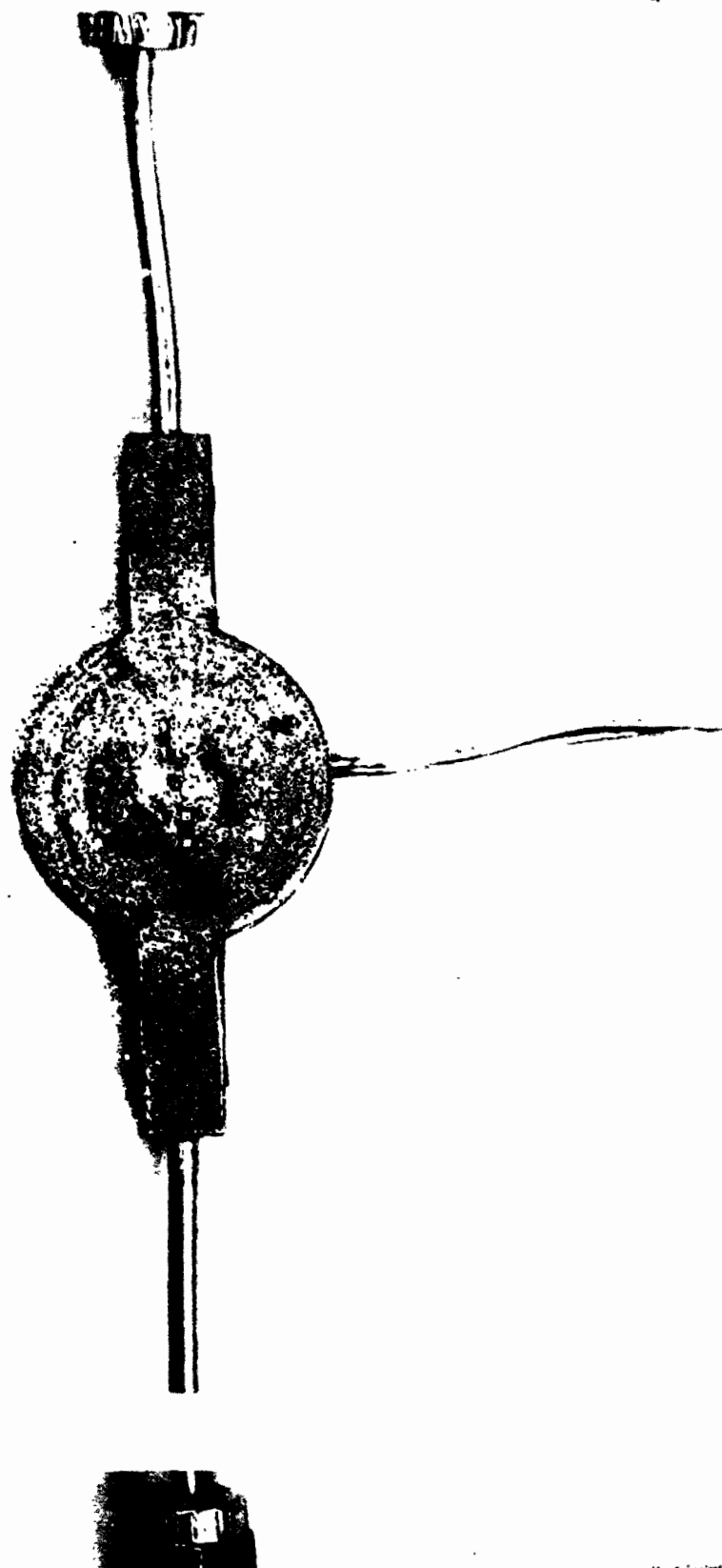


Figure 1. XD-2B Unielement Injector

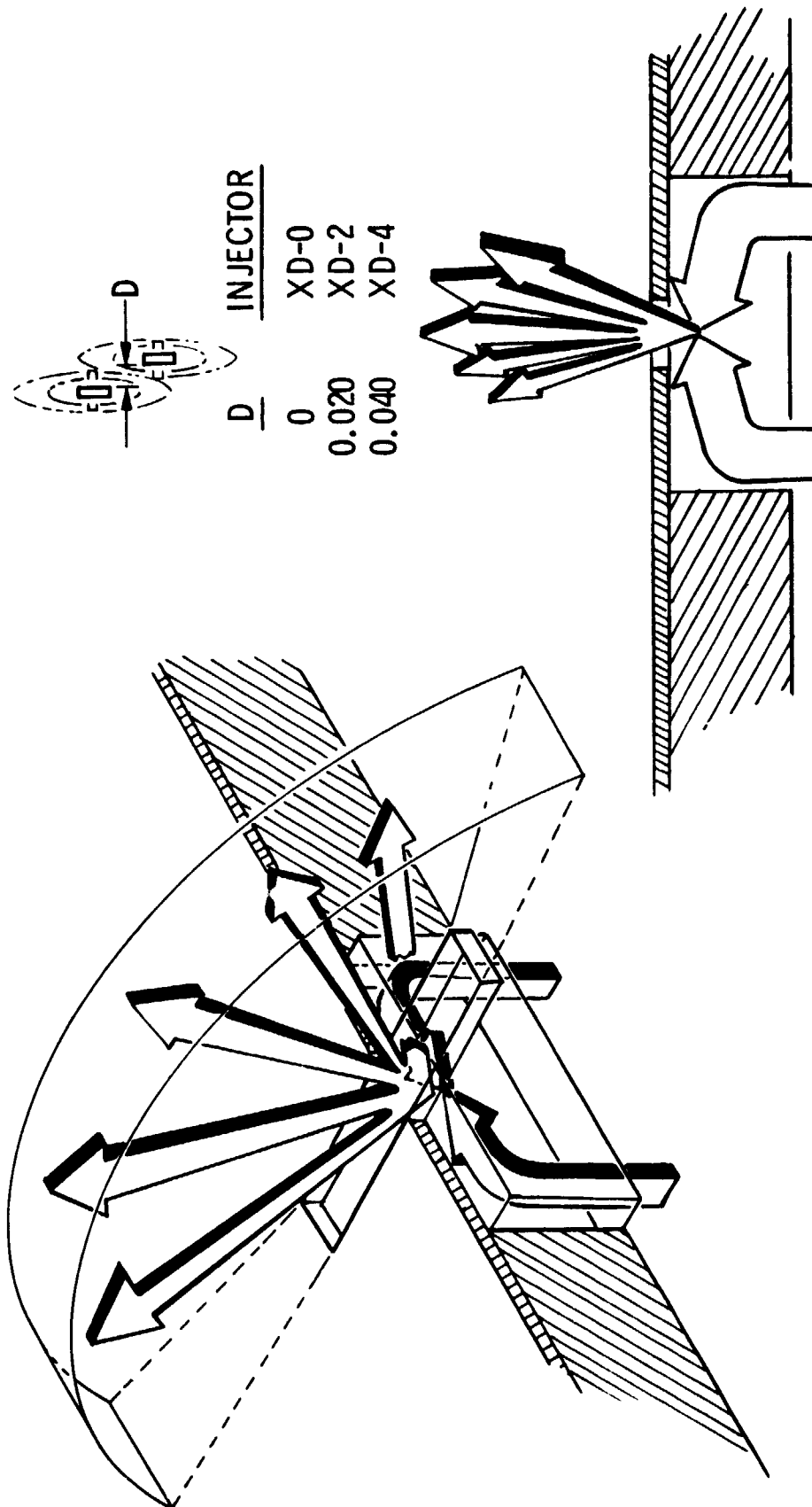


Figure 2. X-Doubllet Element

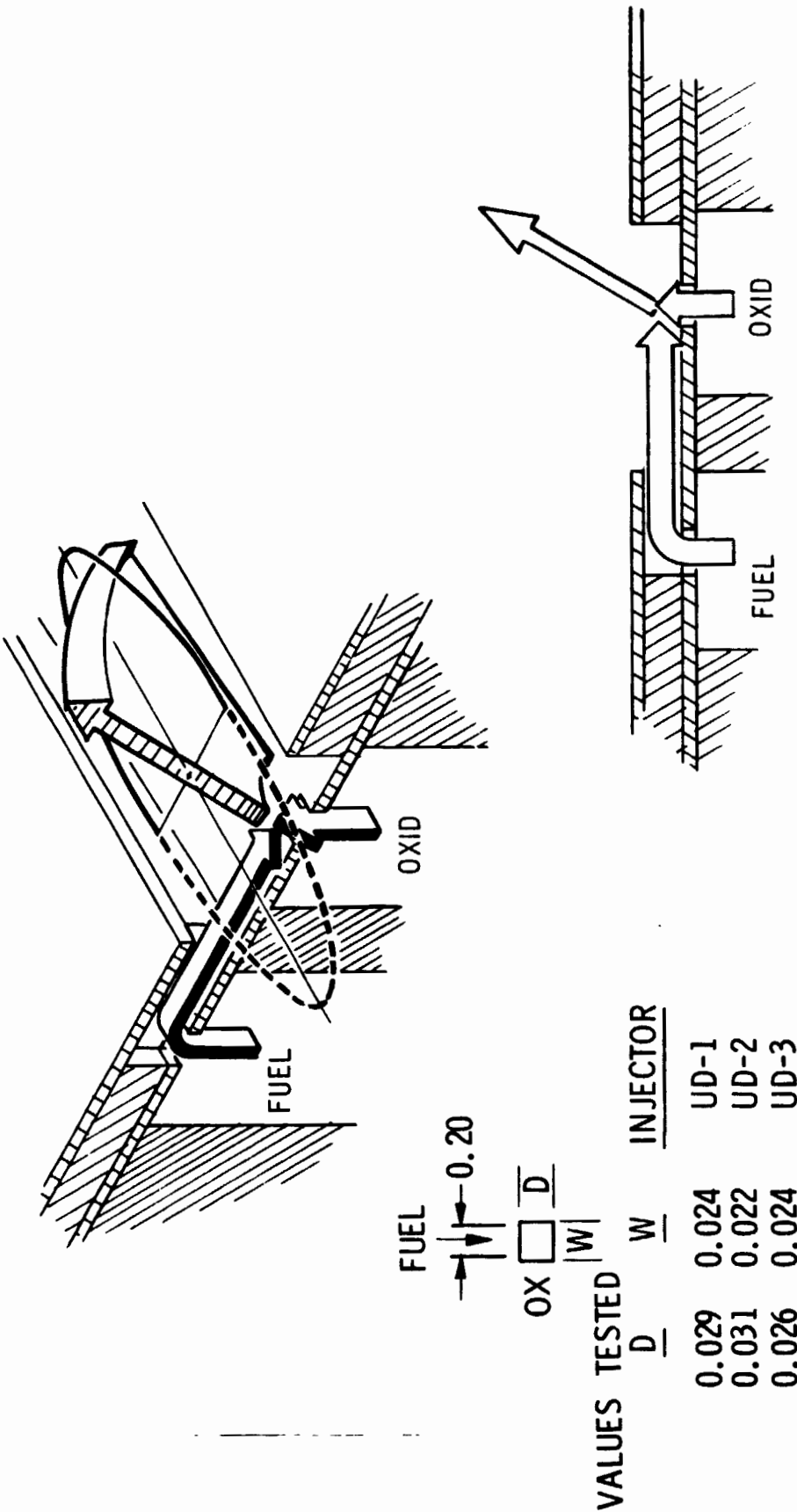


Figure 3. Unlike 90° Doublet Element

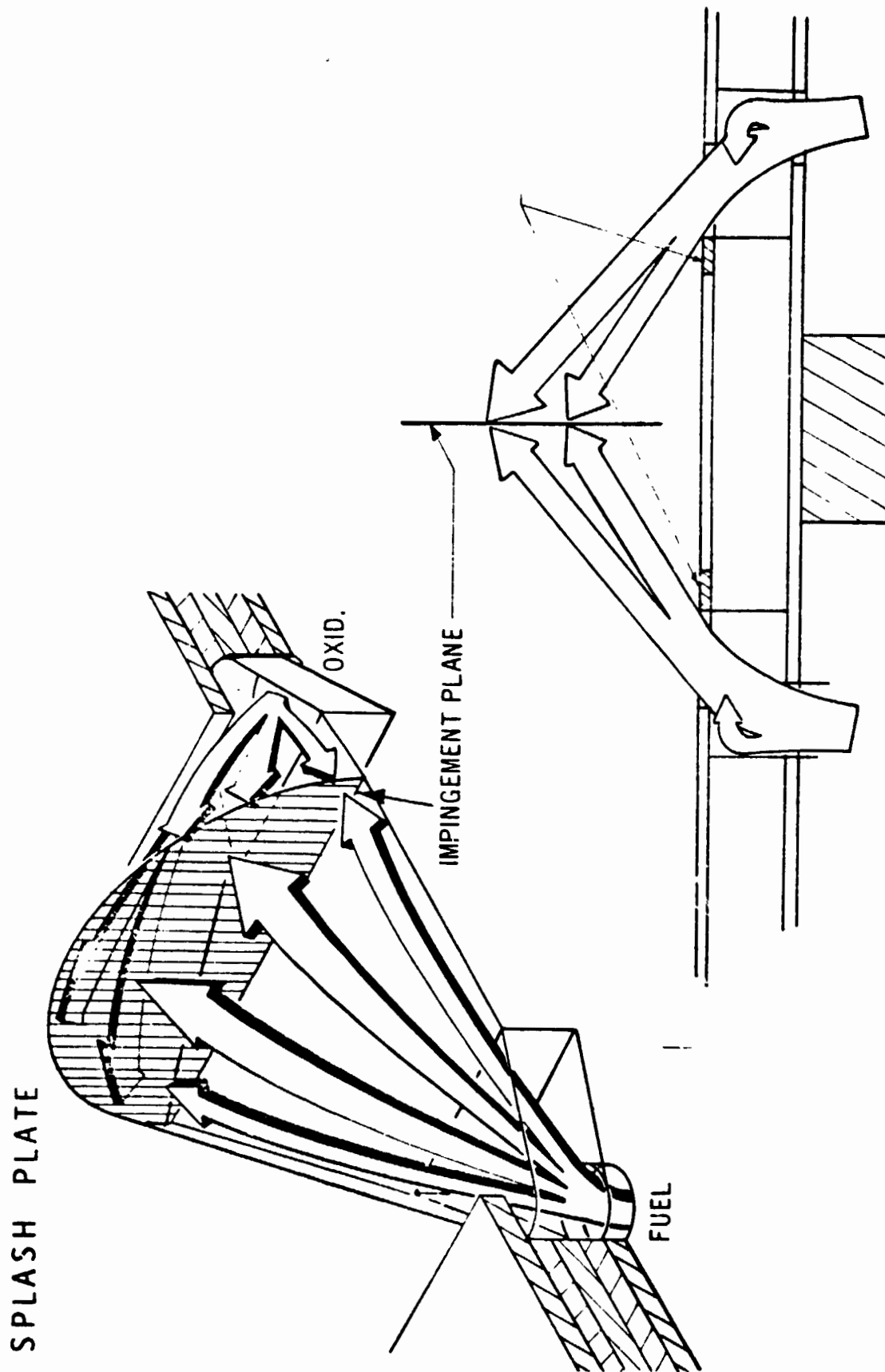


Figure 4. Splash Plate Element

VII,B, Unielement Design (cont.)

0
0
momentum exchange atomization). The unlike-doublet impinged the fuel on the oxidizer; the oxidizer was injected normal to the face and the fuel was normal to the oxidizer, i.e., parallel to the face (unlike momentum exchange atomization). The splash plate involved mechanical atomization of the two propellants by means of direct impingement on the lip of the injection cup and subsequent impingement of the resulting unlike propellant fans.

Following tests with the original configurations, several variations to the original patterns were added and a fourth configuration, a like-doublet, also included; Figure 5 shows the basic like-doublet, which consists of two impinging like-doublet fans, impinging at right angles.

Subsequently, the investigation of various patterns was renewed, with the emphasis on suitability for platelet fabrication techniques, increased passage size, avoidance of passages over ring channel lands, prevention of propellant splashing into the opposite propellant orifice, etc., in addition to the usual considerations of performance, stability, and compatibility. Six conceptual designs were completed and two of them fabricated and spray tested. These two were the V-doublet and vortex patterns, shown respectively on Figures 6 and 7, of which several dimensional variations existed. The V-doublet produced like-impinging fuel and oxidizer doublet fans which were canted toward each other. The vortex elements had either one or two inlets to each vortex cup and had a variety of exit area cross-sections.

Thus there were six basic orifice configurations tested with each pattern having several variations. These are summarized on Table I, which gives pertinent geometrical information for all of the variations.

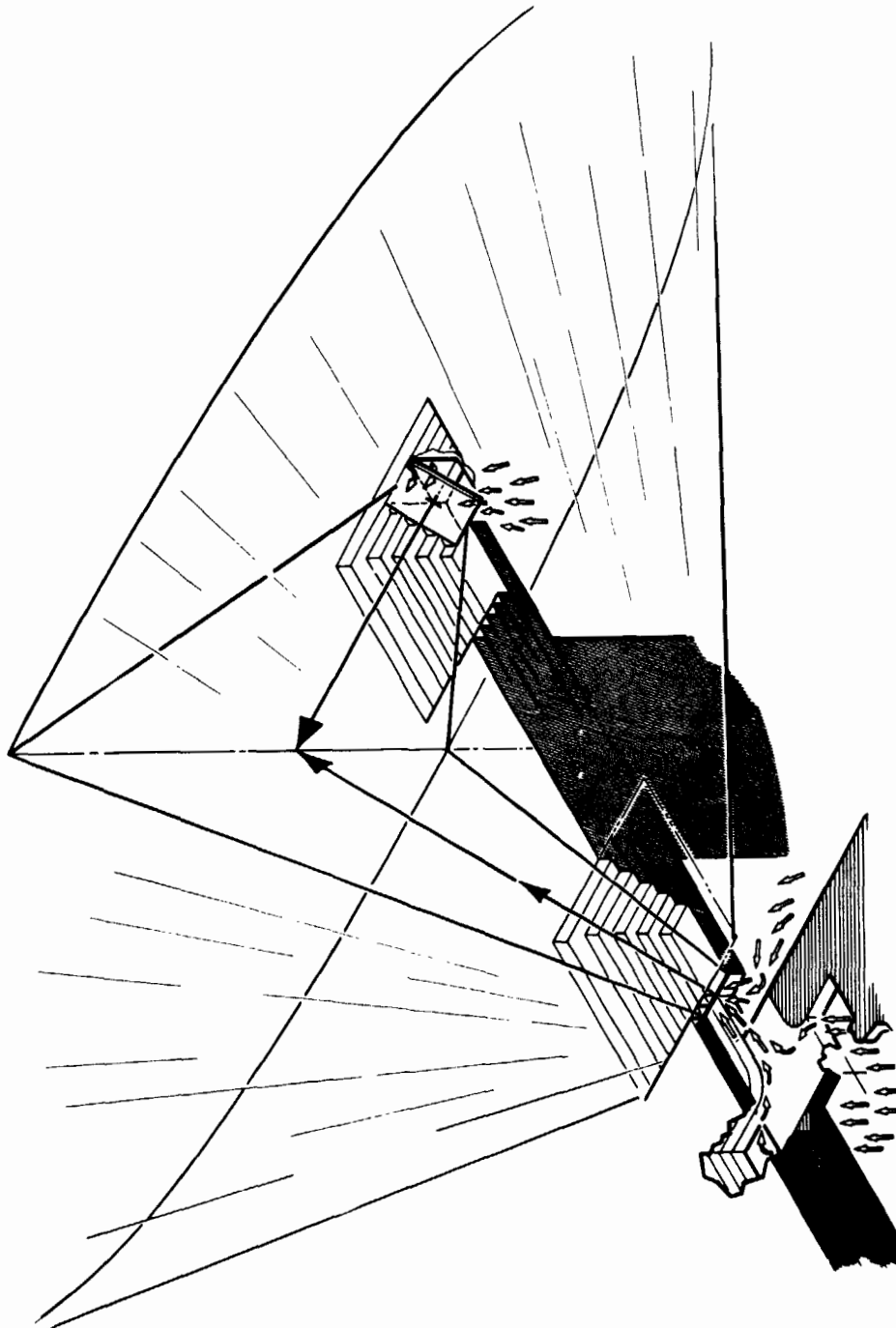


Figure 5. Like Doublet Element

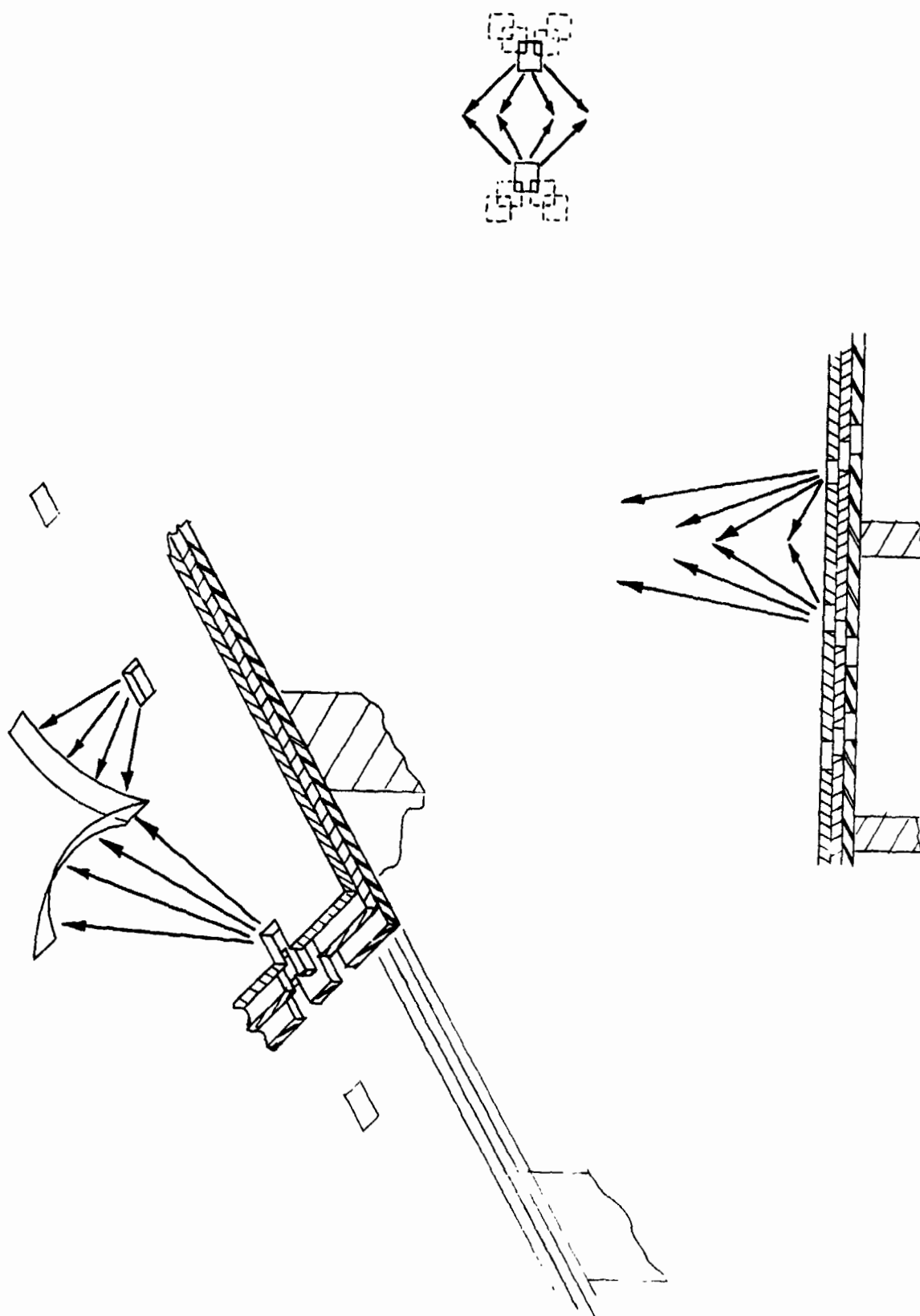


Figure 6. V-Doublet Element

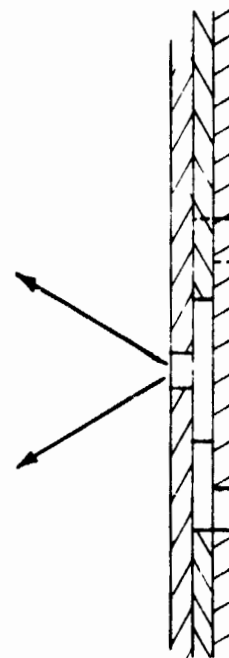
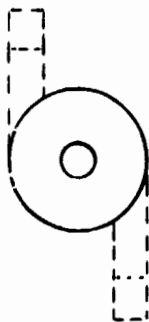
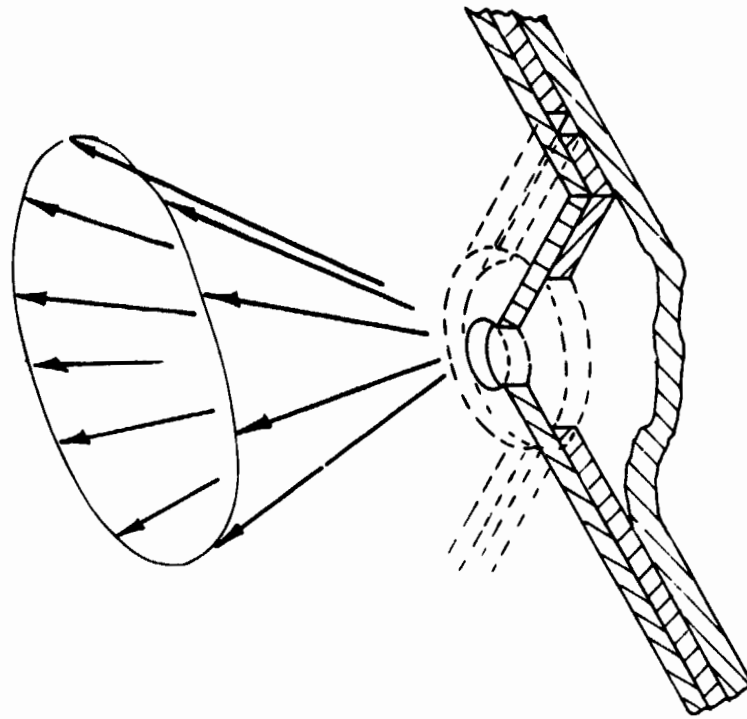


Figure 7. Vortex Element

TABLE I

SUMMARY OF UNIELEMENT PATTERNS TESTED

I. X-Doublet

a. Offset Fans

	Offset	Orifice Size		Slot Size	
		Fuel	Oxidizer	Fuel	Oxidizer
XD-2	.000	.020x.020	.024x.024	.020x.080	.024x.096
XD-2	.020	.020x.020	.024x.024	.020x.080	.024x.096
XD-4	.040	.020x.020	.024x.024	.020x.080	.024x.096
XD-01	.000	.020x.020	.024x.024	.020x.060	.024x.060
XD-02	.000	.020x.020	.020x.024	.020x.060	.020x.060

b. In-Line Fans

XDI-1	-	.020x.020	.024x.024	.020x.080	.020x.080
XDI-2	-	.020x.020	.020x.024	.020x.080	.024x.080

II. Unlike-Doublet

	Oxidizer Orifice	Fuel Orifice
UD-1	.029x.024	.020x.020
UD-2	.031x.022	.020x.020
UD-3	.026x.024	.020x.020

III. Splash Plate

	Orifice Diameter	
	Fuel	Oxidizer
SP-1	.020	.024
SP-2 (relieved)	.020	.024
LSP-1	.025	.030
LSP-2 (relieved .015)	.025	.030
4SP (four elements)		

IV. Like-Doublet

	Cup Size	
	Fuel	Oxidizer
LD-B	.049x.100	.055x.100
LD-FD	.059x.100	.055x.100
LD-FWD	.059x.120	.055x.100
LD-FOWD	.059x.129	.065x.120

V. V-Doublet

	Included Angle	Inlet		Outlet	
		Fuel	Oxidizer	Fuel	Oxidizer
VDT-1	60	.020x.020	.024x.024	.020x.020	.024x.024
VDT-2	60	.024x.020	.024x.024	.020x.020	.024x.024
VDT-3	60	.020x.020	.024x.024	.0226 dia	.0271 dia
VDT-4	60	.024x.020	.024x.024	.0226 dia	.0271 dia
VDT-5	90	.020x.020	.024x.024	.020x.020	.024x.024
VDT-6	90	.024x.020	.024x.024	.020x.020	.024x.024
VDT-7	90	.020x.020	.024x.024	.0226 dia	.0271 dia
VDT-8	90	.024x.020	.024x.024	.0226 dia	.0271 dia

VI. Vortex

	Exit Config	# of Inlets	Cup Diameter		Exit Diameter	
			Fuel	Oxidizer	Fuel	Oxidizer
VTX-A	Circular	1	.120	.100	.029 dia	.033 dia
VTX-B	Circular	2	.120	.100	.027 dia	.030 dia
VTX-C, Ca	Circular	1	.140	.120	.030 dia	.034 dia
VTX-D, Da	Circular	2	.140	.120	.028 dia	.031 dia
VTX-E	Elliptical	1			.0204x.0408	.0234x.0468
	Rectangular	1			.020x.0287	.020x.0354
VTX-F	Elliptical	2			.0204x.0408	.0234x.0468
	Rectangular	2			.020x.0287	.020x.0354
VTX-G	Triangular	1			.0108bx.0093h	.0131bx.0113h
	Cross-Shaped	1			.012	.012
VTX-H	Triangular	2			.0108bx.0093h	.0131bx.0113h
	Cross-Shaped	2			.012	.012

VII, Unielement Testing (cont.)

C. SPRAY TESTS

Spray tests using filtered water as a propellant simulant were conducted to allow visual observation of the injector spray and atomization characteristics. Element pressure drop correlations were simultaneously developed. Backlighting enabled Polaroid photographs to be made of the spray patterns, and Figures 8 and 9 show typical results for some of the first patterns tested. The propellant circuits were flowed separately and then together in these tests.

The spray tests were an inexpensive means of determining droplet size distribution and dispersion, and in conjunction with the mixing tests described below, permitted an estimation of performance and compatibility under hot-fire conditions. The X-doublet, for instance, was observed to give excellent atomization, with well defined and predictable spray; however, the spray width was found to be minimum for good unlike propellant mixing. Neither the unlike-doublet nor the splash plate offered comparable atomization, although the unlike-doublet showed excellent stream alignment and the splash plate a uniform spray field. The like-doublet patterns typically produced a fan similar to the splash plate, possibly with superior atomization. The vortex element produced a conical spray which showed excellent atomization.

D. MIXING TESTS

Mixing tests were performed on the Advanced Injector Distribution (AID) cold flow measurement facility, more commonly called the "milk maid". Figure 10 shows a photograph of the apparatus which involves a collector head placed below the injector face and numerous tubes leading to collector bottles. The tests were conducted using water as a fuel simulant (specific gravity of 1.00 versus 0.79 at the nominal fuel injection temperature) and Freon as the oxidizer simulant (specific gravity of 1.58 versus 1.44 at the nominal point). This favorable density ratio allows the proper momentum ratio to be duplicated. Four unielement

ORIGINAL PAGE IS
OF POOR QUALITY

















INJECTOR MIN. PASSAGE SIZE PRESS DROP, PSI	OX ONLY	FUEL ONLY	BOTH	ROTATED
UD-1 .020 30				
XD-0 .020 30				
XD-4 .020 30				
SP-1 .020 30				

Figure 8. OME Platelet Injector Unielement Cold Flow Characterization












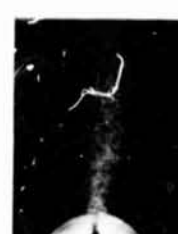




INJECTOR MIN. PASSAGE SIZE PRESSURE DROP, PSI	OX ONLY	FUEL ONLY	BOTH	ROTATED
UD-2 .020 30				
UD-3 .020 30				
XD-2 .020 30				
SP-2 .020 30				

Figure 9. CME Platelet Injector Unielement Cold Flow Characterization

ORIGINAL PAGE IS
OF POOR QUALITY

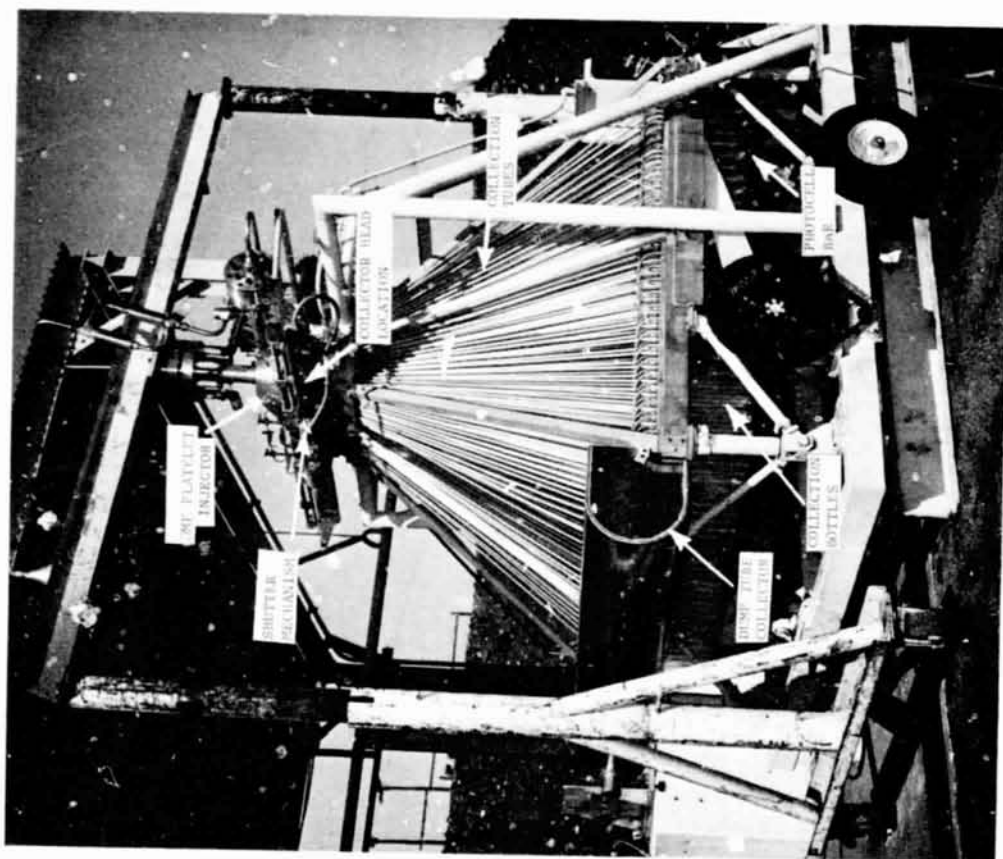


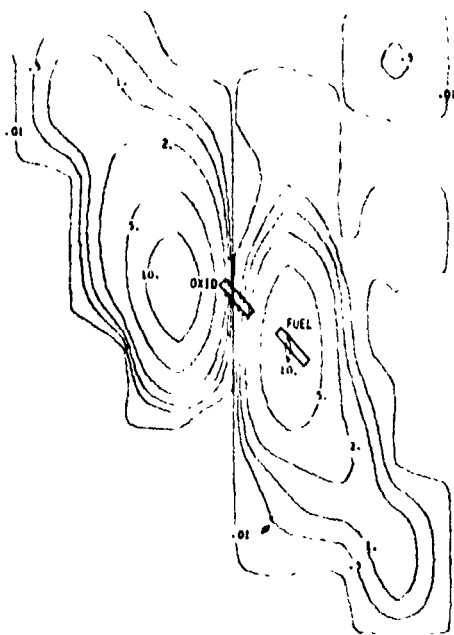
Figure 10. Advanced Injector Cold Flow Collection Apparatus

VII,D, Mixing Tests (cont.)

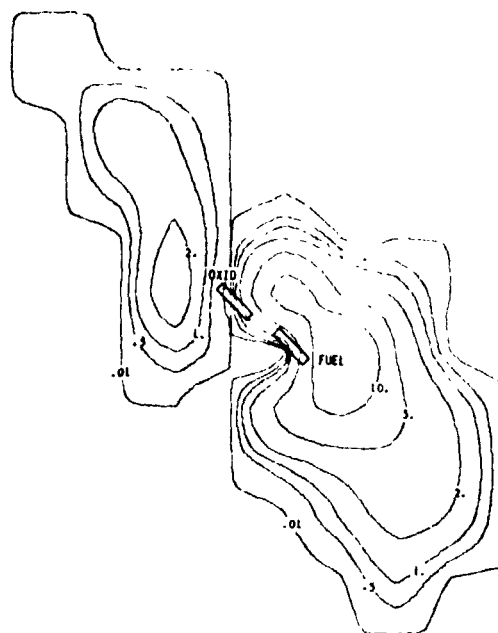
injectors were tested at one time with the collector head located 0.75 in. away on all tests. The head was divided into four quadrants by separator plates, and care was taken to ensure that no liquid struck the separators. The resulting spray grid on each injector was thus a square 1.8 in. on a side.

Based on test measurements, maps of mixture ratio, fuel and oxidizer mass flux, and total mass flux were generated by computer. Figures 11 through 21 show such plots for variations on the X-doublet, in-line X-doublet, unlike-doublet, splash plate, and like-doublet patterns. For the X-doublets, Figures, 11, 12 and 13, the XD-2 configuration appears to have the most condensed spray pattern with both propellants concentrated into single lobes. These results may be misleading in that flow to the XD-2 was somewhat intermittent and the injector would not otherwise be expected to differ so markedly from the XD-0 and XD-4. However, the mixing efficiency is clearly degraded by increasing the amount of offset between orifices; the effect is simply due to increasing the separation between propellant fans. Figures 14 and 15 show the mixture ratio and mass flux maps for the in-line doublets. For these two elements, the propellants are more-or-less concentrated under their respective orifices with the oxidizer tending to surround the fuel fan. The tendency is increased when the oxidizer slot is larger than the fuel slot.

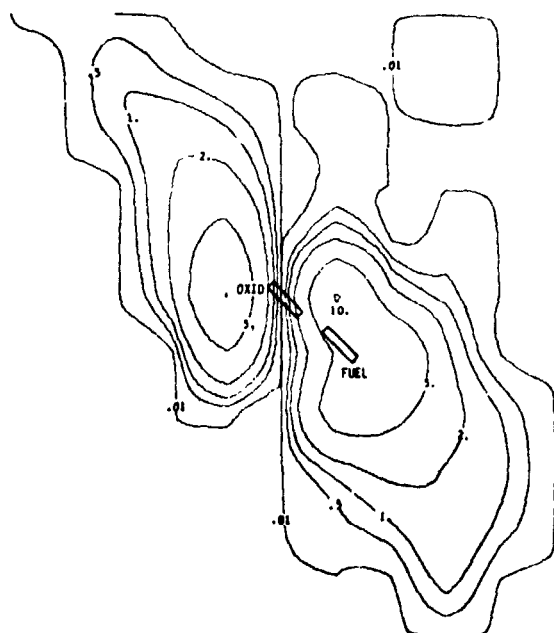
Unlike-doublet test results are given in Figures 16, 17, and 18. The unlike-doublets produced relatively uniform fuel dispersion but rather converged oxidizer flow such that the mass flux and mixture ratio profiles are both centered around the orifice area. The splash plate design, Figure 19, yields relatively uniform mass fluxes and a mixture ratio profile that leans in the direction of high values in the direction of oxidizer flow beyond the fuel orifice. This spray-through characteristic would be checked out on hot test to see if combustion would inhibit this condition. Finally, the like-doublet results given in Figures 20 and 21 show a wide dispersal of both injectants, again with the oxidizer penetrating through the fuel and causing high mixture ratio zones beyond the fuel orifice.



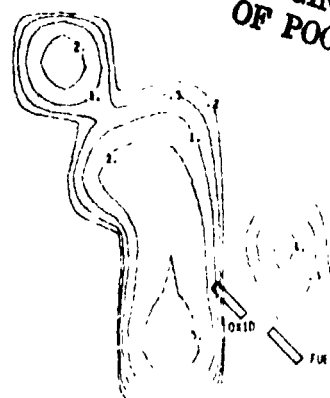
XD-0 Oxidizer Mass Flux Profile in X



XD-0 Fuel Mass Flux Profile in X



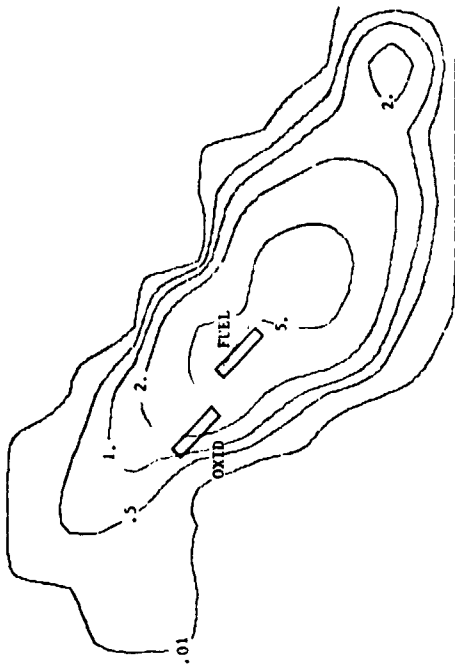
XD-0 Total Mass Flux Profile in X



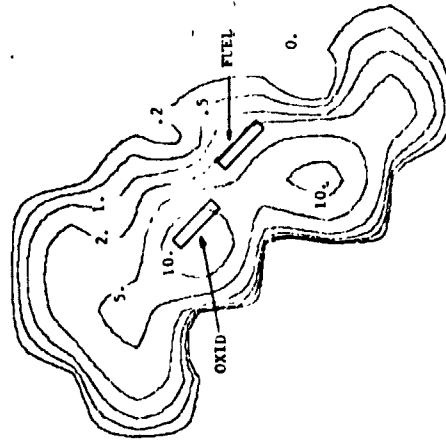
XD-0 Mixture Ratio Profile

ORIGINAL PAGE IS
OF POOR QUALITY

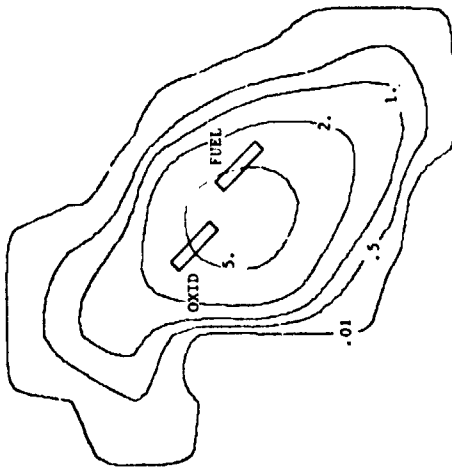
Figure 11. Unielement Propellant Flow Distribution, XD-0 Pattern



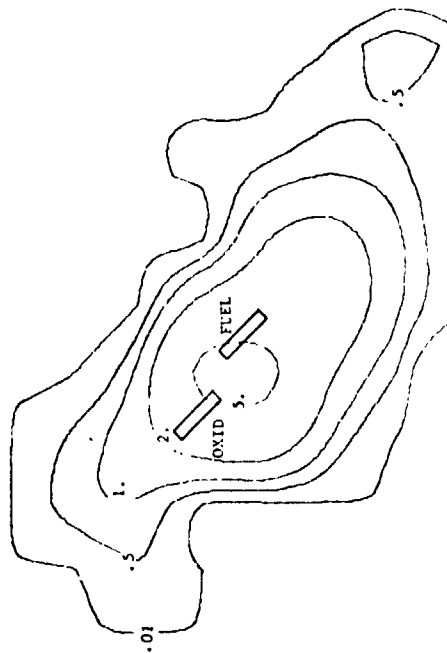
XD-2B Fuel Mass Flux Profile in Z



XD-2B Mixture Ratio Profile

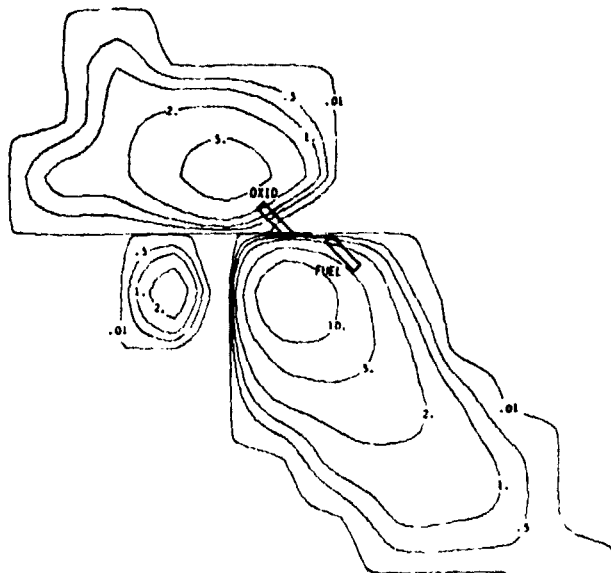


XD-2B Oxidizer Mass Flux Profile in Z

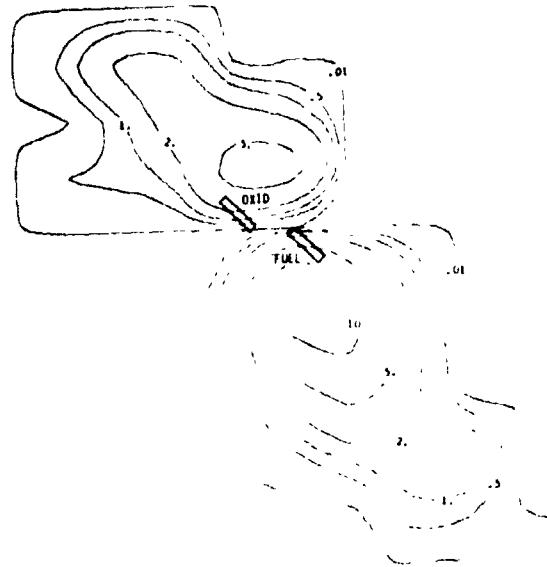


XD-2B Total Mass Flux Profile in Z

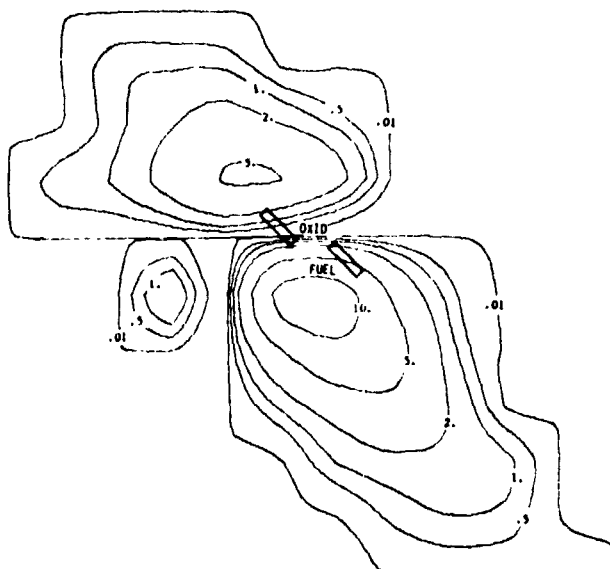
Figure 12. Unielement Propellant Flow Distribution, XD-2 Pattern



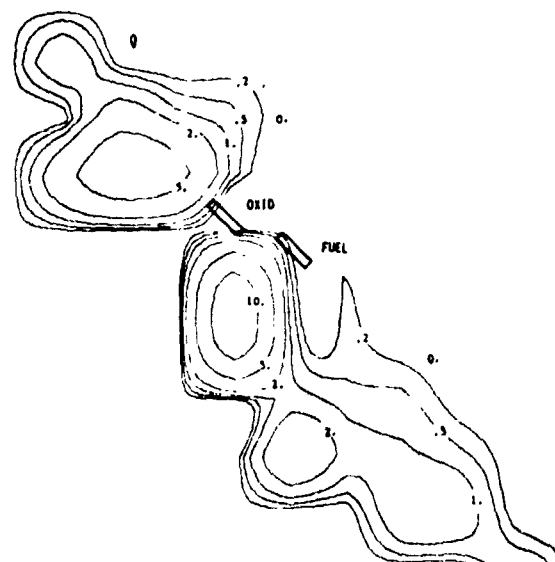
XD-4 Oxidizer Mass Flow Profile in Z



XD-4 Fuel Mass Flow Profile in Z

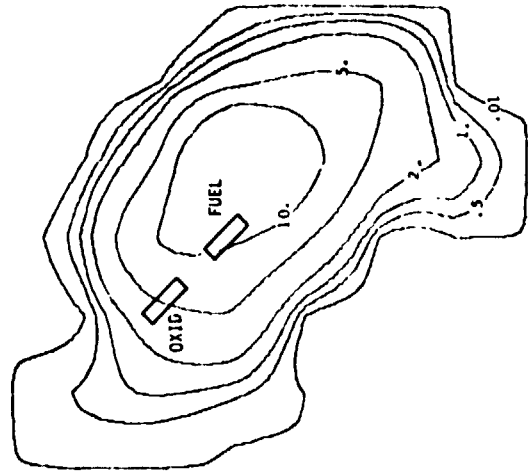


XD-4 Total Mass Flow Profile in Z

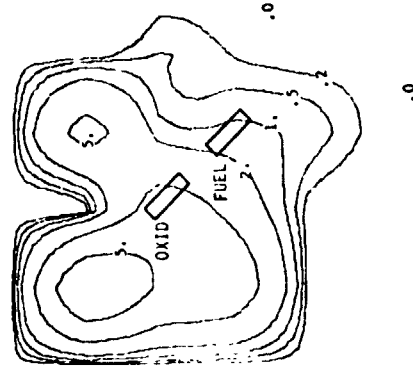


XD-4 Mixture Ratio Profile

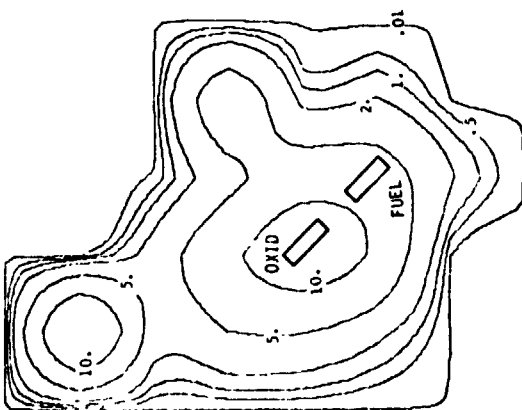
Figure 13. Unielement Propellant Flow Distribution, XD-4 Pattern



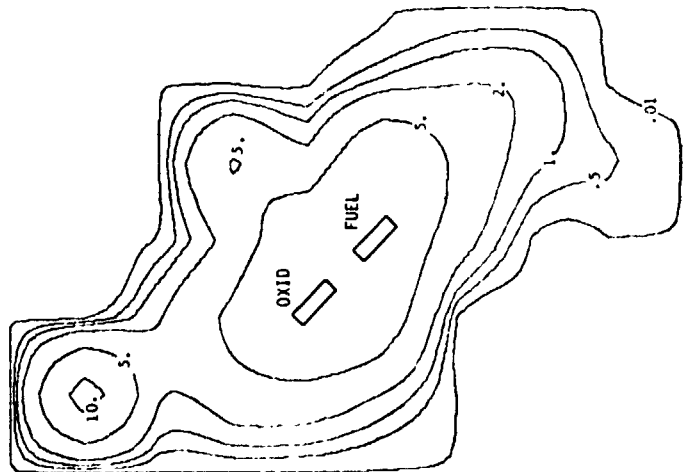
XDI-1 Fuel Mass Flux Profile in Z



XDI-1 Mixture Ratio Profile



XDI-1 Oxidizer Mass Flux Profile in Z



XDI-1 Total Mass Flux Profile in Z

Figure 14. Unielement Propellant Flow Distribution, XDI-1 Pattern

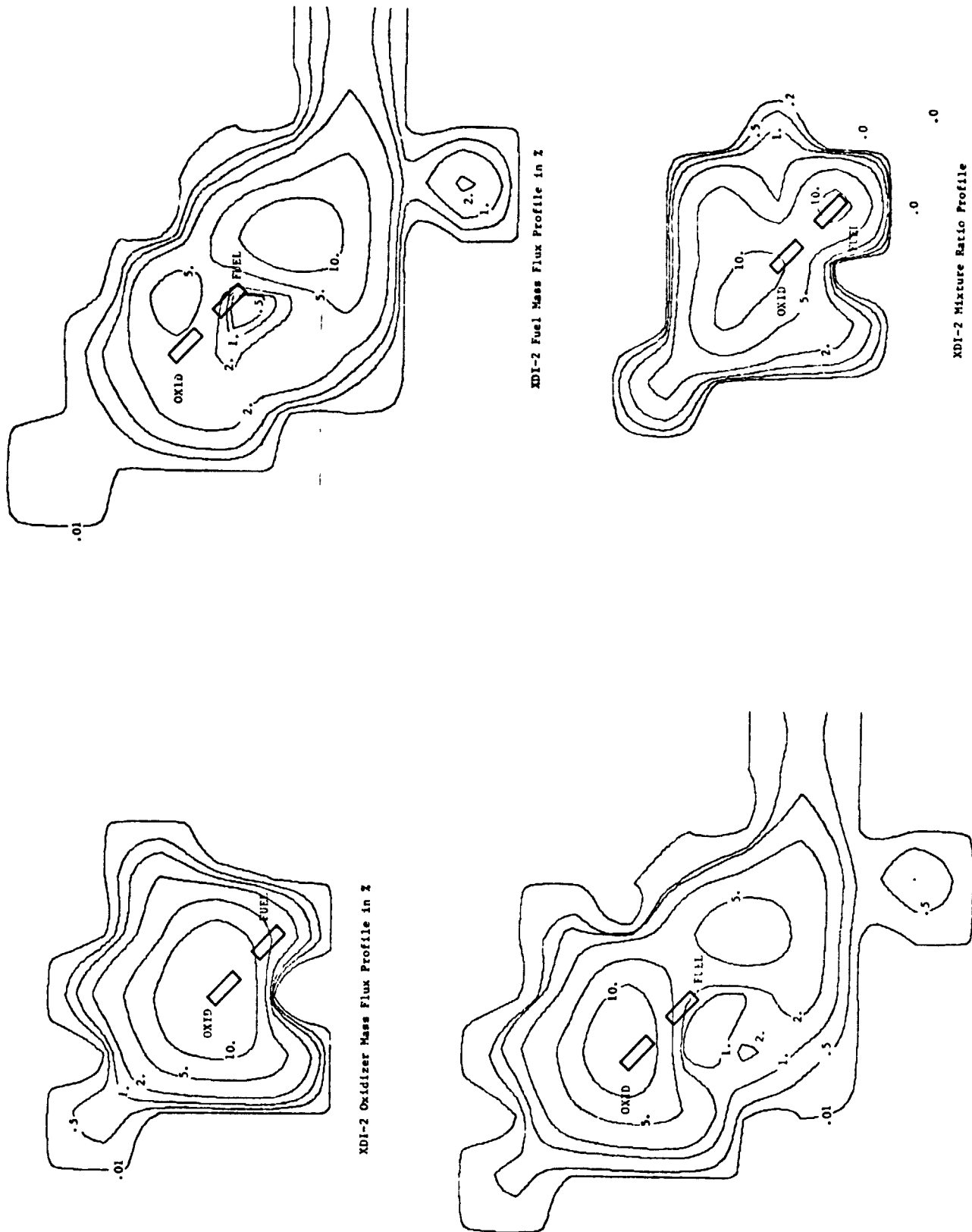
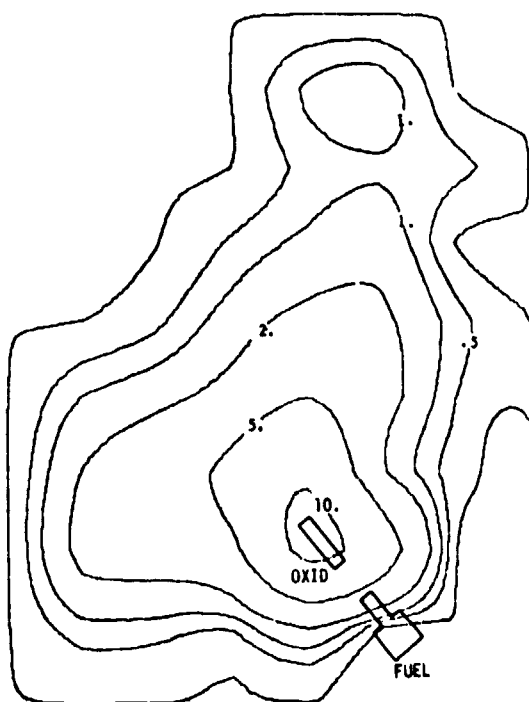
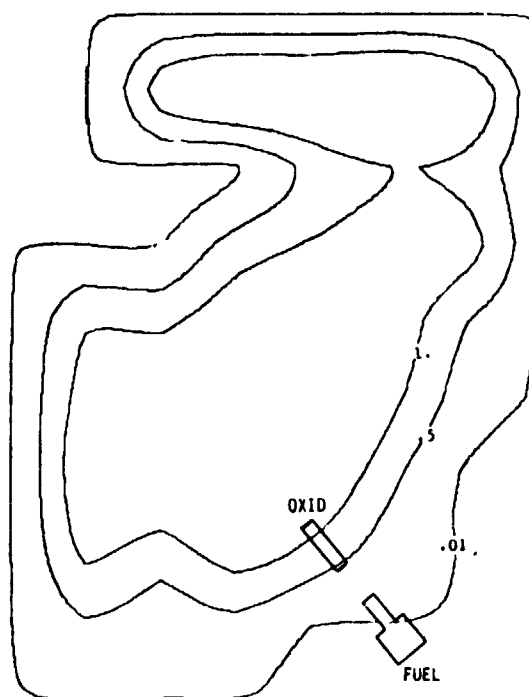


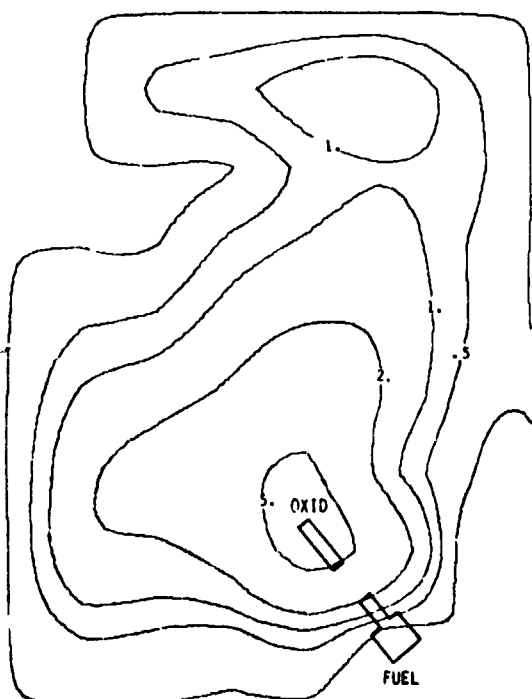
Figure 15. Unelemented Propellant Flow Distribution, XDI-2 Pattern



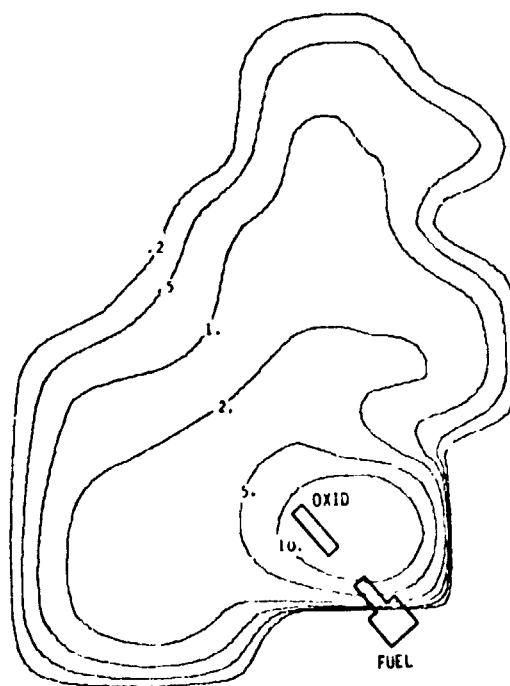
UD-1B Oxidizer Mass Flux Profile in X



UD-1B Fuel Mass Flux Profile in X



UD-1B Total Mass Flux Profile in X



UD-1B Mixture Ratio Profile

Figure 16. Unielement Propellant Flow Distribution, UD-1 Pattern

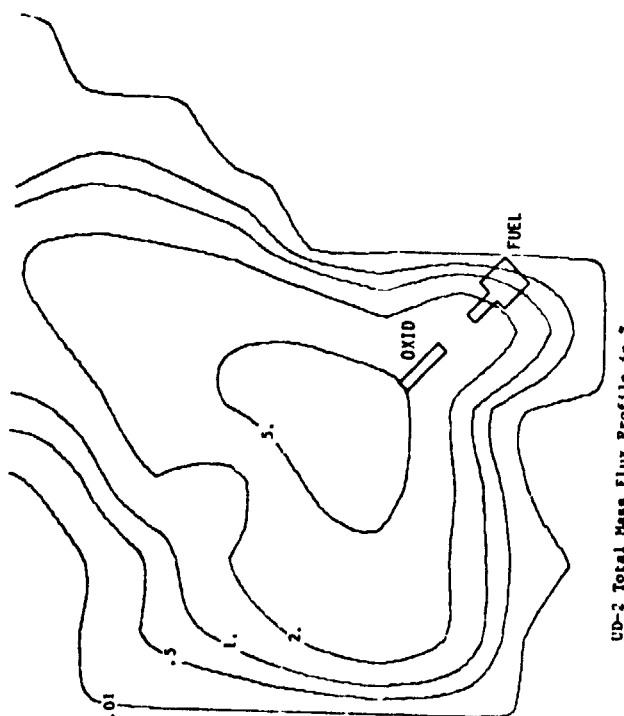
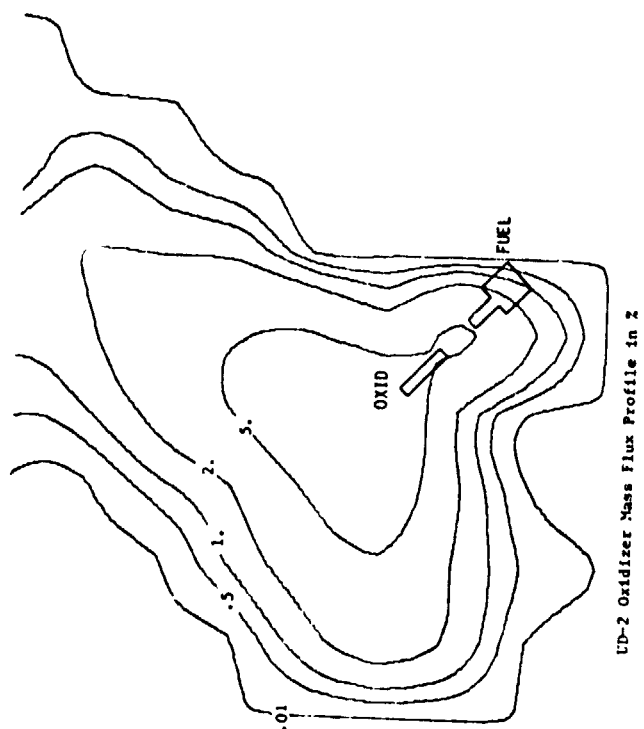
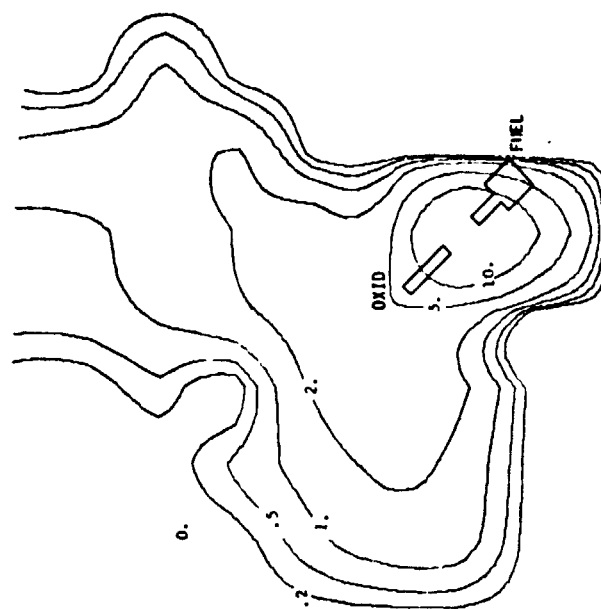
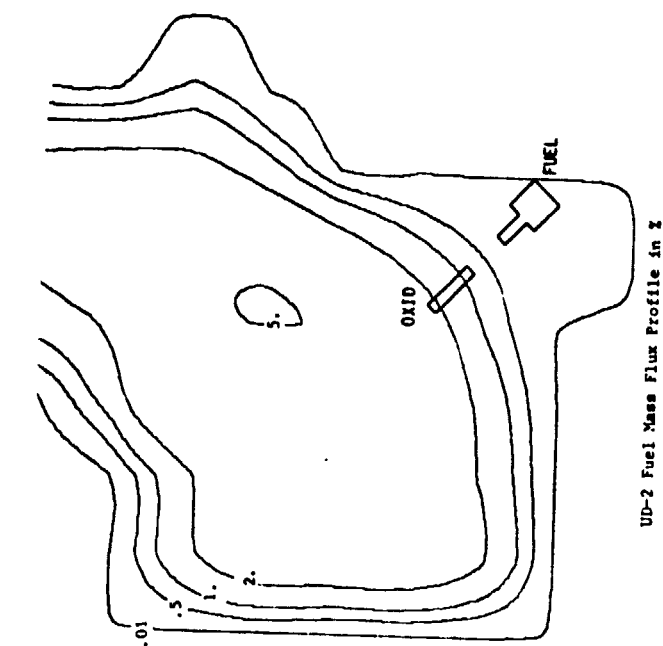
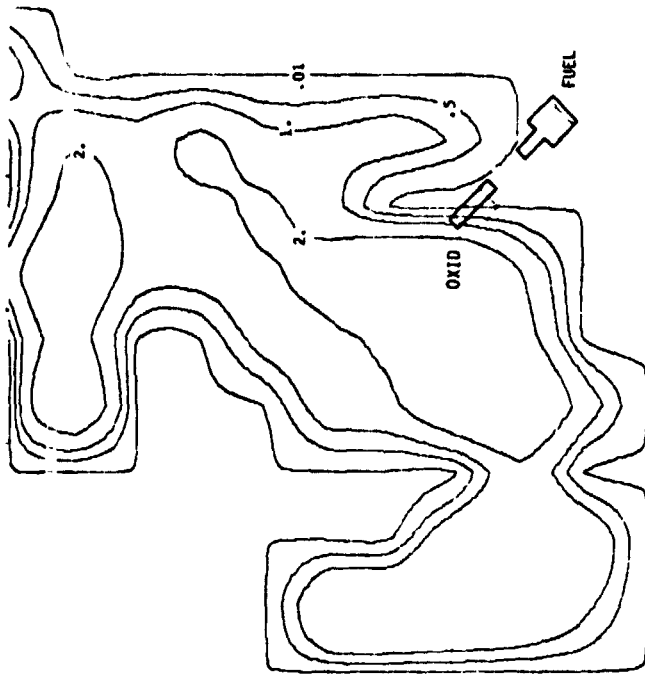
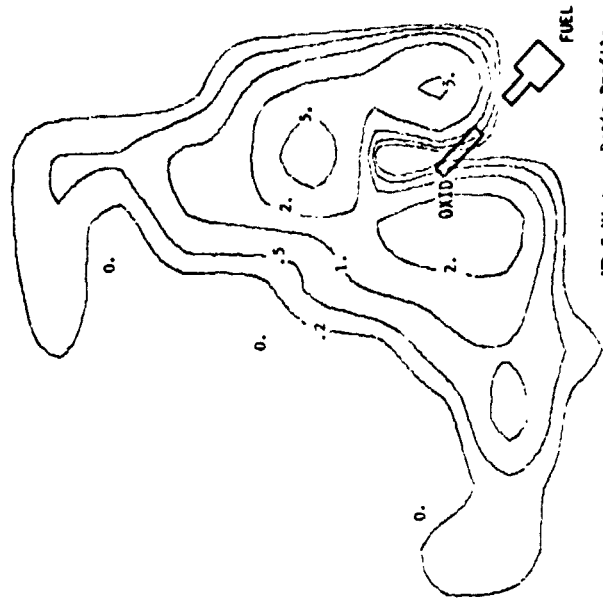


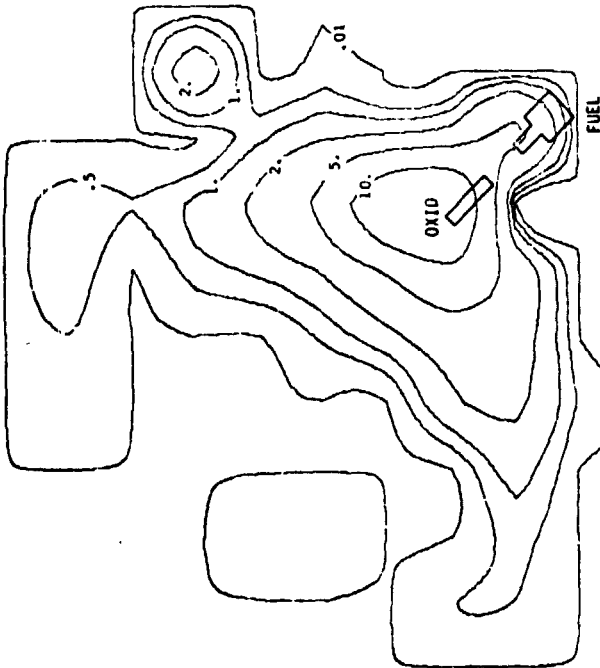
Figure 17. Unelemented Propellant Flow Distribution, UD-2 Pattern



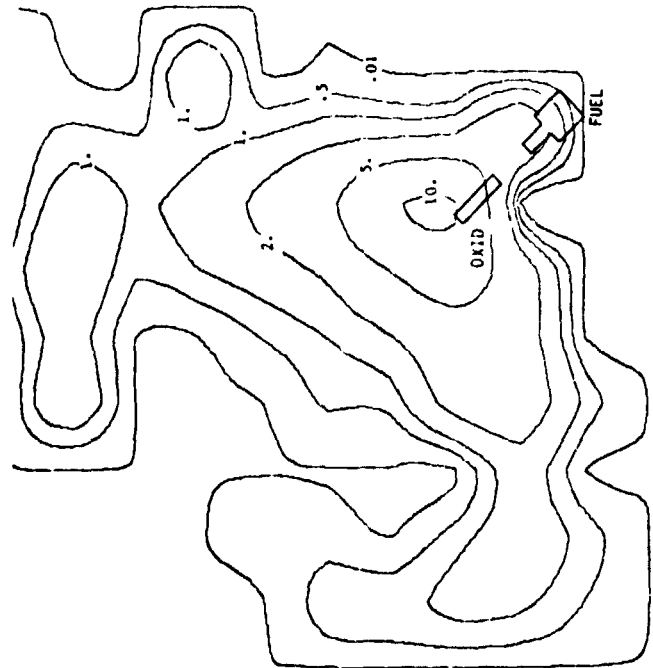
UD-3 Fuel Mass Flux Profile in Z



UD-3 Mixture Ratio Profile

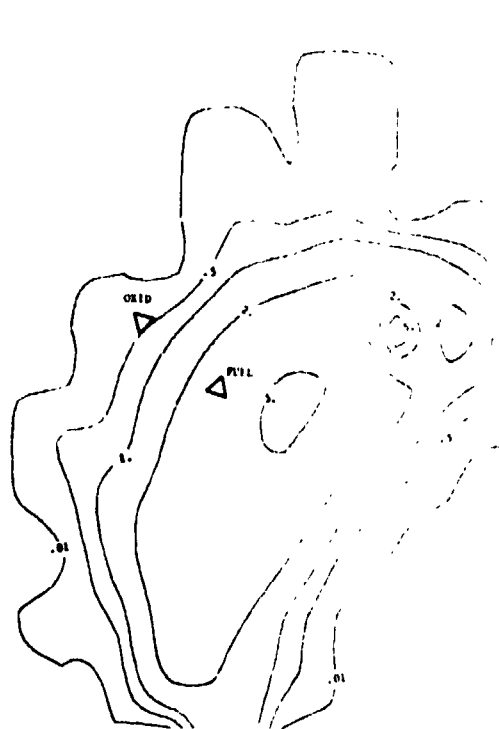


UD-3 Oxidizer Mass Flux Profile in Z

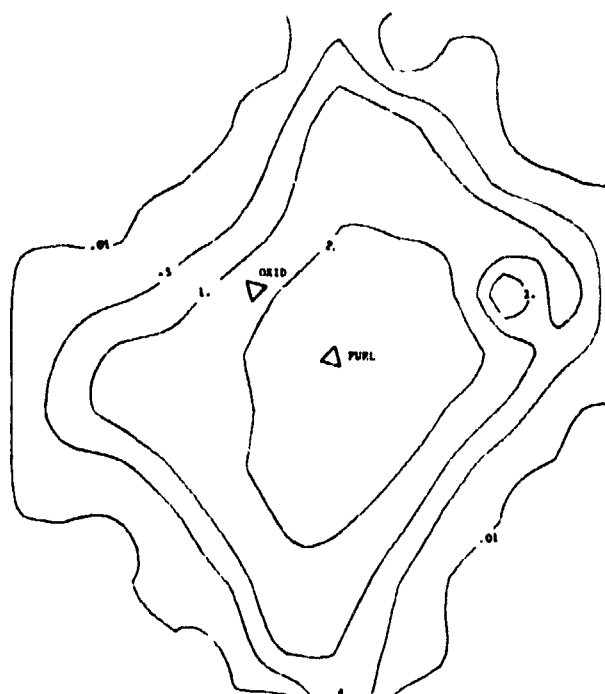


UD-3 Total Mass Flux Profile in Z

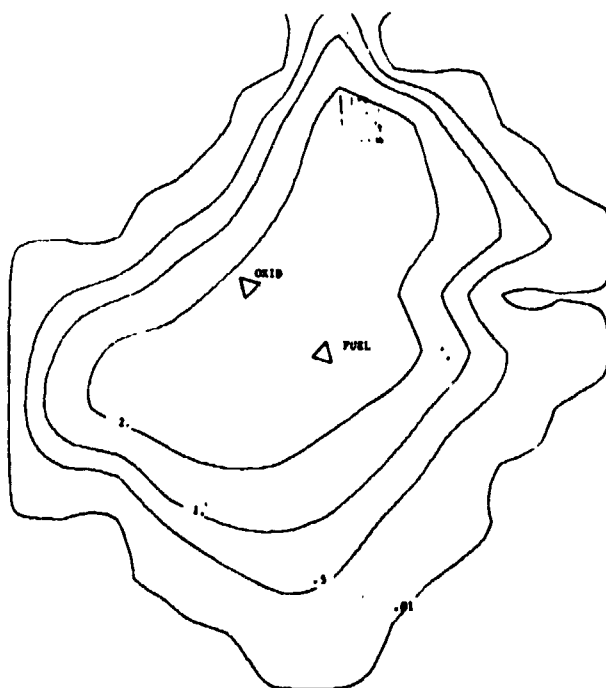
Figure 18. Unelement Propellant Flow Distribution, UD-3 Pattern



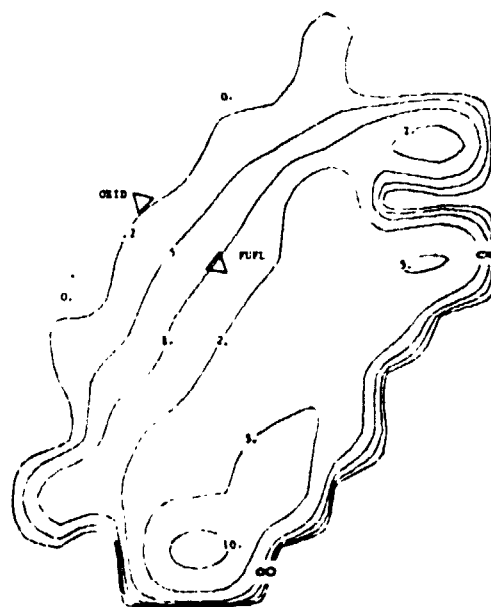
SP-18 Oxidizer Mass Flow Profile in X



SP-18 Fuel Mass Flow Profile in X

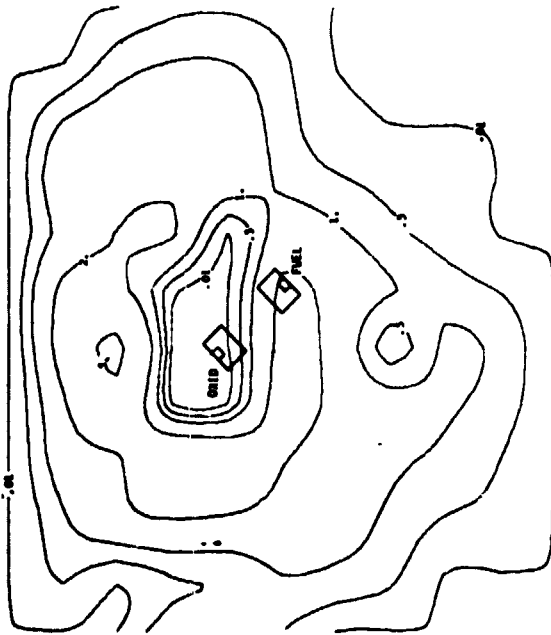


SP-18 Total Mass Flow Profile in X

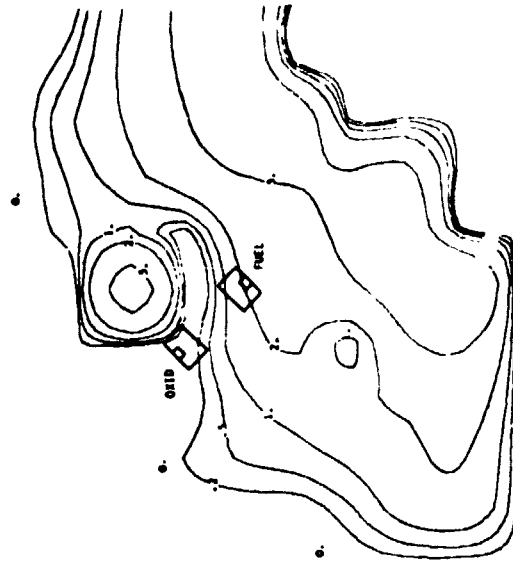


SP-18 Mixture Ratio Profile

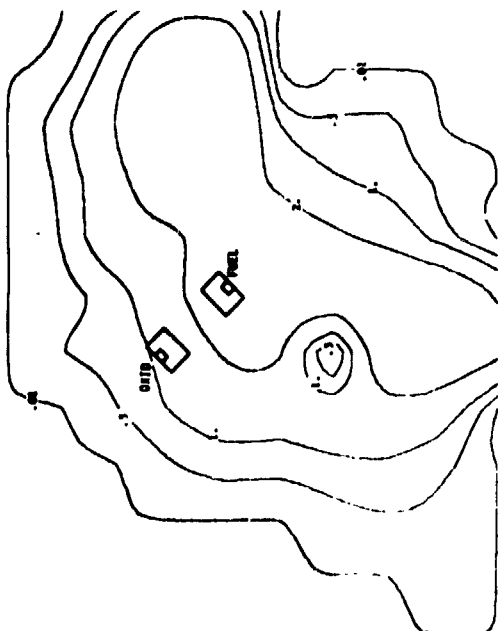
Figure 19. Unielement Propellant Flow Distribution, SP-1 Pattern



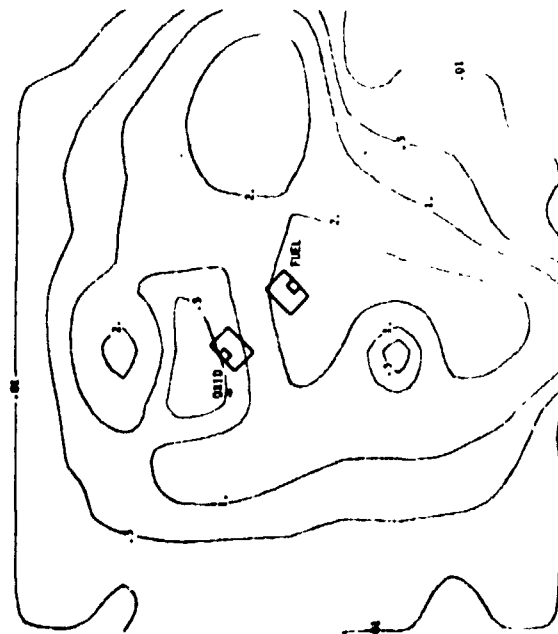
LD-8 Fuel Mass Flow Profile in 2



LD-8 Mixture Ratio Profile



LD-8 Oxidizer Mass Flow Profile in 2



LD-8 Total Mass Flow Profile in 2

Figure 20. Unelement Propellant Flow Distribution, LD-8 Pattern

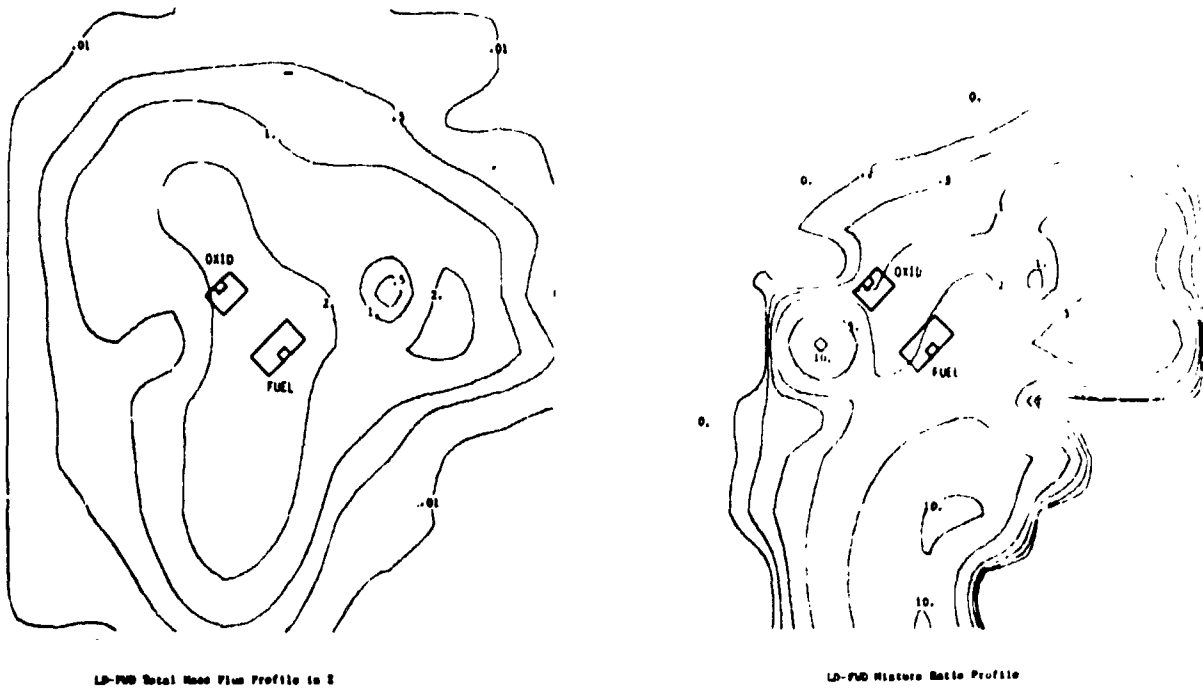
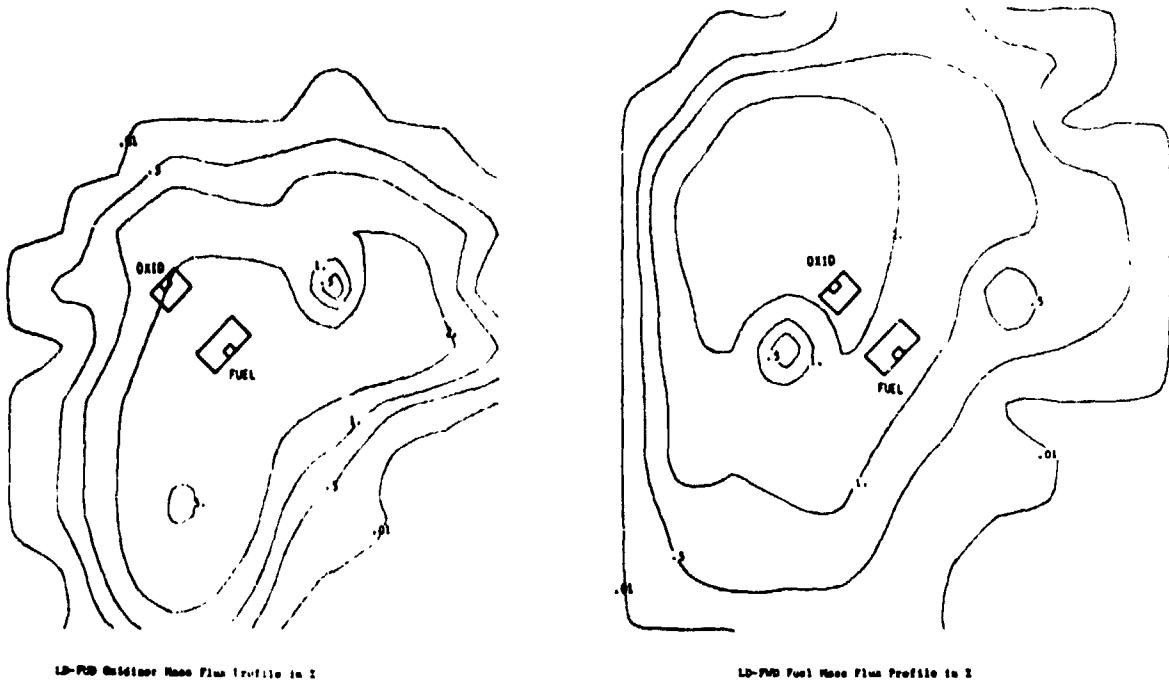


Figure 21. Uniement Propellant Flow Distribution, LD-FWD Pattern

Report 13133-F-1

VII,D, Mixing Tests (cont.)

It should be pointed out that the orifices drawn on the above figures are not to scale, nor accurately located. Also, the explanation for nonsymmetrical profiles from symmetrical orifice configurations is not obvious; presumably, the effect of tolerance differences take on great significance when compared to nominal passage sizes, but also quirks in the test set-up and data reduction techniques may induce a large part of the nonsymmetrical results obtained.

In conjunction with the above tests, the mixing efficiency, Rupe number, and collection area were determined as follows:

<u>Element</u>	<u>Collection Mixture Ratio</u>	<u>Mixing Efficiency</u>	<u>Rupe Number</u>	<u>% Area Collection</u>
XD-0	1.08	50.1	0.70	54.7
XD-2	2.10	44.0	0.38	N/A
XD-4	1.31	35.0	0.62	47.5
XDI-1	N/A	43.6	N/A	N/A
XDI-2	N/A	57.4	N/A	N/A
UD-1	1.06	61.9	0.71	42.2
UD-2	1.72	72.9	0.48	37.1
UD-3	1.65	54.6	0.50	47.2
SP-1	0.98	59.1	0.74	79.6
LD-B	N/A	58.0	N/A	N/A
LD-FWD	N/A	61.2	N/A	N/A

Mixing efficiency, E_m , is defined by the equation:

$$E_m = 100 \left\{ 1 - \sum_j X_j \left[\frac{(O/F)_j - (O/F)}{1 + (O/F)_j} \right] - \sum_i X_i \left[\frac{(O/F) - (O/F)_i}{(O/F) [1 + (O/F)_i]} \right] \right\}$$

where X is the mass fraction in each collection tube, (O/F) is the nominal mixture ratio, and the subscript i and j refer to the samples below and above the nominal mixture ratio, respectively. Mixing efficiency is thus a measure of the weight-summed deviation from uniform mixture ratio condition.

VII,D, Mixing Tests (cont.)

The Rupe Number, R_n , is defined as:

$$R_n = \frac{1}{1 + \left(\frac{1}{O/F}\right)^2 \left(\frac{\rho_o}{\rho_f}\right) \left(\frac{d_o}{d_f}\right)^3}$$

where ρ is the density, d the orifice diameter, and the subscripts o and f denote the oxidizer and fuel respectively. It is a measure of relative momentum and area effects for impinging propellant streams. The mixing efficiency and Rupe Number were developed¹ to express the correlation between propellant mixing and pertinent injection parameters. The last term in the table, the "% Area Collected" is the ratio of collector tubes containing fluid to total collector tubes and is a measure of propellant dispersion.

Although the unielement "milk maid" testing approach cannot account for interelement mixing and various combustion effects, it has proven a useful tool in optimizing injector element design. It is almost axiomatic that a well designed single element can only perform better under hot fire conditions in conjunction with other elements.

E. HOT FIRE TESTS

Eight-eight hot firings were conducted with the unielements, using both 2 in. and 4 in. long chambers. Figure 22 shows the chambers used in these Tests and Table II summarizes test conditions and pertinent results. The following injector patterns were tested: XD-0 and -2, XDI-1 and -2, SP-1 and -2, LSP-2 and 4SP, UD-1 and -2, and LD-B. Figures 23 and 24 show the energy release efficiency (ERE) as a function of mixture ratio for the various patterns tested. In general, the patterns are not mixture ratio sensitive; the splash plate, like-

¹Rupe, J. H., A Correlation Between the Dynamic Properties of a Pair of Impinging Streams and the Uniformity of Mixture Ratio Distribution in the Resulting Spray, Program Report No. 20-209, Jet Propulsion Lab., 28 March 1956

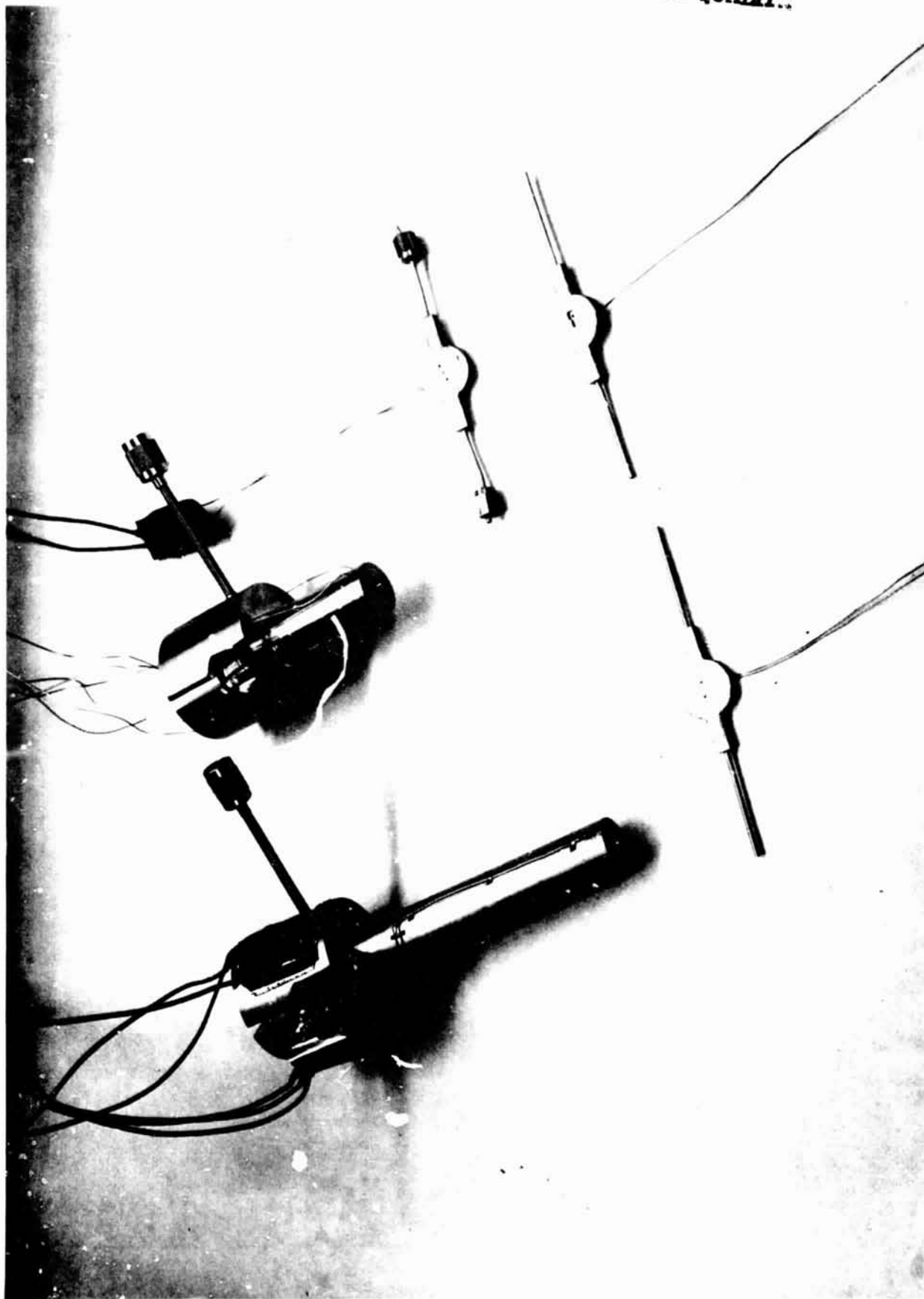


Figure 22. 2 in. and 4 in. Chambers Used in Unilelement Testing

TABLE II

SUMMARY OF UNIELEMENT HOT FIRINGS

Test #	Date	Element	Chamber Length(in)	O/F	Pc	Tox(F)	T _f (F)	Velocity Ratio(F/O)	Momentum Ratio(F/O)	% C*	% Is	ERE
101	11/14/72	XD-2B	2	1.55	44.0	51	51	1.44	.93	54.0	48.8	52.4
102	12/06/72		4	1.35	125.0	43	43	1.66	1.23	81.0	76.9	83.5
103				1.68	112.6	43	43	1.33	.79	78.8	74.5	81.9
104				1.69	117.7	43	42	1.32	.78	78.3	75.1	82.3
105				1.40	98.1	42	42	1.60	1.14	82.5	76.8	83.7
106				1.51	141.6	43	43	1.48	.99	78.3	73.7	80.1
107				1.63	116.6	43	42	1.37	.84	80.7	75.0	82.2
108	12/07/72	SP-1B	4	1.54	102.0	41	41	1.50	.97	88.9	84.9	92.6
109				1.46	119.7	42	42	1.58	1.08	92.0	87.9	95.2
110				1.52	150.0	42	42	1.52	1.00	93.3	86.7	93.9
111				2.04	102.0	42	42	1.13	.56	90.1	85.8	94.4
112		UD-1B		.66	101.0	42	42	3.31	5.02	98.1	87.5	93.0
113				1.45	95.7	42	42	1.51	1.04	94.0	89.6	97.3
114				1.49	145.6	42	42	1.47	.99	94.6	90.8	98.1
115	12/12/72	XD-2B		1.58	120.8	38	109	1.48	.93	81.3	76.0	83.1
116				1.63	121.8	39	84	1.41	.87	79.9	73.4	80.7
117				1.66	120.9	40	110	1.41	.85	80.7	72.3	79.3
118	12/13/72			1.72	122.6	32	109	1.36	.79	80.3	75.1	82.4
119				1.72	121.0	32	161	1.41	.82	80.8	75.1	82.4
120				3.04	107.1	32	166	.80	.26	79.6	75.1	83.2
121	12/14/72			1.60	120.9	32	180	1.53	.96	80.1	74.8	81.6
122				1.69	120.6	32	202	1.47	.87	80.2	74.7	81.8
123				.70	120.8	32	209	1.47	.87	79.3	73.2	80.1
124		SP-1B		1.96	105.1	32	129	1.29	.68	91.1	89.4	98.2
125				1.70	102.7	32	176	1.48	.87	90.5	87.2	95.5
126	12/15/72	UD-1B		1.81	156.0	33	33	1.21	.67	91.7	87.3	95.1
127				2.04	154.3	33	35	1.07	.53	91.4	86.5	94.5
128				1.49	156.4	33	146	1.57	1.06	90.0	85.9	92.8
129				1.64	156.8	34	200	1.48	.90	90.7	85.9	94.4
130	12/18/72	XD-0		1.55	119.6	53	52	1.44	.93	85.3	79.6	86.8
131				1.82	122.5	53	52	1.22	.67	83.8	77.2	84.8
132		UD-2		1.63	155.5	52	52	1.32	.81	92.4	87.8	95.3
133				1.86	155.8	52	52	1.17	.63	92.6	86.1	94.1
134				1.26	146.9	54	198	1.87	1.49	93.0	87.7	94.2

TABLE II (cont.)

Test #	Date	Element	Chamber Length(in)	O/F	Pc	Tox(F)	T _f (s)	Velocity Ratio(F/O)	Momentum Ratio(F/O)	% C*	% Is	ERE
135	N/A	SP-28	4	1.79	104.4	52	52	1.48	.83	91.2	88.0	96.4
136	12/20/72		1	2.04	100.8	52	52	1.30	.64	88.8	86.6	95.1
137			2	1.60	97.1	53	53	1.66	1.03	83.1	86.0	92.0
138			4	1.75	100.9	51	50	1.52	.87	83.3	83.9	92.2
139	01/30/73	XDI-2		1.51	121.3	52	53	1.59	1.06	82.4	78.8	86.2
140	01/31/73			2.08	122.0	53	55	1.16	.56	82.5	77.9	86.2
141				2.49	122.2	53	55	.96	.39	83.0	78.0	86.5
142				1.84	121.7	53	56	1.30	.71	82.1	77.8	85.9
143				1.94	119.4	54	158	1.32	.68	81.0	76.8	84.4
144				1.86	119.7	53	209	1.42	.76	79.5	74.7	82.1
145	02/01/73	LD-B		1.93	159.5	53	54	1.23	.64	90.2	86.8	94.9
146				1.30	154.2	54	54	1.83	1.40	89.4	86.6	93.4
147				1.93	163.8	54	55	1.23	.64	90.9	87.4	95.4
148				2.06	165.9	54	55	1.16	.56	91.3	87.4	95.5
149				1.81	167.0	55	133	1.38	.76	91.5	88.5	96.4
150				1.86	168.2	54	131	1.46	.83	90.5	86.1	94.1
151	02/02/73	XDI-1		1.71	123.7	55	58	1.12	.65	81.6	77.0	84.7
152				1.93	118.2	56	58	.99	.51	82.2	77.7	85.9
153				2.53	148.4	55	56	.85	.33	88.8	85.7	94.3
154		LSP-2		1.41	158.3	56	58	1.52	1.08	90.9	87.7	94.9
155				1.61	167.9	56	60	1.33	.83	91.6	88.1	95.7
156				1.71	168.3	55	59	1.26	.73	91.8	88.3	96.1
157	02/05/73			1.50	163.1	61	163	1.52	1.02	90.7	87.5	94.6
158				1.73	164.4	61	211	1.36	.78	90.6	87.2	94.8
159	02/21/73	SP-28	2	1.78	100.3	57	58	1.47	.82	81.2	77.0	83.2
160				1.69	98.6	58	58	1.55	.92	83.7	81.8	88.0
161				1.07	101.5	57	59	2.45	2.30	88.5	83.9	88.7
162				2.57	94.6	58	59	1.02	.40	81.3	83.0	89.9
163				1.69	103.1	58	59	1.54	.91	87.9	84.4	92.4
164			4	1.58	107.6	62	66	1.38	.87	92.2	87.7	95.6
165		4SP		1.83	106.4	60	62	1.19	.65	91.9	87.4	95.9
166				1.03	103.2	60	60	2.11	2.04	92.1	87.8	94.3
167		LSP-2		1.67	166.7	60	61	1.28	.77	93.7	90.2	97.6
168				1.38	182.9	59	61	1.58	1.13	93.4	89.1	95.6
169				1.53	175.9	60	60	1.40	.92	93.7	89.4	96.2
170												

TABLE II (cont.)

Test #	Date	Element	Chamber Length(in)	O/F	Pc	Tox(F)	T _f (F)	Velocity Ratio(F/O)	Momentum Ratio(F/O)	% C*	% Is	ERE	
171	02/21/73	X00	4	1.62	125.1	60	61	1.38	.85	85.3	79.4	86.8	
172				1.94	121.3	60	61	1.15	.59	85.8	79.1	87.0	
173				1.99	123.9	60	144	1.18	.59	84.8	77.5	85.3	
174				1.93	124.2	60	179	1.24	.64	84.9	77.7	85.5	
175		4SP	2	1.43	98.1	58	65	1.52	1.06	90.2	85.6	91.2	
176				1.71	100.7	59	70	1.28	.75	90.0	85.6	91.9	
177				.98	95.9	61	75	2.24	2.30	90.6	86.3	90.9	
178				1.50	171.1	63	76	.73	.49	92.1	87.9	93.1	
179		LSP-2		1.31	171.5	63	76	.84	.64	91.9	88.2	93.0	
180				1.74	167.6	63	76	.63	.36	92.8	87.1	92.9	
181				1.58	172.6	59	198	1.48	.94	91.8	86.9	94.1	
182				1.95	179.3	59	197	1.19	.61	92.1	84.9	93.6	
183		4SP	4	1.71	110.4	59	157	1.35	.78	92.9	87.5	95.7	
184				1.83	112.1	59	168	1.27	.70	93.1	86.4	95.0	
185				1.70	102.1	59	69	1.54	.91	88.2	85.2	92.9	
186				1.81	109.5	59	68	1.45	.80	88.9	83.8	91.7	
187		SP-28		1.43	107.1	59	65	1.83	1.28	90.2	85.2	92.2	
188				3.00	95.7	59	143	.92	.31	87.9	85.2	94.2	

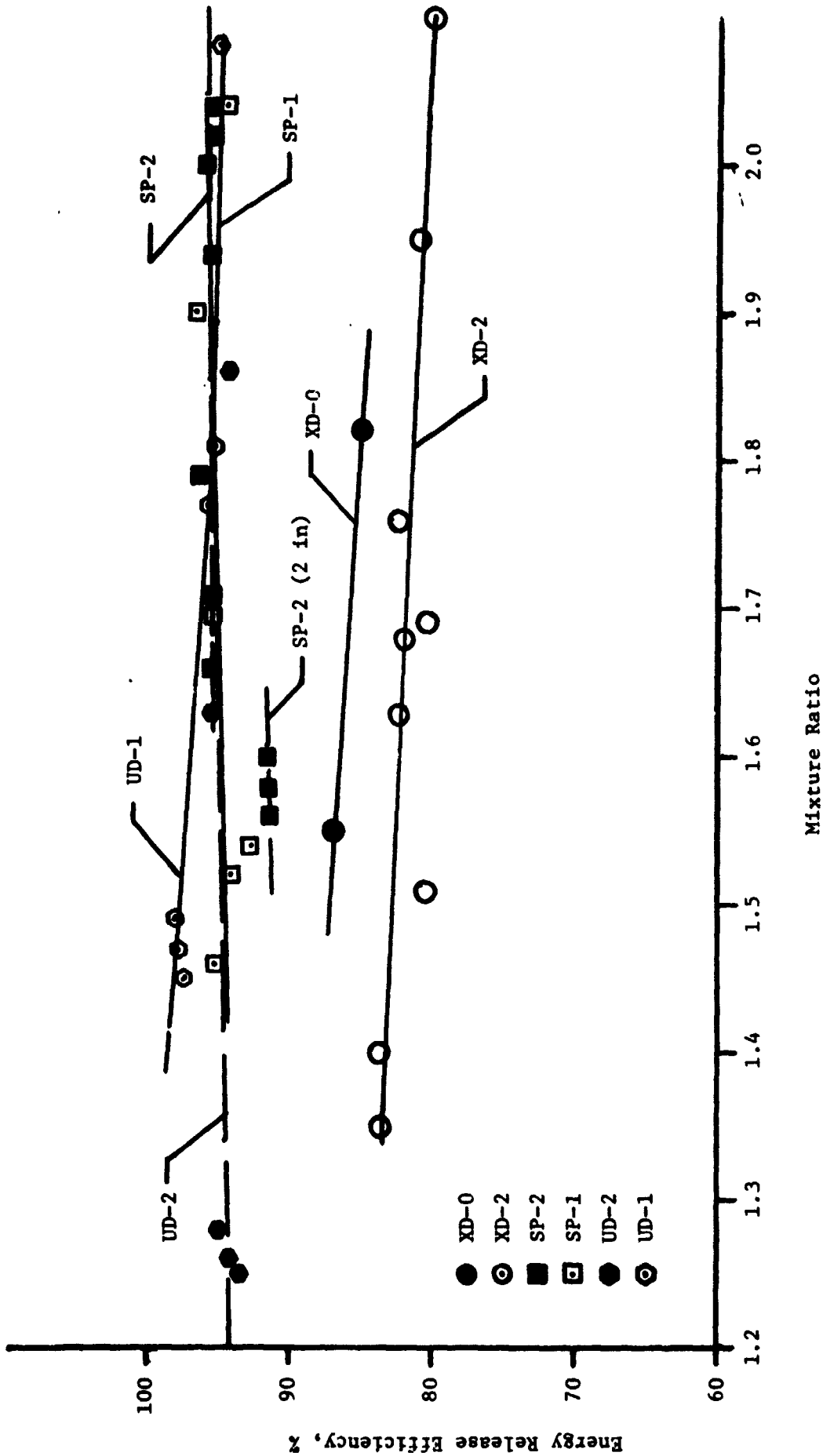


Figure 23. Energy Release Efficiency vs Mixture Ratio

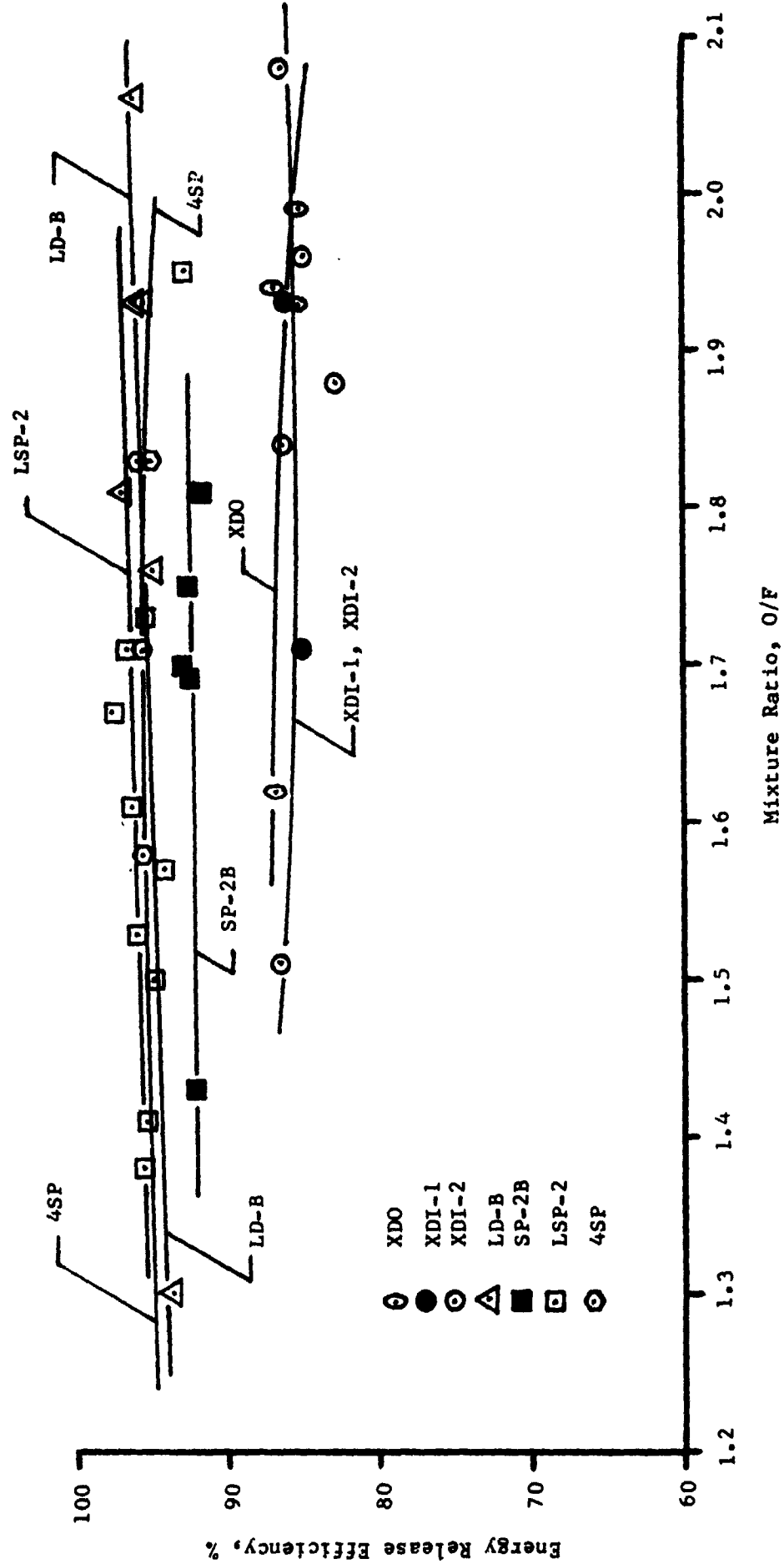


Figure 24. Energy Release Efficiency vs Mixture Ratio

VII,E, Hot Fire Tests (cont.)

doublet, and unlike-doublet configuration tend to be higher performing than the X-doublets. Figures 25 and 26 show ERE as a function of fuel temperature; typically, very little sensitivity to fuel temperature is evident. Likewise, little sensitivity to Rupe Number, velocity ratio or momentum ratio has been determined. Thus, in general, all of the elements appear suitable from the standpoint of insensitivity to operating point condition over the expected range of OMS applicability.

Both injector face temperatures and chamber gas-side wall temperatures were measured in the unielement testing. Figure 27 shows face temperatures as a function of mixture ratio, and Figure 28 as a function of fuel temperature, for the basic patterns tested. Two conclusions are readily apparent: (1) the face temperature is relatively insensitive to mixture ratio or fuel temperature; and (2) the splash plate operates at a much higher temperature than the other configurations. Typically, it registered 800 to 1000°F while the others were in the range of 200 to 400°F. It must be recognized, of course, that these figures are based on one or two thermocouple responses which may not be indicative of the entire face temperature.

Chamber gas-side wall temperatures were measured at six locations axially and circumferentially. Results for the X-doublet pattern are shown on Figure 29. Typically, the responses trend toward the propellant saturation temperatures in the section upstream of the throat, while in the throat they indicate the effects of combustion. The following figure, 30, gives a measure of the average heat flux and the circumferential non-uniformities associated with the basic patterns. In general, the unlike-doublet shows the highest flux in the throat while the X-doublet shows the greatest circumferential variation. These results imply that unlike-doublet and splash plate patterns will cause higher heat fluxes in the forward part of the full scale hardware than the X-doublet, but it is not correct to infer that the X-doublet will be more of a streaker under full scale conditions; such non-uniformities will be washed out in a multi-element environment.

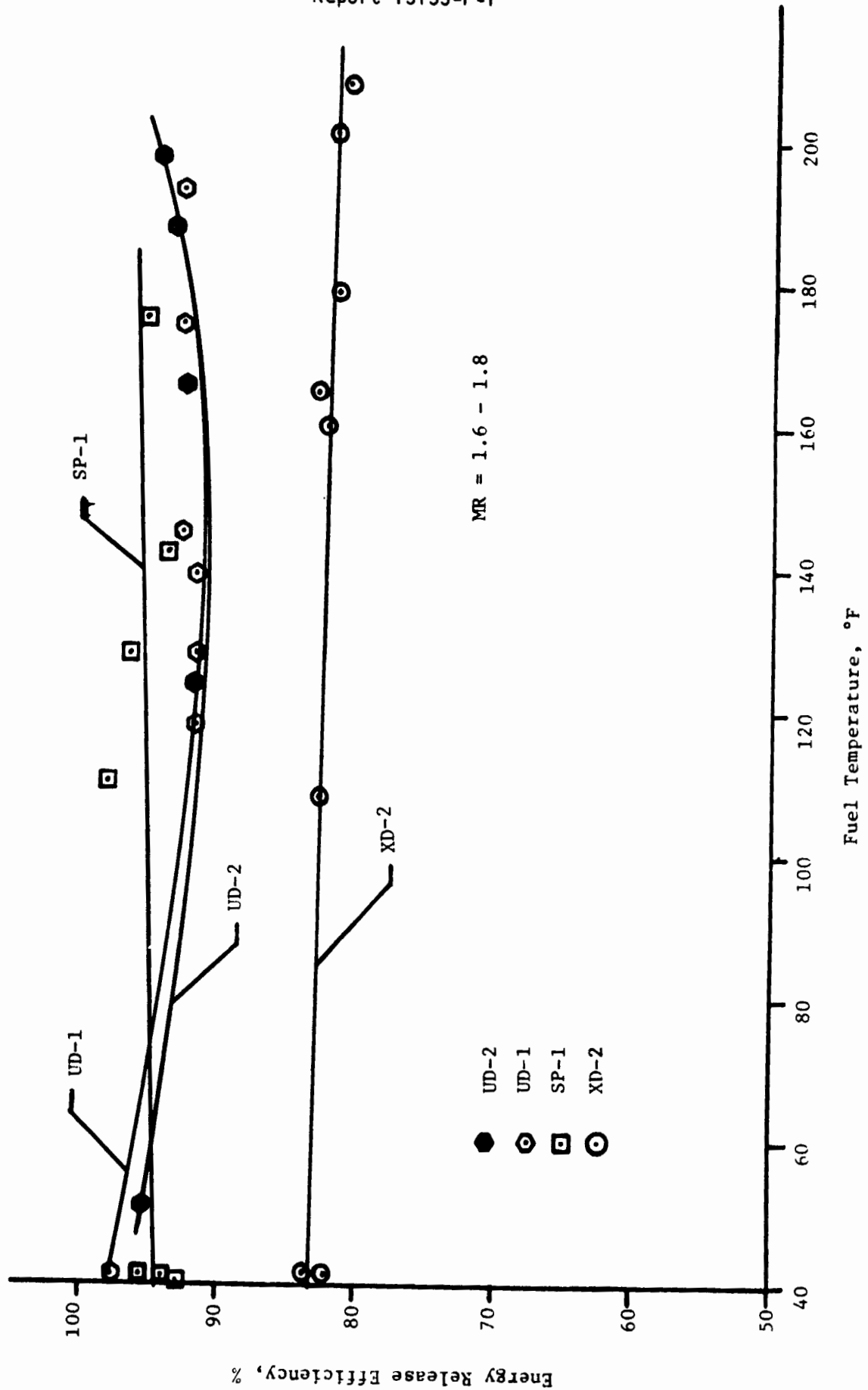


Figure 25. Energy Release Efficiency vs Fuel Temperature

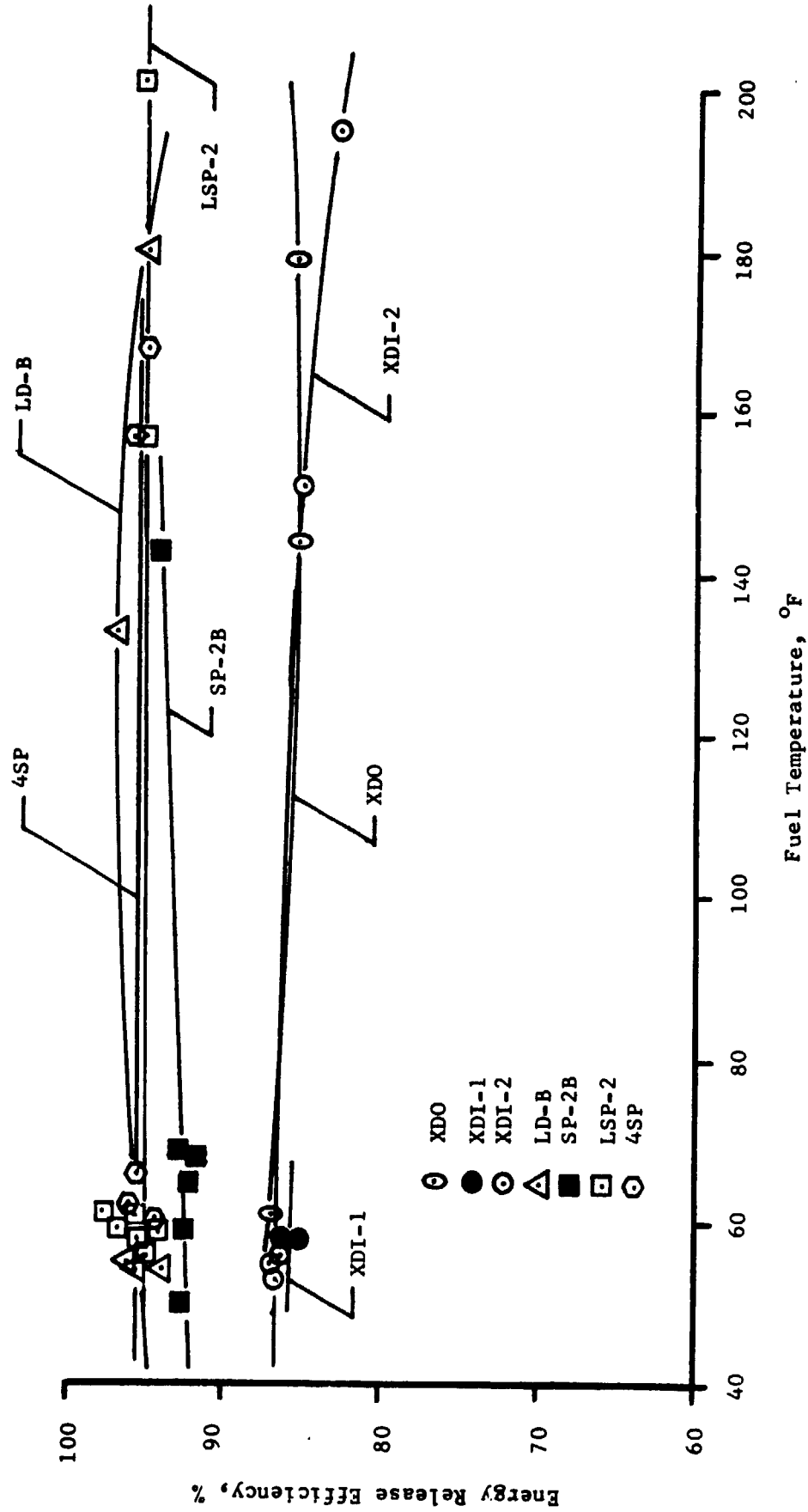


Figure 26. Energy Release Efficiency vs Fuel Temperature

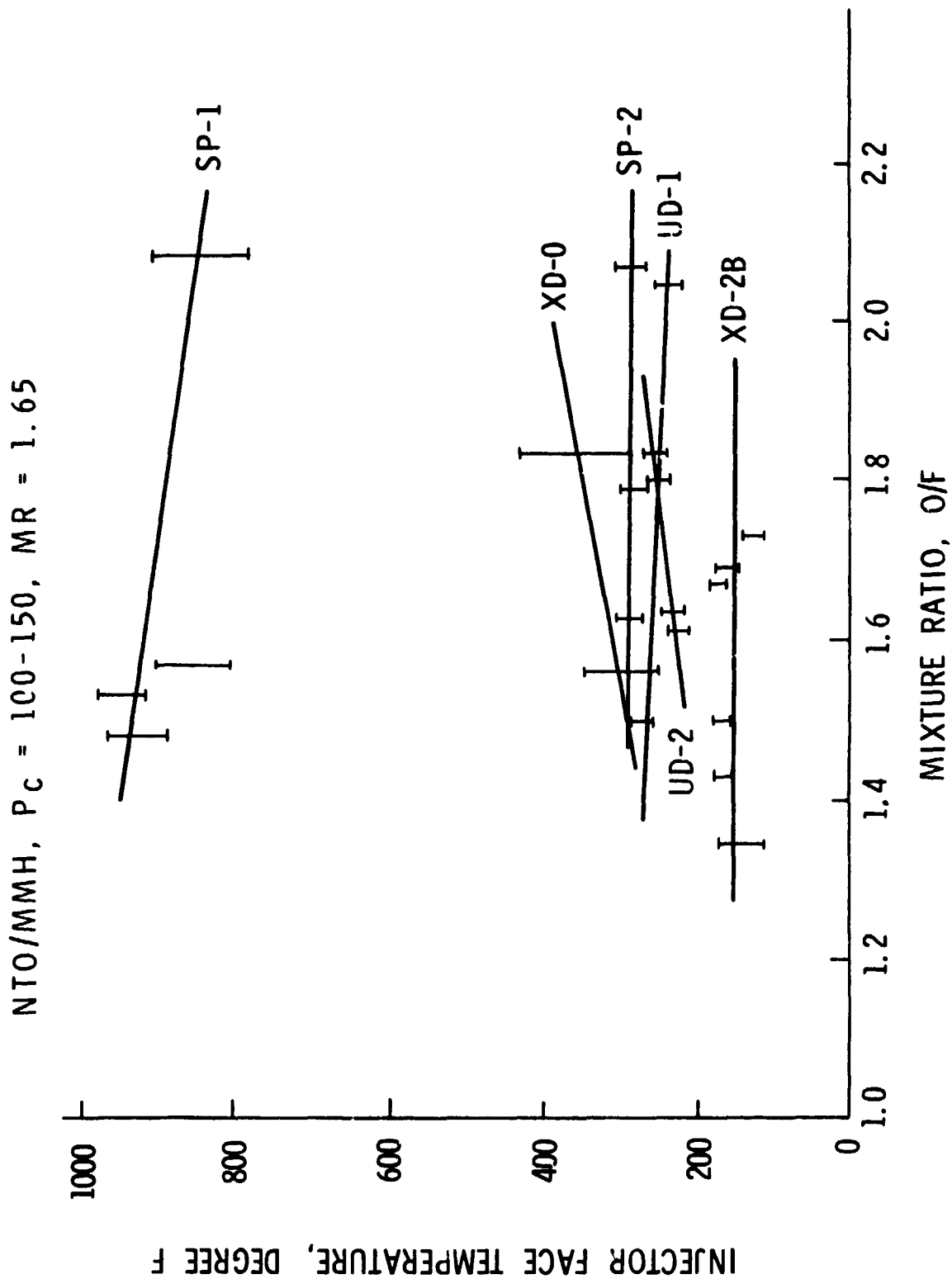


Figure 27. Unielement Face Temperature Characteristics

NTO/MMH, $P_c = 100-150$ PSIA, $MR = 1.65$

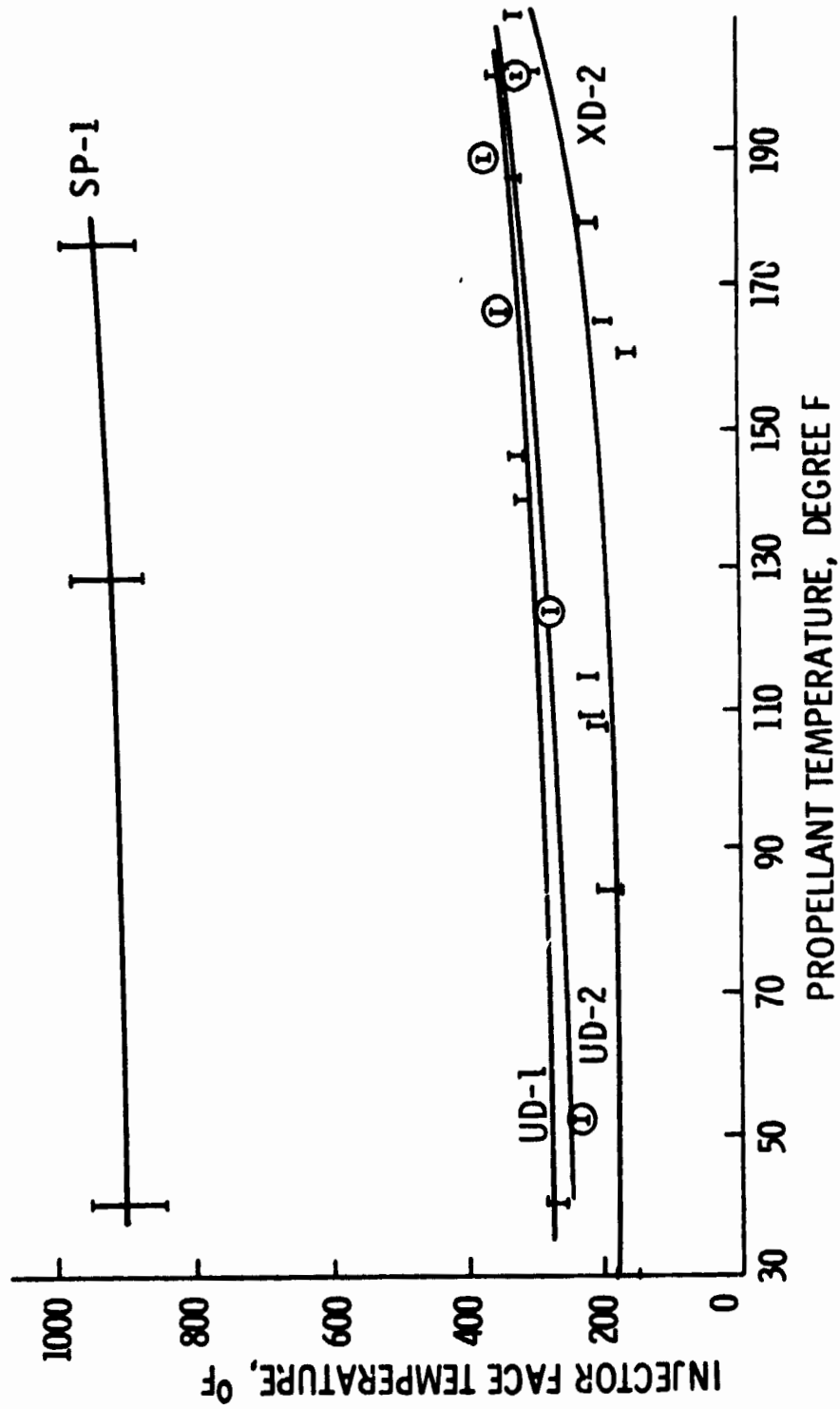


Figure 28. Uniement Face Temperature Characteristics

TYPICAL THERMAL DATA INJECTOR XD 2-B TEST 107

$P_c = 115$ PSIA, $MR = 1.66$

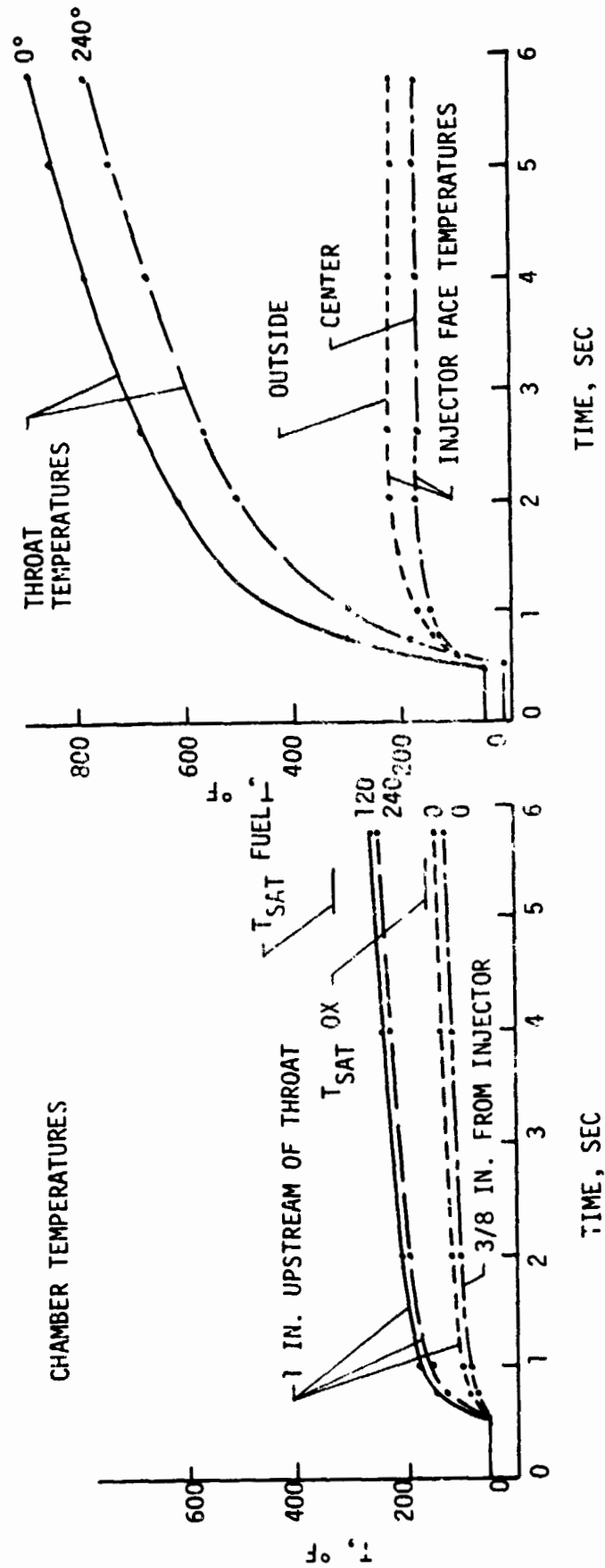
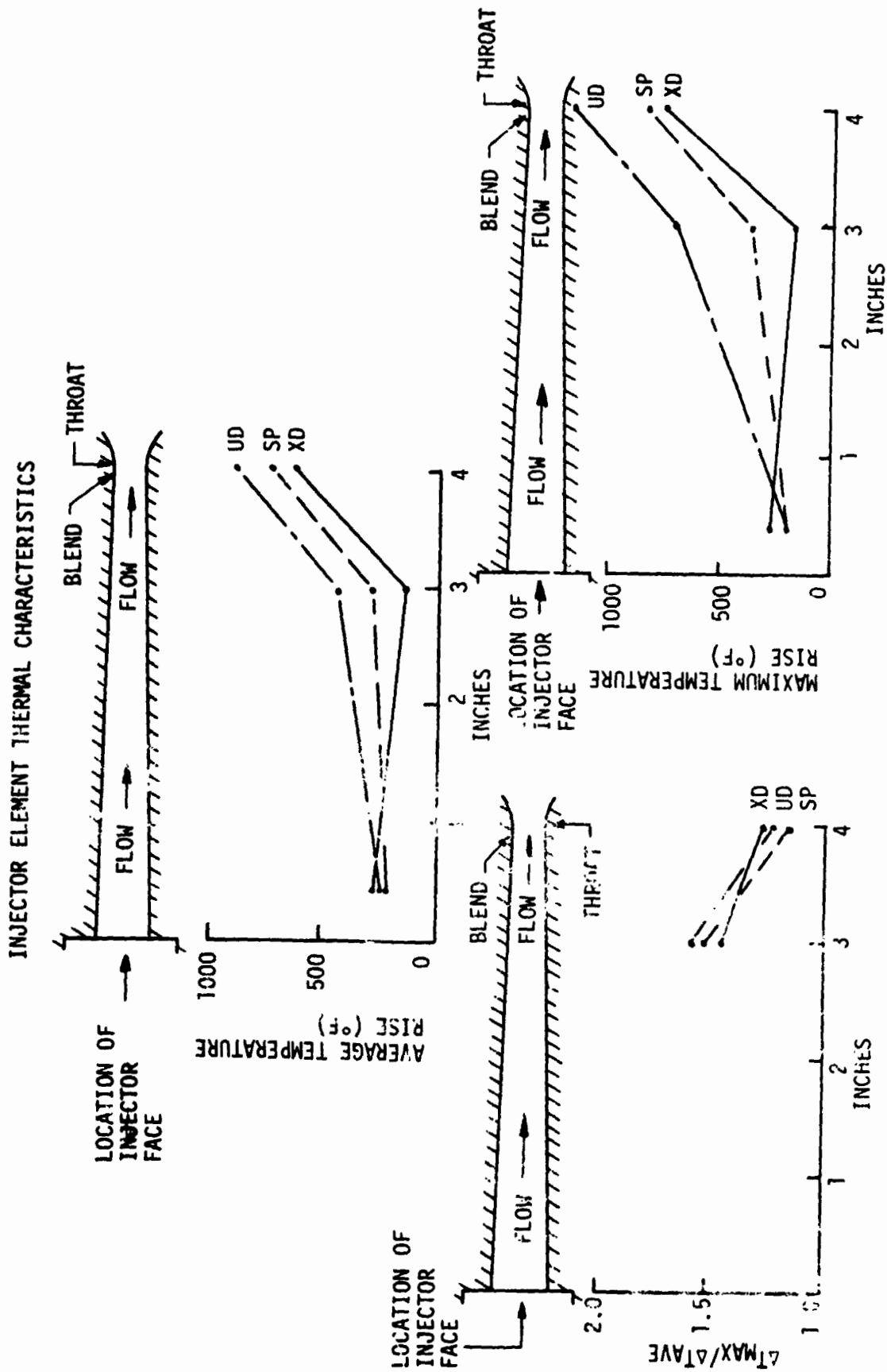


Figure 29. Urielement Hot Fire Testing



TEMPERATURES TAKEN AFTER 2.9 SEC OF FIRING

Figure 30. Unielement Hot Fire Testing

Report 13133-F-1

VII,E, Hot Fire Tests (cont.)

0
0
A special compatibility test was conducted to evaluate the SP spray-through characteristic. This test was accomplished by copper plating the chamber and hot testing to determine the portion of the chamber which was oxidized and reduced. The cold flow observation of spray-through was not verified.

Postfire examination of the unielements showed that all were reuseable except for the unlike-doublet, UD-2, which underwent some distortion of the oxidizer orifice during pulse testing; apparently, fuel dribbled into the orifice region between pulses and exploded to cause the damage. Also, the splash plate SP-1B showed two heat marks on either side of the element, confirming the high face temperatures that were measured.

F. CONCLUSIONS

As a result of the initial unielement testing, the splash plate pattern SP-2 was chosen as the primary candidate for subscale test evaluation. The bases for its selection were high performance, excellent compatibility, and insensitivity to operating point and propellant temperature. The X-doublet, XD-0, (later defined XDT, tangent fans) was chosen as a backup configuration, in part because of its excellent atomization and need for multi-element mixing to achieve desired level of performance. The unlike-doublets, although high performing, were not considered suitable; further development work to eliminate orifice distortion was considered necessary.

In general, the unielement test program met all of its objectives and proved to be an excellent method of screening candidate patterns. It provided a simple and inexpensive means of determining optimum orifice geometry and gave some indication of chamber wall compatibility as well.

ORIGINAL PAGE IS
OF POOR QUALITY

VIII. SUBSCALE PROGRAM

VIII. SUBSCALE PROGRAM

A. OBJECTIVE AND APPROACH

The subscale program was identified as Task II of the program and initiated to evaluate the various platelet element arrays available from the uni-element program. The injector size was chosen such that the first tangential frequency duplicated the single pocket mode of a full scale five bladed baffle OMS injector. The thrust magnitude had to be sufficiently large to allow accurate extrapolation of performance and heat transfer data. The resulting thrust was selected at 600 lb_f. The basic approach was to design the injector manifolding and ring channels to be identical to the central portion of the full scale unit. The injector body also had the requirement of possessing adequate structural integrity to permit bonding of the injector face on a completed injector manifold. This potential rework feature would permit several injector patterns to be evaluated using a minimum of injector bodies.

The program consisted of four parts: design analysis, cold flow investigations, hot test evaluation and cycle life demonstration. Each of these activities are described in the following sections.

The program was initiated in December 1972 and completed in September of 1973.

B. DESIGN

1. Design Point

The subscale hardware was designed per the design point specification shown in Table III. The thrust level was chosen consistent with a size which would acoustically simulate the five bladed baffled pocket mode of a full scale design. Mixture ratio was identical to full scale at 1.65. The necessary film coolant fraction was predicted at 12% of the fuel, thus shifting the core mixture ratio to 1.875. Flow rate was established consistent with a

Report 13133-F-1

TABLE III
SUBSCALE DESIGN POINT
OME PLATELET INJECTOR DESIGN POINT

P_c	= 125 psia
$MR_{O/A}$	= 1.65
FFC	= 12%
MR_{core}	= 1.875
I_s	= 315 sec

Injector	<u>SP-2</u>	<u>XD-0</u>	<u>XDI</u>
F/E	5.609	6.889	6.889
w_o	0.011625	0.01425	0.01425
w_f	0.0062	0.0076	0.0076
C_{D_o}	0.77	0.655	0.655
C_{D_f}	0.59	0.700	0.700
ΔP_o	30.3	35.0	35.0
ΔP_f	30.0	30.0	30.0
Oxidizer orifice, in.	0.024	0.024 x 0.024	0.024 x 0.024
Fuel orifice, in.	0.020	0.020 x 0.020	0.020 x 0.020
Number @ 600 lb	107	87	97
Number @ 6000 lb	1070	870	870

VIII,B, Design (cont.)

315 second vacuum specific impulse prediction for OMS. The injector pressure drop was chosen at 35 psid maximum with a goal of 30 psid if a satisfactory element array could be obtained. The thruster design summary is given in Table IV.

2. Pattern Design

Using the results of the spray and mixing tests from the uni-element program, Section VII, the subscale patterns were formulated.

The resulting patterns are shown in Figures 31, 32, and 33 for the splash plate, X-doublet and unlike-doublet designs. All patterns utilize a cant angle (element center line rotated off a radial line from the injector center) which maximizes the spray overlap and maintains a reducing atmosphere along the chamber wall. The optimum angles were 25 degrees for the splash plate, 30 for the X-doublet and 45 for the unlike-doublet. All designs were presented for NASA approval with the splash plate (SP) and the X-doublet (XD) designs accepted for fabrication. The selected versions of the designs were XD with tangential fans (XDT), with inline fans (XDI), a normal splash plate (SP1) and relieved splash plate (SP2). In addition, two other pattern designs were selected. The XDT2 pattern was produced to evaluate interelement mixing and the effect of the modified cant angle on wall compatibility. The last pattern, a mixed element (ME 1), was produced by merging the very compatible XDI elements with the higher performing splash plate (SP2) design to evaluate if the attractive benefits of each element could be realized with a 60/40 mixture, i.e., 60% X-doublet and 40% splash plate elements. This combination design was accomplished by a simple merging of portions of each artwork.

3. Injector Design

A six channel concentric ring injector manifold design with a single inlet for each circuit was produced as shown in Figure 34. Land widths

Report 13133-F-1

TABLE IV

OME PLATELET INJECTOR
SUBSCALE THRUSTER
DESIGN SUMMARY

Thrust (vacuum), lbf	600
Chamber pressure, psia	125
Oxidizer	N ₂ O ₄
Fuel	MMH
Area ratio (vacuum)	40
Area ratio (sea level)	2.0
Nozzle	15° cone
Contraction ratio	2.05
Chamber length, in.	4.0
Mixture ratio	1.65
Throat area, in. ²	2.78
Chamber diameter, in.	2.70
Throat diameter, in.	1.882
Oxidizer flow, lbm/sec	1.245
Fuel flow, lbm/sec	0.755
Oxidizer pressure drop, psid	35
Fuel pressure drop, psid	35
Injector elements, number	99: X-Doublet 124: Splash Plate 78: Unlike Doublet
Acoustic cavities	
Partitions	12
Width, in.	0.150
Depth, in.	0.600
L* section length, in.	3.0
Film coolant ring	
Weight flow (30%), lbm/sec	0.226
Orifice Diameter, in.	0.024
Chamber	
Bomb port, grains	2.0
Photocon high frequency	307

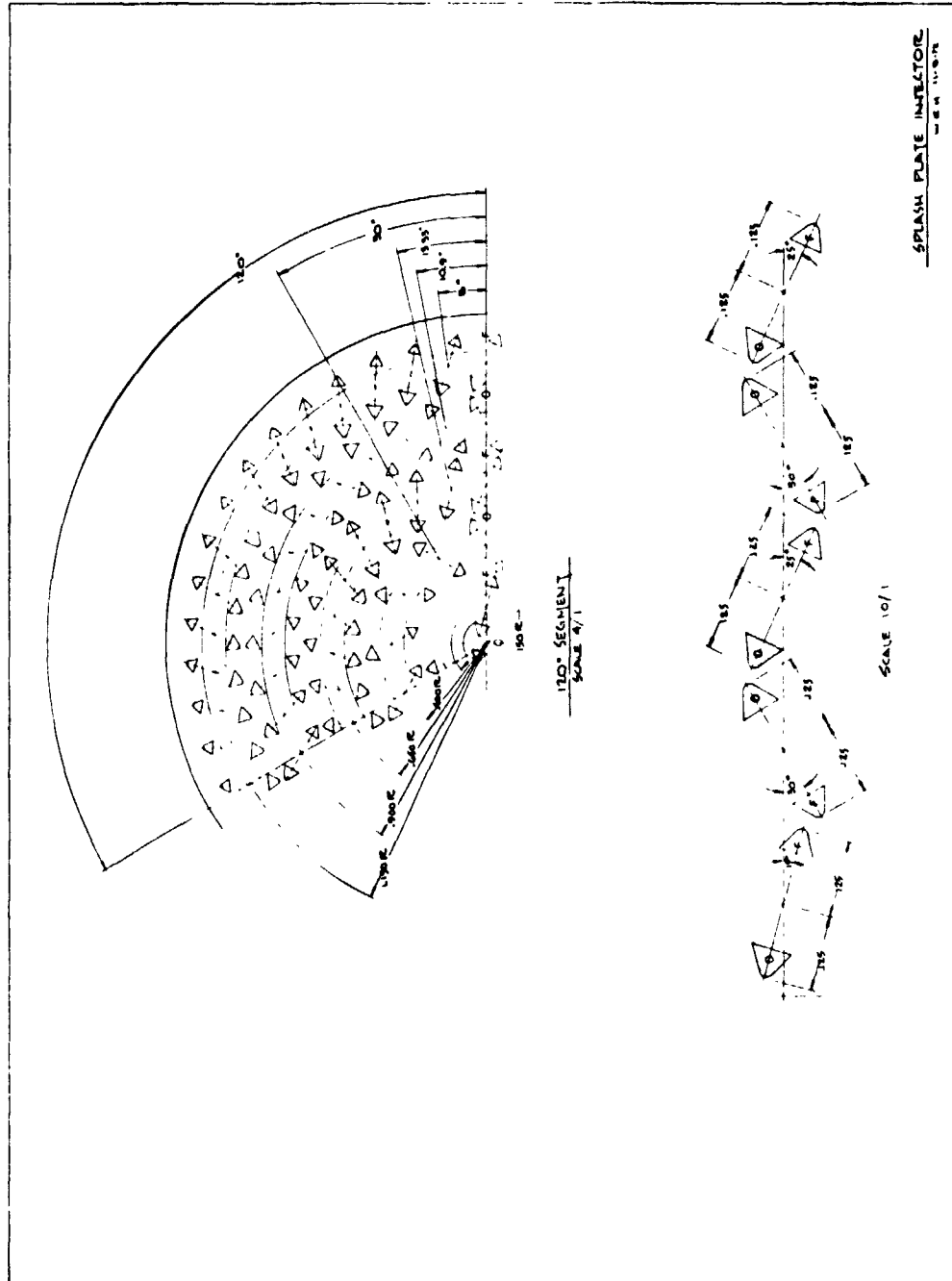


Figure 31. Preliminary Subscale Layout - Splash Plate

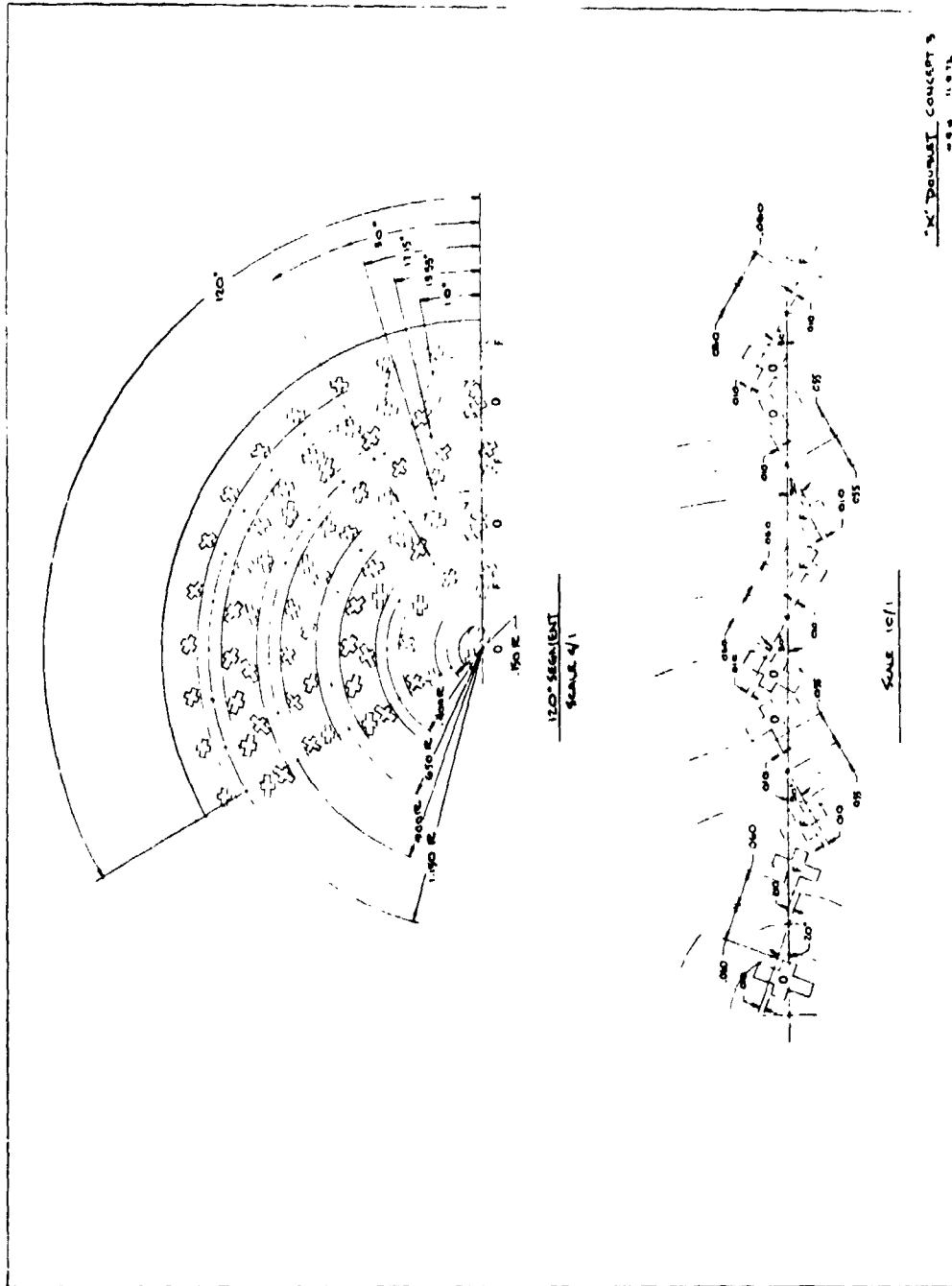


Figure 32. Preliminary Subscale Layout - X-Doublet

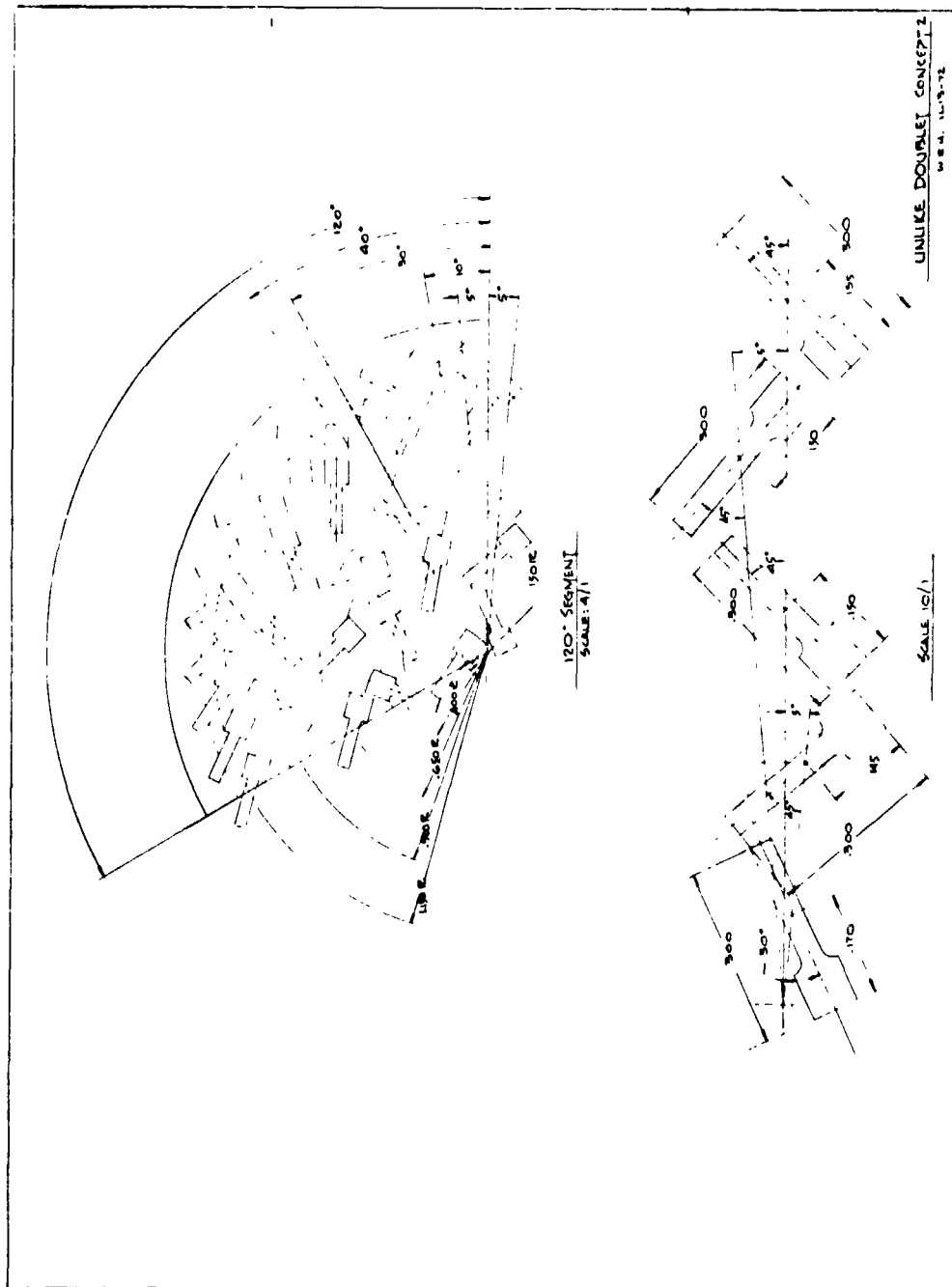


Figure 33. Preliminary Subscale Layout - Unlike Doublet

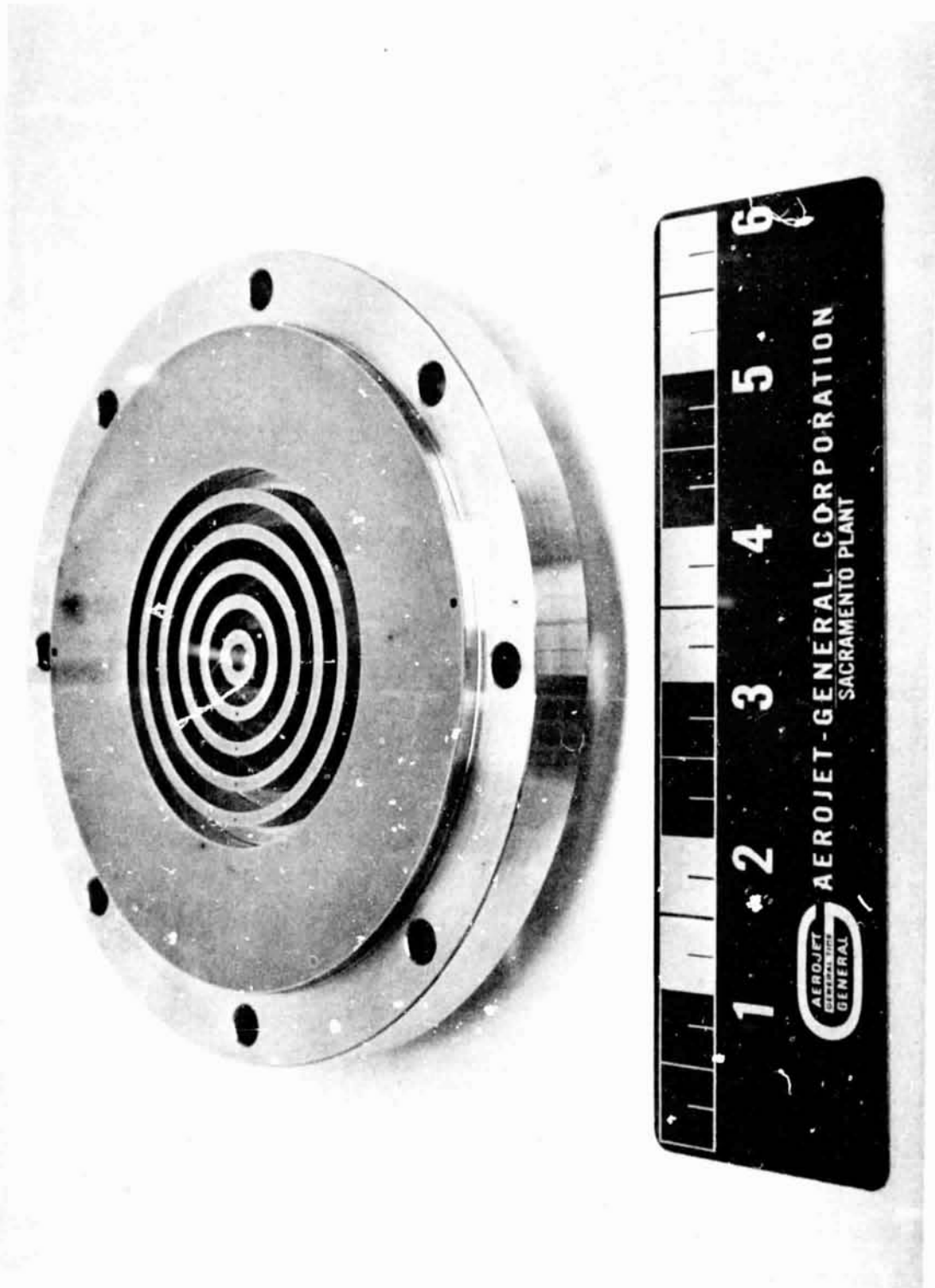


Figure 34. Subscale Injector Manifold

VIII,B, Design (cont.)

between propellant channels were established at .1 in. and the fluid passages .150 in. width. Channel depths were consistent with 15 fps channel velocity and constant over the entire circumference. The channels were eclipsed by a single circular inlet manifold with low velocity drop-through slots. The channels did not provide acoustic ring dams. The body was completely manufactured from 304L stainless steel and was machined using electrical discharge machining (EDM) processes. Manifold face covers were welded using electron beam techniques.

The platelet injector face assembly consisted of five photo-etched plates which developed the particular injector face pattern. Two alignment tabs on four positioning tabs were included to insure proper plate-to-plate and face-to-manifold orientation. All platelets were made of 304L material and diffusion bonded as an assembly. The face assembly was then bonded to the manifold on a separate run. The assembly following bonding is shown in Figure 35. Provisions for four face thermocouples were also included. The SP and XD injector faces are shown in Figures 36 and 37.

4. Thruster Design

An exploded view of the complete subscale assembly is shown in Figure 38. Shown from left to right are the injector, resonator ring, L* section and chamber.

The acoustic cavity consisted of a .150 in. width annular slot, .6 in. deep, located next to the injector face. The annulus was sectioned by 12 radial partitions. The acoustic cavity was sized to be 22% of the injector face area. This part, which sandwiches between the injector and chamber, is shown in Figure 39. Provisions were made in the injector body to record high frequency pressure responses in one cavity compartment with a Kistler 601A transducer. Provisions for cavity temperature measurements were also included.

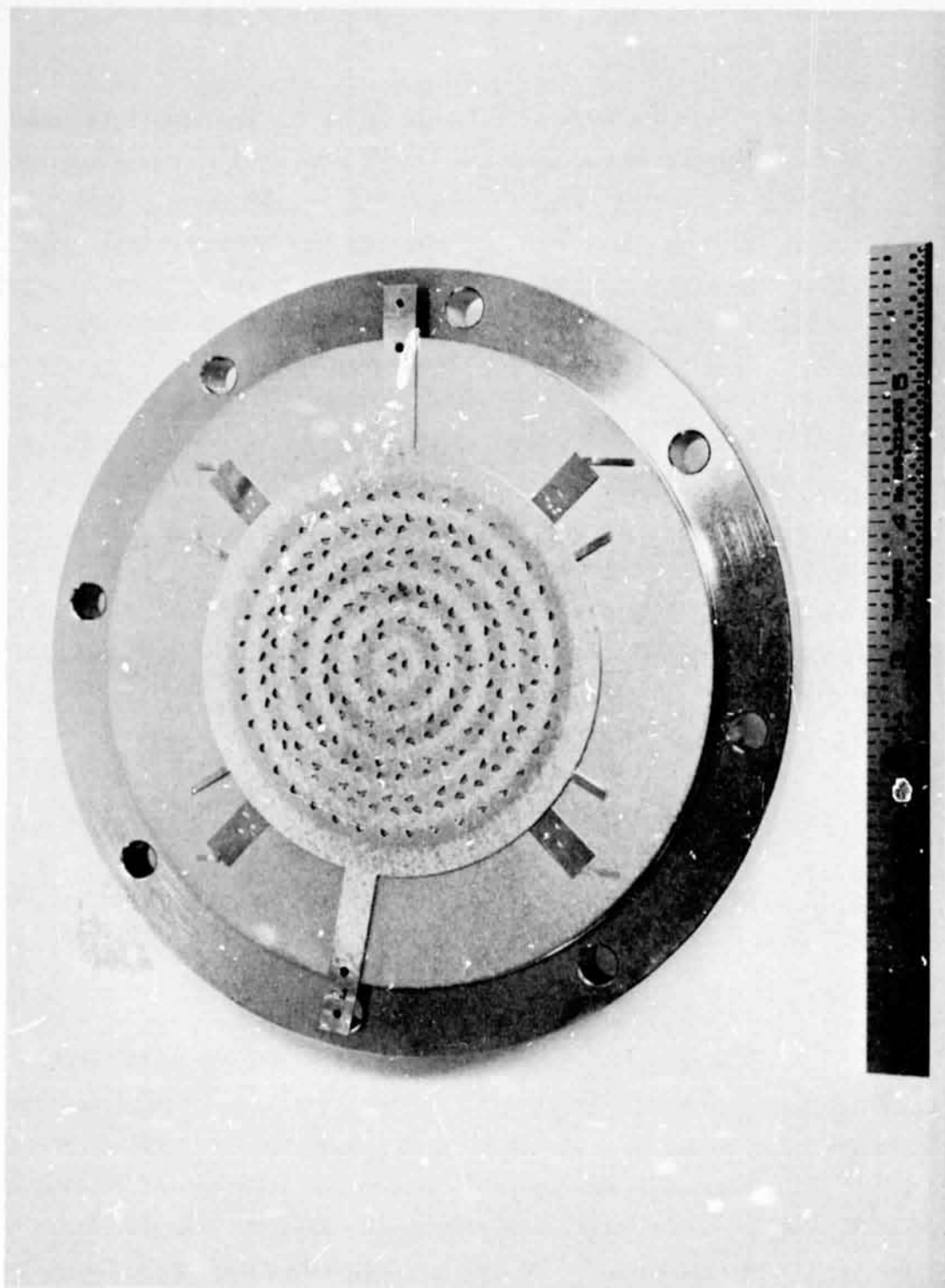


Figure 35. Subscale Splash Plate Injector

ORIGINAL PAGE IS
OF POOR QUALITY

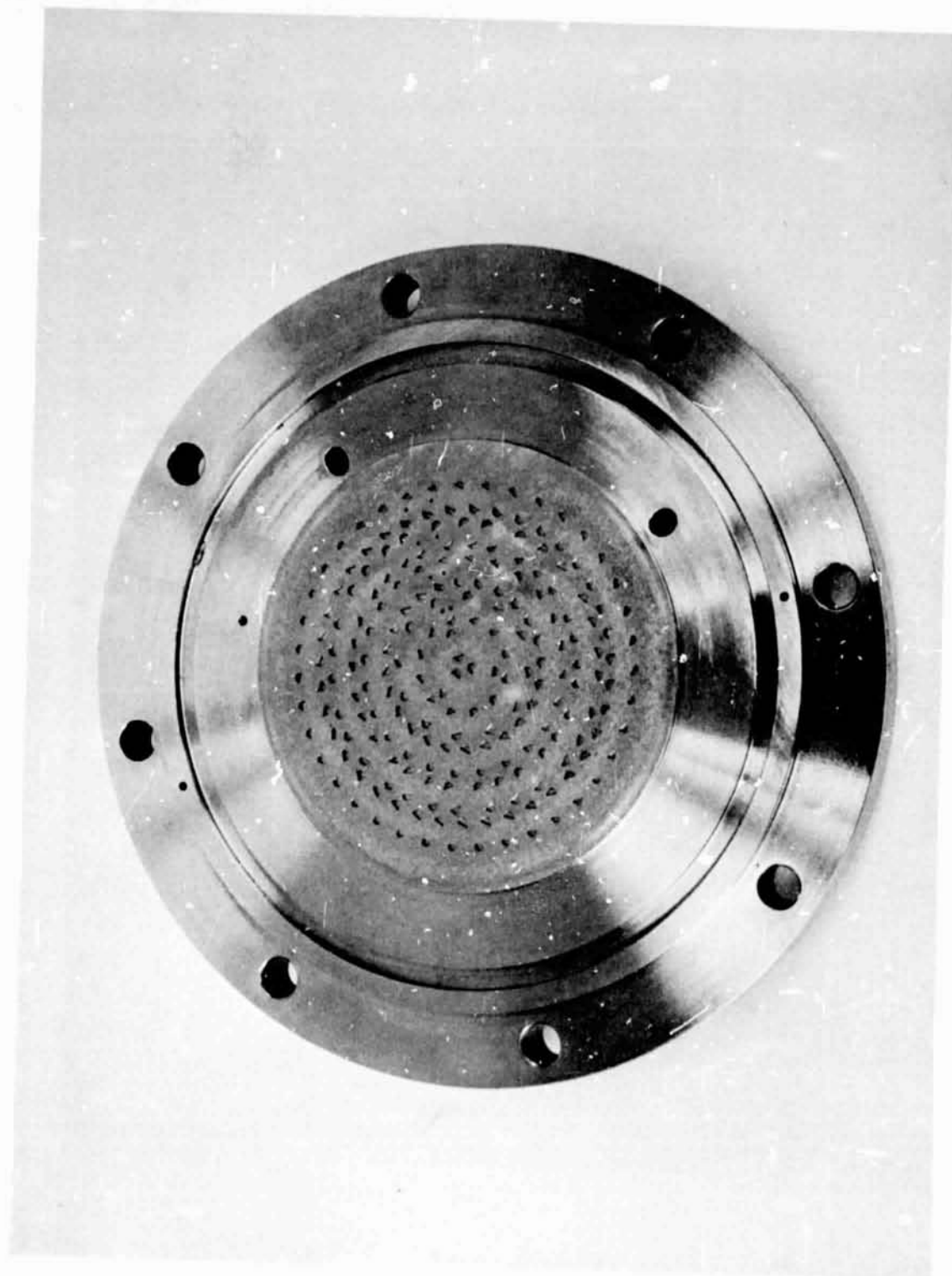


Figure 36. Subscale Splash Plate Injector

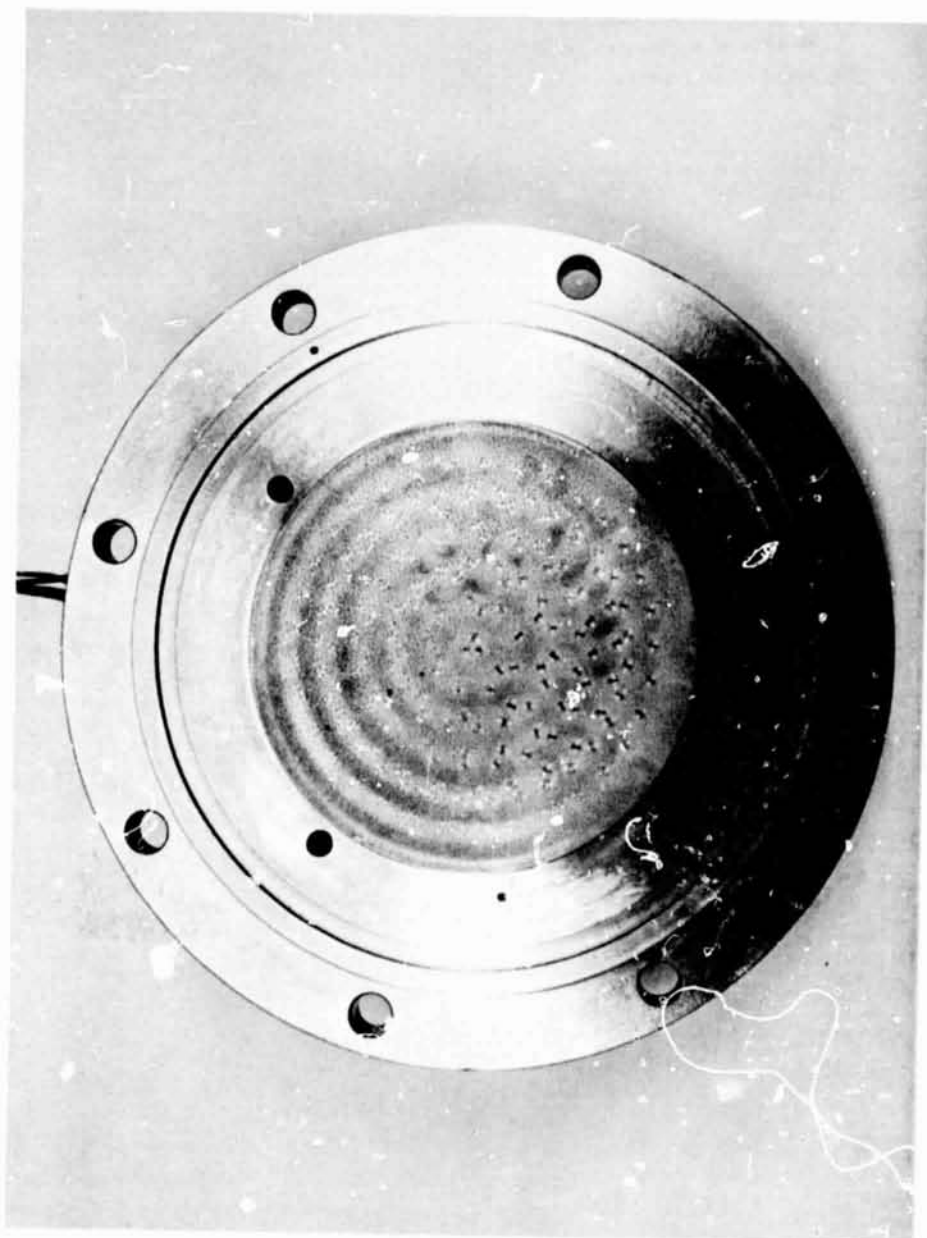


Figure 37. X-Doublet Injector

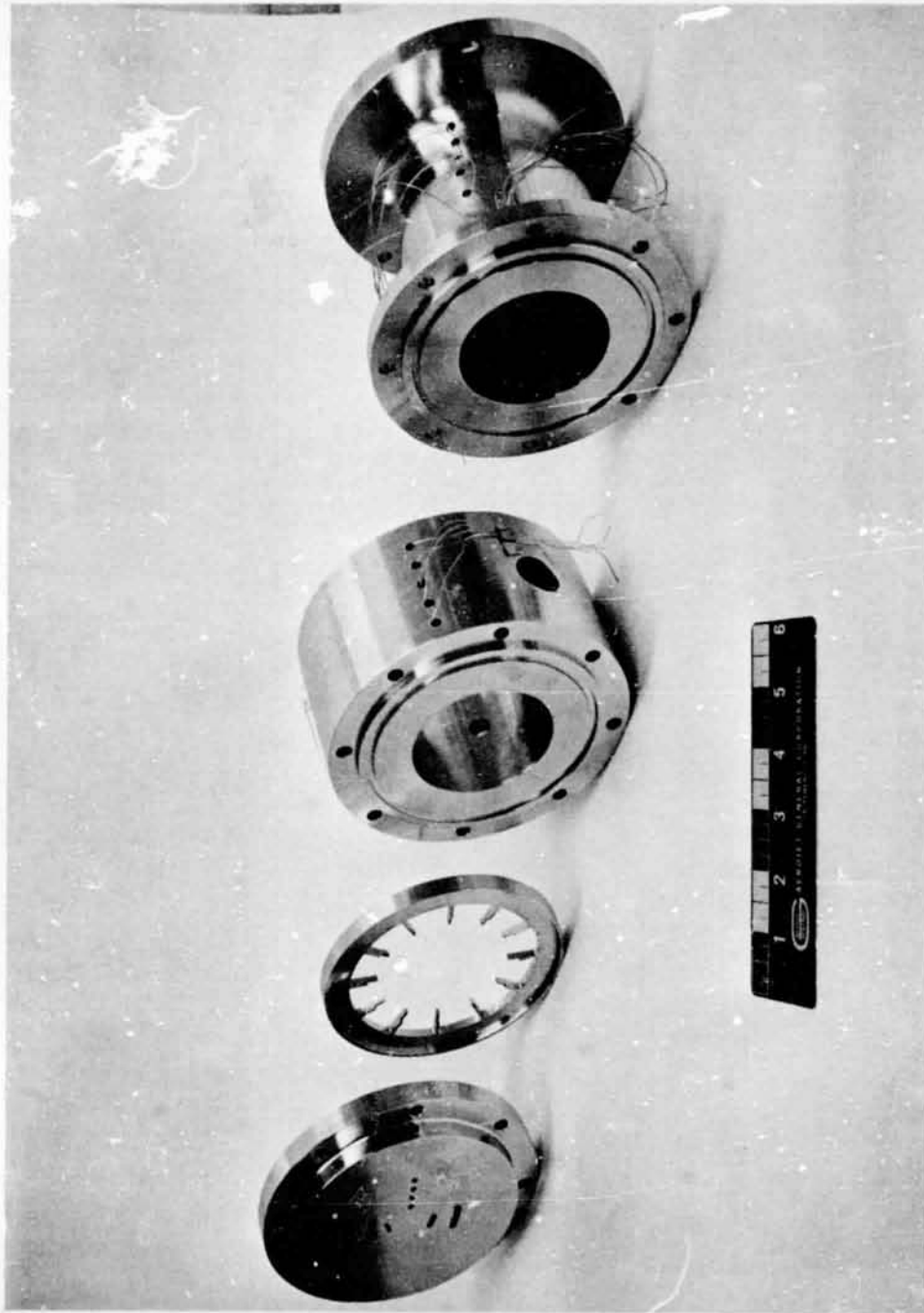


Figure 38. Subscale Hardware Components

C-2

ORIGINAL PAGE IS
OF POOR QUALITY

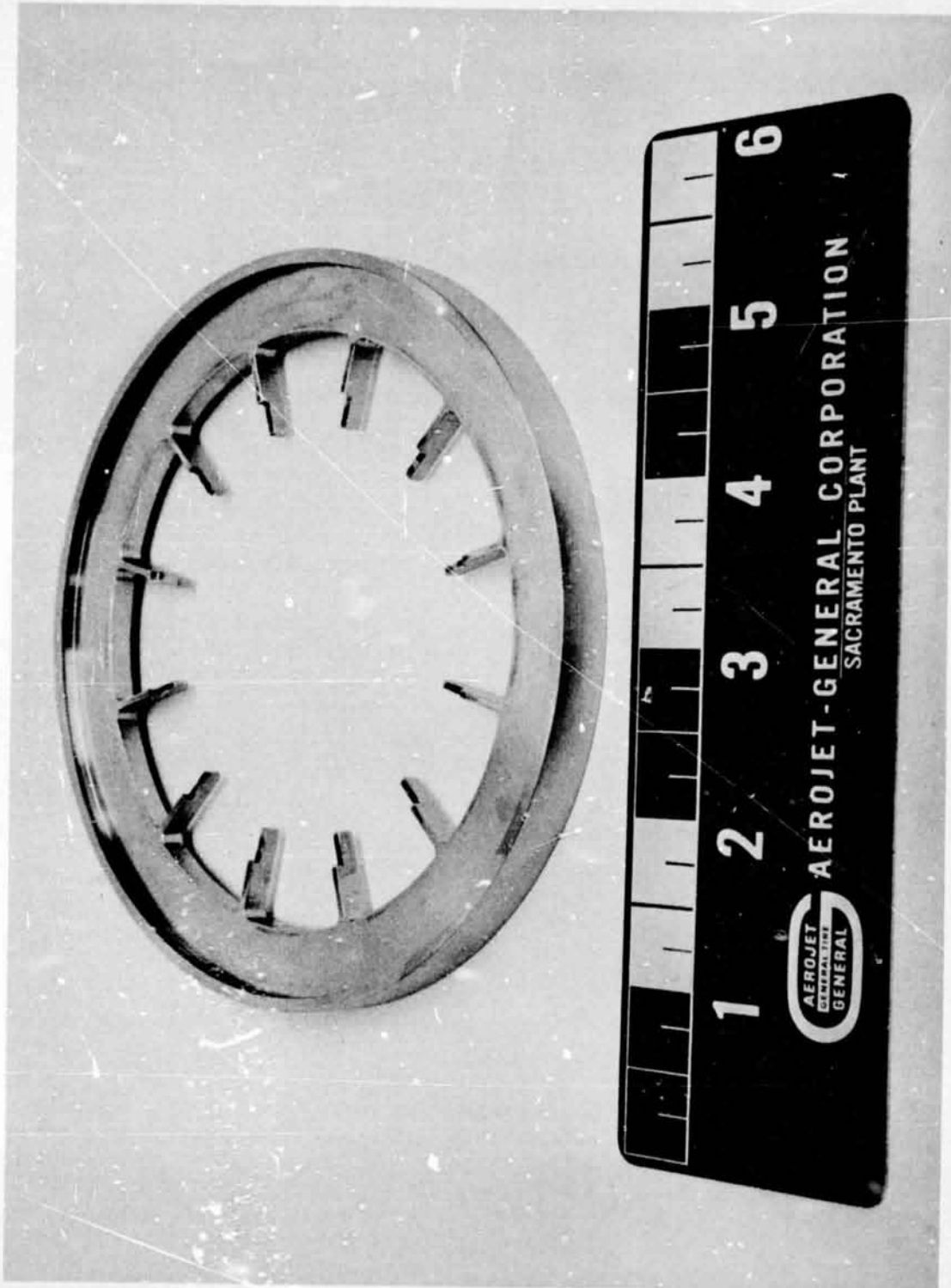


Figure 39. Subscale Resonator Ring

VIII,B, Design (cont.)

The combustion chamber was 4 in. in length and flanged at both ends as shown in Figure 40. The aft flange enabled a pressure test plate to be installed for system leak checks. Two axial rows of thermocouples were included to determine wall heat fluxes. These thermocouples were mounted flush with the inner wall and brazed in place. Also included were two 1/4 in. AN low frequency pressure ports for chamber wall pressure measurements.

A heavy-weight L* section of 3 in. axial length was also fabricated and is pictured in Figure 41. Two axial rows of thermocouples were included together with two photocon 307 high frequency transducer ports. A 2.0 grain bomb port was located in the L* section.

The film coolant ring, Figure 42, could be installed between the resonator and L* section. Up to 30% of the fuel flow was injected through this ring of thirty-six 0.024 orifices. Each orifice was tangentially directed to produce a swirl spray to improve coverage. The ring was fed separately from a special valved supply.

C. COLD FLOW

All subscale hardware was fully characterized with cold flow evaluations. Initially, each injector was water-flowed for visual pattern check.

Following spray evaluations, each injector and the film coolant ring were hydraulically characterized over a range of water flow rates to calibrate the pressure drop of the entire assembly. Mixing evaluation of the splash plate and X-doublet injectors were performed using the Advanced Injector Distribution (AID) cold flow apparatus. This unit collects the injector effluent from immiscible simulants flowing into a 728 tube collector head. The mixture ratio profiles of both injectors as determined from this flow data are shown in Figures 43 and 44.

ORIGINAL PAGE IS
OF POOR QUALITY

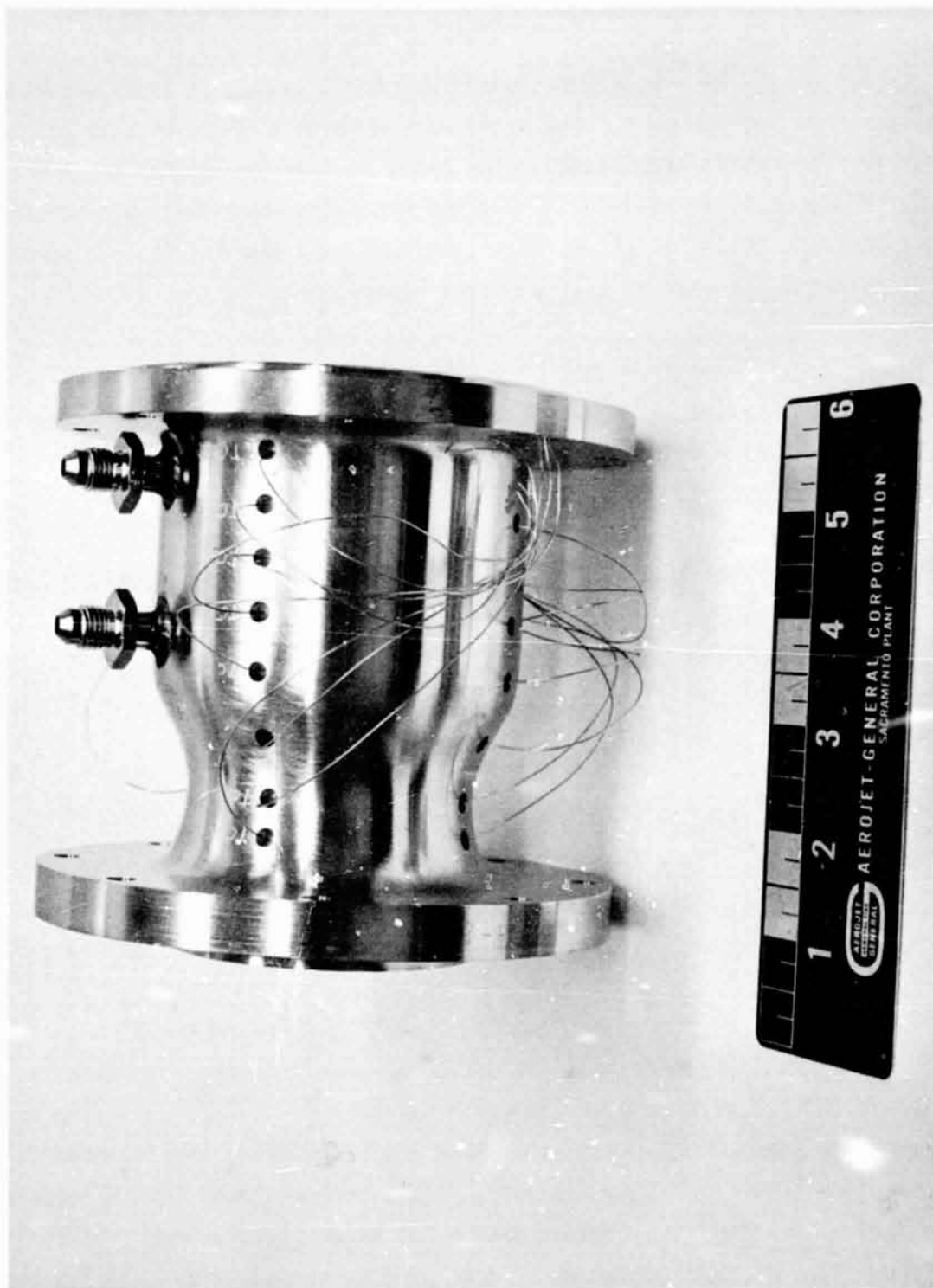


Figure 40. Subscale Chamber (4.0 in.)

ORIGINAL PAGE IS
OF POOR QUALITY

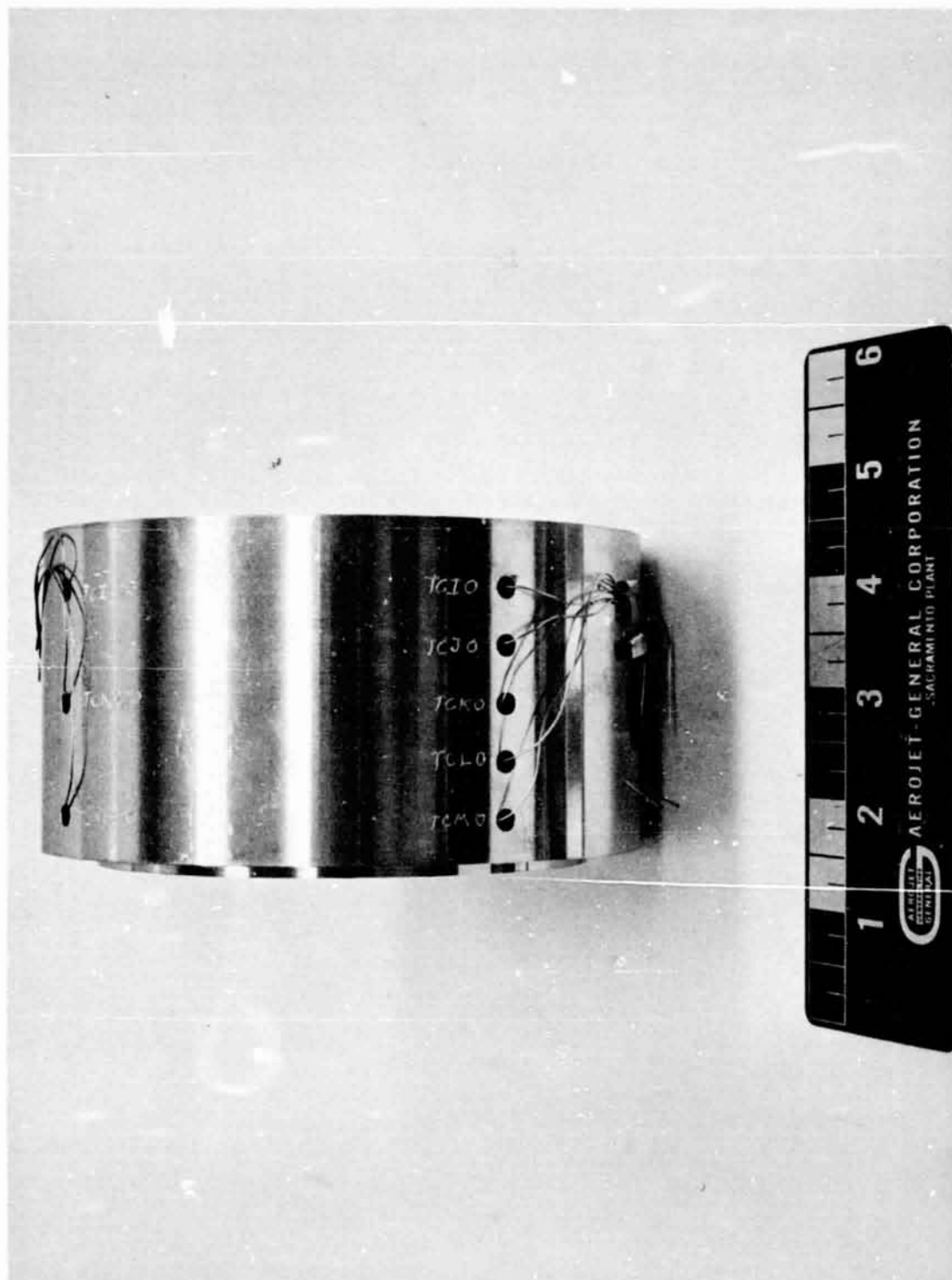


Figure 41. Subscale L* Section (3.0 in.)

ORIGINAL PAGE IS
OF POOR QUALITY

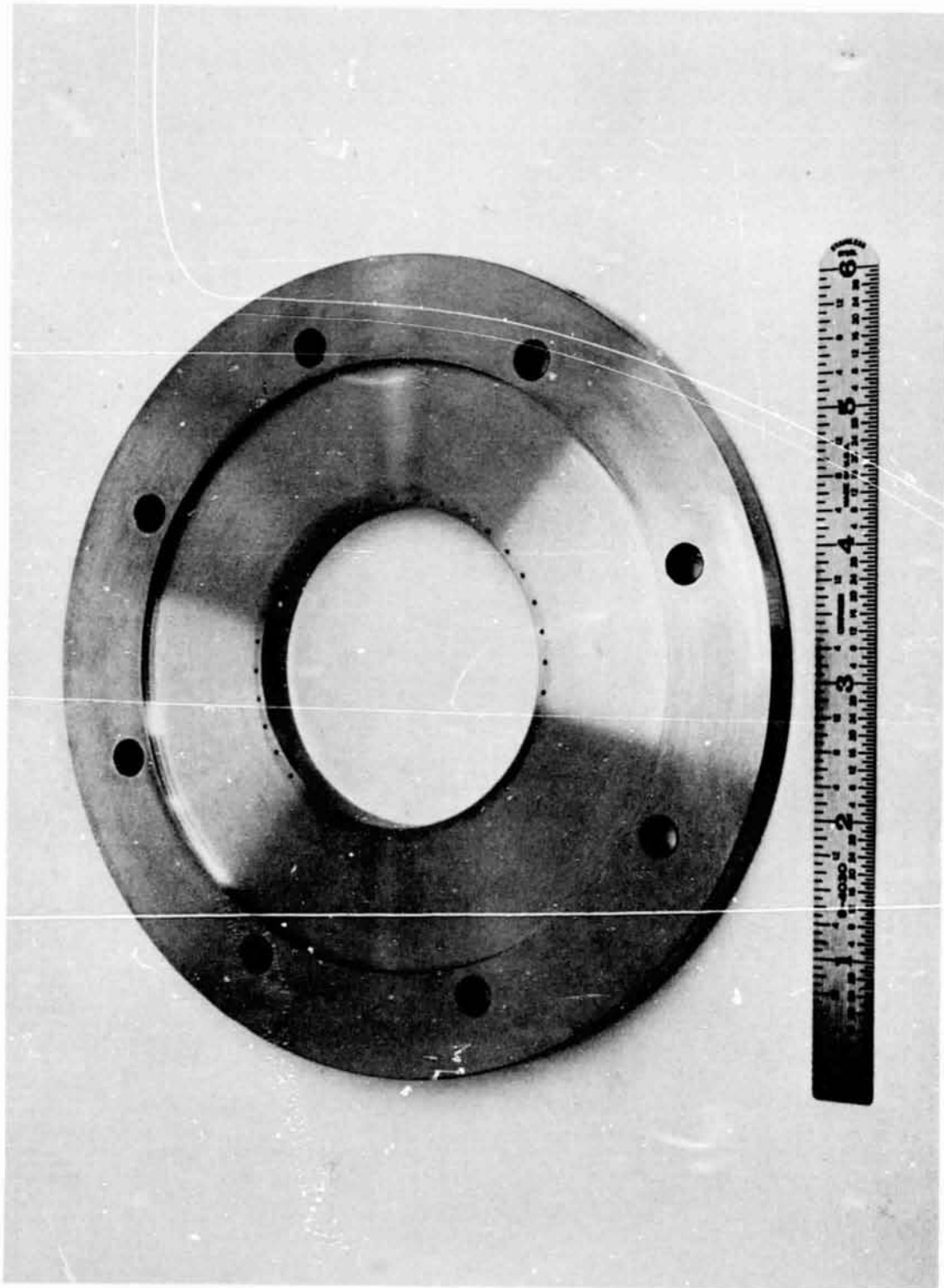


Figure 42. Subscale Film Coolant Ring

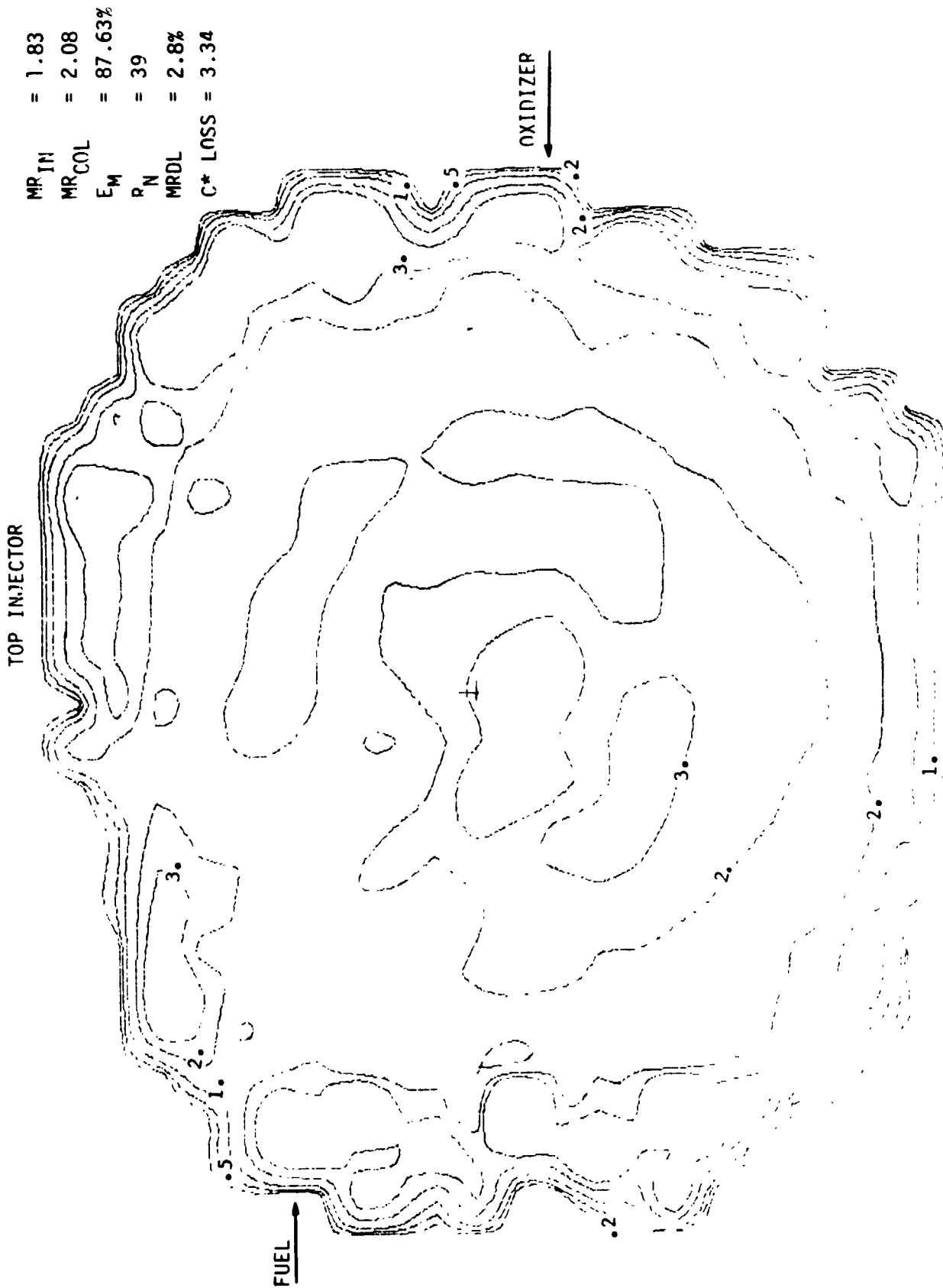


Figure 43. Subscale Splash Plate Mixture Ratio Distribution

$MR_{IN} = 1.83$
 $MR_{COL} = 1.81$
 $E_M = 63.15\%$
 $R_N = 0.46$
 $MRDL = 16.7\%$
 $C^* LOSS = 18.5\%$

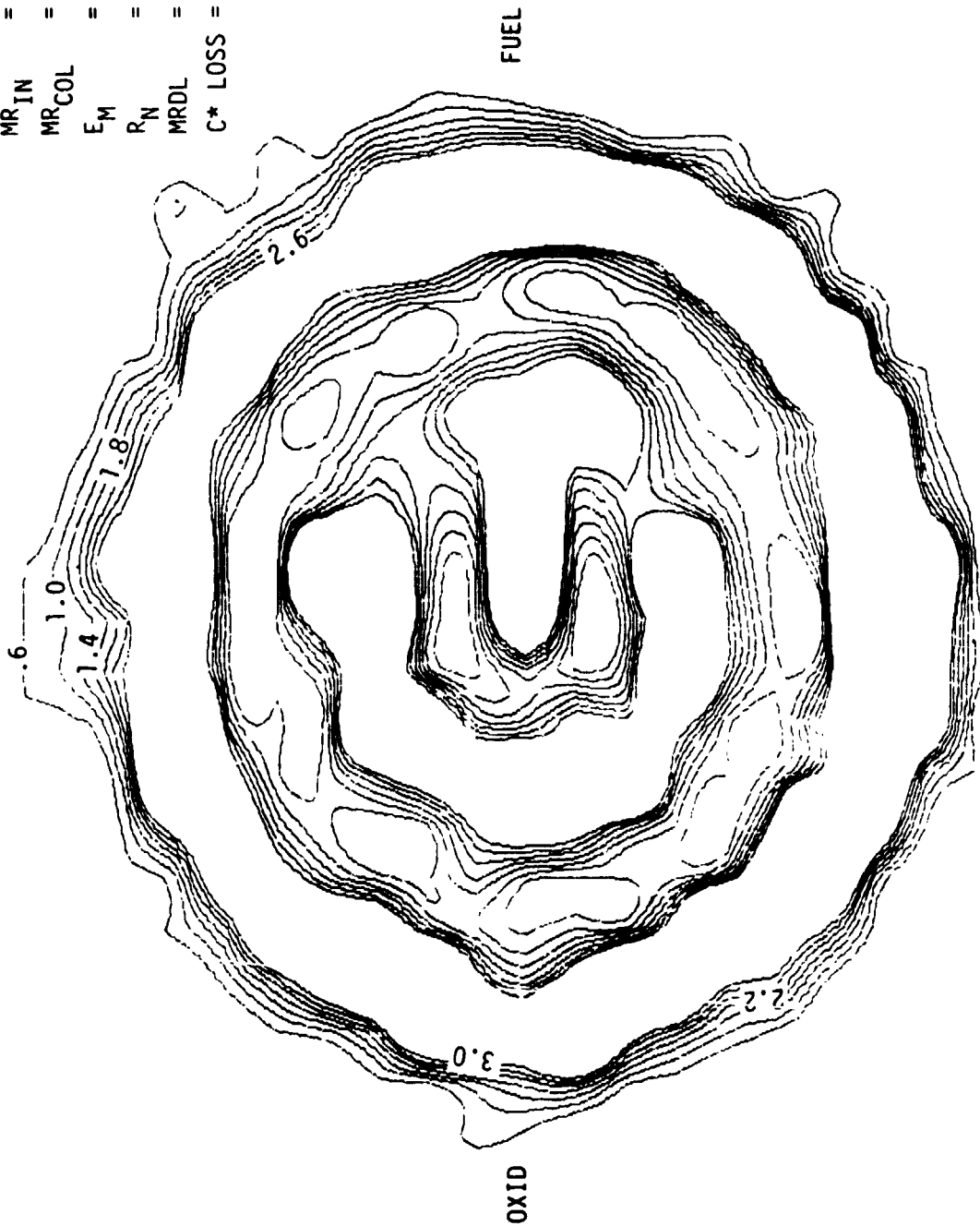


Figure 44. Subscale X-Doublet Mixture Ratio Distribution

VIII,C, Cold Flow (cont.)

The XDT mixing data show an overriding influence of the injector ring channels. This is undesirable from a mixing efficiency point of view, giving a calculated mixing efficiency of only 63%, or a mixture ratio distribution performance loss of 16.7%. A heavy outer fuel-rich zone is also produced, which is excellent for chamber wall compatibility. The splash plate design, on the other hand, corrects the ring channel influence by directing the propellant across the channel lands providing a much higher mixing efficiency of 87% and a corresponding mixture ratio distribution loss of only 7.8%. Again, a fuel-rich outer boundary is produced, indicating excellent compatibility.

D. HOT TESTING

The subscale hardware was evaluated with a hot fire test program conducted in ALRC's Physics Laboratory on Test Stand A-2. The program encompassed 87 tests using six injectors and four chambers with both ambient and heated fuel. A summary of the variations tested is given in Table V. Propellants used were nitrogen tetroxide and monomethylhydrazine. This section provides a description of the test facility and the test program. Interpretation of the significant results is presented in Section E which follows.

1. Test Facility

All subscale testing was performed in the ALRC's Research Physics Laboratory on Test Stand A-2. The facility delivers NTO and MMH through positive displacement flowmeters to insure accurate flow measurements. A single axis, dual bridge load cell was aligned in a single plane through the thrust axis. The thrust measurement system also provided on-line load calibration to accurately determine thrust bias. Flow into the thruster was controlled by a linked bi-propellant valve assembly mounted on the injector backside.

Report 13133-F-1

TABLE V
SUBSCALE TEST SUMMARY

I. Injectors	
Splash Plate (SP)	2 Versions
"X" Doublet (XD)	3 Versions
Mixed Element	1 Version
II. Cold Flow Tests	
Pattern	6
Hydraulic	6
Propellant Distribution	2
III. Hot Tests	
Total Number	87
Ambient Propellants	25
Heated Fuel	62
Film Cooled	10
Bombed	55
Splash Plate Injector	
SP1	14
SP2	27
X-Doublet Injector	
XDT1	25
XDT2	6
XDI	4
Mixed Element Injector	
ME	11
Chamber Length, in.	
4	14
6	8
7	53
10	11
12	1
IV. Test Range	
Chamber Pressure, psia	101-156
Mixture Ratio, O/F	1.6-2.4
Oxidizer Temperature, °F	50-65
Fuel Temperature, °F	50-235
Duration, sec	1-6
V. Posttest Hardware Condition	
Injector Overheat	None
Chamber Overheat	None
Injector Plugging	None
Resonator Partition	Slight Tip Erosion

VIII.D, Hot Testing (cont.)

Propellant conditioning to 235 degrees Fahrenheit was supplied for the MMH fuel circuit to simulate regeneratively heated fuel outlet temperatures for a prototype OMS engine. Heating was accomplished by means of a simple heat exchanger.

Stability evaluation was provided for all testing using 2.0 grain RDX, teflon covered tangentially oriented bombs placed 1.5 in. downstream of the injector face. High frequency measurements were made with an uncooled Kistler transducer mounted in the acoustic cavity and with water-cooled Photocon transducers located in the chamber. An on-line playback system enabled complete evaluation of the high frequency data following testing.

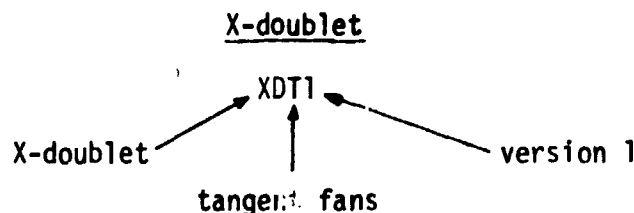
2. Test Program

The test program encompassed a wide range of operating conditions and numerous variations in hardware configuration. A test log describing these variables is included in Table V.

The test program consisted of four major series and is summarized below.

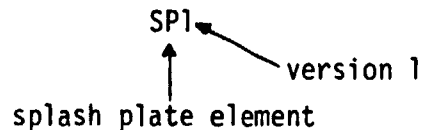
a. Series I - Basic Injector Evaluation

Two basic injection elements were tested in this program, the X-Doublet and the splash plate designs. Pattern nomenclature is defined by the following acronyms:



III,D, Hot Testing (cont.)

Splash plates



Series I consisted of thirty-six tests and evaluated the XDT1 and SP1 elements over a range of chamber length from 4 to 10 in., over a range of mixture ratio from 1.6 to 2.2, and over a range of chamber pressure from 100 to 150 psia. Tests were conducted with ambient and heated fuel, with and without film cooling, with and without acoustic cavities, and with and without stability bombs.

This activity focused on obtaining an understanding of the performance, compatibility, heat transfer, stability and injector operating point sensitivity.

b. Series II - Modified Element Evaluation

Following testing of the two basic element designs, the program proceeded to evaluate modifications to these designs with a 37 test program. The performance for SP1 was lower than expected based on unielement data. This initiated a review of the SP1 design which revealed flow interference between the spray and the injector face. A relieving of the platelet stack beneath the fan produced an element designated as the SP2 version. In an effort to improve the performance of the XD family of elements, a design with inline fans rather than tangent fans was produced and denoted as XDI. The basic XDT1 element matrix was also modified to enhance wall compatibility and was identified as XDT2.

III,D, Hot Testing (cont.)

c. Series III - Mixed Element Evaluations

A mixed element injector was developed combining the desirable characteristics of both designs. This design, designated ME1, was tested 11 times over a range of chamber length, chamber pressure and mixture ratio. The testing also included bomb tests in which the acoustic cavity was removed, to evaluate basic injector stability characteristics.

d. Series IV - Chamber Length Optimization

Following evaluation of the test data, the XDT1 pattern was selected for the full scale design. Stability and compatibility were excellent, with a slight compromise on performance. In order to achieve maximum performance, the chamber length was extended to 12 inches, a length consistent with the full scale regenerative chamber. Three tests were conducted with the 12 inch chamber without incident, thus completing the subscale test activity.

e. Series V - Cycle Life Testing

During the full scale test program, the subscale program was reactivated to explore the cycle life capability of the bonded joint between the platelet face stack and the injector body. To assess the cycle life capability, two injectors were each subjected to 1500 complete thermal cycles. A single cycle consisted of a one second burn followed by a six second coast. The first injector tested was the mixed element injector. No deterioration of the bonded joint was experienced. The second injector, XDT1, was fabricated with a back-up electron beam weld on each land, providing a redundant metallurgical joint consistent with the potential OMS baseline approach. Again, 1500 full thermal cycles were completed without incident or bond joint damage. Hairline cracks were noted in the orifice region of the XDT1 injector, however. These are attributed to structural fatigue of the top platelet; structural and metallurgical evaluation indicated that the condition could be corrected by increasing the top plate thickness or by adding an additional face plate. The latter approach was selected for subsequent designs.

VIII, Subscale Testing (cont.)

E. RESULTS

The following sections describe the pertinent results obtained from the subscale program and are categorized by performance, compatibility, and stability.

1. Performance

All tests were evaluated to determine actual performance and to assess the potential performance of each design at the full scale level. In order to accomplish this task, the JANNAF-approved performance evaluation procedures described in Section X, Full Scale Performance, were employed.

The energy release efficiencies of the various injectors tested were computed for a mixture ratio of 1.88, consistent with a film coolant fraction of 12%, and a chamber length of 7 in., the point where the majority of the testing was conducted. The following ranking of injectors in terms of performance was established:

Energy Release Efficiency

<u>Injector</u>	<u>Ambient Fuel</u>	<u>200°F Fuel</u>
SP2	98.7	99.5
SP1	96	96.5
ME1	94	97
XDT1	91.5	93.0
XDT2	89	92.6
XDI	89	91.2

Figure 45 shows the influence of chamber length on performance. The apparent low performance of the XDT injector can be increased to 98% by

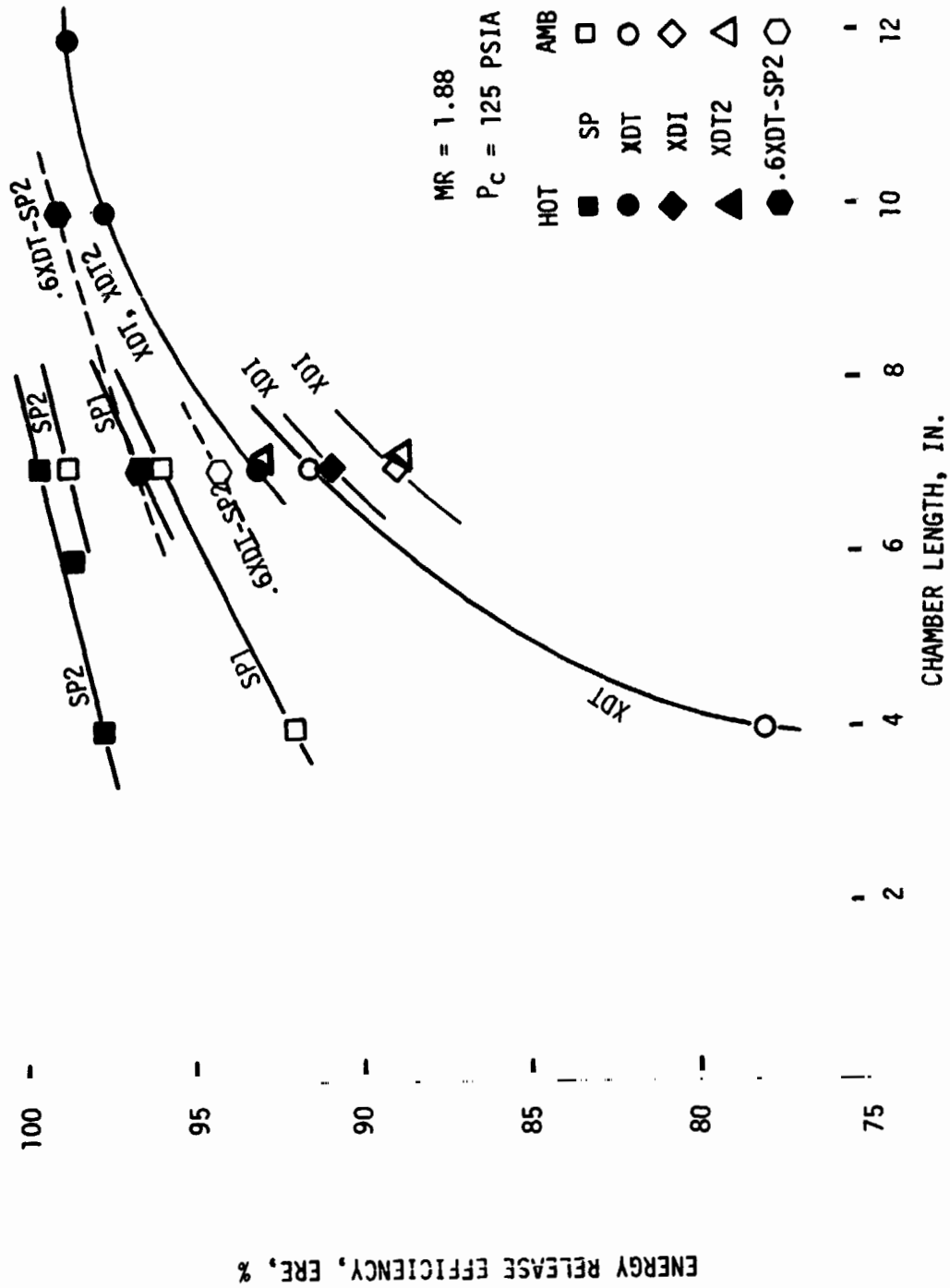


Figure 45. OME Platelet Injector Performance, Subscale Injector

Report 13133-F-1

VIII,E, Results (cont.)

increasing the chamber length to 12 inches, comparable to the splash plate design operating at a 7 inch chamber length, as shown on Figure 46.

The lower XDT performance is most likely the result of incomplete mixing and corresponding slow rate of propellant vaporization. This inefficiency in the mixing process can be most clearly seen in the cold flow mixing test data of Figure 44, which clearly portrays concentric rings of fuel and oxidizer.

The mixed element injector delivered performance consistent with a 60% X-doublet and a 40% splash plate mixture. This result permits a great deal of flexibility in the design of a full scale injector in order to obtain the desired stability, performance or heat transfer characteristics.

A number of injectors were tested with fuel film cooling. They all incurred a performance loss with film cooling as shown in Figure 47. These data are for the X-doublet injectors. Also presented on the figure is the performance accounting for both energy release and film coolant losses. About 2% higher performance obtains with heated fuel.

2. Compatibility

Injector compatibility was assessed on the basis of injector face temperature measurements and inferred heat flux values on the chamber wall.

a. Face Temperature

Thermocouples inserted through the ring channel lands and mechanically joined to the platelet face were used to measure face temperatures. Four thermocouples were installed in a radial line on each injector face with

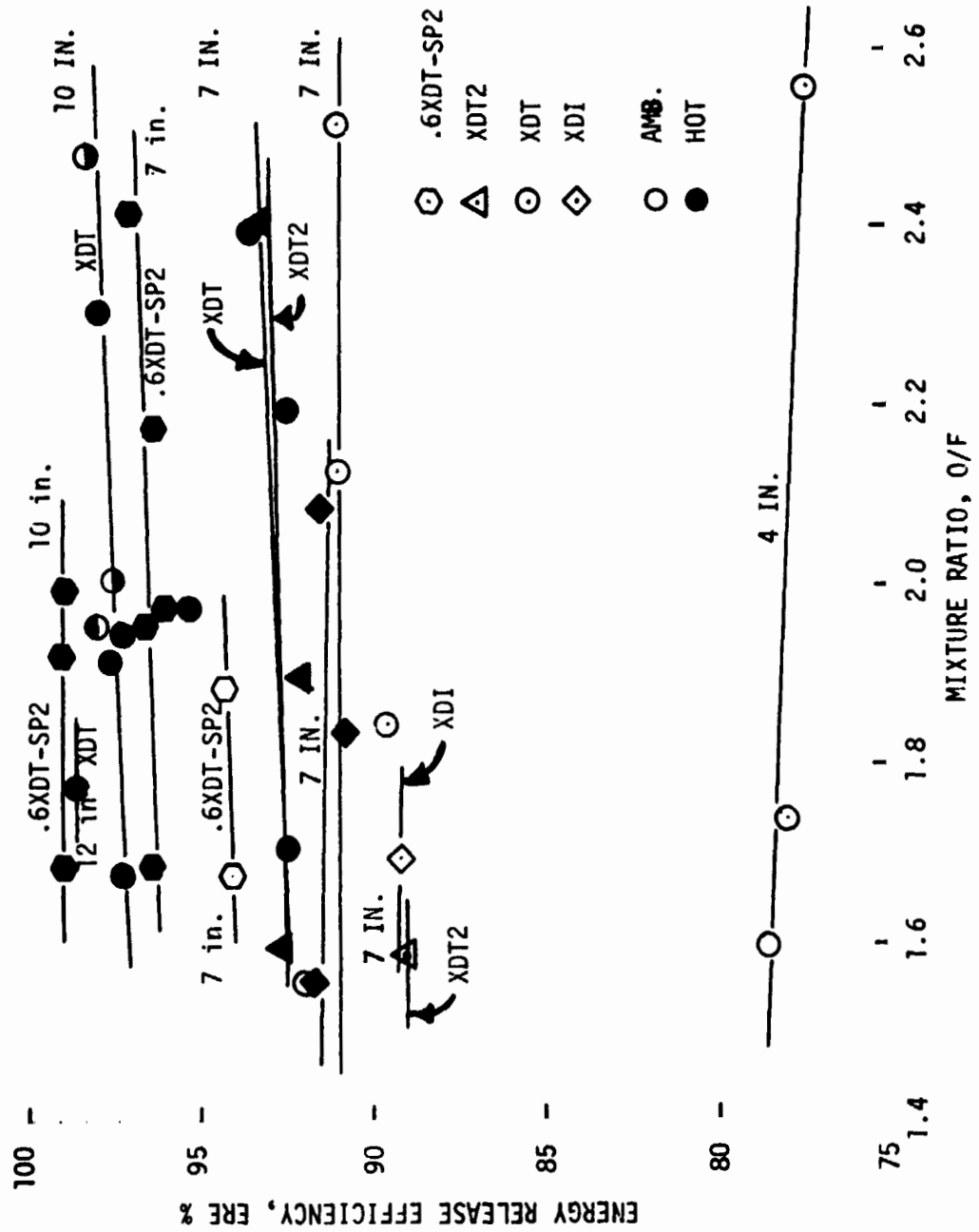


Figure 46. Subscale Injector X-Doublet Performance

Tests 1K-17-115, 121, 124-128

MR = 1.7
P_C = 125 psia

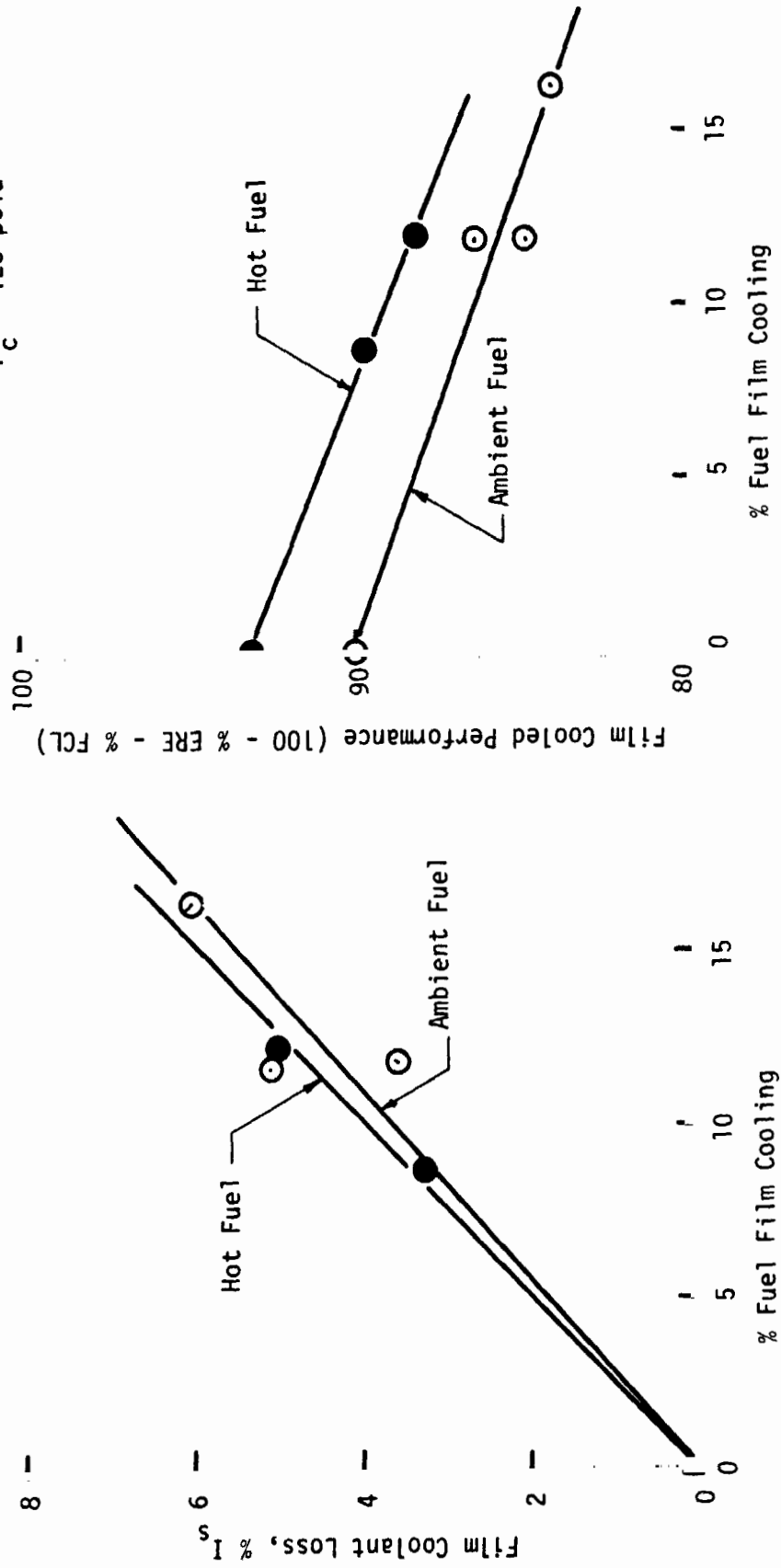


Figure 47. Film Cooled Chamber Performance Data

VIII,E, Results (cont.)

one thermocouple per land. Figure 48 shows the face temperatures measured on the splash plate injector. The spread in measured temperatures, from 300 to 900°F, is a result of thermocouple placement with respect to the injection element. The 900°F temperatures occurred midway between and in line with the ox and fuel splash plates (T3), when testing at elevated fuel temperatures. The 300°F temperatures occur off to the side of the elements and indicate some spray splashback cooling of the face.

The X-doublet injector data are given in Figure 49. The face temperatures range from 400 to 700°F and appear insensitive to high fuel inlet temperature.

b. Chamber Heat Flux

The chamber heat flux was determined from measured gas-side temperature responses. A comparison of the calculated fluxes without film cooling for all injectors is presented in Figure 50. From this figure, it is apparent that the SP and XDT injectors exhibit entirely different forward end flux profiles. The X-doublet family has a very low flux section 1.6 in. long in which very little combustion occurs. The splash plate injectors, on the other hand, show a relatively high flux at the forward end. Both the XDT and SP injectors exhibit comparable fluxes at lengths of 6 in. and beyond.

Heat flux data with film cooling are presented in Figure 51. Again, the X-doublet injectors show improved compatibility relative to the splash plate. The maximum apparent liquid lengths with the splash plate are about 1 inch; with the X-doublet liquid, lengths approaching 3 inches are readily obtained.

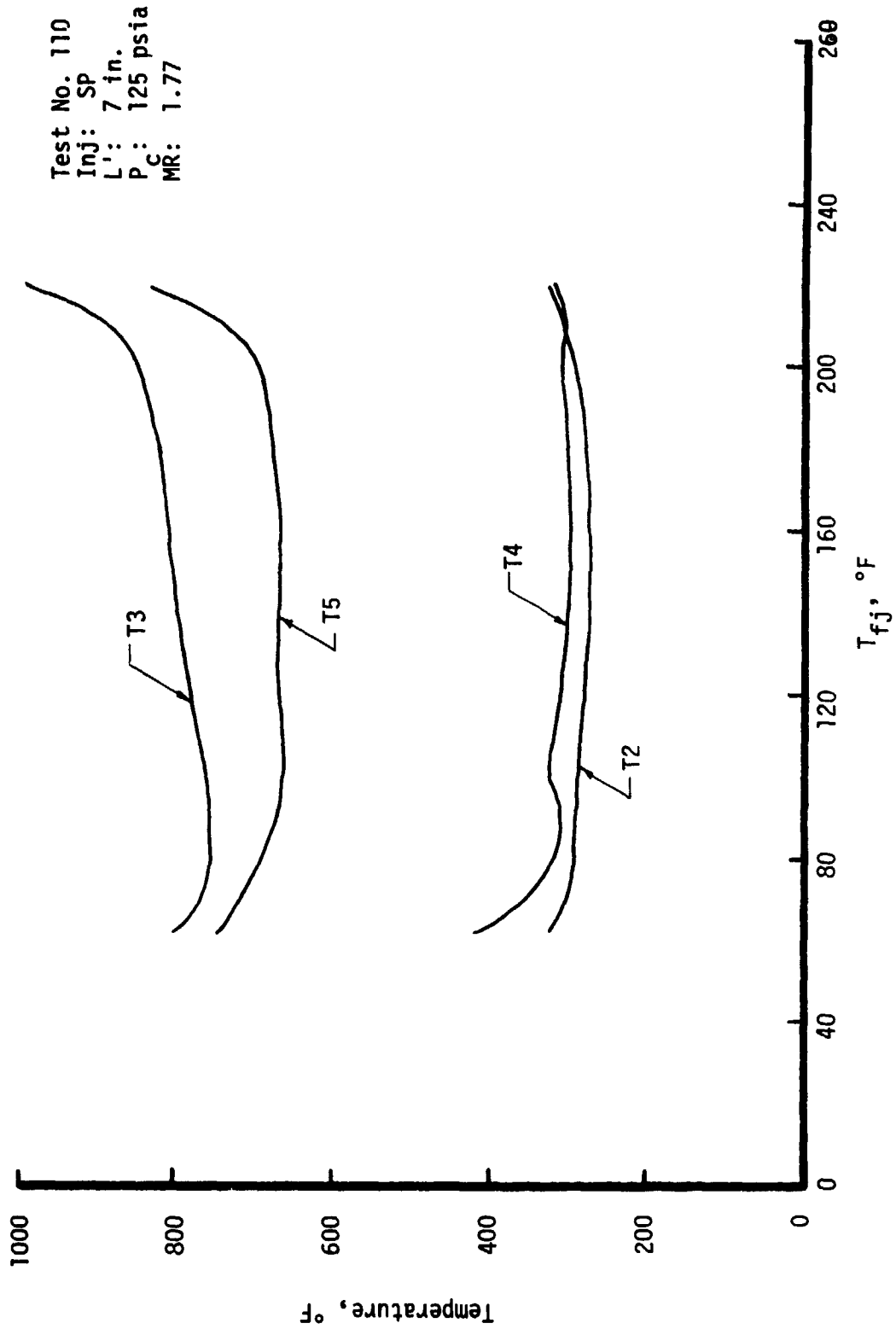


Figure 48. Splash Plate Injector Thermal Characteristics

Test No. 118
 Inj: XDT
 L': 7 in.
 P_C: 125 psia
 MR: 1.66

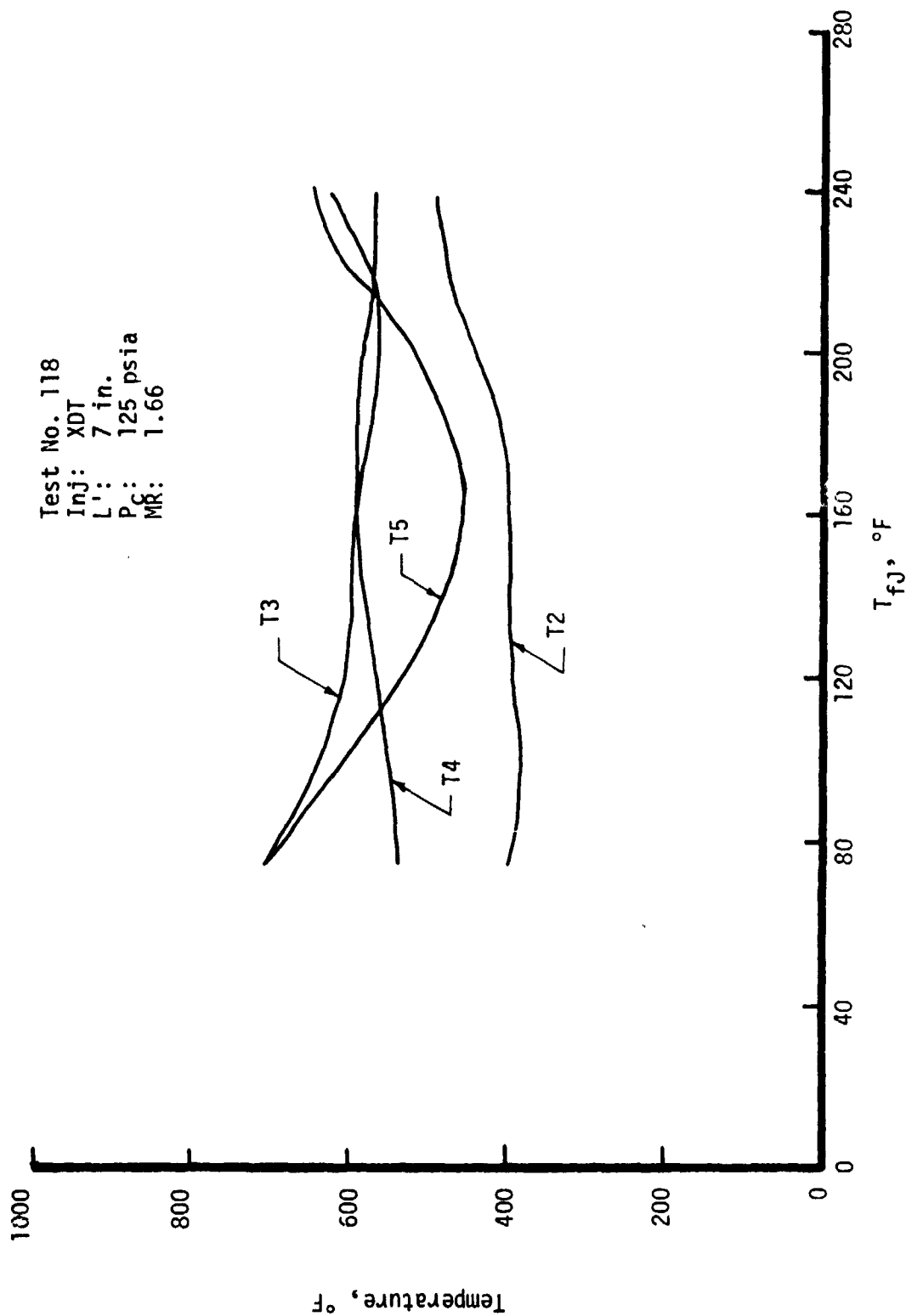
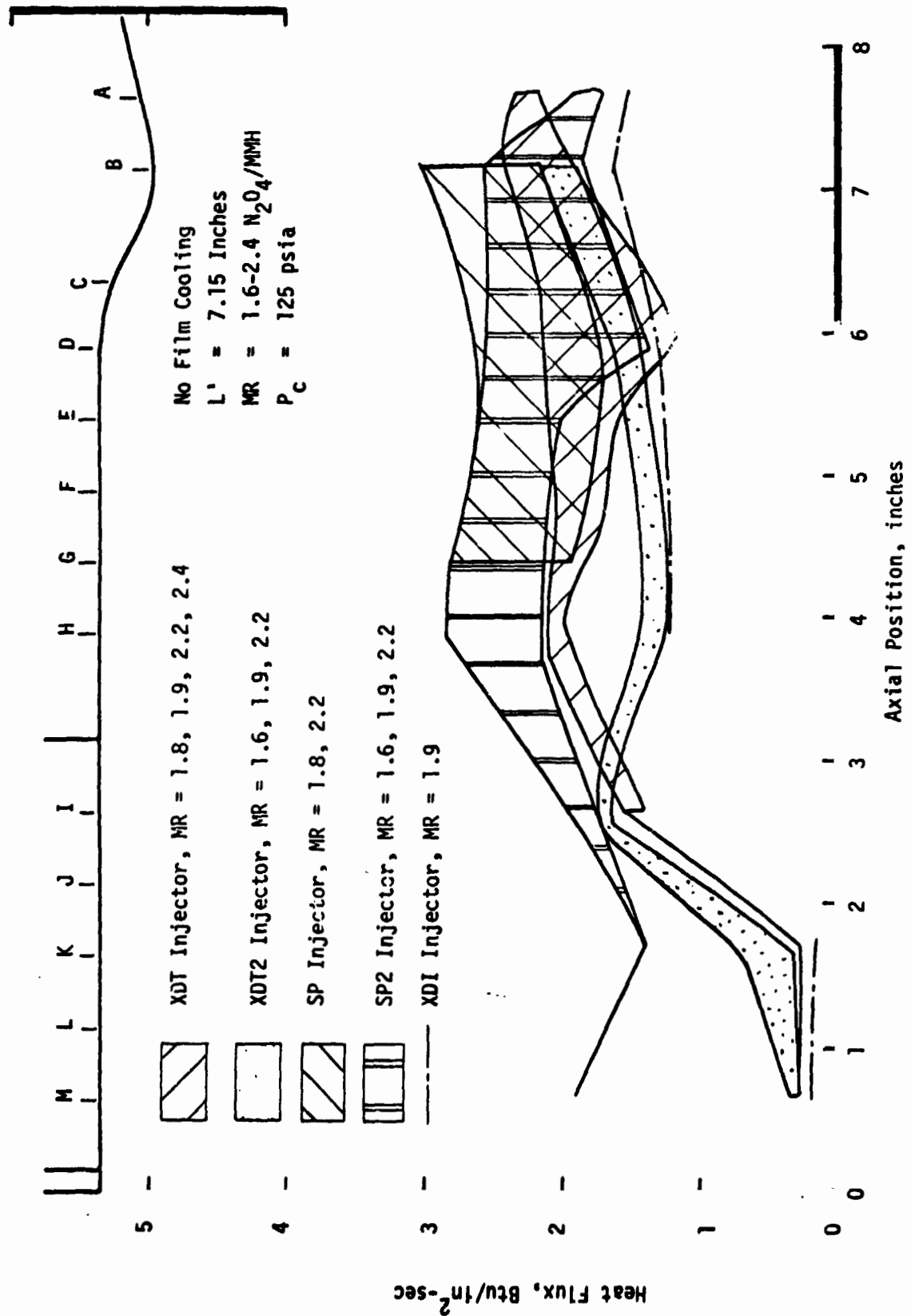


Figure 49. X-Doublet Injector Thermal Characteristics



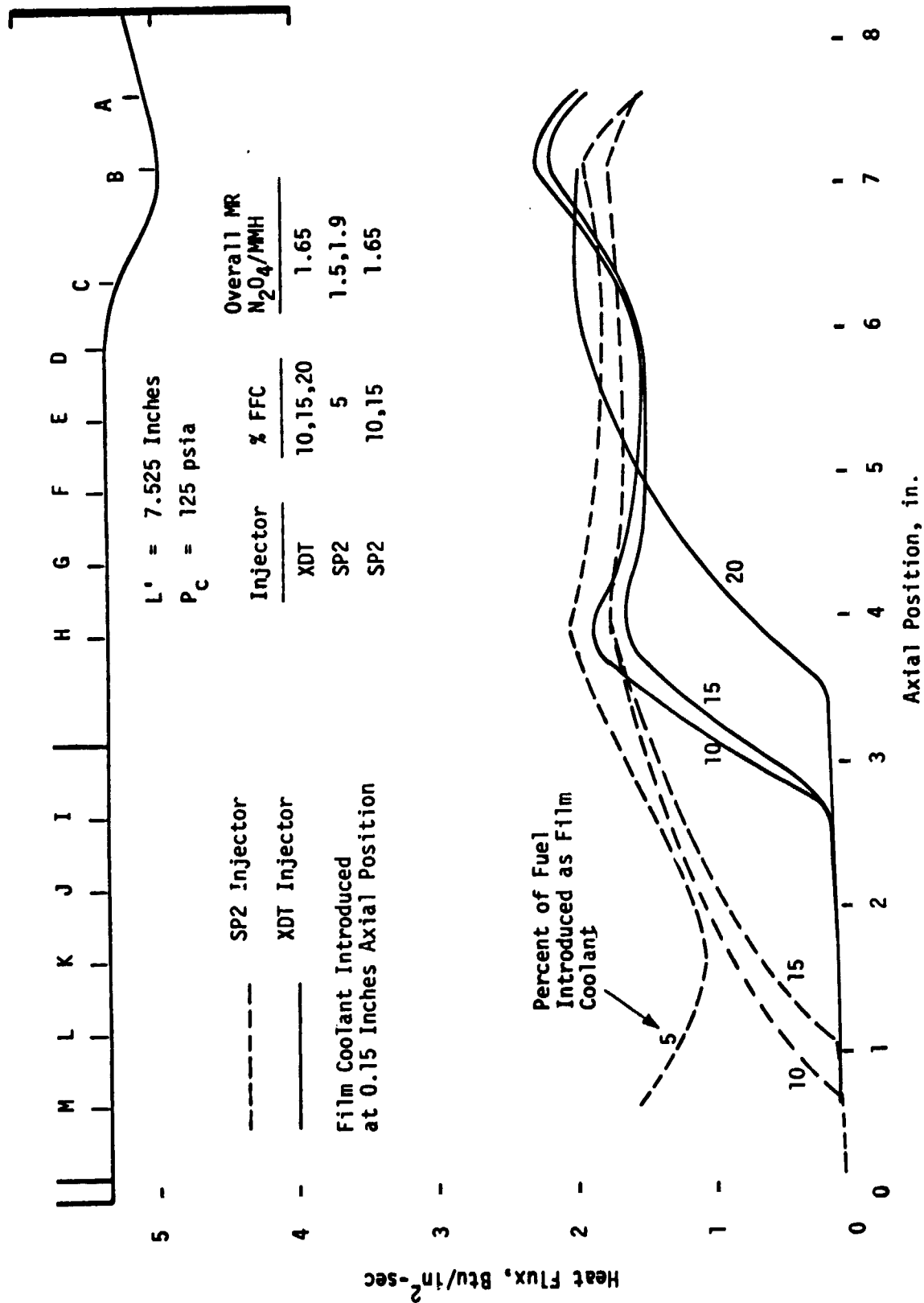


Figure 51. Composite Plot of Film Cooled Chamber Heat Flux Data

VIII,E, Results (cont.)

3. Stability

Stability tests were conducted on the subscale injectors to obtain data on the sensitive frequencies of the different patterns and elements and also to enable ranking of the injectors on the basis of stability. Data were obtained in 55 bomb tests both with and without quarter-wave acoustic cavities. The results are discussed by element type.

a. X-Doublet Injectors

Three types of X-doublet injectors were evaluated for stability: XDT1, XDT2 and XDI. A tabulation of the stability results is presented in Table VI. The range of test variables was:

Fuel temperature, °F	60 - 230
Chamber length, in.	4 - 12
Cavity depth, in.	0 - 0.6
Chamber Pressure, psia	100 - 150
Mixture Ratio, O/F	1.6 - 2.2
Fuel Film Cooling, %	0 - 20

This includes tests conducted without the quarter-wave cavities; such testing was done in 10 in. and 12 in. chambers.

Variations to the basic X-doublet element, i.e., the XDI and XDT2 patterns, showed no difference in stability characteristics.

Several tests on the X-doublet injectors did produce low amplitude chug frequency instabilities. Chug amplitude was approximately 5% of P_c . These tests were generally at high mixture ratios, above 2.2, and at chamber lengths of 7 inches or less. Two tests at these higher mixture ratios were conducted in a 10 in. chamber with no incidence of chugging.

Report 13133-F-1

TABLE VI

OME TRANSVERSE PLATELET 600 LBF TEST SUMMARY
X - DOUBLET INJECTOR

Inj. Type	Test No.	Pc, psia	O/A MR	Comments
<u>AMBIENT FUEL (TEMPERATURE ≈60°F)</u>				
L'=4" XDT	-111	125*	1.9*	5% Pc, 550 Hz
	-112	119	1.75	Stable
	-113	124	1.60	Stable
	-114	120	2.5	Stable
L'=7" XDT	-115	128	1.85	5% Pc, 550 Hz
	-116	129	2.52	5% Pc, 550 Hz
	-124	124	1.70	+13.2% FFC, 1.96 core MR
	-125	125	1.60	+13.2% FFC, 1.85 core, 5% Pc, 550 Hz
	-126	123	1.63	+19.1% FFC, 2.02 core, 5% Pc, 550 Hz
L'=7" XDI	-149	125	1.70	Stable
L'=7" XDT2	-168	128	1.64	5% Pc, 550 Hz
<u>HOT FUEL (TEMPERATURE ≈230°F)</u>				
L'=7" XDT	-117	127	2.20	5% Pc, 550 Hz
	-118	133	1.67	Stable
	-121	125	2.20	Stable
	-122	125	1.75	Stable
	-123	127	2.41	Stable
	-127	127	1.59	+13.5% FFC, 1.84 core MR
	-128	130	1.62	+9.4% FFC, 1.79 core MR
L'=7" XDI	-150	120	1.85	Stable
	-151	133	1.56	Stable
	-152	125	2.23	Stable
L'=7" XDT2	-166	131	1.90	Stable
	-167	125*	1.60*	Stable
	-168	125*	2.20*	5% Pc, 550 Hz
	-169	133	2.45	Stable
	-170	137	1.60	Stable
L'-10" XDT	-134	101	2.45	Stable
	-131	128	1.98	Stable
	-132	129	1.66	Stable
	-133	129	2.31	Stable
	-136	126	1.98	w/o cavity, stable
	-135	157	1.96	Stable

*Planned test conditions.

VIII,E, Results (cont.)

Spectral analyses of a number of tests were conducted to determine the cavity resonant frequency. Figure 52 shows the RMS amplitude for both the cavity and the chamber as a function of frequency for Test 121. A low level activity at .05 psi (RMS) amplitude can be detected at 9600 Hz, the chamber first tangential (1-T) mode. At this frequency, a strong resonance measured by the cavity transducer which shows a 20:1 amplification over the chamber measurement. This resonance shows the 9600 Hz tune at the .6 in. cavity depth and the ability of the acoustic cavity to damp the 1-T kinetic energy of the XDT injectors.

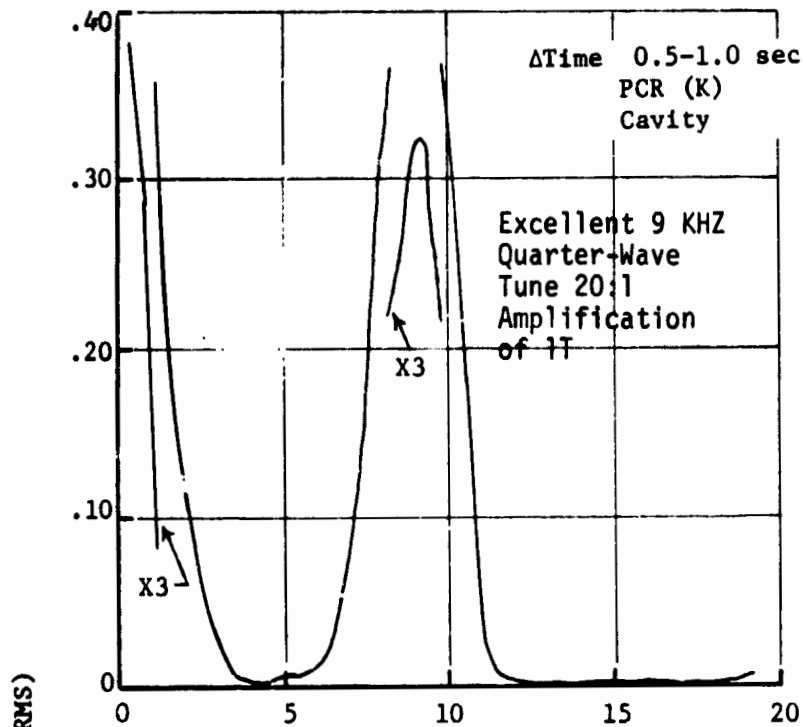
In summary, the X-doublet injectors showed no apparent sensitivity to a transverse mode at 9600 Hz or longitudinal mode at 2600 Hz. This favorable characteristic is believed to be the result of the axially distributed energy release which this element provides.

b. Splash Plate Injectors

Two types of splash plate injectors, SP1 and SP2, were tested during the course of the program in 40 firings, including nineteen bomb tests. A summary of all SP tests, indicating operating condition and chamber length and including comments on stability, is given in Table VII.

Instabilities were encountered at frequencies of about 2000 to 2600 Hz and at 9600 Hz with the splash plate injectors. The lower frequency range corresponds to the first longitudinal (1-L) mode of the chamber. These frequencies were measured on seventeen tests with amplitudes ranging from +5% to +40% of chamber pressure. Since the 1-L mode couples most strongly when the sensitive part of the energy release occurs at a pressure antinode, an attempt was made to stabilize the unit by shifting the 1-L antinode. The acoustic cavity depth was increased to 1.6 in., to make the chamber appear

Report 13133-F-1



MR = 1.6

$T_f = 230^\circ\text{F}$

$L' = 7 \text{ in. and}$
 $.6 \text{ in. cavity}$

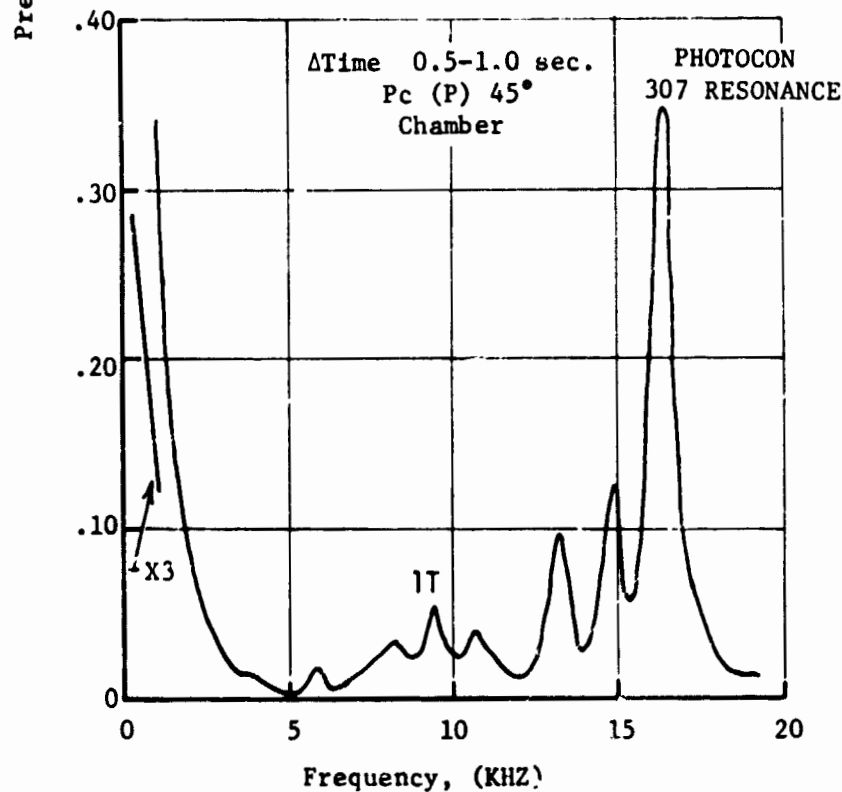


Figure 52. Spectral Analysis of XDT Injector Test 121

TABLE VII

OME TRANSVERSE PLATELET 600 LBF TEST SUMMARY
SPLASH PLATE INJECTOR

<u>Inj</u>	<u>Test</u>	<u>Pc</u>	<u>MR</u>	<u>Comments</u>	
<u>AMBIENT FUEL (TEMPERATURE ≈60°F)</u>					
L'=4"	SP1	-101	100*	1.8*	Chug 970 Hz
		-102	125*	1.8*	Stable 550 & 2000 Hz, 5% Pc
		-103	125*	1.9*	Stable 550 & 2000 Hz, 5% Pc
		-104	136	1.8	Stable
		-105	136	2.16	2000 Hz, 5% Pc
		-106	132	1.73	Stable
		-107	133	1.60	Stable
L'=6"	SP2	-158	125*	1.9*	0.3 sec duration
		-159	125*	1.6*	0.3 sec duration
L'=7"	SP1	-108	137	1.84	2040 Hz, 10% Pc (45 psi on Start)
		-109	132	2.15	2100 Hz, 10% Pc
	SP2	-137	135	1.93	2100 Hz, 10% Pc
<u>HOT FUEL (TEMPERATURE ≈230°F)</u>					
L'=4"	SP2	-141	130	2.0	Stable (225°F, Fuel)
		-142	136	1.54	Stable
		-143	125	2.80	Chug (1000 Hz for 300 ms near start)
L'=6"	SP2	-157	133	1.90	Stable
		-160	140	1.42	Stable
		-171	136	1.76	Stable
		-172	140	1.43	Stable
		-173	132	2.30	2600 Hz, 30% Pc
L'=7"	SP1	-154	102	2.10	2500 Hz for 25 ms at start (218°F, Fuel)
		-110	133	1.78	2500 Hz, 40% Pc (220°F, Fuel)
		-119	126	1.90	2500 Hz, 25% Pc (199°F, Fuel)
		-120	129	2.50	2500 Hz, 10% Pc (180°F, Fuel)
		-129	138	1.81	w/o .6" cavity (9600 Hz at bomb, 100% Pc)
		-130	147	1.78	w/o .6" cavity (9600 Hz at start, 100% Pc)
	SP2	-138	125	2.00	2400 Hz, 30% Pc
		-139	135	1.60	Stable (240°F, Fuel)
		-140	130	2.50	2400 Hz, 40% Pc
		-144	122	1.90	+FFC 14.5% Stable (214°F, Fuel)
		-145	125*	1.65*	+FFC 10%, 2500 Hz, 30% Pc prior to bomb
		-146	125	1.75	+FFC 10%, 2400 Hz, 30% Pc
		-147	121	1.95	+FFC 6.5% Stable (227°F, Fuel)
		-148	133	1.6	+FFC 6.5% Stable (238°F, Fuel)
		-155	125*	1.70*	w/o .6" cavity (9600 Hz at start, 100% Pc)
		-161	134	2.18	1.6" deep cavity, 2500 Hz, 30% Pc
		-162	140	1.56	1.6" deep cavity, stable
		-163	134	2.50	1.6" deep cavity, stable
		-164	138	1.93	1.6" deep cavity, 2500 Hz, 30% Pc, FS-2 9.6Kc
		-153	162	1.85	.6" deep cavity

*Planned test conditions.

VIII,E, Results (cont.)

acoustically longer and thereby shift the pressure antinode into the cavities. Half of the tests, that is 2 out of 4, in this configuration showed the 1-L mode; this indicates only minimal mode modification occurred and/or substantiates the high gain and localized energy release characteristic of the splash plate element.

The 9600 Hz instability was encountered three times, twice spontaneously at the beginning of the test and once following the bomb. The 9600 Hz frequency is the 1-T chamber mode. This mode was present only in tests in which the chamber acoustic cavity was removed. This is significant in that it indicates the acoustic cavities were effective against the transverse mode although they had been ineffective with the longitudinal mode.

It was also observed that the acoustic cavity temperature was about 2200°F with the splash plate elements as compared to about 300°F with the X-doublet. This is consistent with the performance, compatibility, and stability results, all of which indicate the splash plate element to have a much shorter time lag than the X-doublet.

In summary, the splash plate element was capable of coupling with a longitudinal mode and with transverse modes at frequencies up to at least 10,000 Hz. This characteristic was interpreted as making the splash plate a high risk element for the full scale application.

c. Mixed Element Injectors

The mixed element injector was an attempt to blend the desirable performance of the SP element with the desirable compatibility of the XDT element, and to locate the rapid energy release of the SP element away from the injector periphery so as to minimize the 1-L coupling.

Report 13133-F-1

VIII,E, Results (cont.)

The design was tested eleven times as tabulated in Table VIII, and was bombed each time. Only two tests were unstable, both with 10 in. chambers in which the acoustic cavity had been removed. The sensitivity frequency was raised to 9800 Hz which is the 1-T + 1-L mode. No incidence of the 2500 Hz frequency was noted indicating a longer energy release distance had been achieved. The single test of the 10 in. chamber with acoustic cavities was bomb-stable, confirming a positive contribution on the part of the cavities.

d. Stability Summary

The stability testing clearly indicated the attractive character of the XDT element. The injector designs were not sensitive to any hardware or operating point variables. Acoustic cavities were not required for dynamic stability at the 600 lb thrust level.

The SP designs, on the other hand, showed extreme sensitivity to combustion acoustic modes. The 1-T mode could be damped with a .6 in. cavity but modes around 2500 Hz were not easily attenuated. A special deep-cavity design proved statistically inadequate.

Mixing the elements to neutralize the high SP element gain proved quite satisfactory. Instabilities were encountered only in a 10 in. chamber in which the acoustic cavities were absent. At other chamber lengths the cavities could be removed without affecting dynamic stability.

Chugging sensitivity was demonstrated with all designs when tested with short chambers and with low pressure drop injector faces. These conditions were most frequently identified at high mixture ratios, short chamber lengths, and with the SP1 injectors.

Report 13133-F-1

TABLE VIII

OME TRANSVERSE PLATELET 600 1bF TEST SUMMARY MIXED ELEMENT INJECTOR

<u>L'</u>	<u>Inj</u>	<u>Test</u>	<u>P_c</u>	<u>MR</u>	<u>T_f</u>	<u>Comments</u>
7"	ME1	174	125	1.68	94	Stable
		175	127	1.89	96	Stable, no cavity
		176	123	1.98	232	Stable
		177	130	2.42	226	Stable
		178	130	2.42	226	Stable
		179	131	1.69	239	Stable, no cavity
		180	97	2.18	226	Stable, no cavity
		183	127	1.96	235	Stable, no cavity
10"		181	127	2.0	232	Bombed unstable @ 9800 and without cavity
		182	133	1.69	238	Bombed unstable @ 9800 and without cavity
		184	129	1.93	233	Stable after bomb with cavity

ORIGINAL PAGE IS
OF POOR QUALITY

IX. FULL SCALE TESTING AND DEMONSTRATION PROGRAM

Report 13133-F-1

IX. FULL SCALE TESTING AND DEMONSTRATION PROGRAM

A. INTRODUCTION

This section discusses full scale testing, Task VI, done at ALRC following the unielement and subscale hardware testing. It does not include the WSTF testing, which is documented in two separate final reports,^{1,2} nor the stability testing which was conducted at ALRC³ following completion of the second WSTF series. Included in this section will be a description of the injectors, the chambers, designed in Task IV and fabricated in Task V, and the various cavity configurations that were tested, also a chronology of the test sequences and a summary of operating conditions and stability results.

The purpose of the full scale testing was, broadly, to evaluate stability, performance, and heat transfer characteristics, and more specifically, to identify the effects of injector pattern, cavity configuration, chamber length and operating point on those characteristics. The primary thrust of much of the testing was directed toward improving stability margin; thus, many of the firings were stability bombed. Stability results, as well as performance and heat transfer results, are discussed separately in subsequent sections.

B. FACILITY

Full scale tests at ALRC were conducted either in the J-4 test facility or in the A-5 facility. Tests 001 through 038 discussed below were conducted in the J-4 area; all of the remaining tests, numbered 101 through 424, were run in the A-5 facility. Both of these facilities will be briefly described.

¹ WSTF Test Report, Report No. 13133-S-1, 12 December 1973

² 1974 WSTF Test Report, Report No. 13133-S-3, 1 April 1975

³ Report No. 6673:130 PDRD TM05-18, Revision A, Report Development Test OMS Injector, Early Injector Program, July 1975

IX,B, Facility (cont.)

1. J-4 Test Facility

The J-4 facility, shown on Figure 53, can be used for testing either cryogenic or storable propellants either at sea level or altitude conditions. The test hardware is mounted horizontally on a compression flexure firing fixture with in-place force stimulus thrust calibration capability with all propellant lines under pressure. The altitude capability, 70,000 ft equivalent at nominal OME flow rates, is 440 sec and is limited by the steam system capability.

A 2210 gal vessel with 1275 psig capability is used for storing the oxidizer, while the fuel is stored in a 1000 gal vessel with 2160 psig capability. The propellant systems include all of the required support systems such as scrubbers, vent stacks, pressurization systems, temperature conditioning systems, loading stations, and waste ponds.

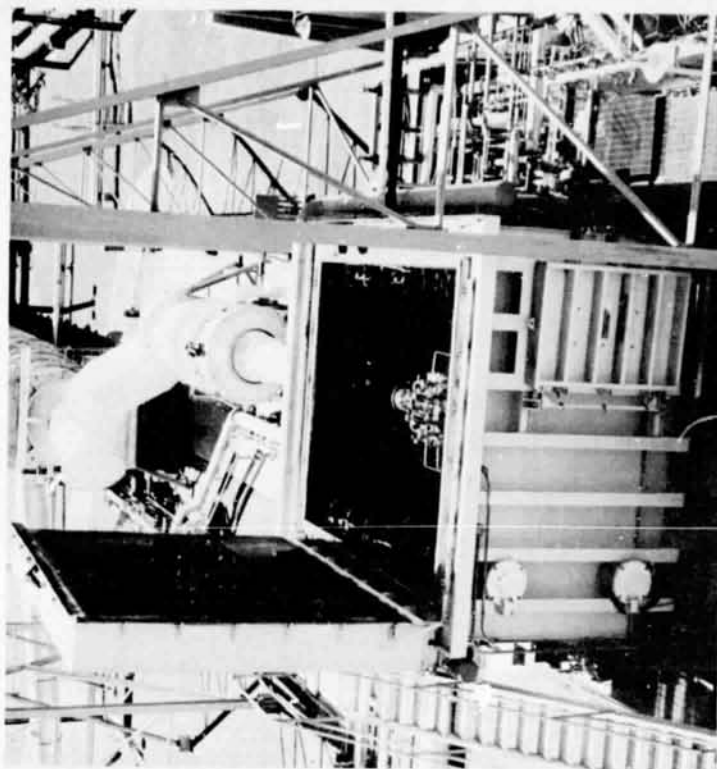
The data acquisition system includes 48 strain gages, 48 thermocouples, 12 RTT's, 6 flow meters, and 12 high frequency channels that can be recorded on 20 brown strip charts, 3 oscillographs, a 120 channel analog-to-digital converter and an Ampex 8-1200 system. Test data are available immediately after each test on strip charts, a direct-writing oscillograph, and an on-line digital printout.

2. A-5 Test Facility

The A-5 test cell is one of seven bays in the A-Area facility, shown on Figure 54. The A-Area, or Physics Lab, as it is commonly called, is well suited to research-oriented work because of the technical background of its personnel as well as the scope of the facility which comprises, in addition to the test bays, the Advanced Injector Distribution measurements system ("milk maid"), centralized control and data acquisition room, shop and assembly

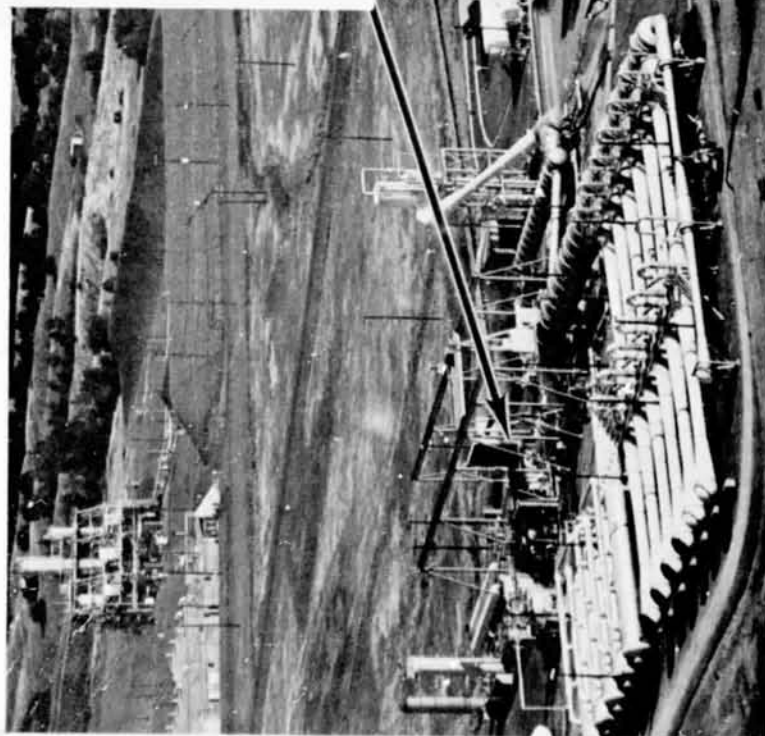
ORIGINAL PAGE IS
OF POOR QUALITY

Report 13133-F-1



J-4 Altitude Chamber (15' X 18' X 10')

- Thruster fires horizontally into 30-in. diameter supersonic diffuser.
- Altitude 70,000 ft., 550 sec.
- Run Tankage Capability \approx 50 sec, 1250 lbF, MR = 4.5



J Area Altitude Test Facility

- Test Cell J-4, Left-Extended Range Thruster Assembly
- Test Cell J-3, Right-Integrated Thruster Assembly
- Foreground: 45,000 lb, 400 psig Steam Accumulators and Ejectors
- Located Left of Cell: 50 gal/1800 psia Vacuum-Jacketed Fuel Tank and 1000 Gal/2160 psig Vacuum-Jacketed Propellant LO₂ Tankage

Figure 53. J-4 Test Facility

RESEARCH PHYSICS LABORATORY - FACILITIES

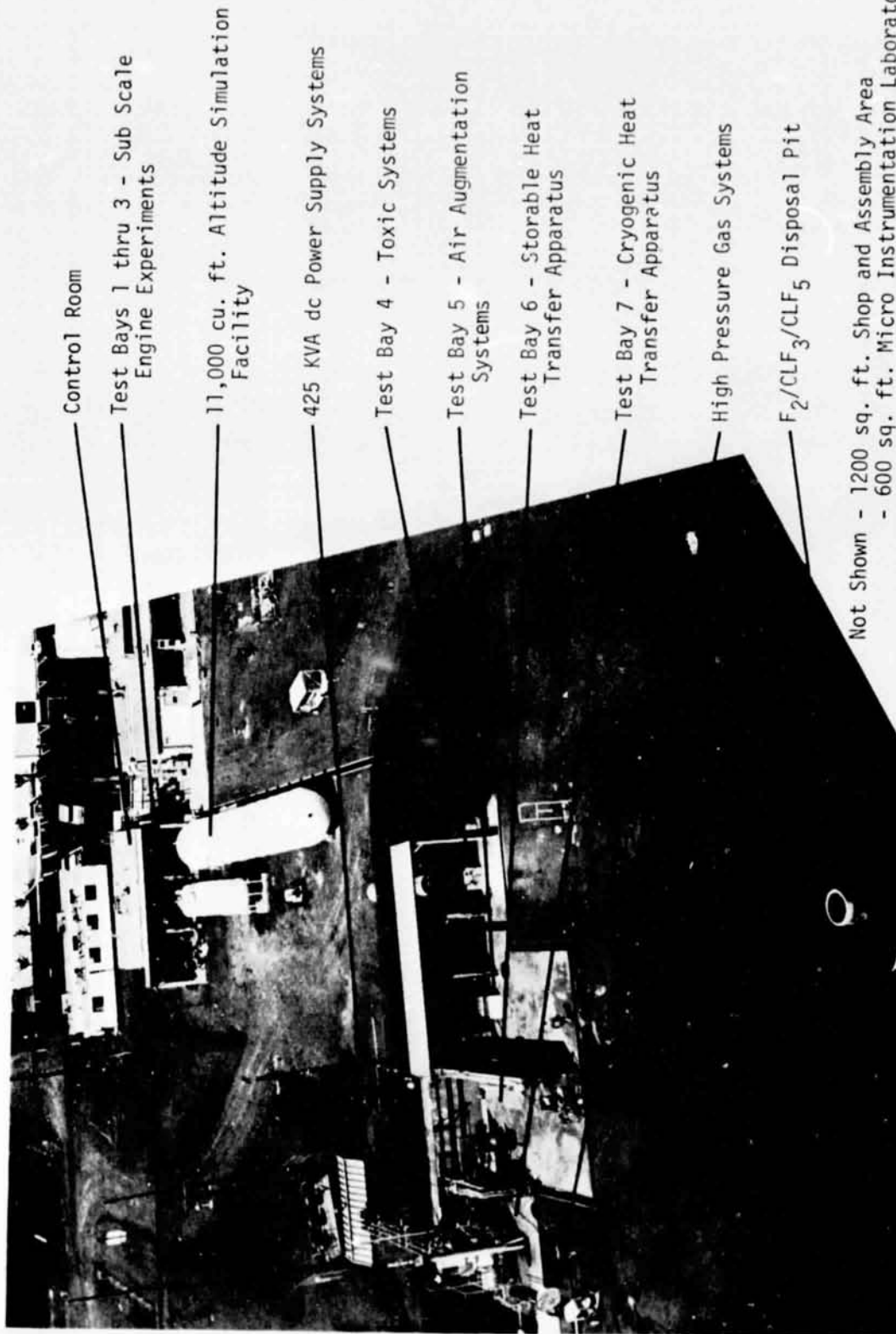


Figure 54. Research Physics Laboratory

Report 13133-F-1

IX,B, Facility (cont.)

area, microinstrumentation laboratory, acoustics laboratory, and data reduction and office area.

The test bays are equipped to conduct small scale rocket firings in the thrust range of 1 to 10,000 lb thrust at both sea level and simulated altitude conditions. Test data are transmitted from the bays via shielded cable to a patch board system located in the central control room. The patch board allows rapid instrumentation change from one bay to another. Wide-band differential instrumentation amplifiers and appropriate signal conditioning convert the low level data signals to high levels required for digital recording, analog taping, and oscillograph galvanometers. Low frequency test data are recorded on a direct writing oscillograph for "quick look" usage and digitized for engineering unit listings. High frequency data are recorded on analog tape which can be played back on the direct-write oscillograph or digitized.

Operating point data are digitized and stored in an on-line HP 2100A computer/real time process controller. This unit controls all test sequencing and malfunction sensing, and it outputs selected data for "quick look" review.

C. CHAMBERS

Except for Sequences 7, 8, and 9 of Series 1 in which the A-1 regenerative chamber was used, all full scale testing at ALRC was accomplished with uncooled, or heat sink chambers. Figure 55 shows an assembly view of a workhorse chamber with the L* section, film coolant ring, injector, and close-out plate (for leak testing) in place. Three chambers were employed in testing two of them residual from a company-funded program. Figure 56 shows a drawing of the 4.000 in. L' chamber; the other two had L' values of 8.000 and 12.000 in. Wall material was 304L stainless steel in all cases and the wall thickness was 0.75 in. The A-1 regeneratively cooled chamber has been previously documented in the two WSTF Test Reports.

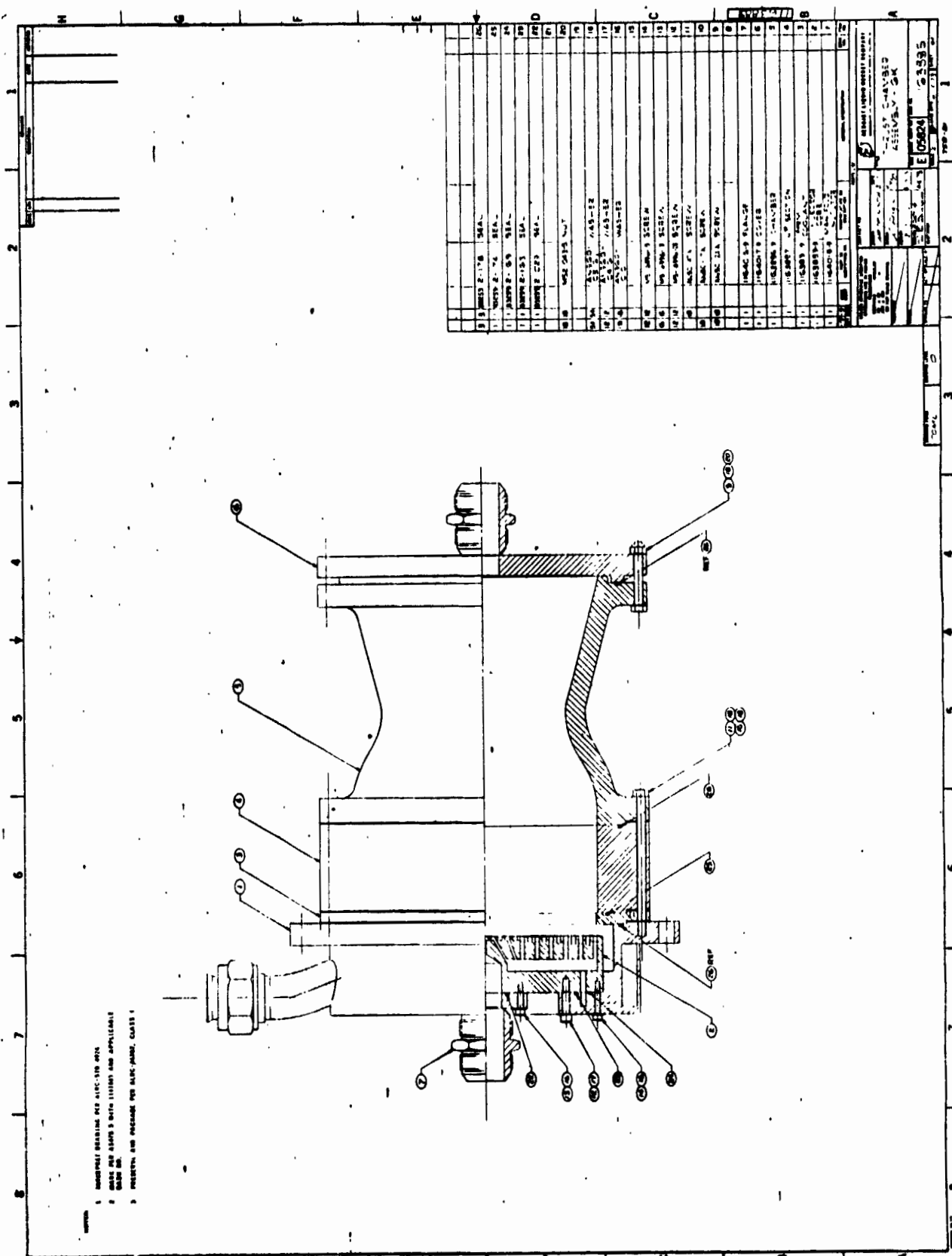


Figure 55. Thrust Chamber Assembly

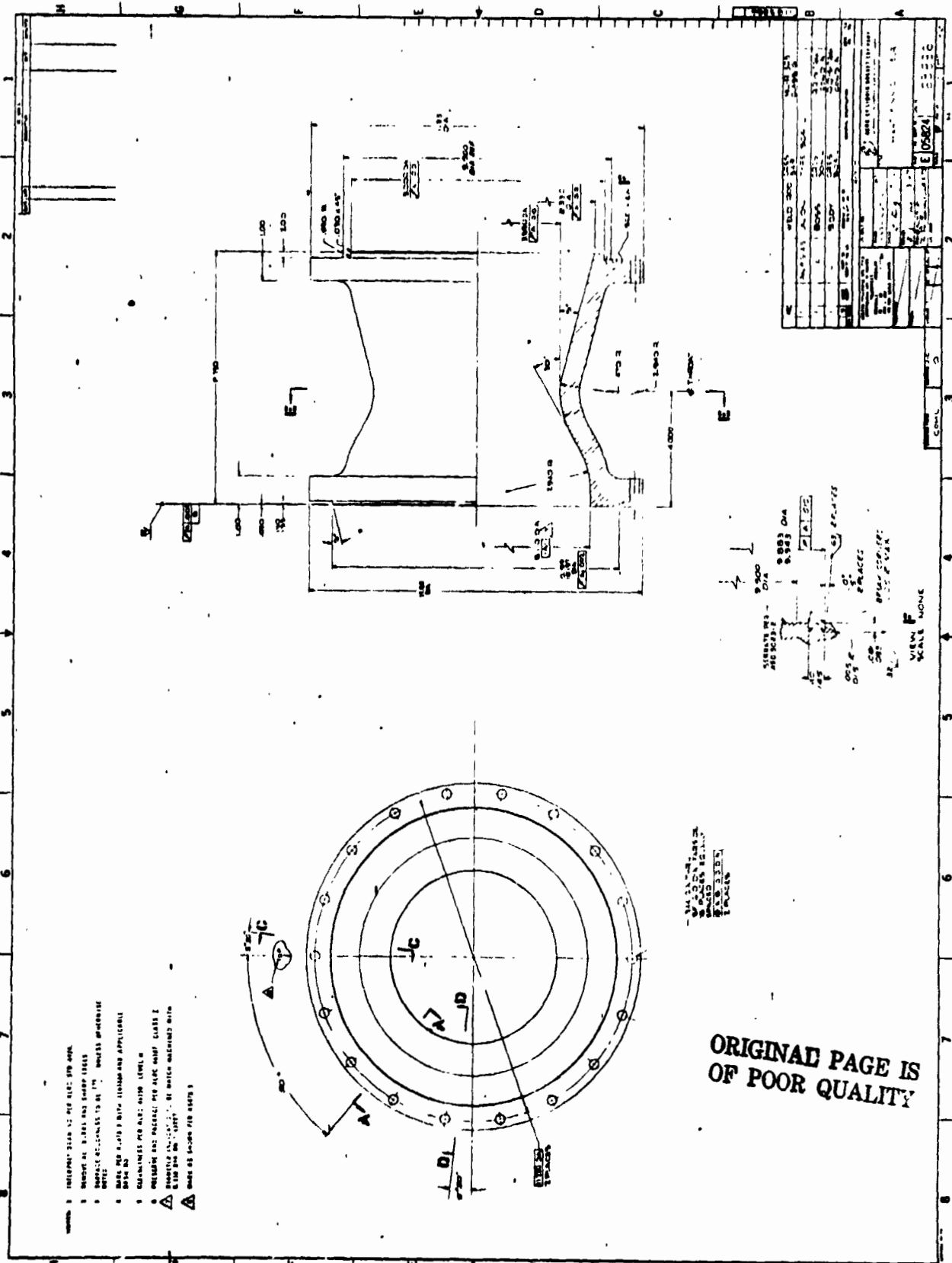


Figure-56. Heat Sink Chamber

ORIGINAL PAGE IS
OF POOR QUALITY

Report 13133-F-1

IX,C, Chambers (cont.)

Three cylindrical L* sections were available for use with these chambers. Their lengths were respectively 2.000, 3.000, and 4.125 in. Wall materials was 347 stainless steel. Figure 57 shows the 3.000 in. section.

Either a stainless steel film coolant ring or a dummy ring could be inserted forward of the L* section. The film coolant ring had 120 orifices 0.0290 in. dia for coolant injection. The dummy ring had no such orifices. The drawing of the ring is presented in Figure 58.

Two nozzles were used during the testing. One, shown on Figure 59, was a 15° conical section with an exit area ratio of 20:1. The other was a contoured nozzle and also had an exit area ratio of 20:1. Both were made of mild steel and bolted on to the aft end of the chamber by means of 18 bolts.

The chamber, as mounted in the A-Area test stand, is shown in Figure 60.

D. CAVITY CONFIGURATION

1. Introduction

A number of geometrical factors, in addition to cavity depth and area, were found to affect combustion stability. It is the purpose of this section to describe these factors in a general way, so as to make the subsequent Test Series Description and Test Summary, Sections F and G, more meaningful. The more important considerations include (1) injector overlap, (2) inlet contour, and (3) corner contour.

2. Cavity Depth

Cavity depth, or length as it is often called, is simply the distance to the bottom of the cavity as measured from the injector face. Using

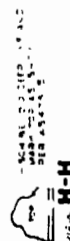


Figure 57. L* Section

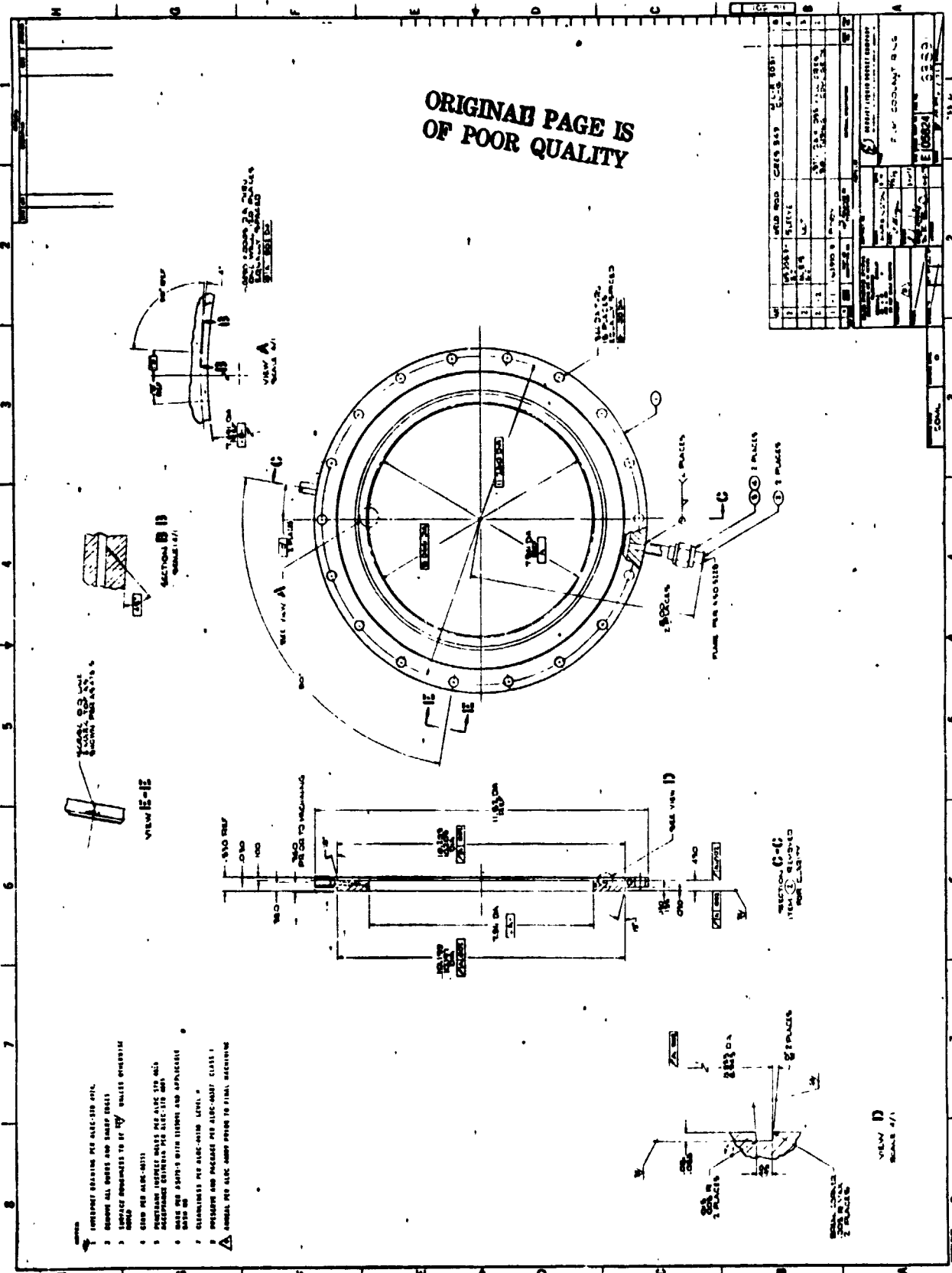
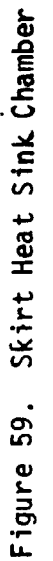


Figure 58, Film Coolant Ring



ORIGINAL PAGE IS
OF POOR QUALITY

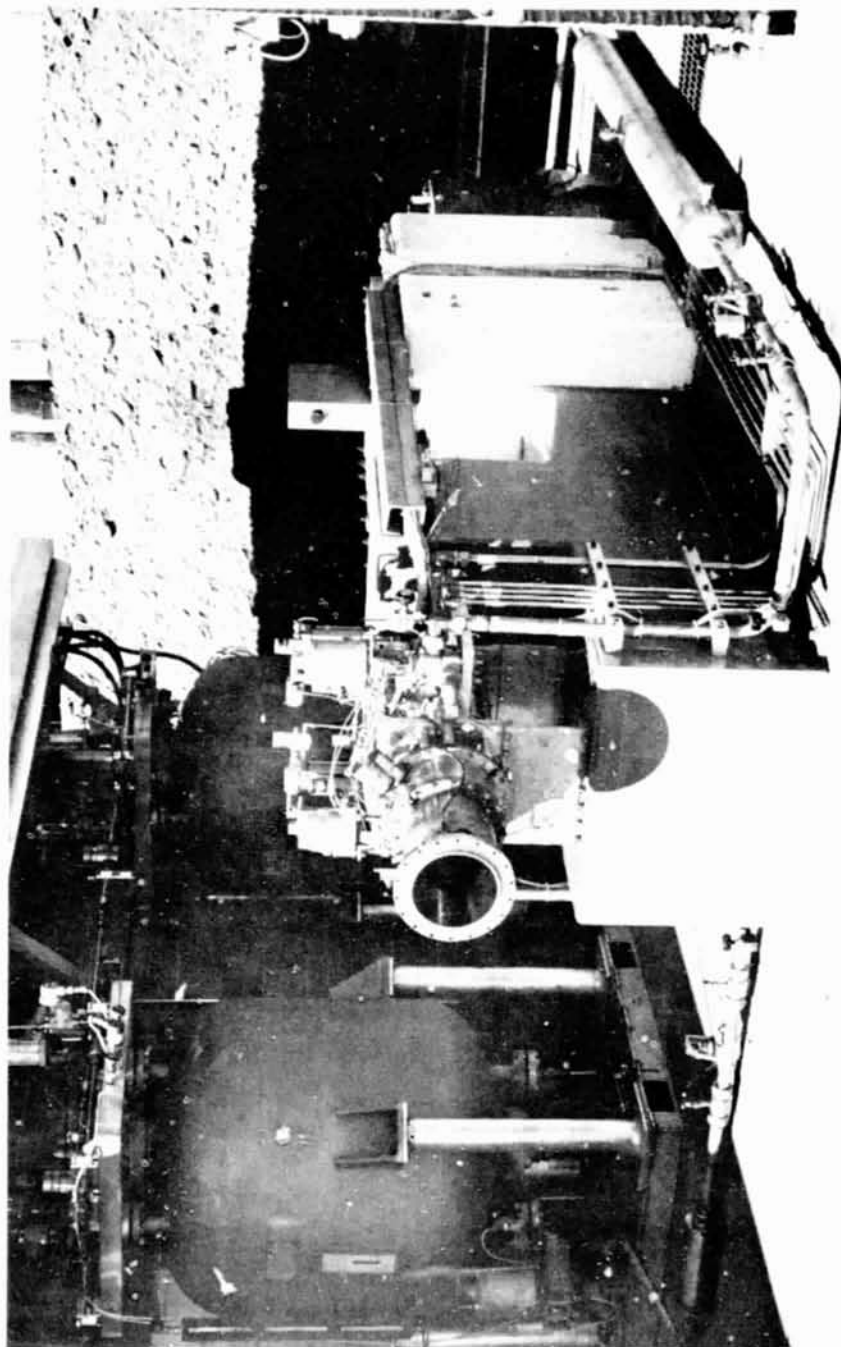


Figure 60. Chamber on Test Stand

IX,D, Cavity Configuration (cont.)

the face as a reference point is arbitrary but in some cases the only realistic way to indicate depth, as for instance, when the outer wall of the cavity is contoured at the downstream end.

After the initial experimentation, it was found necessary to have cavities of two different depths. The longer, or 1-T, cavity was varied in length from 0.4 in. to 1.9 in. The shorter, or 3-T cavity was varied from 0.35 to 0.9 in. The baseline cavity depths were 1.5 in. for the 1-T (eight compartments) and 0.4 in. for the 3-T cavities (4 compartments). In certain tests, the cavities were blocked off to the level of the injector face, leaving only the cavity entrance open. Cavity depth was adjusted by means of blocks that fastened to the bottom of the cavity. The blocks, which were of several lengths, were each held in place by means of two screws.

3. Cavity Area

Cavity open area has usually been expressed as a percentage of the injector face area. The range of 3-T open area percentages varied from 3 to 9% with up to a 20% increase with the inclusion of an additional bolt-on cavity housing. The 1-T values ranged from 10 to 25%. The nominal values were 18% for 1T and 9% for 3T.

4. Injector Overlap

Injector overlap is defined by the excess of injector radius over chamber radius. This is illustrated by Figure 115 in Section XII. Thus positive overlap signifies that the injector diameter is greater than the chamber diameter. In full scale testing, five overlap values were utilized, ranging from -0.007 in. to +0.25 in.

IX, D, Cavity Configuration (cont.)

5. Inlet Contour

The contour of the cavity at the outer diameter of the chamber was tested in three configurations as shown in Figure 114 of Section XII. The first provided a sharp-edged rectangular corner. The second had a small (1/8 in.) radius on the rectangular corner. The third had a larger radius, 1.000 in., which was only used in conjunction with a radiused back corner. The inlet corner contour discussed below were altered by replacing the ring which formed the aft surface of the cavity; curved back corners were achieved by means of tabs protruding into the cavity from the ring.

6. Corner Contour

The back corner of the cavity was also tested with three variations as shown on Figure 114. The first configuration was simply a sharp edged rectangular corner. The second had a 0.600 in. radius which faired into the rectangular inlet contour. The third had a 0.500 in. radius which joined the radiused inlet contour described immediately above.

7. Other Variations

There were a number of other geometrical factors that were altered during the testing and were not found to have as significant an effect on combustion stability as the several items above. These include the chamber profile just downstream of the cavity, the inlet width, the cavity width, the injector edge contour, the location of the outer injection element relative to the chamber wall, and finally, the cavity rib width.

Figure 61 summarizes the several geometrical factors just described and their numerous variations. In two areas, cavity depth and percent open area, the list is not complete and only minimum and maximum values are given. Also indicated is the so-called baseline OMS design.

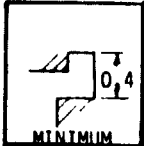
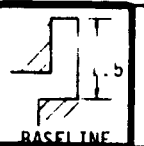
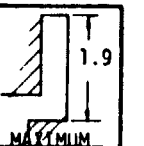
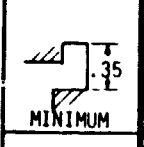
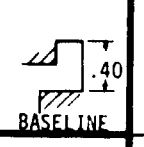
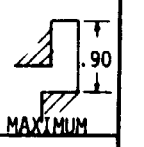
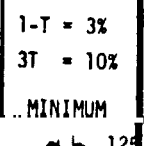
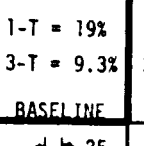
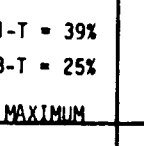
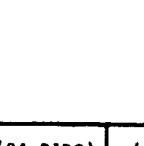

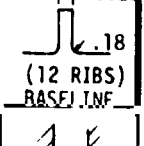
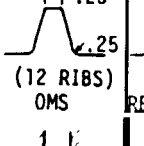
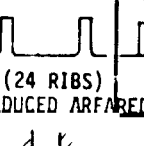
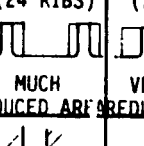
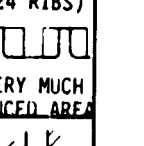
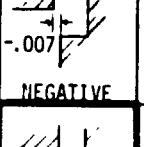
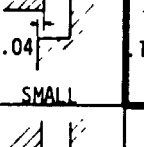
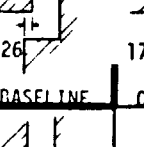
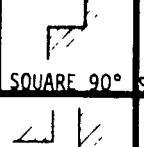
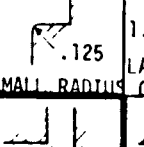
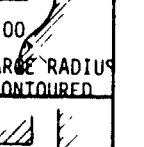
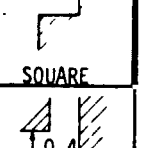
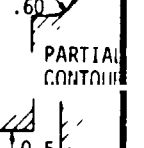
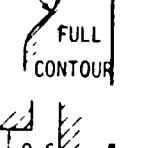
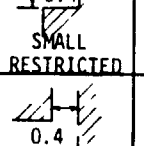
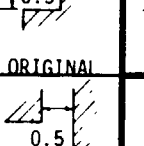
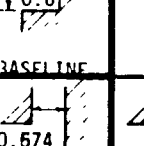
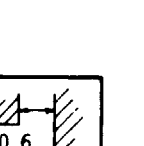
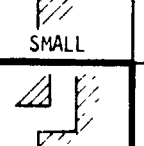
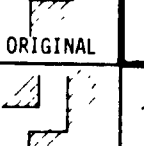
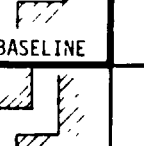
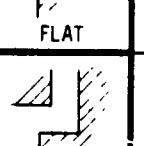
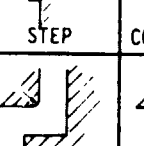
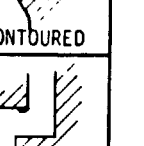
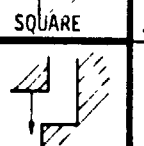
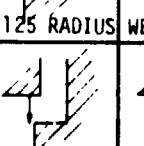
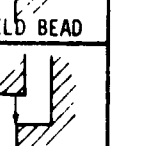
1. 1-T DEPTH	 MINIMUM	 BASELINE	 MAXIMUM		
2. 3-T DEPTH	 MINIMUM	 BASELINE	 MAXIMUM		
3. 1-T & 3-T CAVITY AREA (% OF FACE)	1-T = 3% 3-T = 10% MINIMUM	1-T = 19% 3-T = 9.3% BASELINE	1-T = 39% 3-T = 25% MAXIMUM		
4. RIBWIDTH OR CAVITY AREA	 (12 RIBS) BASELINE	 (12 RIBS) OMS	 (24 RIBS) REDUCED AREA	 (24 RIBS) MUCH REDUCED AREA	 (24 RIBS) VERY MUCH REDUCED AREA
5. OVERLAP INJECTOR-CHAMBER O.D.-I.D.	 NEGATIVE	 SMALL	 BASELINE	 ORIGINAL	 X-LARGE
6. INLET CONTOUR CHAMBER I.D.	 SQUARE 90°	 SMALL RADIUS	 LARGE RADIUS CONTOURED		
7. BACK CORNER CONTOUR	 SQUARE	 PARTIAL CONTOUR	 FULL CONTOUR		
8. INLET WIDTH	 SMALL RESTRICTED	 ORIGINAL	 BASELINE		
9. BACK-SIDE CAVITY WIDTH	 SMALL	 ORIGINAL	 BASELINE	 OMS	
10. DOWNSTREAM CHAMBER I.D. SHAPE	 FLAT	 STEP	 CONTOURED		
11. INJECTOR INLET CONTOUR	 SQUARE	 .125 RADIUS	 WELD BEAD		
12. OUTER INJECTION ELEMENT TO CHAMBER WALL	 BASELINE	 CLOSE	 CLOSER		

FIGURE 61. Acoustic Cavity Configurations

IX, Full Scale Testing (cont.)

E. INJECTORS

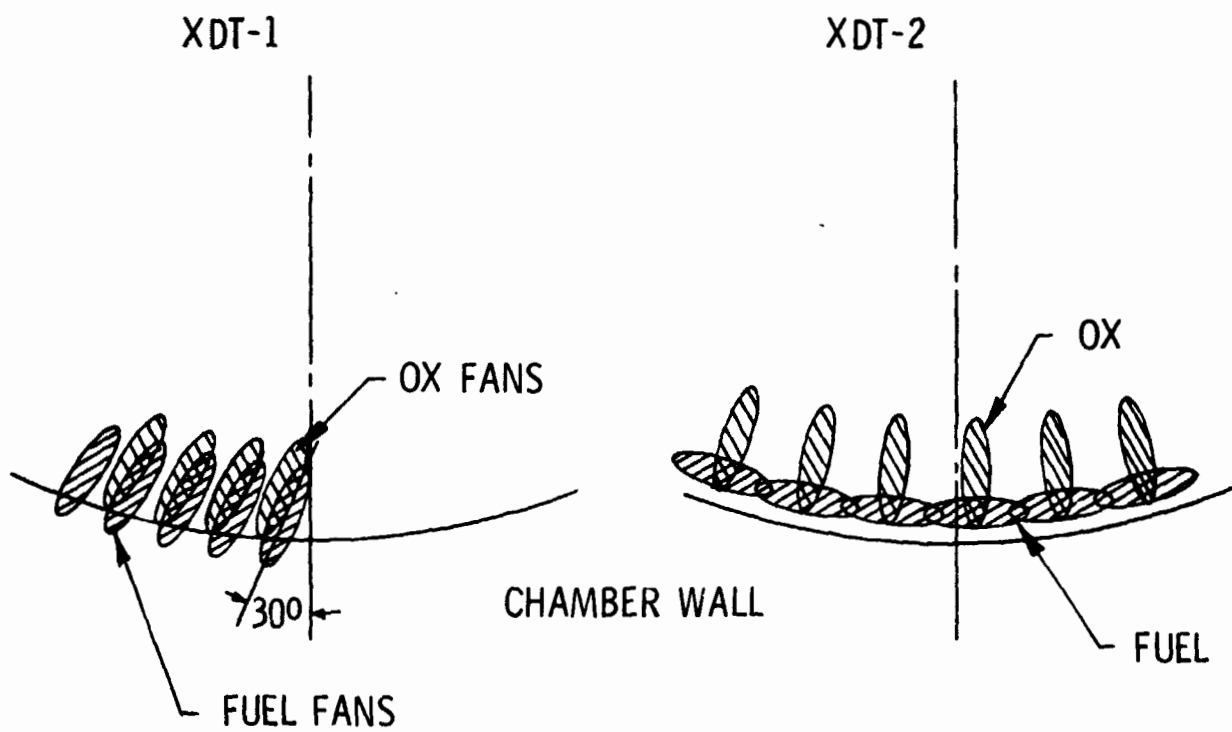
1. Introduction

The frequent replacement of injector faces that was so easily accomplished during the full scale test program has understandably caused something of a nomenclature problem. The terminology is not as incomprehensible as first seems to be the case, however.

There were in fact only two workhorse injector bodies, to each of which four different platelet faces were bonded, and there were two demo injector bodies, one with two faces and the other with a single face. In addition, there was an integral baffle injector and a like-doublet injector that was residual from a company-funded program.

The basic X-doublet pattern was designated by the letters "XDT". Two variations on the XDT pattern existed, denoted on XDT-1 and XDT-2; they differed only in the outer row of elements which altered the fuel fan orientation as shown on Figure 62. Subsequent replacement of the face stack was indicated by a letter suffix to the pattern number. Thus, the four faces on the first workhorse body were designated: XDT-1, XDT-1A, XDT-1B, and XDT-1C. The second workhorse body was first faced with XDT-2, then XDT-2A, and subsequently, with a mixed element and a low pressure drop (actually on XDT-1 pattern) unit.

The demo X-doublet was designated "DXDT" and the pattern again indicated by number. Serial number was then indicated by an additional hyphenated number. Initially, both demo injector bodies were faced with the XDT-1 pattern; thus, they were called DXDT1-1 and DXDT1-2, respectively. A weld repair of DXDT1-1 was labelled DXDT1-1R, and the DXDT1-2 was refaced with the other pattern and subsequently called DXDT2-1, viz, Serial Number 1 of the



NOTE - ALL INBOARD ELEMENT ROWS IDENTICAL ON XDT1 AND 2

Figure 62. Comparison of XDT-1 and XDT-2 Patterns

IX,E, Injectors (cont.)

XDT-2 pattern. Notwithstanding manifold differences between the workhorse and demo bodies, the XDT-1 and DXDT-1 patterns were identical, as were the XDT-2 and the DXDT-2 patterns.

2. Injector Bodies

The workhorse and demo injector bodies were substantially the same in many respects. In both, the oxidizer inlet was at the center and fed outward into three pie manifolds prior to feeding into "downcomers" that supplied the face ring manifolds. Likewise, the fuel in both cases was fed radially inward from a circumferential manifold to three pie manifolds, through the "downcomers", and into the ring manifolds.

The primary differences between the two units affecting fluid dynamic characteristics are: (1) the pie manifolds in the workhorse body are of uniform height while in the demo body they are tapered; (2) the "downcomer" area is smaller on the demo configuration; (3) the retaining structure (and fuel manifold housing) of the demo injector core attaches directly to the regeneratively cooled cavity housing, while on the other it forms the outer wall of the cavity; and (4) the circumferential fuel manifold on the workhorse is fed by a single line while on the demo it is fed from around the periphery.

Figures 63, 64, and 65 present the workhorse injector drawings. Figure 66 reproduces a photograph of the disassembled workhorse injector; it shows the retaining structure, injector core, oxidizer inlet, and several of the blocks which fixed into the forward end of the cavities to effect cavity depth changes. Figures 67 and 68 are photographs of the chamber side and opposite side of the injector assembly, respectively.

The demo injector drawings are given in Figures 69 through 73.

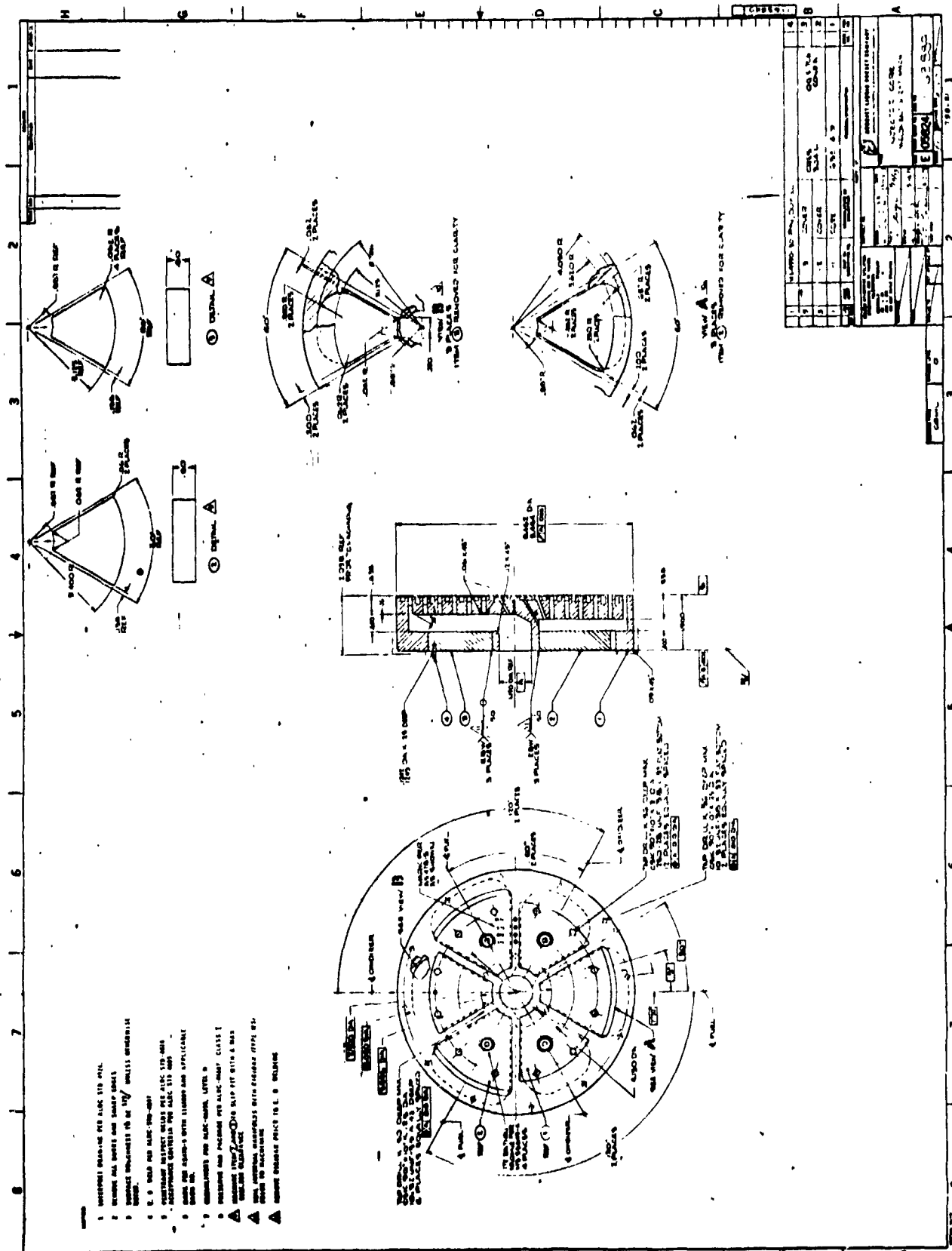


Figure 65. Injector Core Weldment

ORIGINAL PAGE IS
OF POOR QUALITY

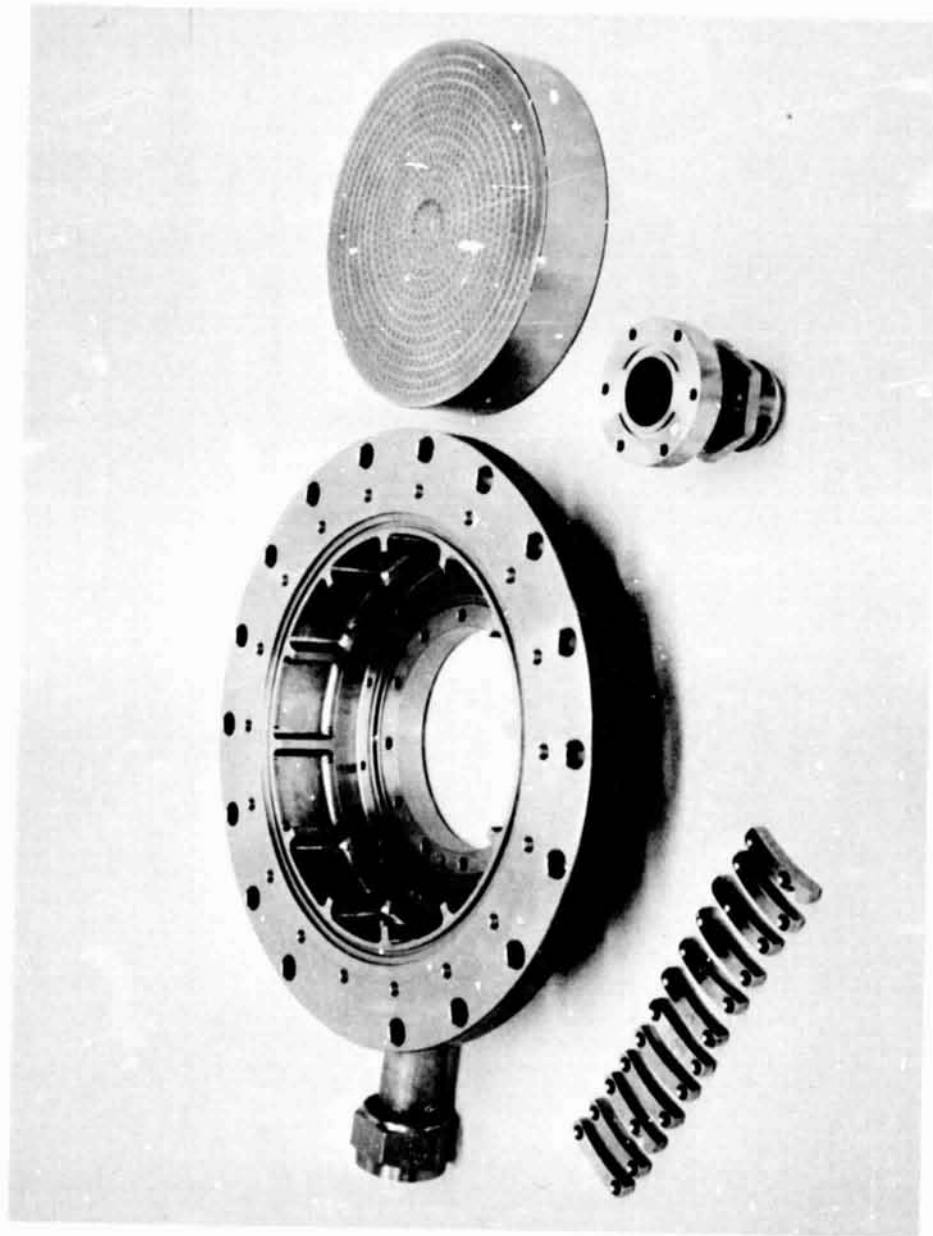


Figure 66. Full Scale Injector Assembly

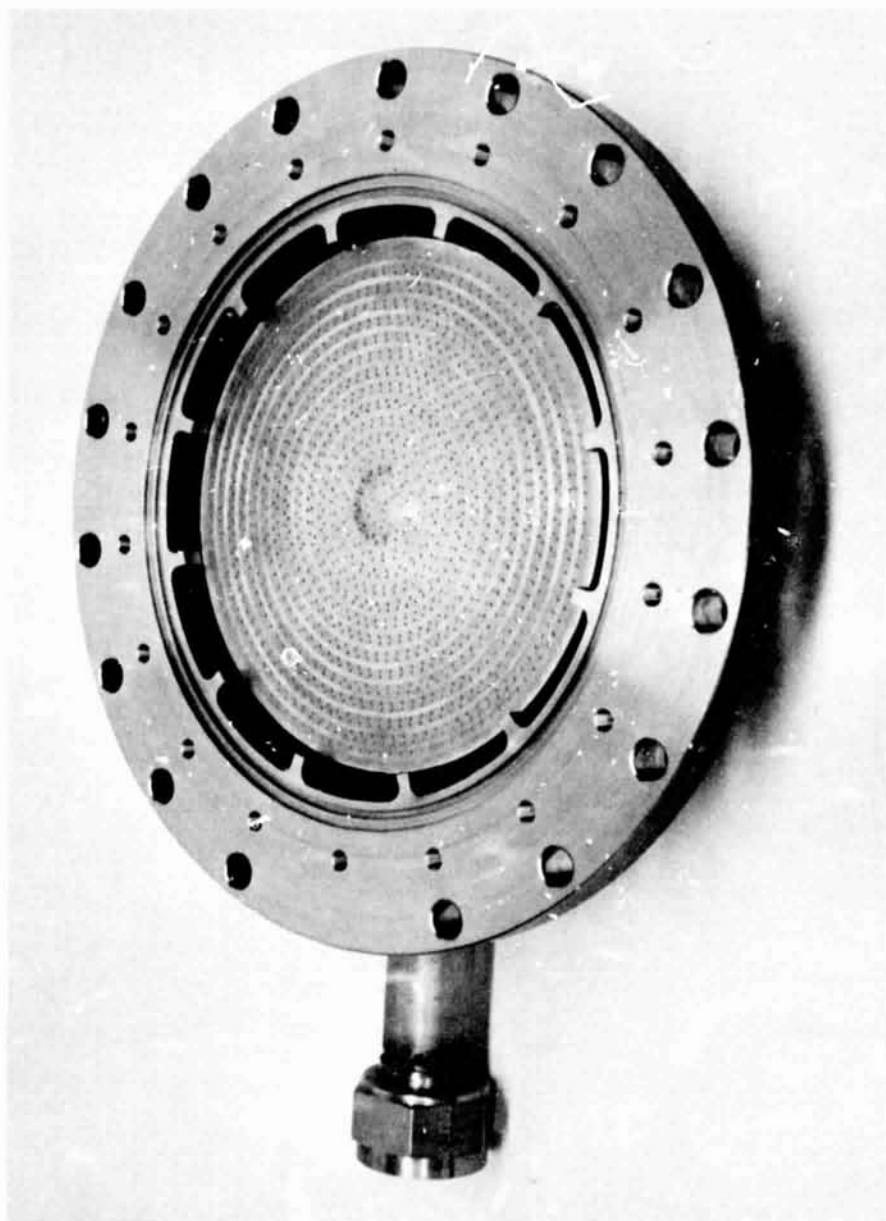


Figure 67. Full Scale Injector (Frontside)

ORIGINAL PAGE IS
OF POOR QUALITY

ORIGINAL PAGE IS
OF POOR QUALITY

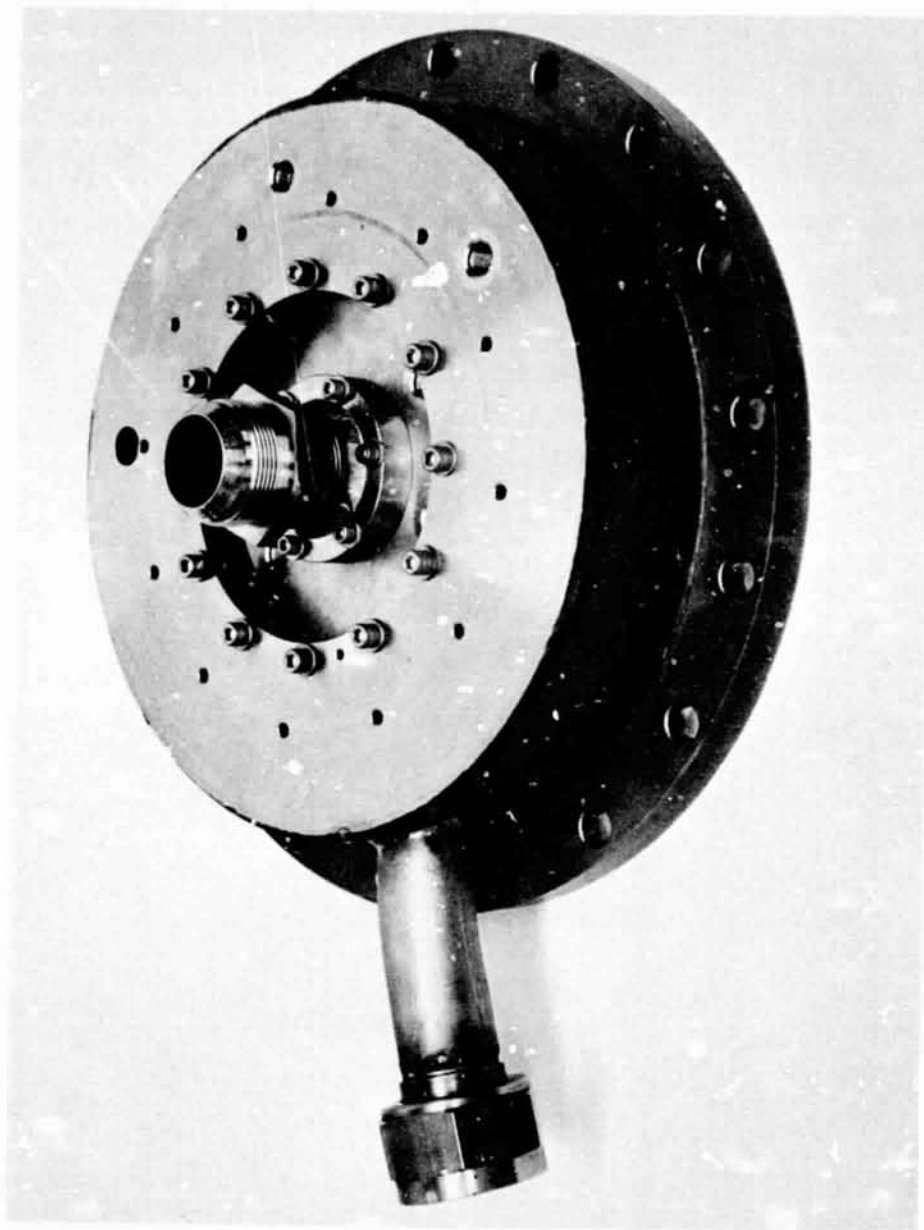


Figure 68. Full Scale XDT Injector (Backside)

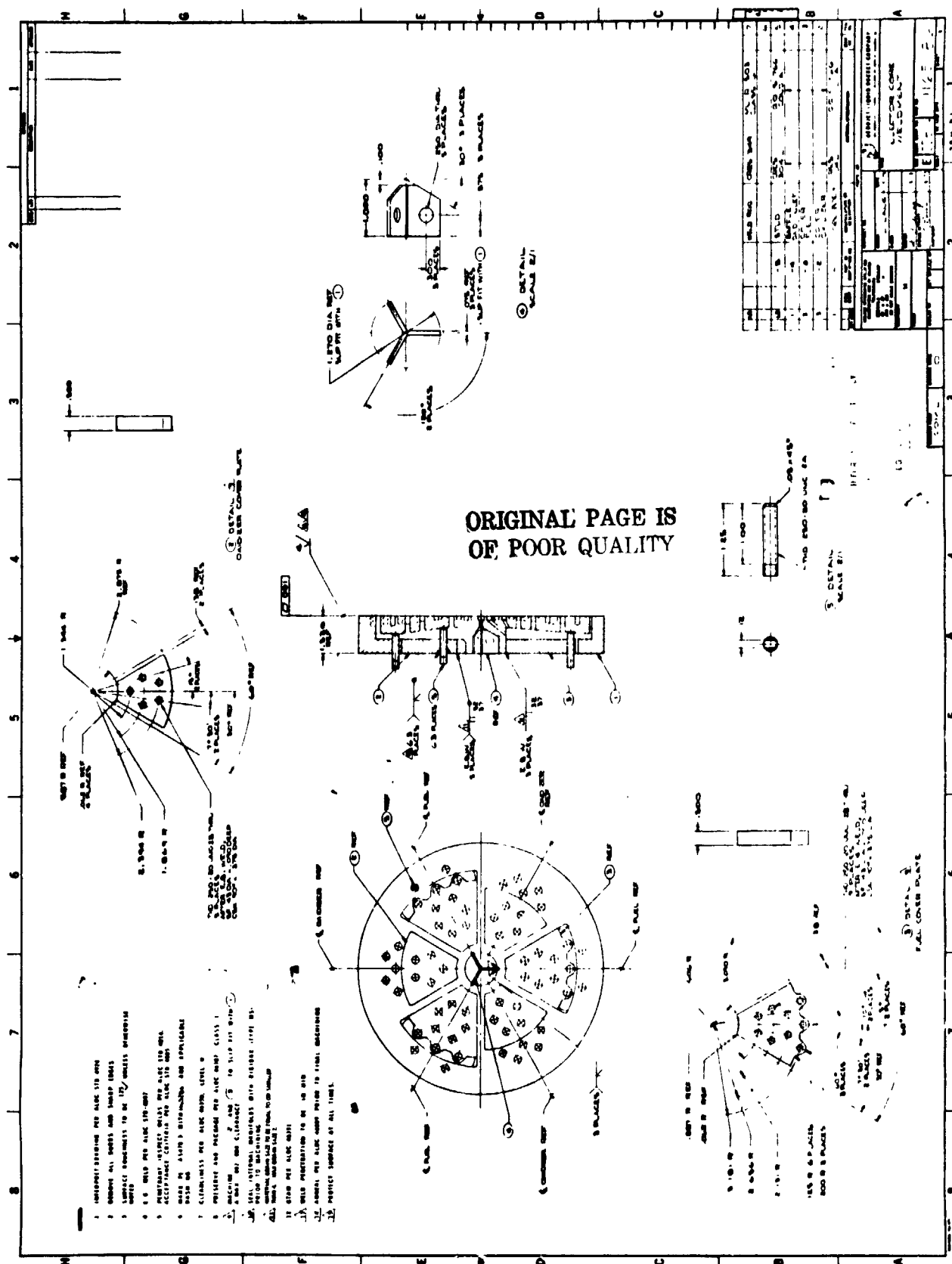


Figure 69. Demonstration Injector Design

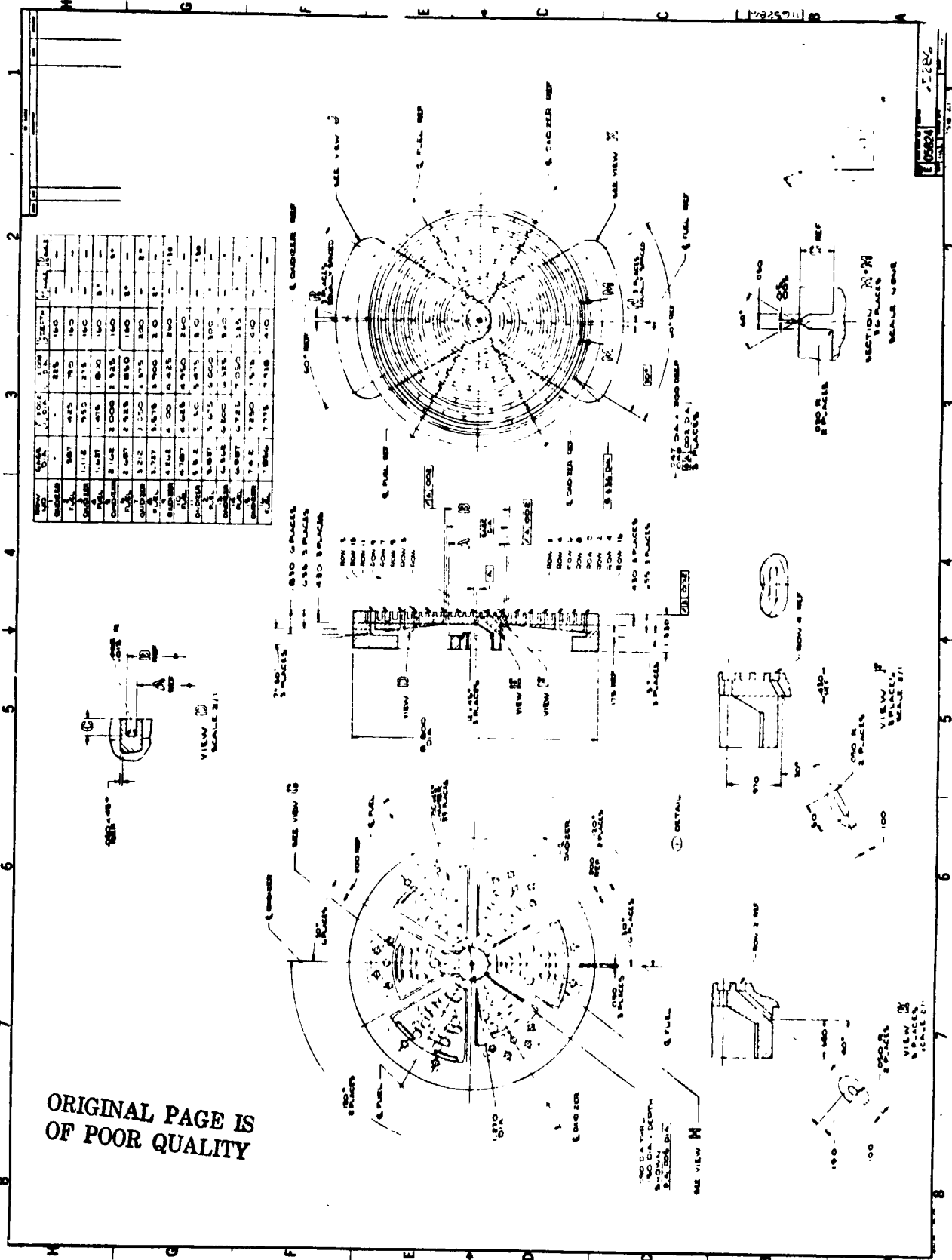


Figure 70. Demonstration Injector Nozzle

Report 13133-F-1

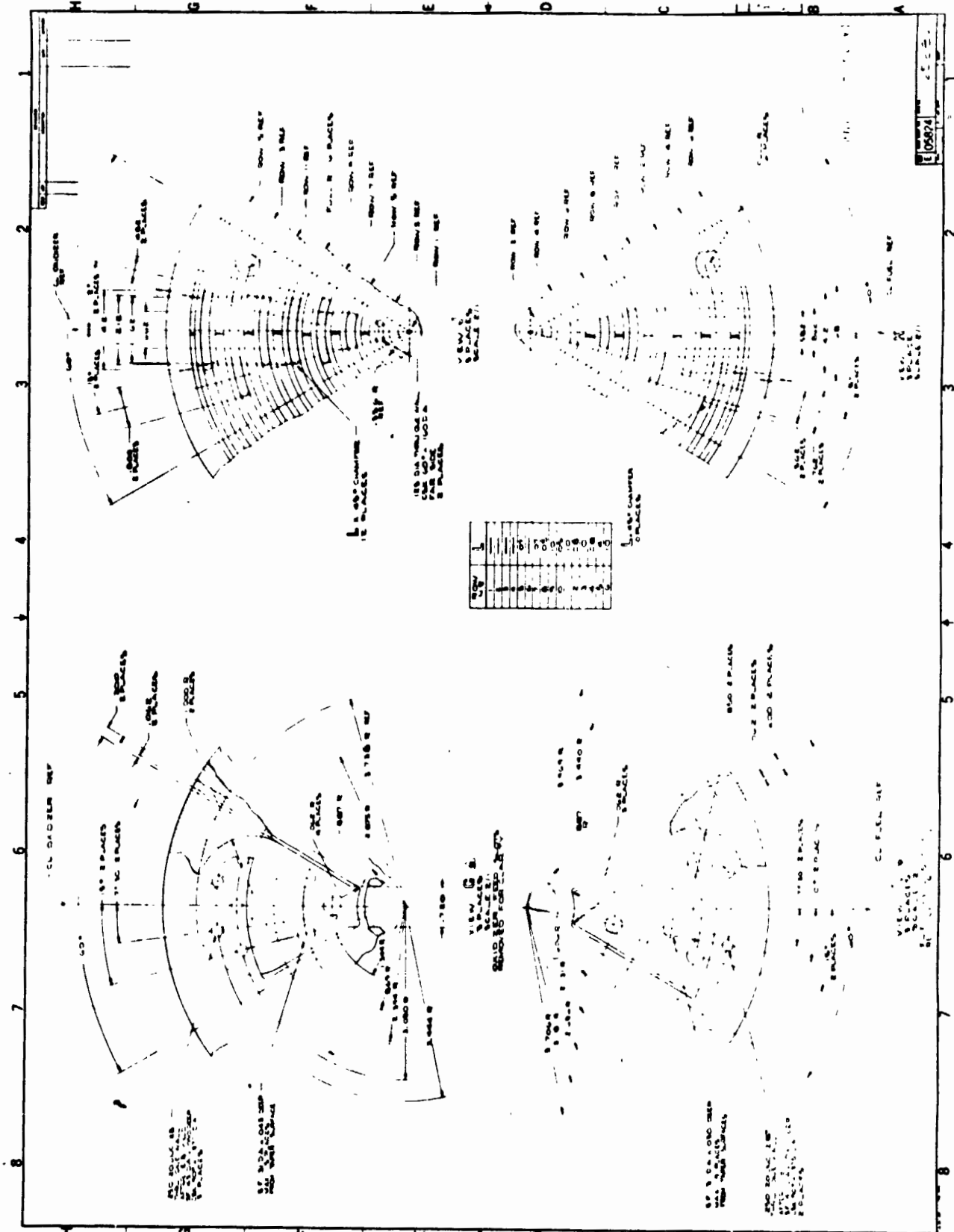


Figure 71. Demonstration Injector Design

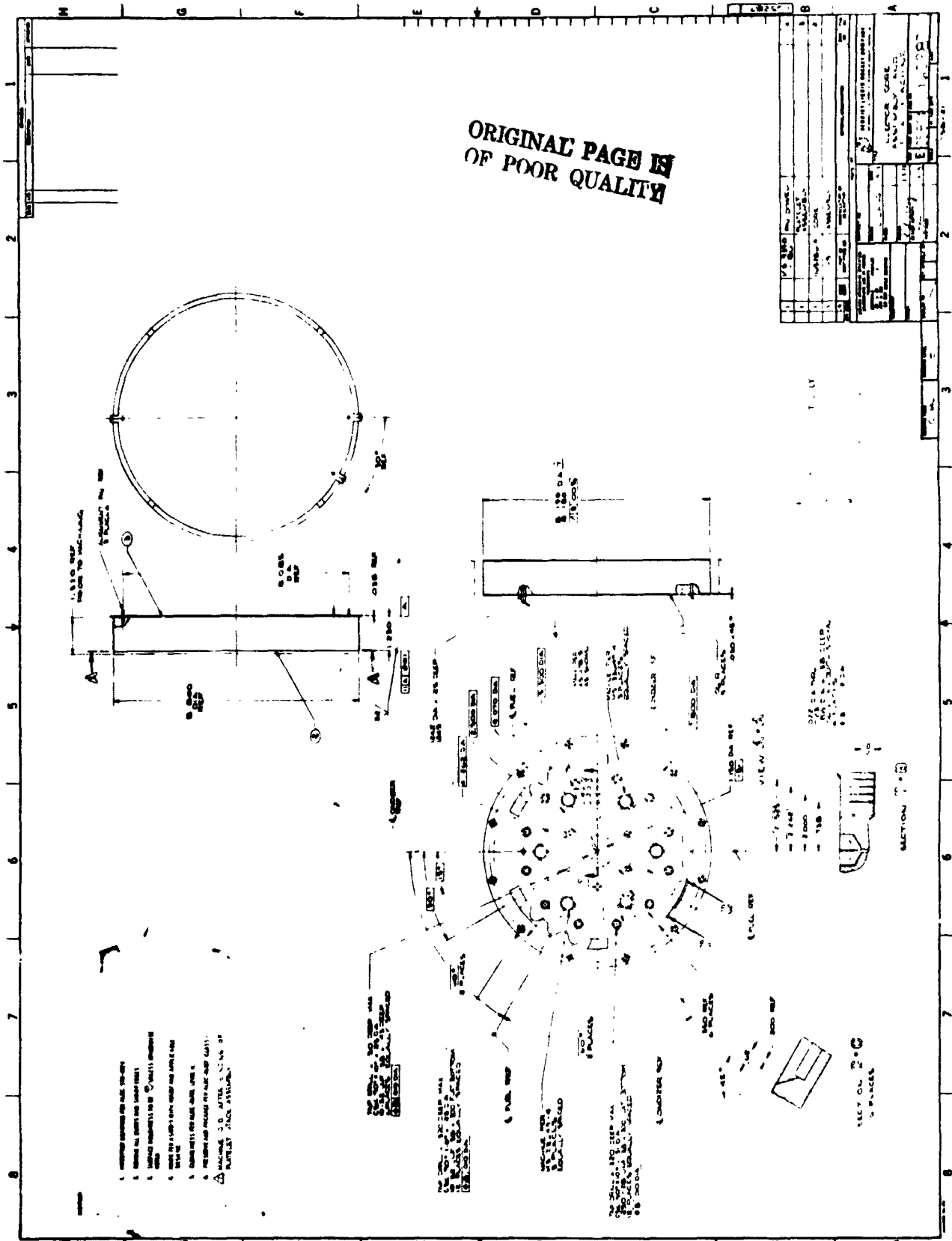


Figure 72. Demonstration Injector Design

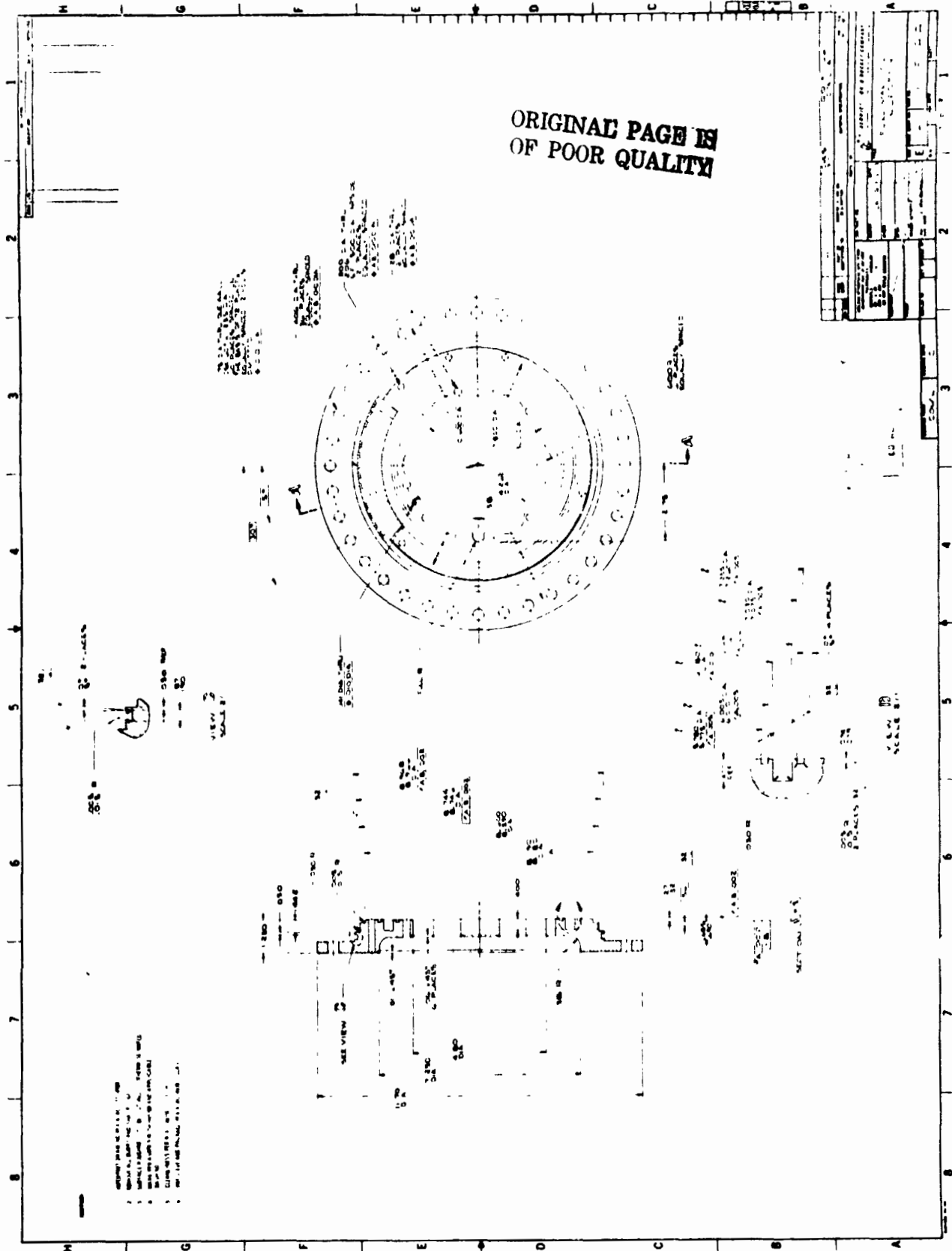


Figure 73. Demonstration Injector Design

IX,E, Injectors (cont.)

3. Injector Faces

0
0
The injector face consisted of a stack of six plates, varying in thickness from .006 to .008 in. These platelets were individually photo-etched and then bonded together to form a single platelet stack which was then bonded onto the injector body.

Testing focused on the XDT-1 and XDT-2 patterns, both of which were composed of 867 elements of the XD-0 variety, described under Unielement Testing, Section VII. Figure 74 shows the X-doublet pattern drawing and Figure 75 produces a photograph of the XDT-1 face.

The mixed element face consisted of both X-doublet and splash-plate elements. It was fabricated with the expectation that it might be higher performing than the X-doublet and more stable than the full splash plate pattern, shown in Figure 76. When this expectation was not fulfilled, testing of the mixed element was discontinued.

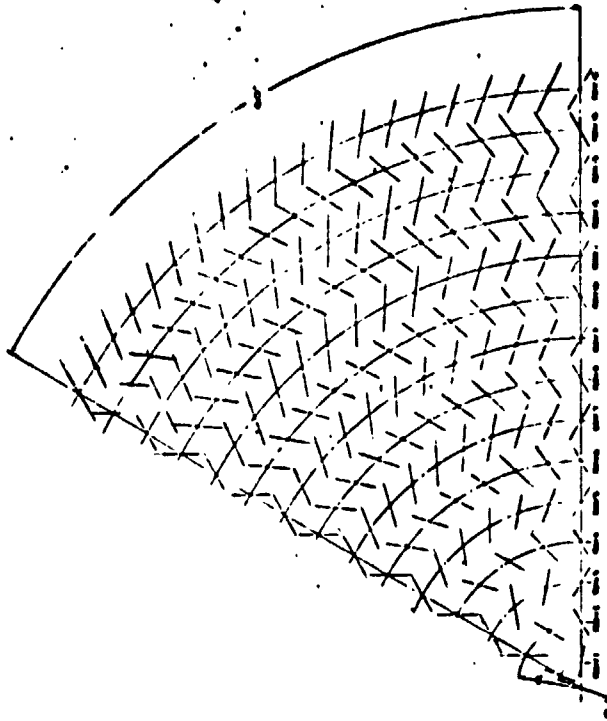
The mixed element-integral baffle unit was designed to produce a low heat flux environment to the oxidizer-cooled baffles. This injector is described in more detail in the next section.

The like-doublet consisted of 544 like-on-like injection orifices which were formed by electrical discharge machining (EDM). The face manifolds were concentric rings as in the platelet designs; "covers" to each manifold, through which the EDM holes were formed, were welded to the injector body.

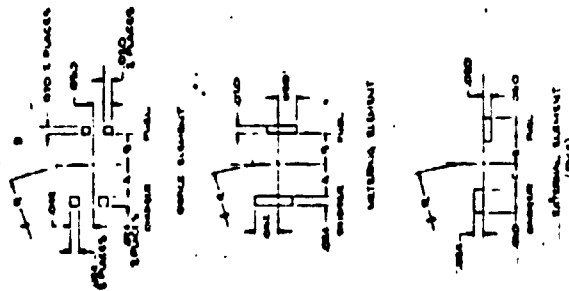
4. Integral Baffle Injector

The integral baffle injector featured three oxidizer cooled radial baffles which were integral with the injector body.

ORIGINAL PAGE IS
OF POOR QUALITY



our Doublet



Row	1	2	3	4	5	6	7	8	9	10	11	12	13	14	15
A	000	000	000	000	000	000	000	000	000	000	000	000	000	000	000
B	000	000	000	000	000	000	000	000	000	000	000	000	000	000	000
C	000	000	000	000	000	000	000	000	000	000	000	000	000	000	000
D	000	000	000	000	000	000	000	000	000	000	000	000	000	000	000
E	000	000	000	000	000	000	000	000	000	000	000	000	000	000	000
F	000	000	000	000	000	000	000	000	000	000	000	000	000	000	000
G	000	000	000	000	000	000	000	000	000	000	000	000	000	000	000
H	000	000	000	000	000	000	000	000	000	000	000	000	000	000	000
I	000	000	000	000	000	000	000	000	000	000	000	000	000	000	000
J	000	000	000	000	000	000	000	000	000	000	000	000	000	000	000
K	000	000	000	000	000	000	000	000	000	000	000	000	000	000	000
L	000	000	000	000	000	000	000	000	000	000	000	000	000	000	000
M	000	000	000	000	000	000	000	000	000	000	000	000	000	000	000
N	000	000	000	000	000	000	000	000	000	000	000	000	000	000	000
O	000	000	000	000	000	000	000	000	000	000	000	000	000	000	000
P	000	000	000	000	000	000	000	000	000	000	000	000	000	000	000
Q	000	000	000	000	000	000	000	000	000	000	000	000	000	000	000
R	000	000	000	000	000	000	000	000	000	000	000	000	000	000	000
S	000	000	000	000	000	000	000	000	000	000	000	000	000	000	000
T	000	000	000	000	000	000	000	000	000	000	000	000	000	000	000
U	000	000	000	000	000	000	000	000	000	000	000	000	000	000	000
V	000	000	000	000	000	000	000	000	000	000	000	000	000	000	000
W	000	000	000	000	000	000	000	000	000	000	000	000	000	000	000
X	000	000	000	000	000	000	000	000	000	000	000	000	000	000	000
Y	000	000	000	000	000	000	000	000	000	000	000	000	000	000	000
Z	000	000	000	000	000	000	000	000	000	000	000	000	000	000	000

Figure 74. X-Doublet Pattern

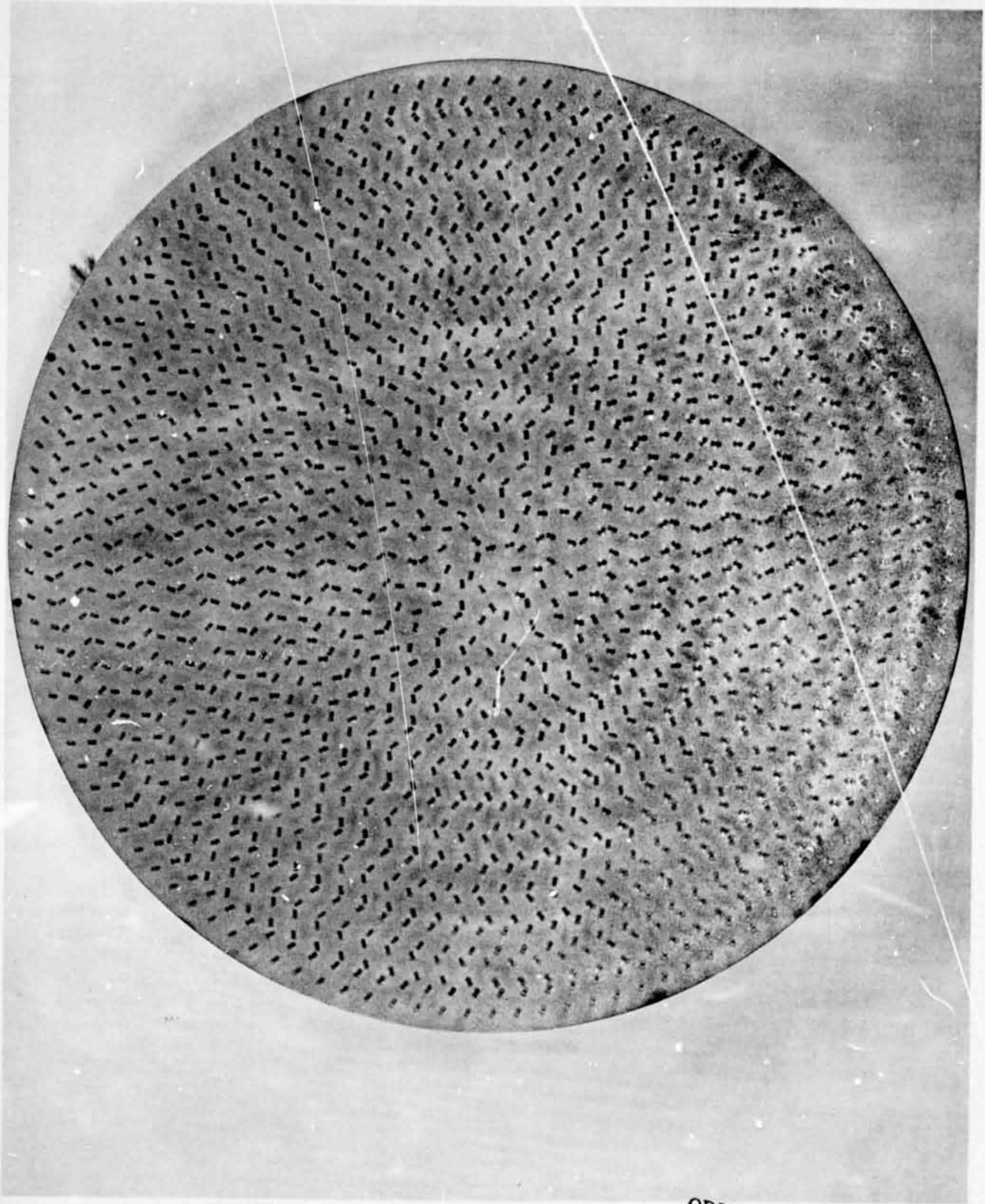


Figure 75. Demonstration Injector Face

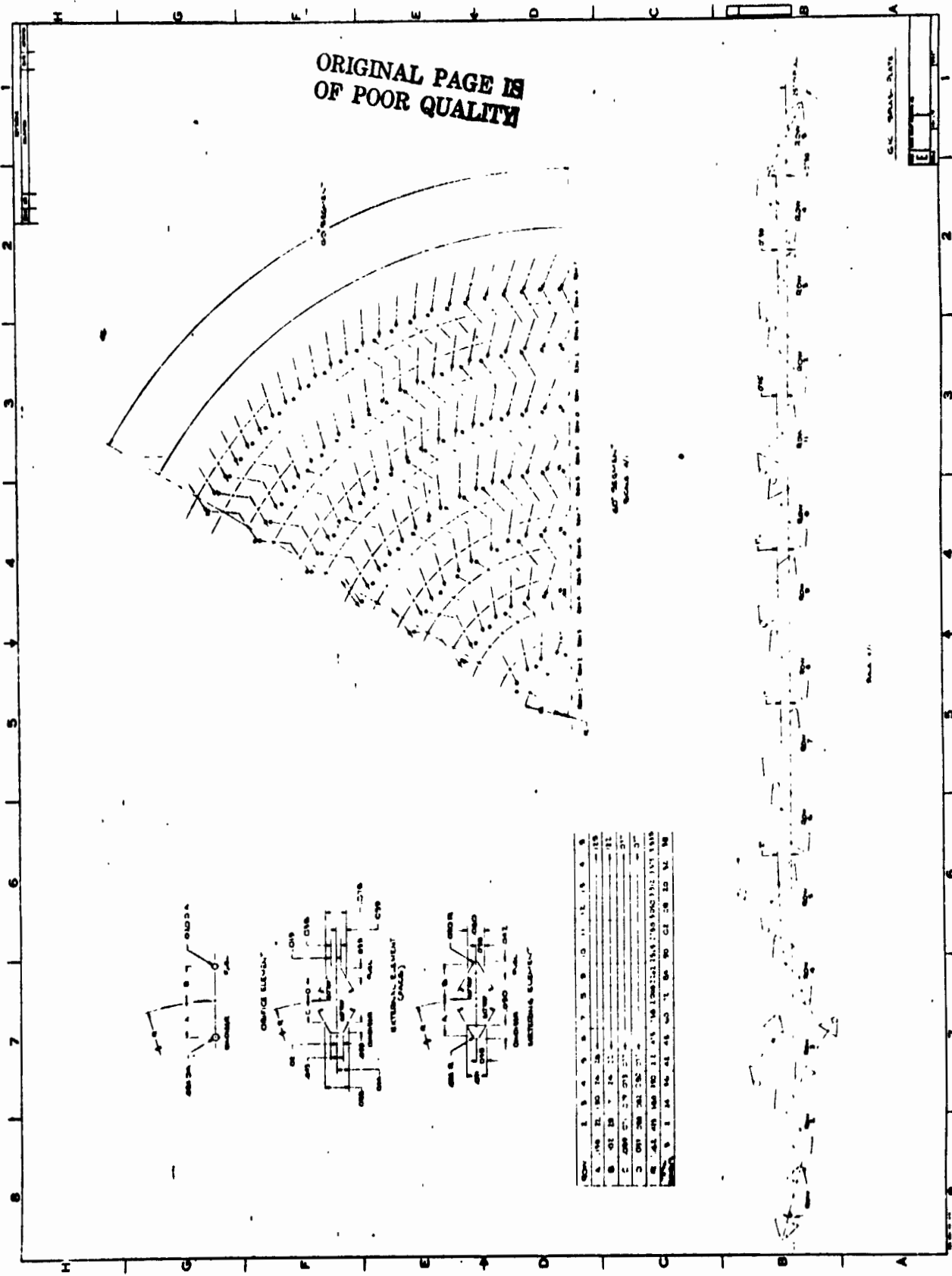


Figure 76. Splash Plate Pattern

Report 13133-F-1

IX, E, Injectors (cont.)

Figure 77 shows the body with baffles attached prior to bonding of the platelet stack. The platelets were photoetched and bonded together in the usual manner and then sectioned into three pie slices for bonding onto the body. The jig for applying the load to the face during the bond cycle is shown in Figure 78. The finished unit is pictured in Figure 79.

5. Testing

The chronology of injector testing is given in Figure 80 which can best be used in conjunction with Section F, Test Series Description, which follows. The chart shows the interplay between testing at ALRC -- all in the A-5 test facility except for the XDT-1 testing in the J-4 facility -- and WSTF. The chart also follows the history of the several injector bodies.

Table IX cites the test history of each of the injector faces and notes the disposition thereof. The like-doublet had 30 firings prior to being used on this program. The XDT-1C injector underwent another 52 firings during related testing at ALRC, following completion of the full scale testing discussed here.

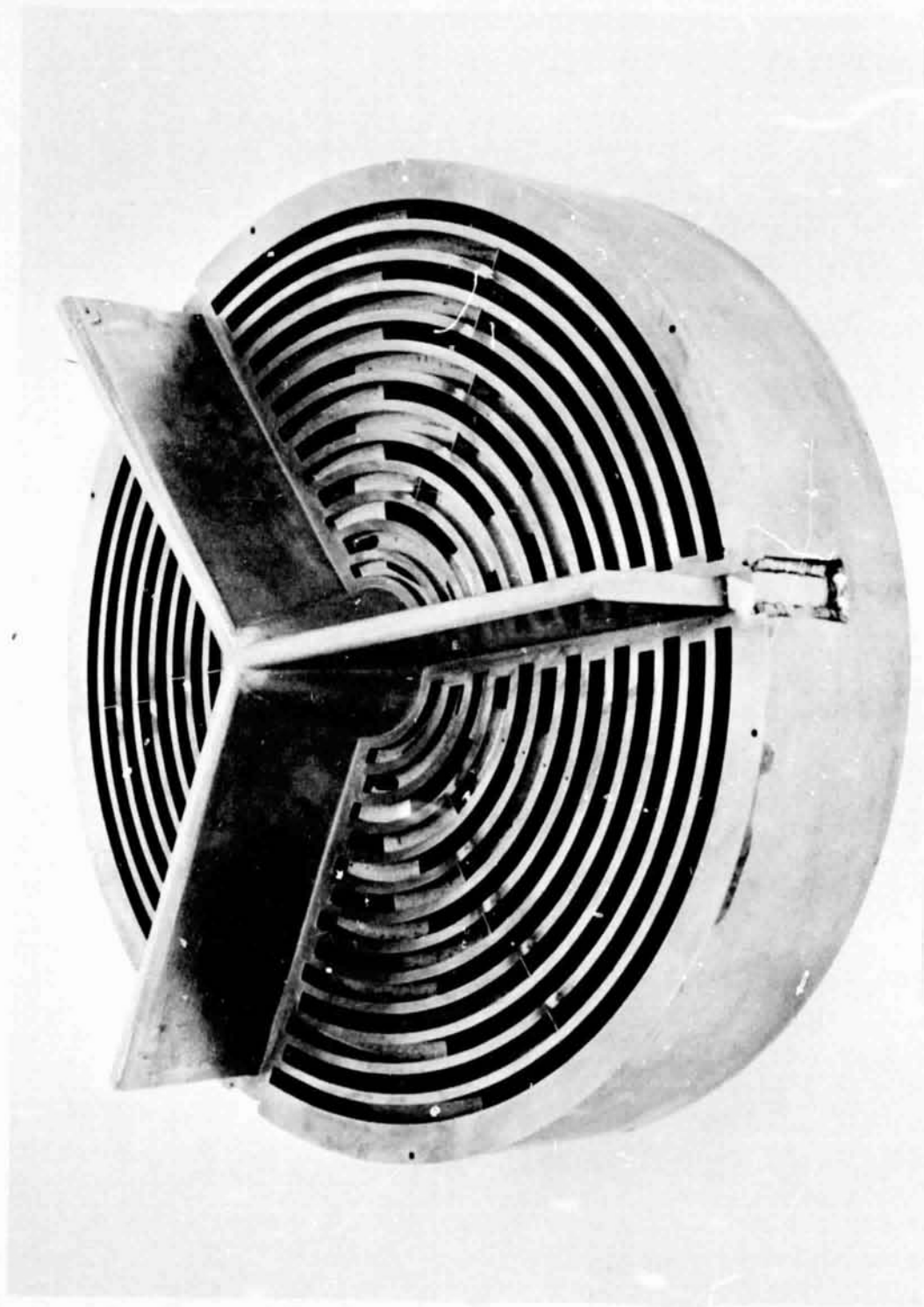


Figure 77. Integral Baffle Injector Core

ORIGINAL PAGE IS
OF POOR QUALITY

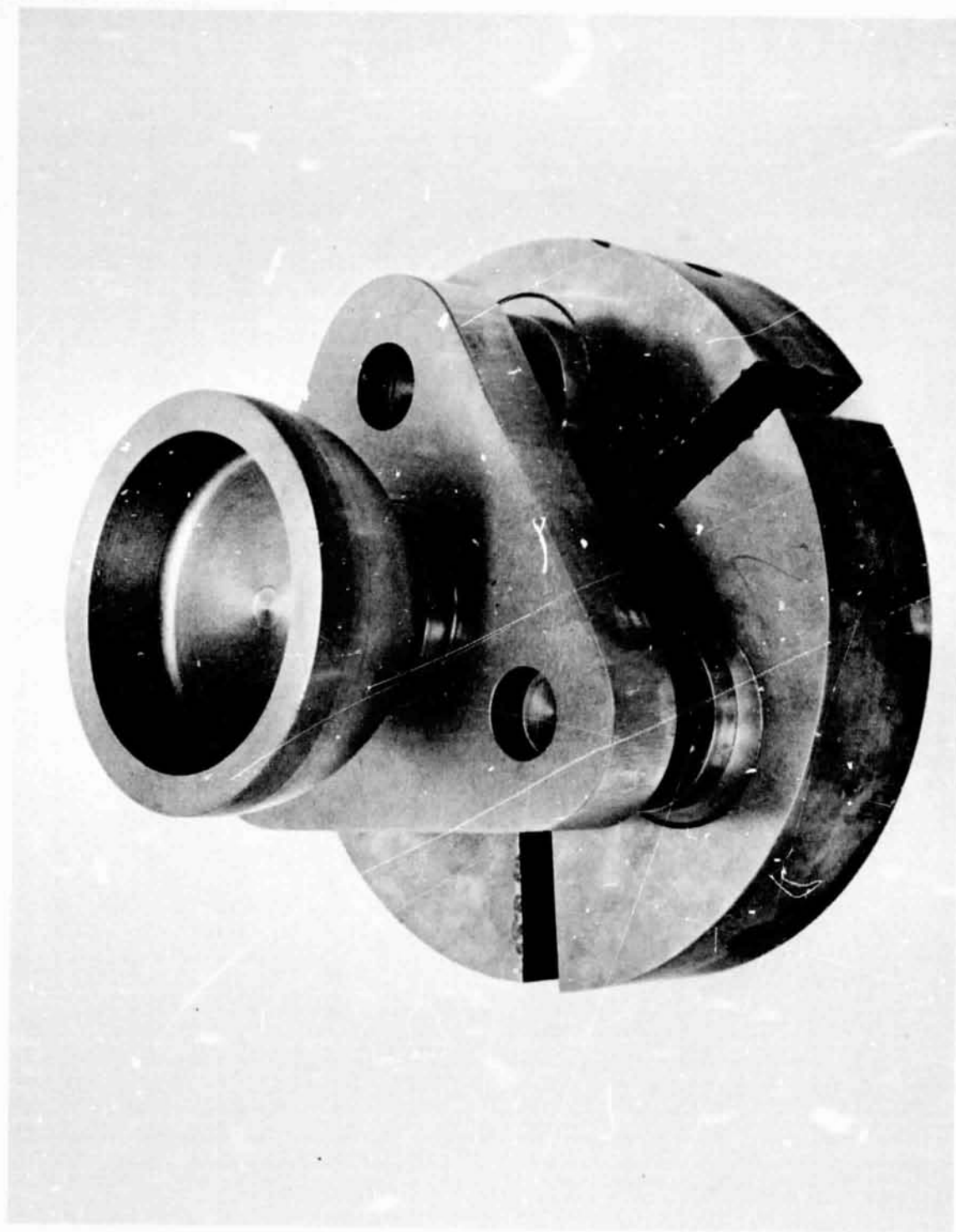


Figure 78. Jig for Bonding Integral Baffle Injector Face

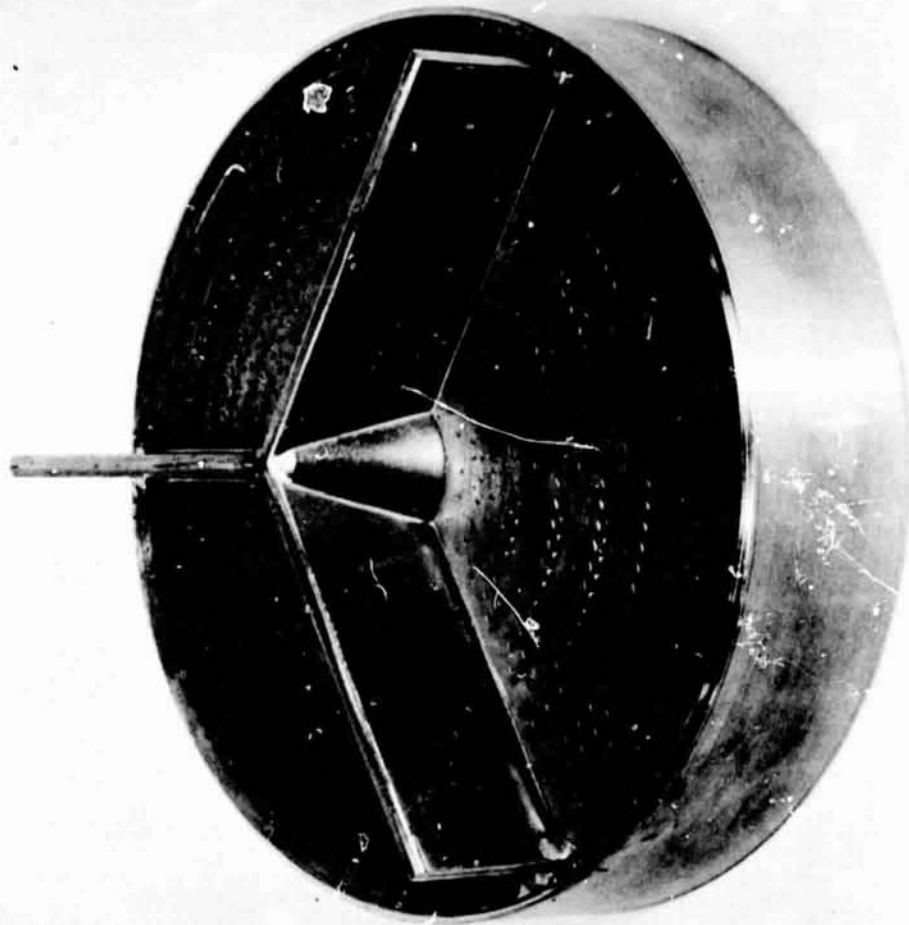


Figure 79. Integral Baffle Injector

ORIGINAL PAGE IS
OF POOR QUALITY

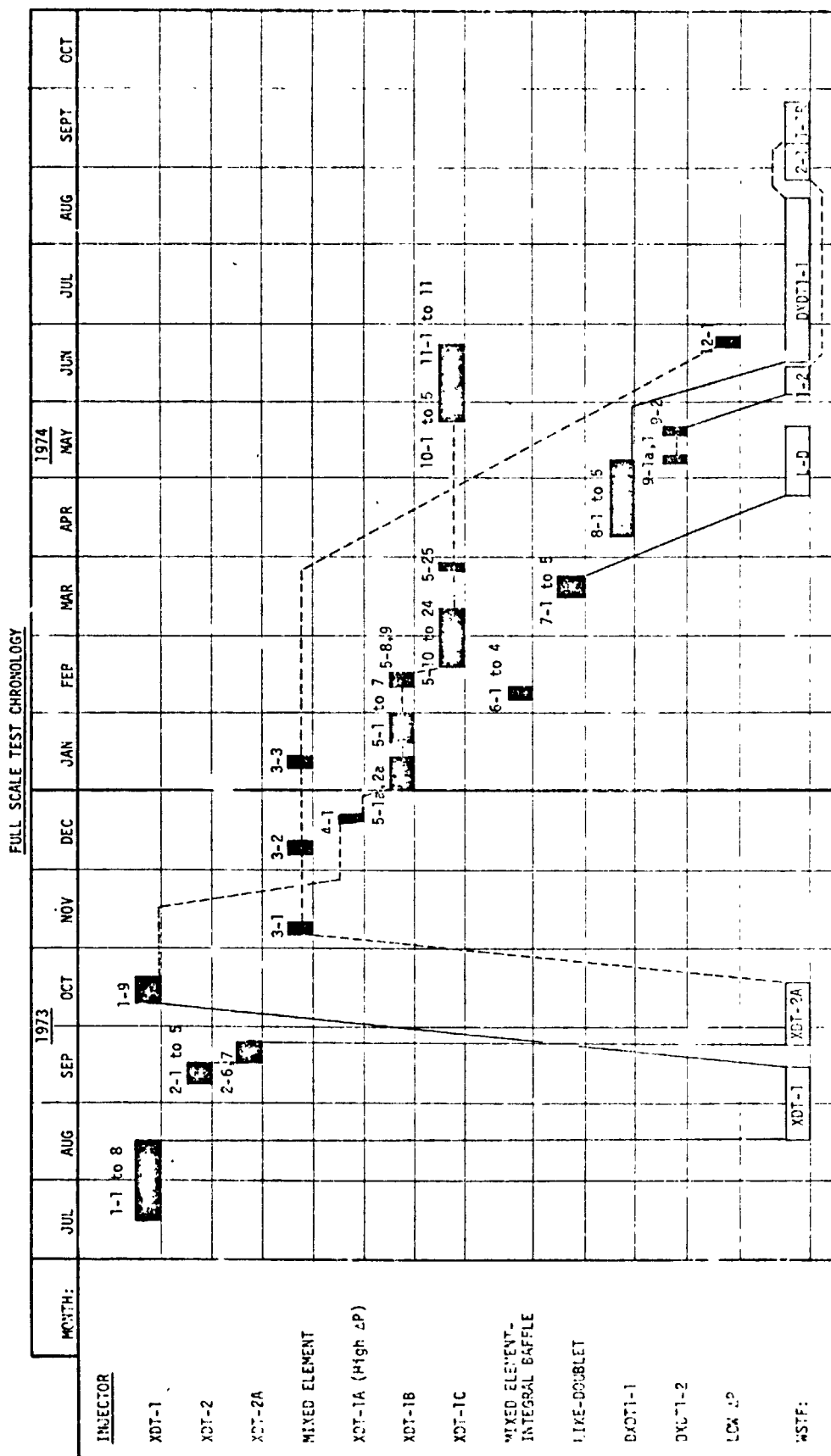


Figure 80. Full Scale Test Chronology

TABLE IX
INJECTOR SUMMARY

<u>Body</u>	<u>Face</u>	<u>Tested</u>	<u>No. Firings</u>	<u>Duration (sec)</u>	<u>Notes</u>
Workhorse #1	XDT-1	J-4	38	170	No face ring dams.
		WSTF	9	22	Unstable.
		A-5	5	10	Confirmed need for dams.
	XDT-1A	A-5	2	4	High injector pressure drop.
	XDT-1B	A-5	38	76	Face leak developed.
	XDT-1C	A-5	134	268	Evaluation of cavity configurations.
Workhorse #2	XDT-2	A-5	24	48	No face ring dams; stability "fixes" evaluated.
	XDT-2A	A-5	14	28	Dams installed; stability achieved.
		WSTF	54	620	Test objectives satisfied.
	Mixed Element	A-5	17	33	High performing, unstable
	Low ΔP	A-5	1	2	Interpropellant leak.
Integrated Baffle	-	A-5	12	24	Unstable
Like-Doublet*	-	A-5	18	36	Evaluation of cavity configurations
		WSTF	56	350	Test objectives satisfied.
Demo #1	DXDT1-1	A-5	33	68	Evaluation of cavity configurations.
		WSTF	76	448	Two orifices slightly burned.
	DXDT1-1R	WSTF	51	220	Also in 40 cold flow tests, 40 sec total duration.
Demo #2	DXDT1-2	A-5	26	52	Chamber length, bomb location, and stability evaluations.
		WSTF	13	90	Delaminated platelet stack, burned face.
	DXDT2-1	WSTF	41	181	Replaced with more representative unit.
			662	2750	

*IR&D residual

IX, Full Scale Testing (cont.)

F. TEST SERIES DESCRIPTION

What follows is a short description of each of the test series of the ALRC full scale test program. Since so much of the program was related to stability, the primary emphasis of this reporting will be on those factors which affected stability. As much as possible, the thoughts of the moment, i.e., at the time of testing, will be recorded. The resurging instability mentioned frequently in the description, is discussed in detail in Section XII, Full Scale Stability. The tables and figures of Section G, Test Summary, which follows, may improve the overall understanding of the test program.

1. Series 1, Pre-dam XDT-1 Injector

Testing commenced June 16, 1973, in the J-4 facility with the XDT-1 injector. Sequence 1 was primarily for checkout purposes and involved an 11 in. uncooled chamber with twelve cavities 1.2 in. long. This cavity depth was selected in an effort to obtain both 1-T and 2-T damping by using a cavity tuned midway between these modes. Two tests, 001 and 002, were conducted using ambient propellants. Performance was found to be low due to heavy concentrations of water in the oxidizer. Both tests were stable.

The oxidizer was replaced and testing continued with a 13 in. chamber in Sequence 2, which consisted of Tests 003, 004, and 005. Heated fuel was used. All three tests were unstable; 003 resurged in the 1-T mode; 004 demonstrated "footballing", and 005 showed a weak resurge with very high frequency, around 8000 Hz.

The cavity depth was then extended to 1.6 in. for sequence 3, to improve the 1-T damping; spontaneous instabilities in the 3-T mode resulted in two tests, 006 and 007. In all of the foregoing tests, a nominal mixture

IX,F, Test Series Description (cont.)

ratio of 1.9 was maintained in anticipation that the fuel film cooling would eventually be required, thus bringing about a nominal overall value while the core operated at the higher value tested.

At this point, it appeared that cavities for the 3-T mode were required. A bolt-on cavity housing was installed; it contained twelve radial cavities 0.9 in. long. Sequence 4 followed, comprising tests 008 through 018. These were run over a matrix of operating points with heated fuel. The first five tests, 008 through 012, were spontaneously unstable with resurging. At the time, the resurging characteristic was thought to be a classical chugging mode, that is, a feed system-linked instability, and to eliminate it, high pressure drop orifices were installed in both propellant circuits immediately downstream of the valves, following Test 012. Thereafter for the first time, stability bombs were used in testing; all of the latter tests of the sequence were bombed with cork encapsulated 6.5 grain RDX bombs located 2 in. from the face. These bombs were triggered by an electrical detonator controlled by the engine sequence computer. The cost per bomb was approximately \$50. All tests were stable, although on Test 015, a brief resurge followed the bomb. Thus there seemed to be ample justification to ascribe the instabilities to a chugging mechanism, since the orifices virtually eliminated unstable tendencies.

The chamber length was then shortened to 11.7 in. for Tests 019, 020, and 021 -- Sequence 5 -- which ensued. Test 012, which a relatively low mixture ratio test, showed resurging.

Film cooling was added to the next sequence of tests and the chamber length was increased to 14 in. All tests of this group, Sequence 6, which comprised tests 022 through 026, were stable. Film coolant flow rates ranged from 9 to 15% of the fuel.

The chamber length was shortened to 13 in. for the next Sequence, 7, consisting of Tests 027, 028, and 029. The film coolant flow was 8% of the fuel and all those firings were stable although an erroneous CSM shutdown occurred on the first test.

Report 13133-F-1

IX,F, Test Series Description (cont.)

0
0

The workhorse, or A-1, regenerative chamber was used for the first time in the next sequence of tests, Sequence 8, which was the last sequence to be conducted in the J-4 Test Facility. Nine firings were made, the last four with film cooling to ensure chamber integrity. A brief resurge was experienced at 0.5 sec into Test 031 but the system recovered and the test continued for 18 sec duration. Two small resurges occurred during Test 034, following which an EB-weld failure was noted on the film coolant ring. Test 035 showed a resurge, which actually had more the appearance of a pop, and Test 036 had a "blip" or small pop. It was hypothesized that the "blips" and other minor perturbations were due to tank pressurant coming out of solution as the fuel passed through the cooling jacket as a result of the long delay between tests causing vapor bubbles to be ingested into the chamber. Test 037 was therefore conducted on a quick turnaround basis following Test 036; as was hopefully expected, there were no perturbations. Before this hypothesis could be tested further, however, it was recognized that the fuel circuit pressure drops were gradually changing. The coolant jacket pressure drop was decreasing and the injector pressure drop was increasing. This trend was evident during an individual test as well as between tests. Wax used to fill the coolant channels during the electroforming of the outer chamber was suspected of being still present and melting. Test 038 ended with 430 Hz chugging. Testing was thereupon terminated. The need to flush the wax both the chamber and the injector was evident; a gate valve had to be replaced, and most important, the WSTF test stand had become available for use. Postfire flushing proved that wax had remained in the coolant channels of the chamber and had passed into the injector, in which about 20% of the fuel orifices were plugged. Thus the blips were credited to wax plugging the orifices, perhaps in conjunction with pressurant coming out of solution.

2. Series 2, XDT-2 Injector

Following cleansing of the wax from the chamber and XDT-1

Report 13133-F-1

IX,F, Test Series Description (cont.)

injector, both units went to WSTF for testing. The WSTF work is reported separately¹ and will not be discussed in detail here. The XDT-1 injector did show a recurrent 430 Hz instability that could not be stabilized even with the installation of 50 psi orifices in the propellant circuits. Testing was temporarily suspended at WSTF and resumed at ALRC's A-5 Test Facility, with the XDT-2 injector. This injector differed from the XDT-1 only in the outer row of elements.

In Sequence 1 of Series 2, there were two checkout tests using ambient fuel, both stable. The cavity configuration used contained eight 1-T cavities 1.6 in. long and four 3-T cavities 0.5 in. long, with square inlet and corner contours and a 0.126 in. injector overlap. The chamber length was 11.7 in. for these tests.

In the following sequence, Number 2, the same hardware was used but tests were conducted over the matrix of mixture ratio and chamber pressure points and the fuel was heated to 200°F. Of the first seven tests Numbered 103 through 109, only one was stable with some evidence that the problem was a feed system-linked instability. To eliminate the participation of the fuel circuit with the combustion process, an accumulator can was added to the fuel circuit; this can had a 6 in. diameter, was 12 in. long, and was orificed at its outlet. In addition, a " ΔP ring" was installed in the injector fuel manifold to increase the system pressure drop, as shown in Section XII. Also, three dams were added to the fuel manifold upstream of the injector pies to eliminate crosstalk. The pies were still in acoustic contact via the face ring manifolds at this point; however, Test 110 which followed was stable and the orifice in the fuel accumulator can was subsequently removed.

¹WSTF Test Report, Report No. 13133-5-1, 12 December 1973

Report 13133-F-1

IX,F, Test Series Description (cont.)

0
0

The three tests of the following sequence 3, were all unstable. Radial cavities for the 1-T mode were added at that point, there being twelve cavities 1.9 in. deep in the radial housing, and an orifice was added to the oxidizer circuit.

Sequence 4, consisting of Tests 114 through 119, was run over a matrix of operating points. Ambient fuel was used in the first two tests, heated fuel in the last four, two of which were unstable. The radial 1-T cavity housing was then replaced by the axial unit, and an accumulator can was also added to the oxidizer circuit. The can installed on the fuel circuit after Test 109 was still in place.

Sequence 5 had five tests, the last four of which used heated propellant. Two of them were unstable. It became clear that these "little fixes" were not eliminating the supposed feed system-linked instability and that the one remaining circuit of acoustic communication in the propellant systems -- the face ring manifolds which formed a series of unbroken circumferential paths around the face from pie to pie -- had to be eliminated. The face of the injector was machined away and three dams welded into each ring manifold at the null point under the opposite propellant pie. An identical face was bonded back on and the unit designated XDT-2A. The entire rework process was accomplished in less than three days.

The next sequence of tests, Sequence 6, consisted of eight tests numbered 125 through 132. The 1-T cavity was shortened to 1.5 in. from 1.9 in. but otherwise the configuration was identical to that of the previous group of tests. The first six tests were all stable, over a matrix of operating points, and so the orifice in the oxidizer line was removed. The two tests which followed were stable, although one of them had three postbomb blins. All firings of the sequence were bombed. Another sequence (7) of firings

Report 13133-F-1

IX,F, Test Series Description (cont.)

ensued, this time with a 16 in. chamber. Six tests, 133 through 138, were conducted over a matrix of operating points. All tests were bombed and all were stable although on the last test there were two postbomb blips. The ring dams were thus judged to be the critical factor in remedying the feed system-linked instability and the injector shipped back to WSTF for continued testing at that facility. At WSTF there followed 54 firings of more than 600 sec duration without incident. The XDT-2 pattern was consequently considered to be the primary candidate for demonstration ("demo"), or prototype, injector testing on the OMS hardware.

To close the loop of the test logic, the XDT-1 injector was returned to the A-5 test stand and fired with the same cavity and feed system configuration as was used previously in Sequence 7 at the XDT-2 testing. This sequence of tests on the XDT-1, without ring dams, is designated herein as Sequence 9 of Series 1, and is thus grouped with the first eight sequences discussed above for that injector. All five tests of the sequence came out unstable, which seemed conclusive proof that the ring dams had eliminated the resurging problem.

At this point, a "baseline" cavity configuration consisting of eight 1-T cavities 1.5 in. deep and four 3-T cavities 0.4 in. deep had become established.

3. Series 3, Mixed Element Injector

Upon completion of the WSTF testing, the face of the XDT-2A injector was removed and replaced with the mixed element pattern. The first sequence of tests comprised ten firings, numbered 144 through 153, and was conducted over the matrix of operating points. All except the first test involved heated fuel, and all firings were bombed. The baseline cavity con-

IX,F, Test Series Description (cont.)

figuration was used in the first two tests; the first firing went unstable with resurging going into the 1-T mode; the second was spontaneously unstable in the 2-T mode. To get better 2-T coverage, the 1-T cavity depth was reduced from 1.5 to 1.2 in. The following test, 146, was spontaneously unstable in the 2-T mode. The 3-T cavity depth was then increased from 0.4 to 0.6 in., whereupon Test 147 was unstable in the 3-T mode. The 1-T depth was further reduced to 0.95 in. and the 3-T depth lowered to 0.35 in. Again, on Test 148, there was an instability in the 2-T mode. The bolt-on radial cavity was installed to provide 2-T coverage; it consisted of twelve cavities 1.2 in. deep and had an entrance area equal to 20% of the face area. The following five tests were stable although an erroneous CSM shutdown occurred on Test 151.

Sequence 2, which followed with the same cavity arrangement, was run specifically to see if the A-50 could be substituted for MMH as the fuel. The results proved negative: both tests of the sequence (154 and 155) were unstable.

Sequence 3, consisting of tests 168 through 172, was undertaken to obtain heat flux and performance data with a short chamber of 12 in. length. The cavity configuration was unchanged from the two prior sequences. The intended result was to determine the trade-off between heat loss to the wall, or equivalently bulk temperature rise with a cooled chamber, and performance. Instead, three of the firings proved spontaneously unstable and a fourth was bombed unstable. Further testing of the mixed element was discontinued. The pattern was concluded to be very high performing - 319-320 seconds specific impulse - but rather inclined toward unstable operation.

4. Series 4, XDT-1A (High ΔP) Injector

During the mixed element testing, the XDT-1 injector underwent face removal, had dams welded in the ring manifolds as was done with the other

Report 13133-F-1

IX,F, Test Series Description (cont.)

unit, and was refaced with an XDT-1 platelet stack. The refurbished injector was designated XDT-1A. Because of underetching of the orifices -- by 0.0010 to 0.0015 in. on all dimensions -- the pressure drop was about 20% high for both propellants. Consequently, the injector was only tested twice, in Tests 156 and 175. It was stable in both tests but was low on performance.

5. Series 5, XDT-1B Injector

The face of the XDT-1A injector was replaced with a correctly etched identical pattern and the unit was then called the XDT-1B. Sequence 1a of the XDT-1B testing consisted of Tests 158 through 164 and was run over the usual matrix of operating points with the baseline cavity configuration and 16 in. chamber. All seven firings were bomb-stable.

Sequence 2a was a chugging evaluation and comprised Tests 165 through 167. Two of the firings, with chamber pressures of 66 psia, chugged; the third, with a chamber pressure of 76 psia, did not chug. These first two sequence numbers were both assigned a letter subscript to differentiate them from the following sequences which were numbered identically at the time of testing.

The next test series was designed to evaluate stability margin. The intent of this series was to establish the minimum cavity area required for stable operation by systematically reducing the cavity area and changing tune to determine the minimum area and optimum tune configuration. From this the design margin of the baseline cavity, in terms of cavity area, could be established. Also, to this point all testing had been done with the square-entrance workhorse cavity configuration. A question existed as to the possibility of employing a contoured inlet with the regeneratively cooled chamber being designed for testing at WSTF. Sequence 1 was the first testing of the

Report 13133-F-1

IX,F, Test Series Description (cont.)

contoured cavity inlet and involved six tests (173 through 178) in a survey of operating point conditions. The cavity areas had been reduced to 15.2% and 8.1% on 1T and 3T cavities respectively as the first step in the design margin testing. The chamber was bombed in every firing; Test 173 was marginally stable and resurges were experienced on Tests 175 and 178, with the resurging going into pure 1-T on Test 175. Since the cavity depths were comparable to those of Sequence 1a, but the area percentages were less, the 1-T cavity area was increased to correspond to that of Sequence 1a to determine whether the instability was the result of the decreased 1T cavity area.

Sequence 2 which followed consisted of 3 firings, Tests 180 through 182, all bomb-unstable with resurging. The 3-T cavity area was increased to agree with the baseline configuration.

Sequence 3 had four firings, Tests 183 through 186, which were bombed unstable. The bomb failed to explode on Test 183 which was the stable test. Since the pertinent cavity parameters, length and open area, were now the same for the contoured inlet cavity as for the rectangular inlet baseline, it was quite clear that the inlet configuration was itself an important factor, for reasons not totally clear at the time. The question arose as to whether the change in contour was equivalent to a change in effective cavity length. Based on a power spectral density analysis of the data obtained from the high frequency transducer in the 1-T cavity, it was considered necessary to shorten the cavity to bring it into tune. Thus, the following four sequences each investigated incremental reductions in the 1-T cavity length.

In Sequence 4, the cavity was reduced to 1.25 in. from 1.50 in. In three firings, Tests 187 through 189, there were two bomb induced instabilities. In Sequence 5 the cavity was further reduced to 1.07 in., and both tests of the sequence were bombed unstable. Sequence 6 had two firings, Tests 192 and 193,

IX,F, Test Series Description (cont.)

with a 0.825 in. 1-T cavity, and both were bombed unstable. Throughout these sequences, the frequency of the 1-T mode was increasing. Finally, in Sequence 7 the 1-T cavity depth was reduced to 0.535 in. and the 3-T depth to 0.212 in. from 0.43 in. Following the first firing, Test 194, which was unstable, a local fuel leak at the periphery of the injector -- at the bond line of the platelet stack and the injector body -- was discovered and the testing stopped for injector rework. During the progress of these five sequences it became apparent that the high frequency measurements were being compromised by the cavity tuning block. Subsequently, the transducer ports entered directly into the cavities rather than passing through the adjustable tuning blocks at the end of the cavities. In any event, it was quite apparent that there exists a frequency depression with increasing cavity depth, as was hypothesized some time earlier.

6. Series 5, XDT-1C Injector

The face of the XDT-1B injector was machined off and replaced with an identical face; the unit was now called the XDT-1C injector. Sequence numbers were continued consecutively following the XDT-1B test sequence 7. e.g., the first sequence of XDT-1C testing was labeled number 8. It consisted of six checkout firings, Tests 206 through 211, over the matrix of operating points; the baseline rectangular cavity configuration was used to confirm the stability and performance characteristics of the basic injector pattern. All six tests were bomb-stable.

The following sequence, 9, had only one test and confirmed the stability of the unit with 1.9 in. 1-T cavities in place of the 1.5 in. cavities used in the previous sequence.

Thereafter, the rectangular inlet cavities were replaced with the contoured inlet cavities. The 1-T depth was maintained at 1.9 in. and the open

Report 13133-F-1

IX,F, Test Series Description (cont.)

area kept at 19%. The object of the next sequence, Tests 213 through 218, was to determine whether the fuel leak experienced with the XDT-1B injector testing was a contributing factor to the instabilities experienced, since the raw fuel was squirting directly into the cavity region, or whether the instabilities were entirely due to effects brought about by the contoured inlet. Two firings of Sequence 10 were marginally stable, showing postbomb resurges: six on Test 216 and two on Test 218.

The I-T cavity depth was reduced to 1.5 in. for Sequence 11, which consisted of Tests 219 and 220. The first was marginally stable with two postbomb resurges, and the second was bombed unstable with resurges going into the I-T mode. Thus, the destabilizing effect of the contoured inlet was confirmed.

There followed a dozen sequences to determine exactly what factors were being influenced by the inlet configuration. The first approach was to determine whether the contoured inlet with its cleaner hydraulic configuration was resulting in reduced kinetic energy dissipation of the jet flowing into and out of the cavity and thereby reducing the cavity damping. Thus, most of the geometrical changes made in subsequent sequences involved inlet variations resulting in significant alteration of the flow resistance.

The first of these sequences, 12, involved the partial contour inlet configuration (Figure 114). Tests 211 through 225 of this sequence were all bomb-stable.

Sequence 13 utilized a restricted inlet area configuration. This restricted inlet configuration was calculated to have the same effective flow area ($C_p A$) as the square inlet and thus addressed whether the ratio of flow area to cavity volume was a significant parameter. Generally, as the inlet area of a cavity is reduced, the cavity begins to behave more like a Helmholtz resonator and less like a quarter wave tube. Of the four tests, Numbers 226

Report 13133-F-1

IX, F, Test Series Description (cont.)

through 229, three were bomb-stable and the fourth, wherein the fuel temperature was significantly higher, was marginal. It showed two postbomb resurges. This sequence indicated improved stability over that obtained with the contoured inlet. However, it still left an open question as to whether it was the changed inlet contour or the shift downward in cavity tune resulting from the restricted inlet which was the stabilizing factor. This led to Sequence 14.

With the same inlet configuration but a shortened 1-T cavity, the single test of Sequence 14 was conducted. This test was intended to determine whether the restricted contoured inlet of Sequence 13 and the normal contoured inlet behaved the same at similar cavity tune conditions. Following the bomb, the system went into the 1-T mode.

At this point it appeared the injector was very sensitive to cavity tune. To verify this, the partial contour was reinstalled, and the 1-T cavity depth left at 1.1 in. as in the previous sequence. All five bomb tests, Number 231 through 235, in Sequence 15, were stable.

The rectangular inlet configuration replaced the partial contour unit for the next sequence, with the same 1-T cavity depth, and all tests -- Numbers 236 through 240 -- were stable. In Sequence 17 which followed, the cavity depth was further reduced to 0.64 inches. All tests were again stable, although the last showed a large postbomb surge.

The partial contour device was again installed with the 1-T cavity depth maintained at 0.64 in. Throughout all of these XDT-10 tests, the 3-T depth was held at 0.4 in. All four tests of Sequence 18 were bomb-stable. In Sequence 19, which consisted of Tests 250 through 254, the 1-T depth was further reduced to 0.40 in.; thus, all twelve cavities, 1-T and 3-T were the same length. The four tests of Sequence 20 were bomb-stable, which, contrary to the conclusion from Sequence 14, indicated that combustion stability was not

Report 13133-F-1

IX,F, Test Series Description (cont.)

particularly affected by cavity tune as commonly calculated in terms of cavity depth; vis., something else was permitting the combustion process to go unstable.

In Sequence 21, the rectangular inlet configuration was replaced with the high C_D inlet. As shown in Figure 116 this inlet had a 0.125 in. radius on its downstream edge to give it a high C_D while still maintaining the general configuration of the baseline cavity. It was intended to differentiate between the effects of cavity entrance direction or location and entrance hydraulic resistance. One test was bombed unstable in the 1-T mode indicating this configuration was much more sensitive to tune than the low C_D sharp edged configuration.

In Sequence 23, therefore, the 1-T length was reduced to 1.1 in. The second of the two firings went unstable in the 1-T mode, indicating that the 1-T cavity length was still insufficient. Thus the length was extended to 1.9 in. and the operating point matrix repeated in Sequence 24. All four tests were bomb-stable although the last test, Number 270, had a small postbomb resurge.

Finally in Sequence 25, the last of this group, the cavities were all blocked shut to determine whether the presence of cavities might be contributing to the instability and also to establish to what mode the injector appeared most sensitive. Both tests were bombed unstable in the 2-T mode with no resurging present. This confirmed that cavities indeed were effective damping devices but also implied that resurging was associated with the pressure of cavities.

7. Series 6, Mixed Element-Integral Baffle Injector

The mixed element-integral baffle injector tests were conducted during the interval that the XDT-1B injector was being refaced. The primary objective of this activity was to demonstrate that the platelet fabrication

IX,F, Test Series Description (cont.)

technique could be successfully employed with baffled injectors and that the baffles could be regeneratively cooled with N_2O_4 .

The mixed element-integral baffle injector had two types of injection elements -- X-doublets and splash plates. The X-doublet elements were located around the periphery and along the baffle walls. The splash plate elements were located in the central core region between the three baffle blades. Approximately 60 percent of the elements were X-doublets and 40 percent were splash plate elements.

In Sequence 1, which consisted only of Test 179, there were no 1-T cavities, under the assumption that the baffles would eliminate the 1-T mode. All of the cavities were adjusted to the 3-T depth. The firing was spontaneously unstable in the 1-T mode indicating the baffles were not supplying sufficient damping. It was reasoned at the time that the slight gap (approximately 0.020 in.) that existed between the baffle and the chamber wall allowed some acoustic communication between baffle pockets. This gap had been demonstrated to be the source of an instability on a Transtage injector program conducted previously at ALRC. The gaps were eliminated by spot welding L-shaped metal pieces to both the baffle and the chamber wall to preclude gas flow between pockets.

For Sequence 2, five of the cavities were fixed to a short 1-T length, 1.3 in., the first test in this configuration was stable, the second spontaneously unstable in the 1-T mode. The metal pieces plugging the gaps were all lost during the unstable test. Since the instability started with them in place, it was concluded that suppressing the communication between pockets via the gap was not an important consideration. The metal inserts were therefore not replaced. Of the remaining five tests of the sequence, four were stable -- two of them with bombs -- and one spontaneously unstable in the 1-T mode.

The 1-T cavity depth was increased to 1.9 in. for Sequence 3, which had an instability on the second test, Number 203, again in the 1-T mode.

IX,F, Test Series Description (cont.)

The number of 1-T cavities was increased by one, so that half of them were tuned to the 1-T mode. Sequence 4 which followed again, had a 1-T mode spontaneous instability on the second of two tests. At this point it was concluded that the presence of the slow mixing X-doublets and the film cooling of the baffle blades was resulting in too much of the energy release occurring well downstream of the baffles, rendering them ineffective. Since the primary objectives of demonstrating fabricability and baffle cooling had been met, it was decided to terminate testing of the baffled injector.

The stable tests did allow calculation of injector performance which was found to be comparable to that for an X-doublet pattern, viz., the expected improvement due to the splash plate was not realized. This agreed with the conclusions reached from the stability results.

8. Series 7, Like-Doublet Injector

The like-doublet injector, residual from a company-funded program, was evaluated after the XDT-1C injector testing. The purpose of running these tests was to determine whether the sensitivity to cavity inlet geometry was characteristic of the X-doublet element or had more general applicability. The first sequence of tests involved the high C_D cavity inlet contour and consisted of Tests 271 through 275. All of the cavities, 1-T and 3-T, were 0.4 in. deep. All tests were bomb-stable.

The contoured inlet was used in the second sequence, again with 0.4 in. cavities. One of the four bombed firings was marginally stable with a 0.009 sec recovery, while another was unstable in the 1-T mode.

The 1-T cavity depth was increased to 1.1 in. for Sequence 3, with no other changes being made to the configuration. All four firings, Tests 280 through 283, were bomb-stable. Thus it was apparent that although the like-doublet injector showed some sensitivity to cavity inlet geometry, it was much less sensitive than the X-doublet injector.

IX,F, Test Series Description (cont.)

The rectangular inlet cavities were installed next and all cavity depths adjusted to 0.4 in. All four tests of Sequence 4 were bomb-stable. Finally, to show that the cavities were essential for stable operation, they were all blocked shut; the single test of Sequence 5 was bombed unstable in the 1-T mode.

9. Series 8, DXDT1-1 Injector

Serial Number 1 of the demo XDT-1 pattern, which was designated DXDT1-1, was then available for testing prior to shipment to WSTF. The partial contour cavity configuration was used in the first sequence of tests. Six of the fifteen firings of this sequence, which encompassed Tests 191 through 305, were bomb-unstable. The unstable test points appeared to be at the high pressure, low mixture ratio end of the operating "box". The cause of the instabilities was suspected to be a poor seal noted between the injector and the adapter manifold. This seal was replaced following Sequence 1 and Sequence 2 proceeded with otherwise identical hardware.

Sequence 2 consisted of Tests 306 through 310. The second test of the group, 307, was a chugging test and chugging was attained at a chamber pressure of 65 psia. Three of the other four tests were bombed unstable in resurging, however, indicating that the seal was not the cause of the instabilities experienced in the previous sequence. A review of all the configuration differences between the DXDT1-1 and prior XDT-1 injectors was therefore conducted. The primary difference noted was in the injector overlap, viz, the excess of injector radius over chamber radius. All prior testing was conducted with an overlap of 0.126 in. The DXDT1-1 unit had a slightly negative overlap, -0.007 in., which resulted from the requirement that injector be compatible with another contractor's hardware for WSTF testing. In order words, the injector diameter was very slightly smaller than the chamber diameter, whereas formerly it was somewhat larger.

Report 13133-F-1

IX,F, Test Series Description (cont.)

To regain whatever effects were lost with the change in overlap, two overlap rings were fabricated. Both of these rings protruded into the chamber. The one provided an overlap of 0.126 in., the same as in all prior tests, while the other provided 0.042 in. overlap.

Sequence 3 was undertaken with the 0.126 in. overlap ring in place. All eight firings over the matrix of operating points were bomb-stable. Two of them, 316 and 317, had small pops just after chamber pressure rise; these were thought to be caused by the explosion of fuel trapped in the cavity. In any event, it was clear that the 0.126 overlap had a stabilizing effect.

The subsequent sequence utilized the 0.042 in. overlap ring. Every test of Sequence 4 was marginal, with single postbomb resurges occurring on Tests 319, 320, and 321, and a double surge on 322.

The larger overlap ring was reinstalled for the single test of Sequence 5. The purpose of the test was to determine if the pops experienced in Sequence 3 were purely start transient phenomena or if they could occur later in the firing. Thus, the firing duration was extended to 4 sec from the nominal 2 sec value commonly used. No pops occurred during this test.

10. Series 9, DXDT1-2 Injector

Serial Number 2 of the demo XDT-1 pattern, designated as DXDT1-2, was then tested. The 0.126 overlap ring was altered such that its downstream edge faired smoothly into the chamber surface. Sequence 1a of Series 9, which was at the time labeled Sequence 6 of the previous series, employed the same hardware configuration as Sequence 5 of that series except for the contoured downstream edge of the overlap ring. All thirteen tests of the sequence, number 324 through 336, were bomb-stable.

IX,F, Test Series Description (cont.)

Sequence 1 consisted of five firings, Tests 337 through 341, with the 0.126 overlap ring brazed into the cavity housing. All five tests were bomb-stable.

The subsequent Sequence 2 investigated performance with a reduced chamber length, 12 in., and two of the three firings had postbomb resurges. The question then arose as to whether the marginal stability was due to the reduction in chamber length or to the repositioning of the stability bomb which were located 3 in. from the injector face on these three tests, as opposed to 10 in. away in earlier tests.

Thus, in Sequence 3, the chamber length was restored to 16 in., but the bomb location was maintained 3 in. from the face. All five tests, 345 through 349, were stable. Thus, chamber length rather than bomb position was the destabilizing factor, a result which had been indicated earlier in the mixed element injector testing.

11. Series 10, XDT-1C Injector, Inlet Effect Investigation

The XDT-1C injector was returned to service so as to investigate what was the critical factor: overlap or sharp edged cavity inlet. The first sequence consisted of a single test, Number 350, to show that the XDT-1C injector was also unstable with the -0.007 in. overlap condition. It was. Thereafter, a new cavity inlet configuration, with 0.250 in. overlap and 0.125 in. radius on the lip of the cavity, was installed. This was the maximum overlap tested. The purpose of testing this configuration was to establish whether the destabilizing effect which was observed with the high C_D inlet was the result of its lower flow resistance or the result of the radius on the lip simply reducing the effective overlap. With this cavity inlet, the 1-T cavity was progressively detuned, or shortened, during the remaining test sequences to enable the stability of this configuration to be compared to that with the sharp-edged entrance.

IX,F. Test Series Description (cont.)

Sequence 2 was the starting point with the nominal cavity configuration except for the maximum overlap, high C_D inlet. All five tests of the sequence were bomb-stable. In Sequence 3, the 1-T depth was reduced to 1.1 in. from 1.5 in.; again all five bomb tests were stable. The 1-T depth was reduced to 0.8 in. in Sequence 4, and once more all five firings were bomb-stable. Finally, in Sequence 5, wherein all of the cavities were 0.4 in. long, one marginal test resulted. Test 367 showed one postbomb resurge. Thus, it was fairly obvious that overlap and not corner sharpness was the critical factor in stabilizing the combustion.

12. Series 11, XDT-1C, Stability Margin Evaluation

The purpose of this series of tests was to determine the stability margin of the baseline cavity configuration. As noted earlier, the method of doing this involved simultaneously reducing percent open areas for the 1-T and 3-T cavities until a marginal condition was encountered, and then adjusting the cavity depth to evaluate the effect of cavity tune.

Before getting into the stability margin tests, however, a sequence was conducted with the 12 in. chamber length to corroborate the destabilizing effect of the reduced chamber length with the XDT-1C injector. All six tests of the sequence were bomb-stable, indicating that the XDT-1C has somewhat greater stability margin than the demo units.

Sequence 2 was with the 16 in. chamber and with 1-T and 3-T cavity open areas of 14.4% and 7.7% respectively. All five firings, Tests 376 through 380, were bomb-stable. The percent open area of the cavities was reduced to 10.2% for 1-T and 6.2% for 3-T for Sequence 3, and the matrix of test points repeated. One marginally stable firing was experienced. Thus, the limiting point on percent open area had been breached.

Report 13133-F-1

IX,F, Test Series Description (cont.)

Sequence 4 which followed had the same open area percentages but deeper 1-T cavities, 1.9 in. as opposed to 1.5 in. Two instabilities were experienced in the six tests. Thus, it could be concluded that the direction of improved stability was towards shorter, rather than longer, 1-T cavities.

The subsequent sequence therefore employed 1.3 in. cavities. One firing was bombed unstable. The 1-T cavity depth was further reduced for Sequence 6, to 1.1 in. All nine test points were bomb-stable, although two tests each had a single postbomb resurge; the greater number of tests was considered necessary to ensure a meaningful statistical sample. Thus, by sufficiently shortening the cavity depth at this limiting percent open area, the unit was returned to stable operation.

In Sequence 7, Tests 404 through 408, the 1-T depth was decreased to 0.9 in. Two firings were bombed unstable and a third had a slight postbomb resurge, indicating that the limiting minimum cavity depth had also been breached. In other words, for the open area percentages determined in Sequence 3, the 1-T cavity depth for bomb-stability lies between 0.9 and 1.3 in.

The subsequent Sequence 8 was run to determine if the 3-T cavities were really necessary. All of the 3-T cavities were blocked off with the blocks extending 0.125 in. downstream of the injector face; the aft end of the cavity thus still formed a "pocket". The 1-T cavity depth was readjusted to 1.1 in., the stable point determined in the prior sequences for the minimum open areas, which were maintained. Two of the four firings in this configuration had postbomb resurges and a third was unstable in the 1-T mode, indicating that the 3-T cavities were contributing to the 1-T mode stability attained previously.

The following sequence, consisting only of Test 413, was conducted to determine whether the active cavity open area, or the effective

IX,F, Test Series Description (cont.)

open area, is the important parameter. The cavity depths and open areas were the same as in Sequence 6, wherein all tests were stable; the cavity inlet was radiused, however, giving a higher C_D . The assumption was that, if effective area is the critical factor, then the greater effective area resulting from the higher C_D should make the system more stable than in Sequence 6. The instability on the first test of the sequence showed that the radius on the inlet not only fails to provide more margin by reason of some effective area increase but acts to destabilize a heretofore stable condition.

Having found in Sequence 8 that the 3-T cavities are necessary for 1-T stability, in Sequence 10 the 3-T area was cut in half to determine to what extent the 3-T cavities contribute to 1-T stability. The rectangular inlet replaced the radiused inlet configuration and except for the 3-T area change there were no other variations. One of the two tests was bombed unstable in 1-T, while in the other the bomb failed to explode. Thus, the 3-T cavities were again shown to contribute to 1-T stability.

Sequence 11 evaluated the high contraction ratio ($r_c = 4.0$) chamber. This chamber had a nominal throat area equal to 1/2 that of the other chamber. The first five firings, Tests 416 through 420, were at high chamber pressures -- 200 to 300 psia -- and proved bomb-stable. The last three tests were conducted at near-nominal chamber pressure to investigate chugging, which was attained on the final test, 423, at 122 psia chamber pressure.

13. Series 12, Low ΔP Injector

The last series of the program was intended to investigate the characteristics of a low pressure drop injector. This series was aborted after the first test, Number 424, showed an interpropellant leak in the injector. Results of this single test are inconclusive.

IX, Full Scale Testing (cont.)

G. TEST SUMMARY

In the Test Series Description above, tests were designated by a series number, a sequence number, and a test number. This follows the methodology used in WSTF testing but was in fact not used throughout ALRC testing. The series number was assigned after the fact to clarify this listing and was given in accordance to the injector. Thus, all of the XDT-1 injector tests are grouped into Series 1. The sequence number was commonly but not always specified during testing, with each sequence denoting a group of tests all with the same hardware. Generally, every hardware change would call for a new sequence number. Thus, Sequence 1-1 involved 1.2 in. cavities with an 11 in. chamber length, and Sequence 1-2 involved 1.6 in. cavities with a 13 in. length; otherwise, there were no differences in configuration. Finally, the test number was assigned on a consecutive basis with the J-Area tests going from 001 to 038, and the A-Area tests going from 101 to 424. This is somewhat different from the WSTF approach wherein each sequence started anew with Test Number 1.

There were unfortunately some exceptions to this system of designation -- for example, hardware changes within a sequence in a few instances -- that could not be rectified without altering much of the original sequence numbering. To avoid confusion, this was not done. Such exceptions reflect the fluidity of the test program wherein changes in hardware configuration could be and were accomplished with a minimum of delay.

Figure 80 maps the chronology of the ALRC testing and also the interaction with WSTF testing although the latter is not broken into individual test sequences. In conjunction with the Test Series Description, it helps explain the rationale of the test program. The figure also traces the replacement of injector faces on the four injector bodies.

IX,G, Test Summary (cont.)

Table X summarizes the elements of the hardware configuration that are deemed important from the standpoint of stability. These include: chamber length, cavity inlet contour, chamber wall shape at the cavity, contour of the back corner of the cavity, inlet height, cavity width, injector overlap, cavity depth, and cavity open area as a percent of injector face area. These elements are described fully in the section above entitled Cavity Configuration.

Table XI summarizes the operating conditions for each test of the entire program. These include chamber pressure, mixture ratio, and propellant temperatures; the use of stability bombs and the resulting stability characteristics are also indicated. In most cases, specified values are nominal rather than exact. An exception to this is that measured ("exact") fuel temperatures are commonly given for the tests with instabilities; these values were measured at the start of the instability.

H. CONCLUSIONS

From the review of the full scale testing, it is apparent that the majority of the tests conducted on this program were directed towards combustion stability. Although a stable injector-acoustic cavity configuration was established early in the testing, it was the intent of the program to explore the limits of stability, i.e., to determine at what point various changes in hardware configuration or test conditions cause the combustion to go unstable. It was felt this information was required to establish the desired OMS technology base. Two factors combined to make the program much more complex than originally anticipated. First, the appearance of resurging instability produced a significant departure from existing combustion stability technology and the analytical tools which have been developed. Second, the great sensitivity to cavity inlet geometry was also unique with no previous technology to rely upon. As a result, much exploratory experimental work had to be performed. Although at the present time, no definitive statements can be made about either resurging or cavity inlet geometry, the testing conducted during this program has resulted

TABLE X
SUMMARY OF HARDWARE CONFIGURATIONS IN FULL SCALE TESTS AT ALRC

Series	Test #	Date	Chamber Length	Inlet Contour	Chamber Shape	Corner Contour	Inlet Height	Cavity Width	Overlap	Cavity Depth $\frac{1I}{3I}$	Cavity Area (%) $\frac{1I}{3I}$
XDT-1 Injector (No Ring Dams)											
1-1	001,002	06/16/73	11	Square	Flat	Square	.50	.50	.126	1.20	25.
2	003-005	07/19/73	13	Square	Flat	Square	.50	.50	.126	1.20	20.
3	006-007	07/20/73	13								
4	008-018	07/24/73	14								
5	019-021	07/26/73	12								
6	022-026	07/31/73	14	Square	Flat	Square	.50	.50	.126	1.20	20.
7	027-029	08/10/73	13								
8	030-038	08/13/73	13								
9	139-143	10/12/73	12								
XDT-2 Injector (No Ring Dams 2-1 through 2-5)											
2-1	101,102	09/07/73	11	Square	Flat	Square	.60	.574	.126	1.60	19.
2	103-110	09/08/73	11	Square	Flat	Square	.60	.574	.126	1.60	19.
3	111-113	09/11/73	14								
4	114-119	09/14/73	13								
5	120-124	09/15/73	13								
6	125-132	09/18/73	13	Square	Flat	Square	.60	.574	.126	1.50	19.
7	133-138	10/10/73	16								
Mixed Element Injector											
3-1	144-153	11/08/73	17	Square	Flat	Square	.60	.574	.126	1.50	19.
2	154-155	12/11/73	17	Square	Flat	Square	.60	.574	.126	1.50	20.
3	168-172	01/14/74	12								
4-1	156,157	12/19/73	16	Square	Flat	Square	.60	.574	.126	1.50	19.
XDT-1A (High ΔP) Injector											
											9.5

TABLE X (cont.)

Series	Test #	Date	Chamber Length	Inlet Contour	Chamber Shape	Corner Contour	Inlet Height	Cavity Width	Overlap	Cavity Depth 1T 3T	Cavity Area (%) 1T 3T
<u>XDT-1B Injector</u>											
5-1a	158-164	01/10/74	16	Square	Flat	Square	.60	.574	.126	1.50	19. 9.5
2a	165-167	01/10/74	16	Square	Flat	Square	.60	.574	.126	1.50	19. 9.5
1	173-178	01/18/74	16	Contour		Contour	.60	.574	.126	1.50	15.2 8.1
2	180-182	01/29/74	16							1.50	19. 8.1
3	183-186	01/28/74	16							1.25	9.5
4	187-189	01/29/74	16							1.07	
5	190,191	01/29/74	16							.83	
6	192,193	01/30/74	16	Contour	Flat	Contour	.60	.574	.126	.43	19. 9.5
7	194	01/30/74	16							.21	16.2
<u>XDT-1C Injector</u>											
8	206-211	02/13/74	16	Square	Flat	Square	.60	.574	.126	1.50	19.0 9.5
9	212	02/14/74	16	Square		Square				1.90	
10	213-218	02/15/74	16	Contour		Contour				1.90	
11	219,220	02/18/74	16	Contour		Contour	.60			1.50	
12	221-225	02/21/74	16	Partial		Partial	.40			1.50	
13	226-229	02/22/74	16	Res. Contour		Contoured	.40			1.10	
14	230	02/25/74	16	Res. Contour		Contoured	.40			1.10	
15	231-235	02/25/74	16	Partial		Partial	.60			1.10	
16	236-240	02/27/74	16	Square		Square				.64	
17	241-245	02/28/74	16	Square		Square				.64	
18	246-249	02/28/74	16	Partial		Partial				.40	
19	250-254	03/04/74	16	Partial		Partial				.40	
20	255-259	03/06/74	16	Square		Square				.40	
21	260	03/07/74	16	High C _D		Contour				.40	
22	261-264	03/07/74	16							1.50	
23	265-266	03/08/74	16							1.10	
24	267-270	03/08/74	16	High C _D	Flat	Contour	.60	.574	.126	1.90	19.0 9.5
25	289,290	03/25/74	16								

Report 13133-F-1

TABLE X (cont.)

Series	Test #	Date	Chamber Length	Inlet Contour	Chamber Shape	Corner Contour	Inlet Height	Cavity Width	Overlap	Cavity Depth <u>1T</u> <u>3T</u>	Cavity Area (%) <u>1T</u> <u>3T</u>
<u>Mixed Element - Integral Baffle Injector</u>											
6-1	179	01/23/74	12	Contour	Flat	Contour	.60	.574	.126	.35	27.6
2	195-201	02/05/74	16	Square		Square				1.30	11.5
3	202,203	02/06/74	16							1.90	16.1
4	204,205	02/08/74	16	Square	Flat	Square	.60	.574	.126	1.90	16.1
										.35	13.8
<u>Like-Doublet Injector</u>											
7-1	271-275	03/12/74	16	High CD	Flat	Square	.60	.574	.126	.40	19.
2	276-279	03/21/74	16	Contour		Contour				.40	9.5
3	280-283	03/21/74	16	Contour		Contour				1.10	
4	284-287	03/21/74	16	Square	Flat	Square	.60	.574	.126	.40	19.
5	288	03/21/74	16								9.5
<u>DXDT 1-1 Injector</u>											
8-1	291-305	04/05/74	16	Partial	Flat	Partial	.60	.60	-.007	1.50	19.
2	306-310	04/16/74	16								9.5
3	311-318	04/24/74	16		Step				.126		
4	319-322	04/25/74	16						.042		
5	323	04/26/74	16	Partial	Step	Partial	.60	.60	.126	1.50	19.
<u>DXDT 1-2 Injector</u>											
9-1a	324-336	05/02/74	16	Partial	Contour	Partial	.60	.60	.126	1.50	19.
1	337-341	05/06/74	16								9.5
2	342-344	05/21/74	12								
3	345-347	05/21/74	16	Partial	Contour	Partial	.60	.60	.126	1.50	19.

C-3

TABLE X (cont.)

Series	Test #	Date	Chamber Length	Inlet Contour	Chamber Shape	Corner Contour	Inlet Height	Cavity Width	Overlap	Cavity Depth	Cavity Area (%)
<u>XDT-1C Injector</u>											
10-1	350	05/23/74	16	High C _D	Square	Square	.60	.574	-.007	.40	9.5
2	351-355	05/24/74	16		Step				.257		
3	356-360	05/30/74	16								
4	361-365	05/30/74	16								
5	366-369	05/31/74	16	High C _D	Step	Square	.60	.574	.257	.40	9.5
<u>XDT-1C Injector</u>											
11-1	370-375	06/09/74	12	Square	Flat	Partial	.60	.574	.126	.40	9.2
2	376-380	06/06/74	16							.48	18.5
3	381-384	06/07/74	16								14.4
4	385-390	06/10/74	16								10.2
5	391-394	06/11/74	16								
6	395-403	06/11/74	16								
7	404-408	06/13/74	16							.48	6.2
8	409-412	06/17/74	16							-.125	
9	413	06/18/74	16	Square Radius						.48	6.2
10	414-416	06/18/74	16	Square	Flat	Partial	.60	.574	.126	.48	3.1
11	416-423	06/25/74	16	Square						.40	9.4
<u>XDT-1 Injector</u>											
21-1	424	06/26/74	16	Square	Flat	Partial	.60	.574	.126	.40	9.4

Report 13133-F-1

TABLE XI

SUMMARY OF OPERATING CONDITIONS FOR FULL SCALE TESTS AT ALRC

<u>Series</u>	<u>Test</u>	<u>P_c</u>	<u>O/F</u>	<u>T_{ox}</u>	<u>T_{fuel}</u>	<u>Bomb Location</u>	<u>Stability Results</u>
<u>XDT-1 Injector (no ring dams)</u>							
1-1	001	125	1.9	70	70	None	
	002				"		
1-2	003				200		Resurge
	004						Resurge
	005						Resurge
1-3	006						Resurge
	007	135					Resurge
1-4	008	125					Resurge
	009	125					Resurge
	010	130	1.6				Resurge
	011	130	2.2				Resurge
	012	140	1.9				Resurge
	013	115					
	014	115				2	
	015	125	1.6				Marginal
	016	114	2.2				
	017	104					
	018	102	1.8				
1-5	019	125	1.9			None	
	020		2.2				
	021		1.6				Resurge
1-6	022						
	023						
	024						
	025						
	026						
1-7	027		1.8				
	028						
	029						
1-8	030	120			170		
	031	116			104		
	032	119	1.6		200		
	033	105	1.8		200		
	034	121	1.6		215		Resurge
	035	121	1.8		215		
	036	105			199		
	037	105			230		
	038	121			187		Resurge
1-9	139	120	1.6		200	6	Resurge
	140	140	1.4	70	200	6	Resurge

All test stable except as noted under "Stability Results"
Bomb Location: distance from injector face.
Indicated values may be nominal.

Report 13133-F-1

TABLE XI (cont.)

<u>Series</u>	<u>Test</u>	<u>P_c</u>	<u>O/F</u>	<u>T_{ox}</u>	<u>T_{fuel}</u>	<u>Bomb Location</u>	<u>Stability Results</u>
1-9 (cont.)	141	106	2.0	70	200	6	Resurge
	142	126	1.65				Resurge
	143	110	1.45				Resurge
XDT-2 Injector (no ring dams 2-1 through 2-5)							
2-1	101	123	1.76	70	70	None	
	102	123	1.76	70	70	None	
2-2	103	127	1.65		200	2	Resurge
	104	127	1.45				Marginal
	105	158	1.66				Resurge
	106	102	1.65				
	107	114	1.99				Resurge
	108	118	1.85				Resurge
	109	111	1.90				Resurge
2-3	110	125	1.60		135		
	111	116	1.65		200		Resurge
	112	130	2.00		200		Resurge
	113	124	1.70		70		Resurge
2-4	114	122	1.68				
	115	139	1.98				
	116	123	1.73		200		
	117	136	1.97				Resurge
	118	140	1.45				Resurge
	119	110	1.95		210		
	120	140			70		Blip
2-5	121	140			136		Resurge
	122	132	1.51		180		Resurge
	123	110	2.09		214		Marginal
	124	122	1.67		208		Blip
2-6	125	138	2.10		202	6	
	126	136	1.44		209		
	127	109	1.88		214		
	128	107	1.39		217		
	129	122	1.63		217		
	130	125	1.64		220		
	131	119	1.55		210		
	132	143	1.98		221		Blip
2-7	133	138	1.90	65	193		
	134	138	1.90		197		
	135	137	1.43		195		
	136	109	1.89		190		
	137	108	1.49		191		
	138	123	1.70		214		Blip

Report 13133-F-1

TABLE XI (cont.)

<u>Series</u>	<u>Test</u>	<u>P_c</u>	<u>O/F</u>	<u>T_{ox}</u>	<u>T_{fuel}</u>	<u>Bomb Location</u>	<u>Stability Results</u>
<u>Mixed Element Injector</u>							
3-1	144	122	1.70	70	70	6	Hi freq
	145	123	1.70	70	200		Hi freq
	146	123	1.70				Hi freq
	147	120	1.65				Hi freq
	148	119	1.70				Hi freq
	149	124	1.67				
	150	138	1.87				
	151	138	1.44				
	152	108	1.88				
	153	107	1.41				
	154	125	1.65				Hi freq
	155	125	1.45				Hi freq
3-2	154	125	1.65			None	
	155	125	1.45			6	
3-3	168	125	1.64	51		2	Resurge
	169	150	1.65				
	170	125	1.64				Resurge
	171	140	1.84				Resurge
	172	140	1.65		208		Resurge
<u>High ΔP Injector</u>							
4-1	156	125	1.65	70	200	6	
	157	140	1.85	70	200	6	
<u>XDT-1B Injector</u>							
5-1a	158	122	1.64	45	205	6	
	159	123	1.86	44	197		
	160	122	1.49	37	198		
	161	148	1.88	41	205		
	162	146	1.46	41	214		
	163	99	1.85	41	202		
	164	99	1.53	41	200		
	165	76	1.65	70	200		
	166	66	1.69	70	200		Chug
	167	66	1.44	70	200		Chug
5-2a	165	76	1.65	70	200	None	
	166	66	1.69	70	200		
	167	66	1.44	70	200		
	173	125	1.71	56	200	6	Marginal
	174	100	1.91		200		
5-1	175	150	1.48		204		Resurge
	176	150	1.93	57	197	None	
	177	150	1.93	57	199	None	
	178	100	1.54	56	188	6	Resurge
	180	100	1.45	70	200	6	Resurge
	181	150	1.45	70	200	6	Resurge
	182	125	1.65	70	200	6	Resurge

Report 13133-F-1

TABLE XI (cont.)

Series	Test	P _c	O/F	T _{ox}	T _{fuel}	Bomb Location	Stability Results
5-3	183	125	1.65	70	200	None 6	Resurge Resurge Resurge Resurge
	184	125	1.65	47	195		
	185	100	1.90	47	190		
	186	150	1.45	49	110		
5-4	187	125	1.65	70	200	None 6	Resurge Resurge Resurge
	188	100	1.90				
	189	150	1.45				
5-5	190	125	1.65			None 6	Resurge Resurge
	191	150	1.45				
5-6	192	125	1.65			None 6	Resurge Resurge
	193	150	1.45				
5-7	194	150	1.45			None 6	Resurge Resurge
5-8	206	125	1.65	48	204		
	207	150	1.45	48	194	None 6	Marginal
	208	110	1.40	43	193		
	209	150	1.90	44	197	None 6	Marginal Marginal
	210	100	1.90	45	178		
	211	125	1.65	47	190	None 6	Resurge
5-9	212	150	1.40	47	190		
5-10	213	125	1.65	50	159	None 6	Marginal Marginal
	214	150	1.45	49	179		
	215	100	1.9	51	179	None 6	Marginal
	216	100	1.9	47	177		
	217	150	1.9	47	180	None 6	Marginal Marginal
	218	100	1.4	47	179		
5-11	219	100	1.9			None 6	Resurge
	220	100	1.4				
5-12	221			50	186	None 6	Marginal
	222						
	223		1.9			None 6	Marginal
	224	150			182		
	225	150	1.4		195	None 6	Marginal
5-13	226	100	1.9	48	188		
	227	100	1.4	48	193	None 6	Marginal
	228	150	1.4	49	218		
	229	150	1.9	49	198	None 6	Hi freq
5-14	230	100	1.4	50	200		
5-15	231	100	1.4		190	None 6	Hi freq
	232	100	1.9				
	233	125	1.65			None 6	Hi freq
	234	150	1.4				
	235	150	1.9			None 6	Hi freq
5-16	236	100	1.4				
	237	100	1.9			None 6	Hi freq
	238	150	1.4				
	239	150	1.4			None 6	Hi freq
	240	150	1.9				

Report 13133-F-1

TABLE XI (cont.)

<u>Series</u>	<u>Test</u>	<u>P_c</u>	<u>O/F</u>	<u>T_{ox}</u>	<u>T_{fuel}</u>	<u>Bomb Location</u>	<u>Stability Results</u>			
5-17	241	100	1.4	50	190	6	Marginal			
	242	150	1.9			6				
	243	100				None				
	244	100				6				
	245	150	1.0							
5-18	246	150	1.4	47						
	247		1.9							
	248	100	1.4							
	249		1.9							
	250	150	1.4					45	183	None
251		1.9	188	6						
252		1.9								
253	100	1.4								
254	100	1.9								
5-20	255	150			1.4					
	256	150	1.9							
	257	100	1.4	180						
	258	100	1.9		182					
	259	150	1.4							182
5-21	260	150	1.4			70	200	6	Hi freq	
	261	150								
	262	100								
	263	150	1.9							
	264	100								
5-23	265	150	1.4							
	266	100								
5-24	267	150								
	268	100								
5-25	269	150	1.9				Marginal High freq High freq			
	270	100								
	289		1.4			10				
	290							10		

Mixed Element Integral Baffle Injector

6-1	179	125	1.65	70	200	6	Hi freq
6-2	195	125	1.65			6	Hi freq
	196	110	1.9			None	
	197	125	1.65				
	198					6	
	199					6	
6-3	200	150	1.4			None	Hi freq
	201	110	1.9				
	202	125	1.65				
	203	110	1.9				
6-4	204	125	1.65			None	Hi freq
	205	110	1.9				

Report 13133-F-1

TABLE XI (cont.)

<u>Series</u>	<u>Test</u>	<u>P_c</u>	<u>O/F</u>	<u>T_{ox}</u>	<u>T_{fuel}</u>	<u>Bomb Location</u>	<u>Stability Results</u>	
<u>Like-Doublet Injector</u>								
7-1	271	150	1.4	70	200	None		
	272	150			190	10		
	273	100			200			
	274	150	1.9		201			
	275	100	1.9		192			
7-2	276	150	1.4		200	3	Hi freq	
	277	100						
	278	150						
	279	150	1.9					
7-3	280		1.4		204			
	281	100			194			
	282	150			196			
	283	100			196			
7-4	284	150	1.9		200			
	285	150	1.4					
	286	100	1.4					
	287	100	1.9					
7-5	288	100	1.4					
<u>DXDT1-1 Injector</u>								
8-1	291	125	1.65	70	206	10		
	292	100	1.45		202			
	293	150	1.65		203			
	294	100	1.65		217			
	295	150	1.4		203			Resurge
	296		1.65		185			
	297		1.4		210			
	298	165	1.4		200			Resurge Resurge
	299	165	1.25					
	300	135	1.25					
	301	135	1.25					Resurge
	302	135	1.55					
	303	165	1.55					
	304	135	1.4					Resurge Resurge Resurge
	305	150	1.55					
8-2	306	150	1.4	210				
	307	65	1.65	222	Chug			
	308	100	1.95	209				
	309	150		201	Resurge Resurge			
8-3	310	125				206	None 10	
	311	150	1.4		200			
	312							
	313							
	314		1.9					
	315	100	1.4					
	316		1.9					
	317							
	318	150				Pop Pop		

Report 13133-F-1

TABLE XI (cont.)

<u>Series</u>	<u>Test</u>	<u>P_c</u>	<u>O/F</u>	<u>T_{ox}</u>	<u>T_{fuel}</u>	<u>Bomb Location</u>	<u>Stability Results</u>
8-4	319	150	1.4	70	200	10	Marginal Marginal Marginal Marginal
	320		1.9				
	321	100	1.9				
	322		1.4				
8-5	323		1.9				

DXDT1-2 Injector

9-1a	324	150	1.4	70	200	10		
	325	150	1.9					
	326	100	1.9					
	327	100	1.4					
	328	165	1.25		216			
	329	165	1.55					
	330	125	1.65		200			
	331		1.9					
	332		2.25					
	333	100	2.25					
	334	125	1.41					
	335	125	1.43					
	336	85	2.25					
	9-1	337	125				1.6	68
338		100	1.4					
339		150	1.4					
340		100	1.9					
341		150	1.4					
9-2		342	125	1.4			3	
		343		1.65				
		344		1.9				
	345		1.81					
	346		1.9					
	347		1.65					
	348	150	1.9					
	349	100	1.9					
					Marginal			
					Marginal			
			</					

XDT-1C Injector

10-1	350	125	1.65	70	200	10	Resurge	
10-2	351							
	352	150	1.9					
	353	150	1.4					
	354	100	1.4					
10-3	355	100	1.9					
	356	150	1.4					
	357							None 10
	358	150	1.9					
	359	100	1.4					
	360	100	1.9					

Report 13133-F-1
TABLE XI (cont.)

<u>Series</u>	<u>Test</u>	<u>P_c</u>	<u>O/F</u>	<u>T_{ox}</u>	<u>T_{fuel}</u>	<u>Bomb Location</u>	<u>Stability Results</u>
10-4	361	150	1.4	70	200	10	Marginal
	362	150	1.9				
	363	100	1.5				
	364	100	2.0				
	365	100	1.4				
10-5	366	150	1.4				
	367	150	1.9				
	368	100	1.4				
	369	100	1.9				
<u>XDT-1C Injector</u>							
11-1	370	125	1.65	70	200	3	Marginal
	371	125	1.9				
	372	150	1.4				
	373	100	1.4				
	374	100	1.4				
11-2	375	150	1.4				
	376	100	1.9			10	
	377	100	1.9			None	
	378	150	1.9			10	
	379	100	1.4			None	
11-3	380	100	1.9				
	381	100	1.4				
	382	100	1.9				
	383	150	1.4				
	384	100	1.9				
11-4	385	100	1.9			Resurge	
	386	100	1.4				None
	387	100	1.4				None
	388	100	1.9				10
	389	100	1.4				None
11-5	390	100	1.9				
	391	150	1.9				
	392	100	1.9				
	393	150	1.4				
	394	100	1.9				
11-6	395	100	1.9			High freq Marginal	
	396	150	1.9				None
	397	150	1.9				10
	398	-	-				10
	399	150	1.9				None
	400	100	1.4				None
	401	150	1.9				10
	402	100	1.9				Marginal
403	150	1.4					

Report 13133-F-1

TABLE XI (cont.)

<u>Series</u>	<u>Test</u>	<u>P_c</u>	<u>O/F</u>	<u>T_{ox}</u>	<u>T_{fuel}</u>	<u>Bomb Location</u>	<u>Stability Results</u>
11-7	404	100	1.4	70	200	10	Hi freq
	405	100	1.9				
	406	150	1.4				Hi freq
	407	100	1.9				
	408	150	1.9				
11-8	409	100	1.4				Hi freq
	410	100	1.9				Marginal
	411	150	1.4				Resurge
	412	150	1.9				
11-9	413	100	1.4				Hi freq
11-10	414	100	1.4				Hi freq
	415	150	1.9				Hi freq
11-11	416	200	1.4	71	225		
	417	200	1.9	72	220		
	418	250	1.65		218		
	419	300	1.4		227		
	420	300	1.9		217		
	421	143	1.65		207		
	422	131	1.58		200		
	423	122	1.63		200		
							Chug

XDT-1 Injector

12-1	424	127	1.66	70	200	10
------	-----	-----	------	----	-----	----

Report 13133-F-1

IV,H. Conclusions (cont.)

in greatly increased insight into both areas. A quantitative model, based on these test results and described in Section XII, has been constructed to provide a more complete understanding of these factors.

ORIGINAL PAGE IS
OF POOR QUALITY

X. FULL SCALE PERFORMANCE

X. FULL SCALE PERFORMANCE

A. INTRODUCTION

This section discusses the performance analysis for 160 of 362 tests conducted at ALRC to determine the performance level of eleven injector configurations. Five different injector patterns were tested as follows:

(1) The XDT1 pattern on seven units designated XDT1 (without face ring dams), XDT1-A, XDT1-B, XDT1-C, demonstration injectors DXDT1-1, DXDT1-2, and a low pressure drop unit XDT1-LP.

(2) The XDT2-A injector pattern (XDT2-without face ring dams was not analyzed for performance due to a high incidence of surge instability).

(3) The unbaffled mixed element pattern ME-1 consisting of 60% X-doublet and 40% splash plate elements.

(4) The mixed element pattern with integral baffles designated IBME-1. and

(5) The (non-platelet) like-doublet injector pattern which was designed and fabricated with ALRC IR&D funding, but which was also tested on the platelet OME Program.

Testing was conducted under a variety of test conditions which included the following:

(1) Two basic chamber configurations (11-in. to 16-in. heat sink and 13-in. regen chambers).

(2) Three nozzle configurations (15° conical nozzles with 2:1 and 2.6:1 area ratios and a Rao contoured nozzle truncated at 20:1 area ratio).

(3) Two different test stands (J-4 and A5).

X,A, Introductions (cont.)

Variable operating conditions included testing with and without fuel film cooling, over an oxidizer inlet temperature range from 40 to 100°F, and over fuel injection temperature range from 140 to 240°F. A summary of the various injector performances based on this analysis is presented as a function of chamber axial length in Table XII. Not all tests are included in the performance summary because many tests were conducted primarily to evaluate combustion stability, acoustic cavity damping margin, or chug stability margin.

Details of the performance analysis are presented in the following subsections. The specific test data and analysis results are presented in Section B, while the interpretation of the performance results with respect to each other and WSTF test results is in Section C. A description of the data analysis and performance extrapolation techniques is included in Section D.

B. DATA ANALYSIS RESULTS

The statistically averaged performance for each injector configuration and chamber length tested is summarized in Table XII in terms of the nominal measured specific impulse extrapolated to the OMS baseline design configuration (55:1 nozzle area ratio) and operating condition ($P_c = 125$ psia and $O/F = 1.65$). Table XII includes a description of the tested chamber configuration (length and coolant type), test series and run number, the total number of tests fired with each injector configuration, the number of those tests analyzed for performance, and nominal OMS performance together with any pertinent comments.

A test-by-test analysis from which Table XII was derived is given for all performance tests in the data appendix at the end of this section (pages 219 through 242.) This tabular summary contains a listing of the pertinent measured test parameters, calculated performance and injector hydraulic parameters, and extrapolated performance estimates. A description of the nomenclature used in the appendix is included in Table XIII which precedes it.

The following parameters were determined to have first order influences upon delivered performance.

TABLE 12 - INJECTOR PERFORMANCE SUMMARY

INJECTOR CONFIGURATION	COMBUSTION CHAMBER LENGTH (in.)	TYPE	TEST NUMBER IDENTIFICATION	TOT. NO. TESTS	NO. PERF. TESTS	NOMINAL OMS ⁽¹⁾ Isp ($\epsilon = 55$)	COMMENTS
Test Series: 2018-D01-0A-XXX							
XDT1 (Without Face Ring Dams)	11 to 13	Heat Sink	-001 to -007	7	0	-	Checkout Tests
	13.5	H.S.	-008 to -018	11	5	312	Extrapolated from low Pc & High O/F
	11.5	H.S.	-019 to -021	3	2	304	Extrapolated from low Pc & High O/F
	13.9	H.S. (9 to 15% FFC)	-022 to -026	5	3	312	With 9% FFC
	12.9	Regen (9% FFC)	-027 to -033	7	4	309.8	With 9% FFC
	12.9	Regen	-034 to -038	5	5	311.8	20:1 Truncated Rao Nozzle
			(TOTAL):	(38)	(19)		
Test Series: 6K-2B-XXX							
XDT2 (Without Dams)	12	Heat Sink	-139 to -143	5	0	-	Resurge. Performance not Analyzed
	12	H.S.	-101 to -124	24	0	-	Resurge. Performance not Analyzed
XDT2-A	12.8	H.S.	-125 to -132	8	8	311.8	(All injectors below this point tested with face ring dams)
	16.4	H.S.	-133 to -138	6	6	316.7 ⁽²⁾	
XDT1-A	16	H.S.	-156 to -157	2	2	311.7	High Injector ΔP
XDT1-B	16	H.S.	-158 to -167	31	26	313.8	
			-173 to -178				
			-180 to -194				
XDT1-C	16	H.S.	-206 to -270	133	19	314.5	
			-289 to -290				
			-350 to -415				
DXDT1-1	16	H.S.	-291 to -336	46	36	313.4	DEMO-1
DXDT1-2	16	H.S.	-337 to -349	13	13	313.2	DEMO-2
ME-1	16.7	H.S.	-144 to -155	12	7	317.5	.6XDT + .4 SP
ME-1	12	H.S.	-168 to -172	5	2	313.4	Extrapolated from High Pc
IBME-1	16	H.S.	-179 & -195 to -205	12	7	313.1	High Oxid. ΔP Across Baffle
HICR XDT1-C	16	H.S.	-416 to -423	8	6	314.2	Extrapolated at Design Injection Vel.
XDT1-Lo ΔP	16	H.S.	-424	1	1	313.3	Inter-Manifold Leak
Like Doublet	16	H.S.	-271 to -288	18	8	314.7	Non-Platelet IR&D Injector
			(TOTAL):	(324)	(141)		

NOTE: (1) I_{sp} corrected to $P_c = 125$ psia, O/F = 1.65 and extrapolated to OMS baseline design (Regenerative Chamber/55:1 nozzle)

(2) Questionable Thrust Data

X,B, Data Analysis Results (cont.)

(1) Mixture Ratio, (O/F) - In the tested O/F range from 1.4 to 1.9, all injector configurations at all chamber pressures and all chamber lengths demonstrated monotonically increasing specific impulse at the higher mixture ratios. Delivered performance is approximately proportional to the ODK specific impulse indicating relatively constant energy release efficiency over this range.

(2) Chamber Pressure, (Pc) - In the range from 90 to 150 psia chamber pressure, all injector configurations tested showed increased specific impulse at higher Pc's. Only part of the performance increase at high Pc can be ascribed to a reduction of the nozzle kinetic loss; the remainder represents an increase in the injector energy release efficiency.

(3) Chamber Length, (L) - All injectors showed improvement in energy release efficiency at longer chamber lengths. The magnitude of performance increase was on the order of +4 sec. I_{sp} going from 12 in. to 16 in. axial chamber length.

It can be seen by inspecting Table XII that the number of tests fired with each injector configuration varied widely from as few as a single test (XDT1-LP) up to as many as 133 tests (XDT1-C). Thus not all configurations have equal statistical significance although all injectors quote an "average performance" and all averages were obtained using the Multiple Co-Variance Analysis Computer Program. In the paragraphs to follow, the data will be presented by injector configuration for units having the greatest numbers of tests and highest confidence level first with the expectation that similar injector configurations of like pattern probably have similar performance characteristics. Discussion of subsequent units will be primarily limited to differences rather than similarities.

1. DXDT1-1 Injector

A total of 46 tests were conducted with the DXDT1-1 (DEMO-1) injector of which 36 tests have been analyzed to determine its performance characteristics. Results from all platelet injector tests have been statistically

X, B, Data Analysis Results (cont.)

correlated with the multiple covariance computer program to determine the effects of mixture ratio and chamber pressure on specific impulse. The variation of specific impulse with mixture ratio and chamber pressure for the DXDT1-1 injector in a 16 in. L¹ chamber is shown in Figure 81. The performance characteristic shown in Figure 81 is typical of all injectors; i.e., increasing specific impulse at higher mixture ratio and higher chamber pressure. The best fit correlation equation picked by the multiple covariance program through all the DEMO-1 test data is also shown on Figure 81 and the correlation influence coefficients are given as a function of P_c , O/F , and $(O/F)^2$.

2. DXDT1-2 Injector

The DEMO-2 injector is identical in design and was fabricated as a carbon copy of the above DEMO-1 injector. Thus, by every expectation it should behave identically to DEMO-1. In fact, Table XII shows that their difference in nominal Isp is only 0.2 sec lower for DEMO-2 which is well within the experimental accuracy. The DEMO-2 performance shown in Table XII is very similar to Figure 81. One set of additional data obtained with DEMO-2 in a 12 in. L¹ chamber is shown in Figure 82. A performance reduction of approximately 5.5 sec is indicated with the shorter chamber.

3. XDT1-C, -B, and -A Injectors

One hundred and thirty-three tests were conducted on the XDT1-C injector. An additional eight tests were conducted in the high contraction ratio (reduced throat diameter) chamber which will be discussed separately. Many of these tests were conducted for stability objectives and performance data were not analyzed. The 19 tests which were analyzed for performance in a 16 in. chamber are plotted on Figure 83.

Also shown on Figure 83 are the 26 data points obtained with the XDT1-B injector. It was observed that often the first test of the day showed wider scatter (generally lower) than the other tests within the correlation.

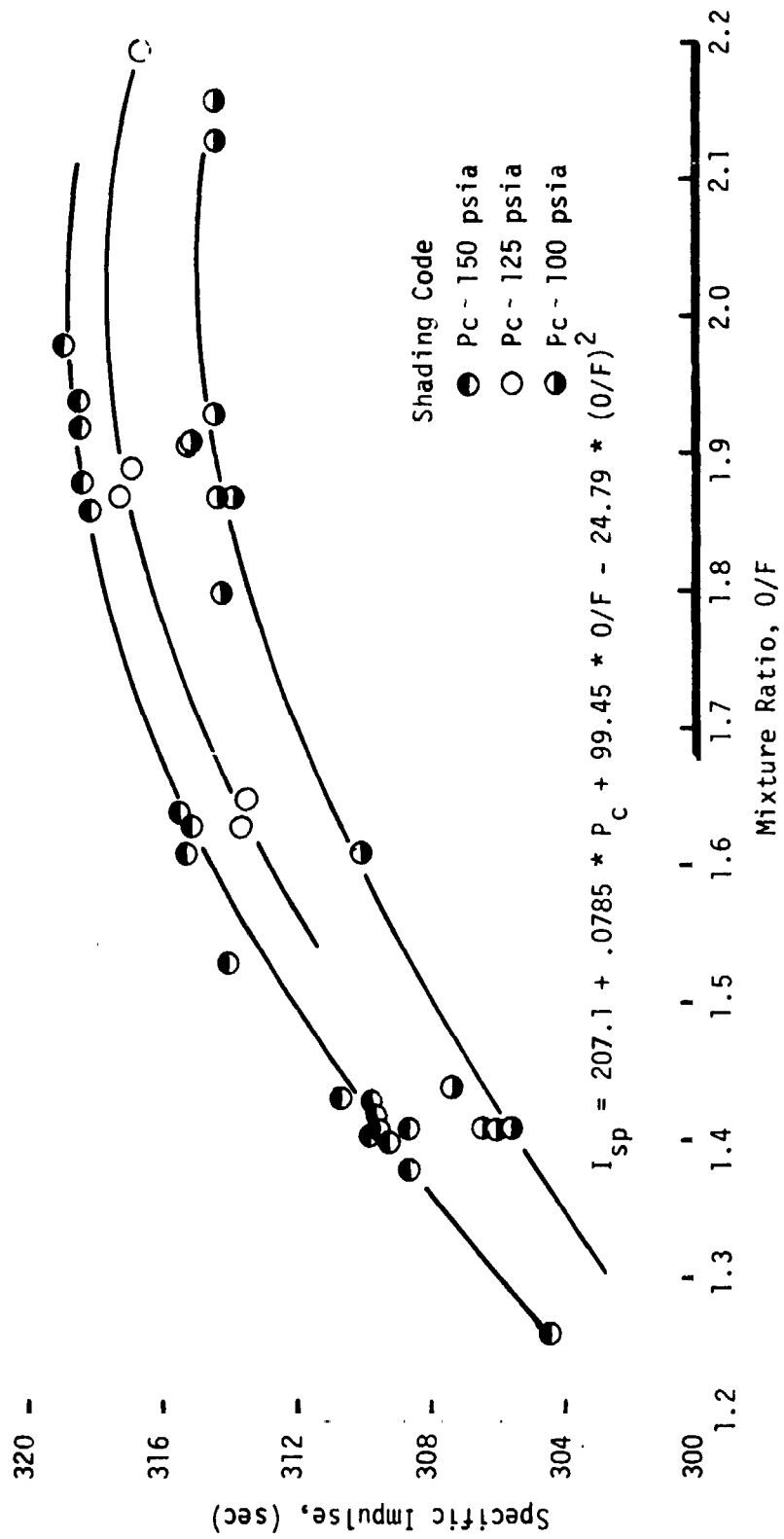


Figure 81. Specific Impulse Obtained with the DXDT1-1 Injector with 16 in. Chamber Length Configuration

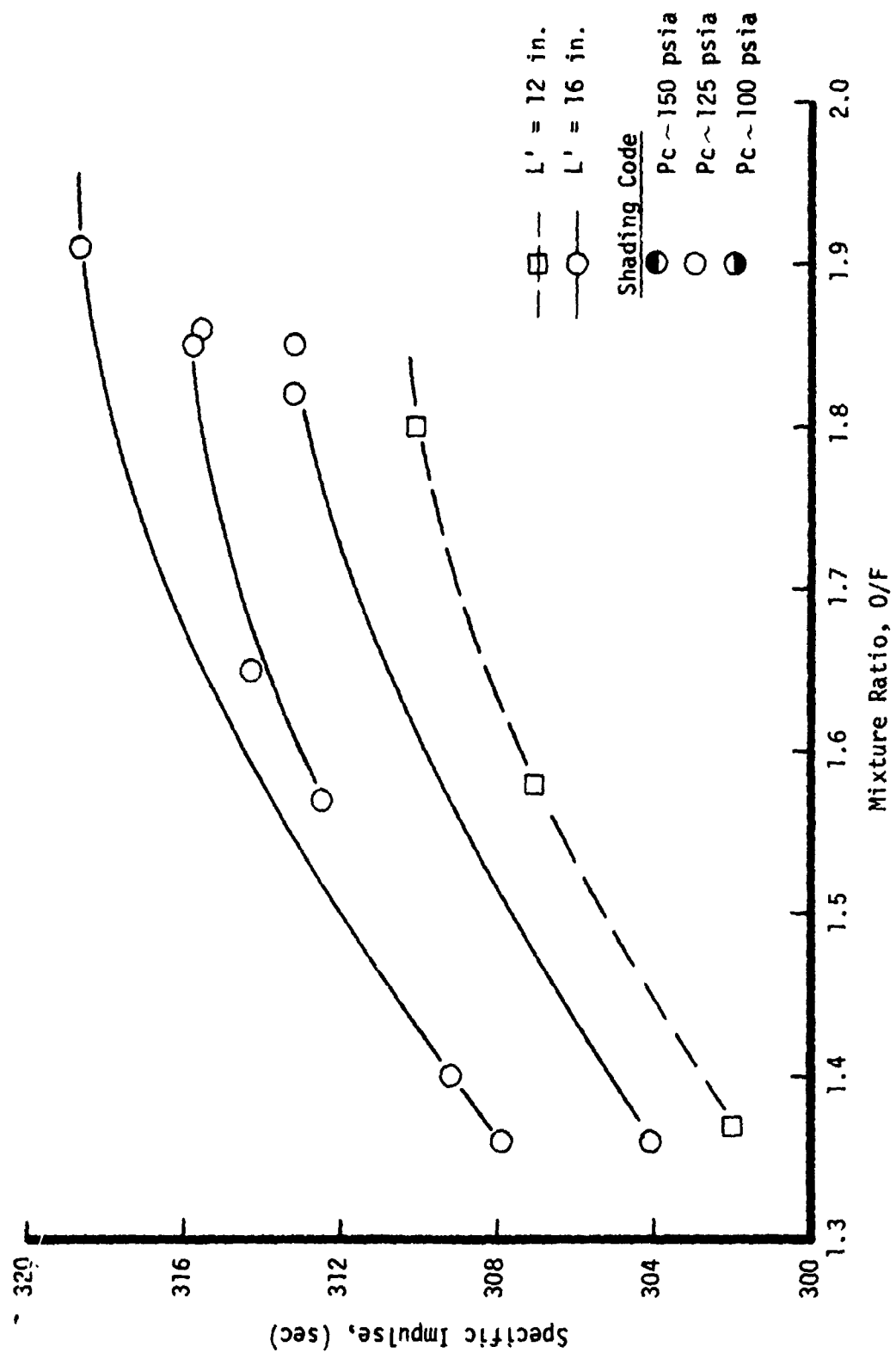


Figure 2. Specific Impulse Obtained with the DXDT1-2 Injector With 12-in. and 16-in. Length Chambers

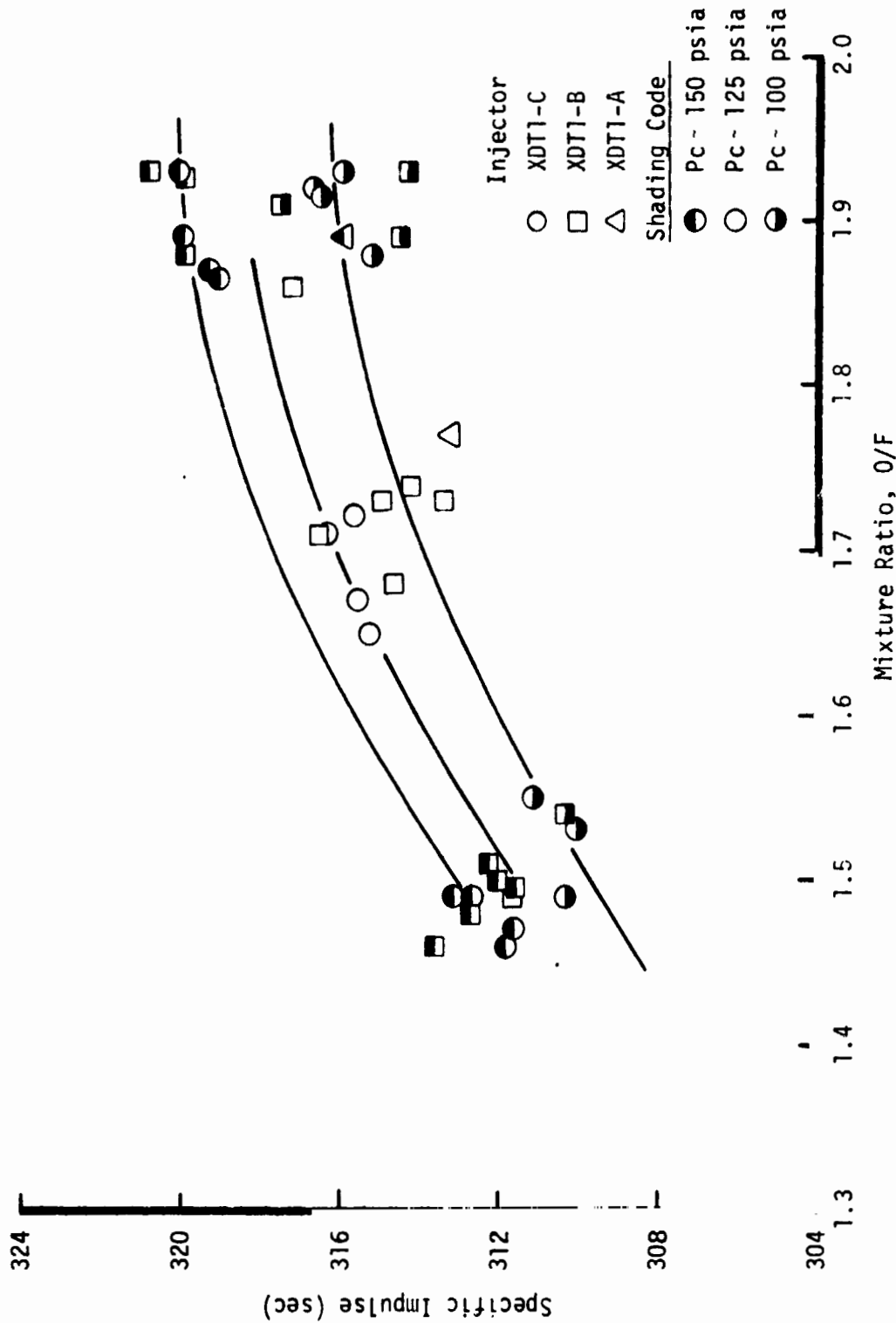


Figure 83. Specific Impulse Obtained with XDT1-A, -B, -C Injectors with 16 in. Heat Sink Chambers

X,B, Data Analysis Results (cont.)

Testing was terminated after only 2 tests on the XDT1-A injector. The performance for these 2 tests are also shown on Figure 83. The specific impulse of the XDT1-A injector appears to be approximately 4 sec. lower than for XDT1-C.

4. Mixed Element Injectors

In order to attempt to reap the high performance benefit of the splash plate element which was demonstrated at the single element and sub-scale thrust levels together with the excellent chamber compatibility and benign combustion stability characteristics of the X-doublet, two mixed element injector patterns were fabricated and tested. The patterns consisted of approximately 60% X-doublet elements distributed around the chamber wall and along the baffles of the integral (3-bladed) baffle unit for compatibility, and at the injector axis for stability because of local sensitivity to the first radial mode. The remaining 40% splash plate elements were placed within the injector core away from solid boundaries.

Although persistent low amplitude combustion instability was triggered during bomb testing by both units, performance was summarized for stable tests and is shown for both injectors on Figure 84. The (unbaffled) ME-1 injector specific impulse is 3 to 4 sec. higher than XDT injectors in 16 in. chambers. Limited testing in a 12 in. chamber indicated that its performance is comparable to XDT injectors in 16 in. chambers. The higher performance of the ME-1 injector (and its degraded stability) must be attributed to the splash plate injection elements.

The baffle length of the integral baffle unit, IBME-1, apparently was insufficient to suppress the 1T-mode instability. In spite of the splash plate elements, its performance was only comparable to other XDT injector performances. The reason for the lower performance of the integral baffled unit is suspected to be caused by a greater mixture ratio maldistribution loss (probably on the order of 4 sec. Isp). The experimentally measured oxidizer pressure drop to regeneratively cool the integral baffles was 115 psid; this excessive value resulted from weld penetration into the flow passages. The oxidizer outflow from the baffle coolant fed directly into the oxidizer manifold and the high baffle outlet velocity head probably degraded the oxidizer injection distribution.

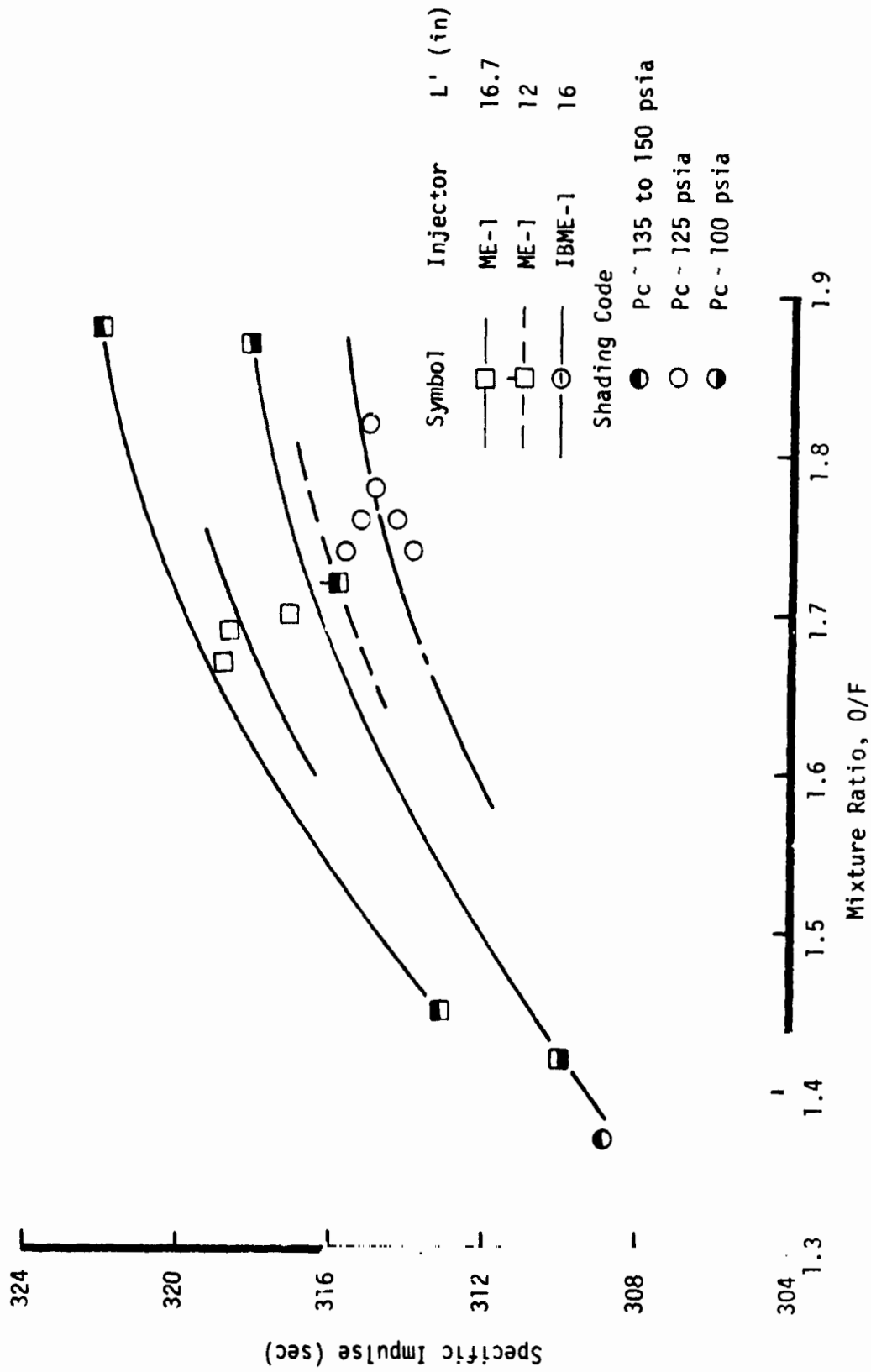


Figure 84. Specific Impulse Obtained with the .6XDT + .4SP Mixed Element Injectors

X,B, Data Analysis Results (cont.)

5. XDT2-A Injector

The XDT2 pattern is identical to the XDT1 pattern in all respects except in the outermost compatibility row element orientation. The compatibility row comprises 13% of the total injection elements. Extrapolated performance for both 12.8 and 16.4 in. chamber lengths is shown on Figure 85. for the XDT2-A injector (dynamically stable with injector face ring dams).

Initial testing of the XDT2 injector configuration without face ring dams resulted in repeated resurge instabilities. Due to the instabilities which could affect injector performance, performance analyses were not conducted for this configuration.

6. Other Platelet Injectors

The XDT1 injector was the first platelet assembly fabricated and tested on the OME Program. Many different parameters were evaluated on this initial unit such as 0 to 15% fuel film cooling, 11 to 14 in. heat sink chamber length, 12.9 in. regeneratively cooled chamber with a 20:1 area ratio truncated Rao contoured nozzle, with both ambient and facility heated fuel. Although many diverse test configurations and operating conditions were evaluated, the quantity of data for any one test condition is scant thus precluding statistical correlation with the multiple covariance computer program. The performance data which were obtained, however, are reported in Table XIV and are plotted on Figure 86. A further complication is that the importance of face ring dams had not been recognized prior to testing this first unit without dams; thus, the occurrence of resurge instability further reduced the number of valid performance tests.

The influence of low injector pressure drop upon performance and stability was intended to be evaluated with a variation of the XDT1 pattern designated XDT1-LP late in the OME Program. After one test firing on this injector, an interpropellant manifold leak was discovered across the platelet stack and further testing was terminated. Based upon performance data for this one test (6K-2B-424) no difference was noted in comparison with other XDT1 injector configurations.

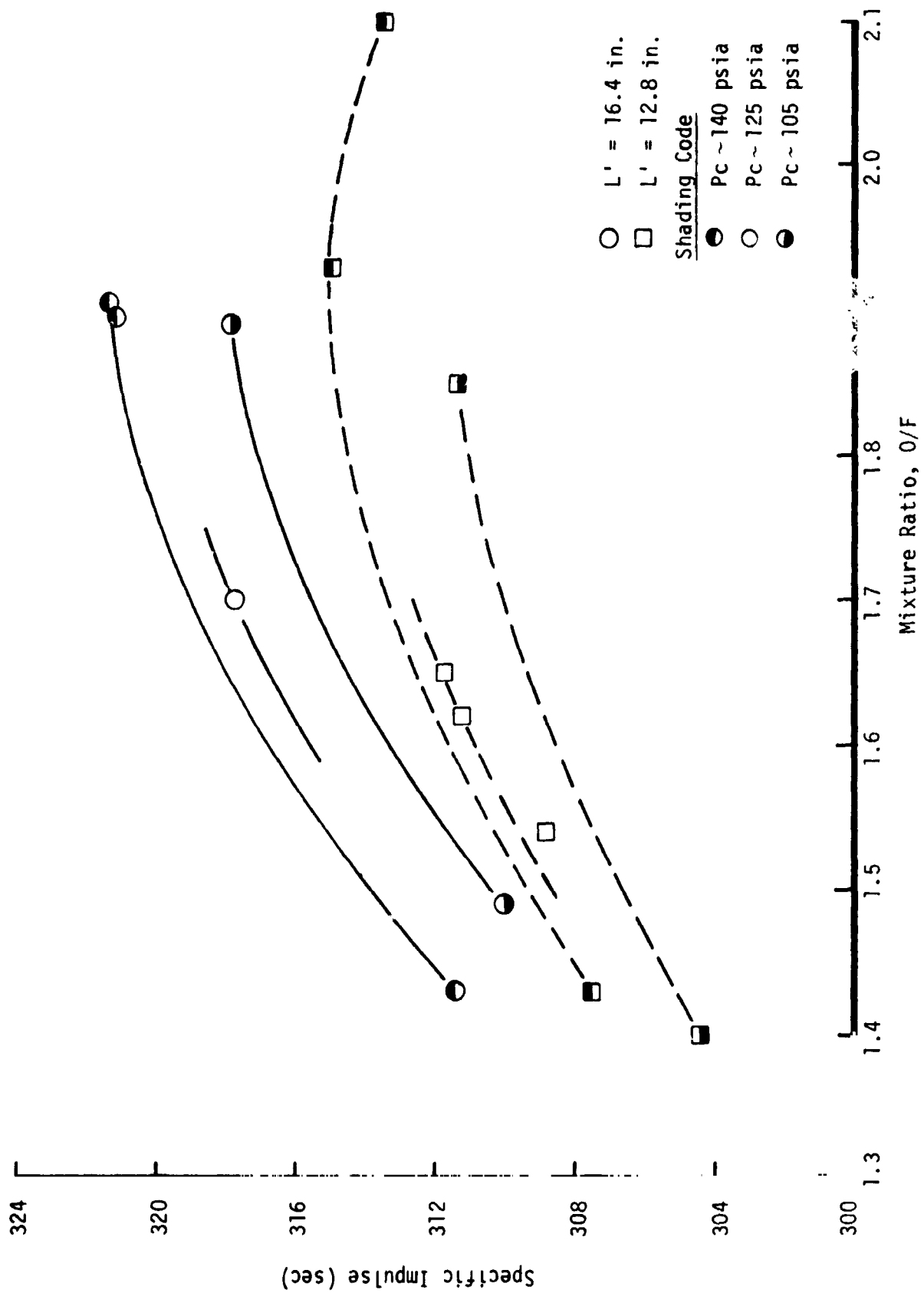


Figure 85. Specific Impulse of XDT2-A Injector with 12.8 and 16.4 in. Length Chambers

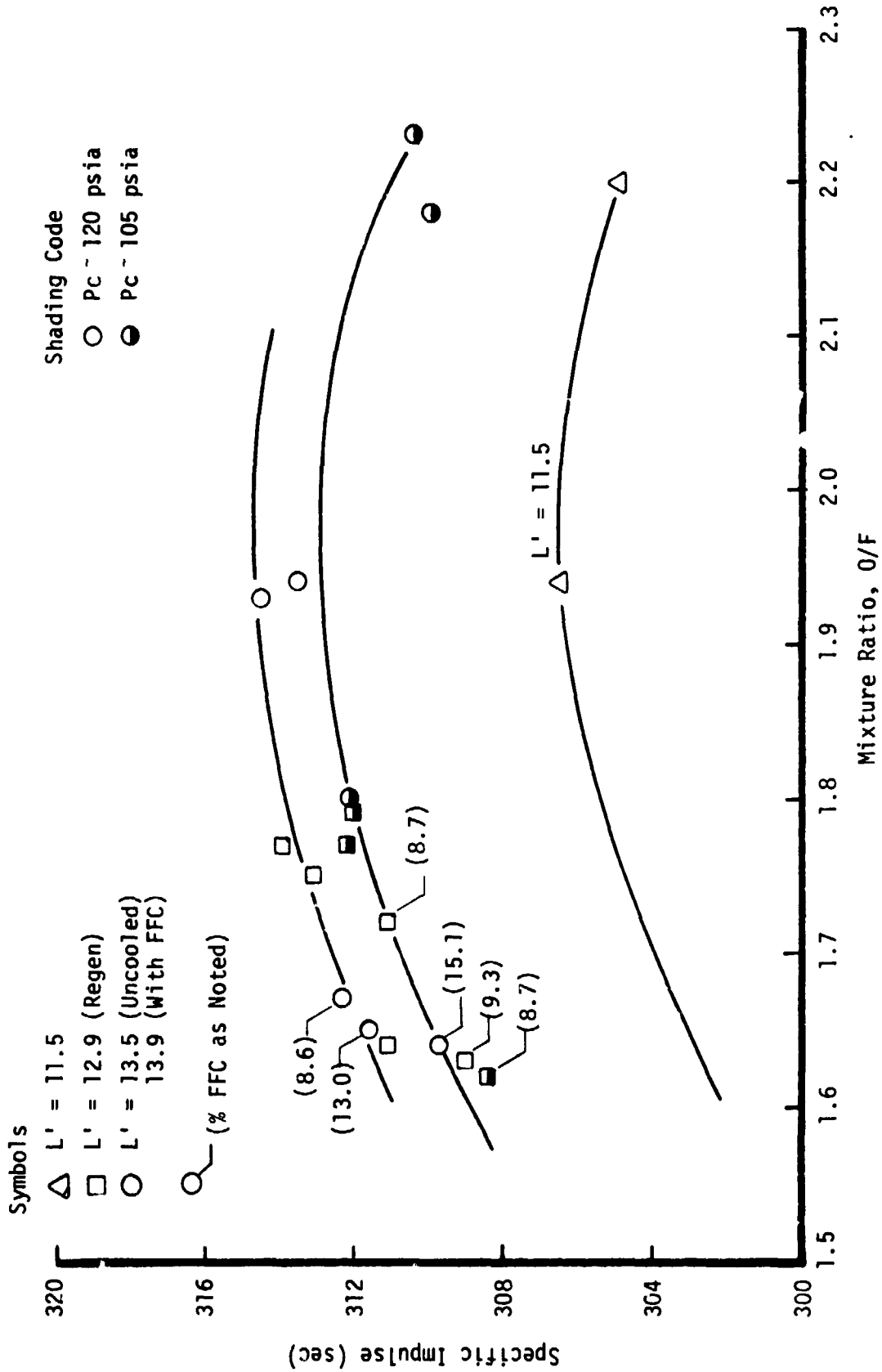


Figure 86. Specific Impulse of XDT1 Injector without Face Ring Dams

X,B, Data Analysis Results (cont.)

The effect of higher contraction ratio on OME stability was also evaluated. Increasing the contraction ratio without increasing injector/chamber diameter necessitated a reduction in throat diameter. To keep P_c constant would have required a reduction in the number of injection elements, if the nominal injection velocities were to be maintained. Since an injector face plate with fewer orifices was not available it was necessary to operate at higher pressures. Thus the XDT1-C injector was used at chamber pressures from 120 to 300 psia, to evaluate chug stability margin. At comparable injection velocities the chamber pressure with the high CR chamber is approximately twice the nominal value. The relative effect of P_c upon performance is similar to the characteristic observed with all of the other injectors as shown on Figure 87. To extrapolate the high CR performance to nominal OMS operating conditions, the nozzle kinetic and boundary layer losses were evaluated at $P_c = 125$ psia; but the injector energy release efficiency was evaluated at nominal design injection velocity, i.e., high CR chamber $P_c \approx 250$ psia. Furthermore, the test nozzle exit area ratio for the high CR chamber was 2.6:1 instead of nominal 2:1 for other sea level tests.

7. Like-Doublet Injector

The like-doublet injector was the only non-platelet injector evaluated on the OME Program. This conventional injector was designed and fabricated on an ALRC funded program. Only the tests conducted on the OME program are included in Tables XI and XIV and in Figure 88.

The like-doublet injector demonstrated excellent high frequency stability characteristics, adequate chug margin and its performance was equivalent to the X-doublet platelet injectors.

C. PERFORMANCE COMPARISON

Four of the injector configurations listed in Table XII were tested both at sea level with 15° conical nozzles having 2:1 area ratio at ALRC, and tested with high area ratio contoured nozzles in the WSTF altitude facility. A comparison between their respective performances is shown in the table below.

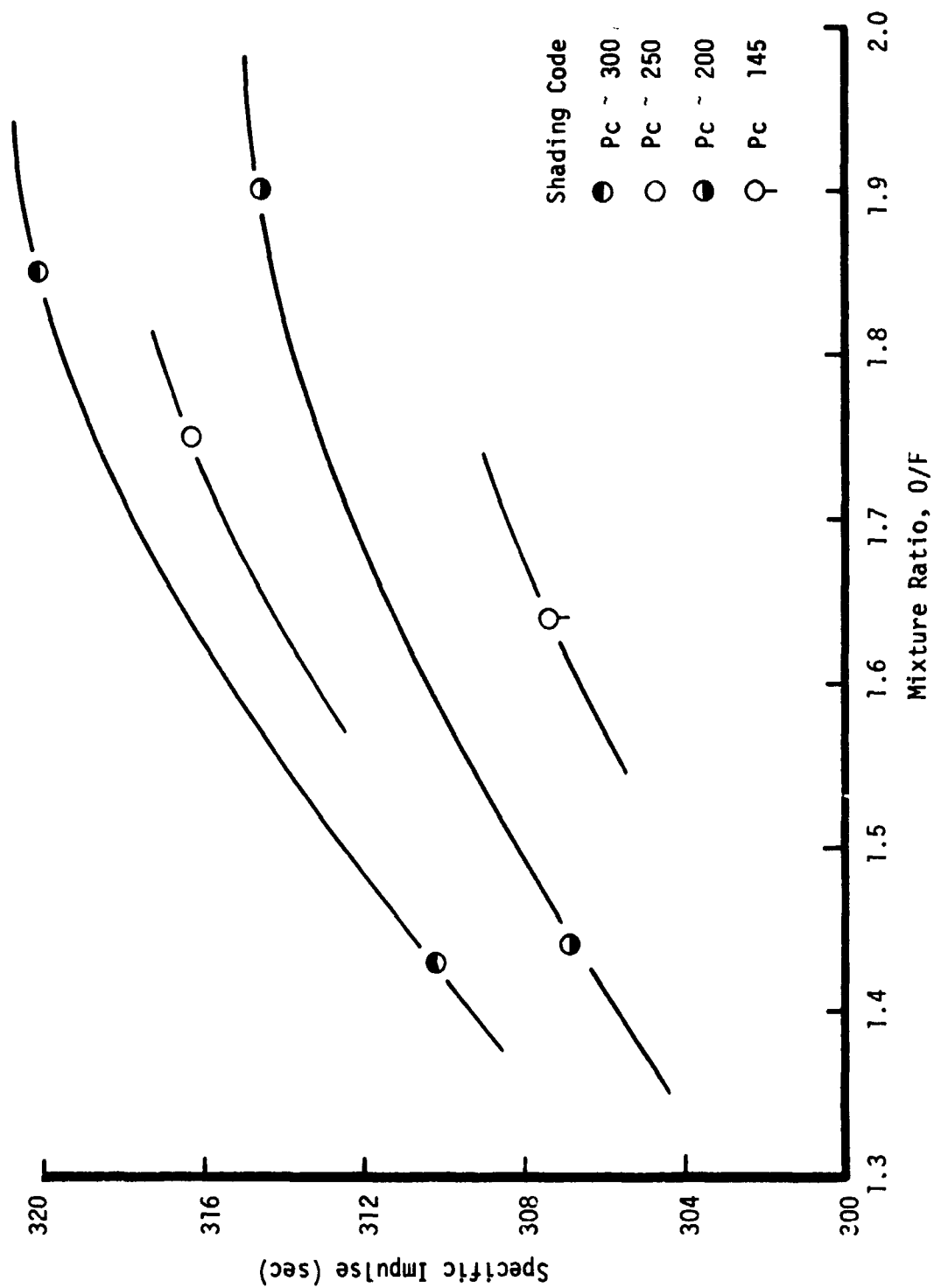


Figure 87. Specific Impulse of XDTI-C Injector with High Contraction Ratio Chamber

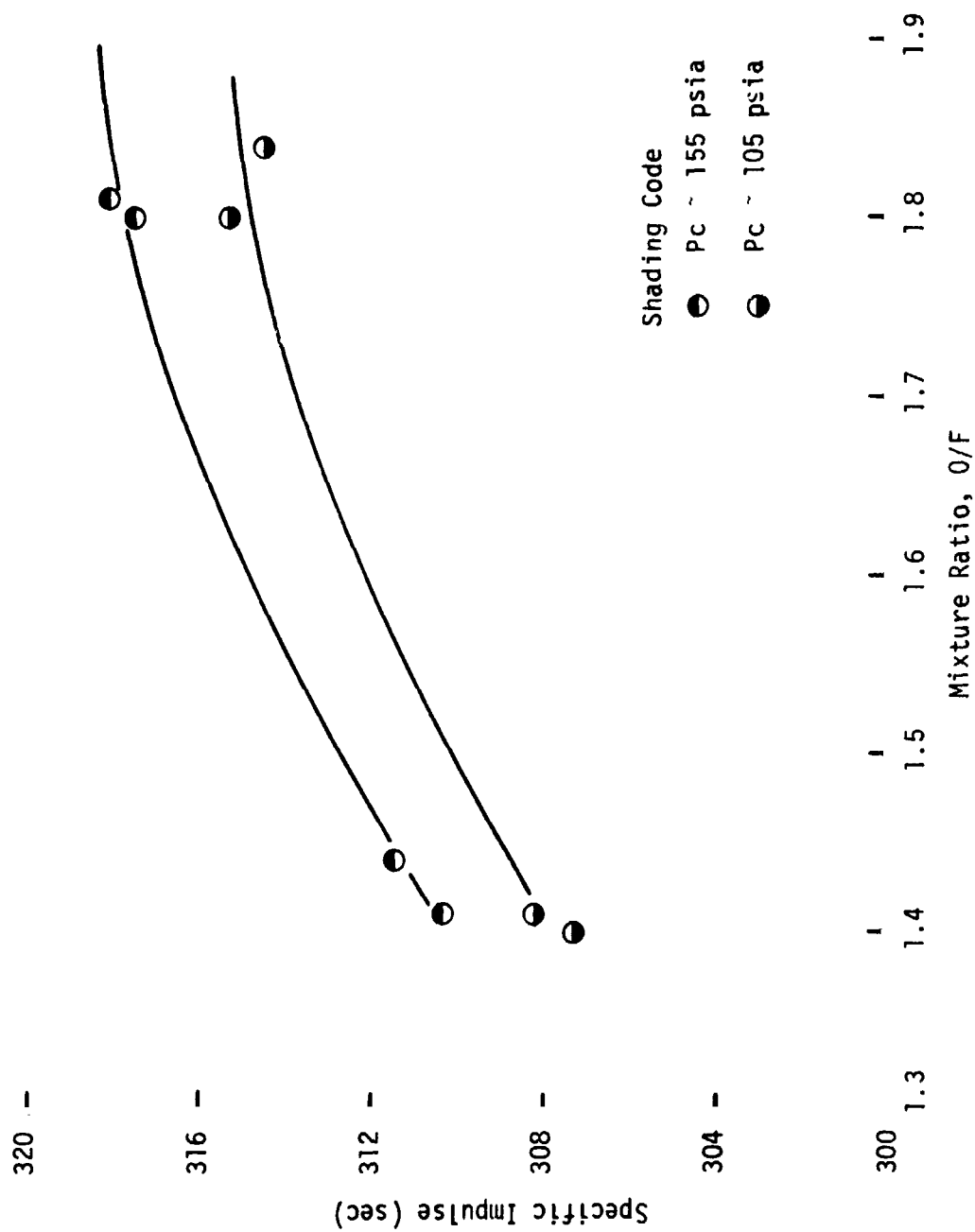


Figure 88. Specific Impulse Obtained with the Like-Doulet Injector with 16 in. Length Chamber

X,C, Performance Comparison (cont.)

COMPARISON OF ALRC PERFORMANCE WITH WSTF DATA

Injector Configuration	<u>L' (in)</u>	<u>ALRC</u>	<u>WSTF</u>
XDT2-A	12.9	311.8	312.6
XDT2-A	16.4	316.7 ⁽¹⁾	314.1
DXDT1-1	16	313.4	316.7
DXDT1-2	16	313.2	318 ⁽²⁾
Like-Doubiet	16	314.7	316.6

- Notes: (1) Questionable Thrust Data
 (2) Questionable Performance; Known Intermanifest Leak

The like-douplet and DEMO-1 injectors delivered 2 and 3 sec. higher Isp, respectively, at the WSTF compared to ALRC sea level extrapolations to the nominal OMS design and operating conditions. This difference is probably due to the limitations of the performance extrapolation technique from 2:1 nozzle area ratio to 55:1. The XDT2-A performance in the shorter chamber shows the closest agreement between ALRC and WSTF performance data of all the configurations listed. The longer chamber ALRC data with the XDT2-A injector is suspect. The thrust measurement cell was replaced subsequent to these tests. Finally, the DEMO-2 data at WSTF is questionable due to a face plate delamination and interpropellant manifold leak which is known to have occurred. Overall, the WSTF performance at least equals or slightly exceeds ALRC performance extrapolations from low area ratio sea level testing. Furthermore, the like-douplet performance and platelet XDT injector performances are equivalent as determined by WSTF altitude testing.

A comparison can also be made between the ALRC performance extrapolations for the various injector configurations summarized in Table XII. Briefly, the performance summary shows that for an equivalent 16 in. chamber length at OMS conditions, eight of the eleven configurations tested delivered between 313 to 315 sec. specific impulse. Of the two injectors which exceeded this performance range, only the mixed element injector is known to have a distinct performance advantage due to the high-performing splash plate elements. The XDT2-A thrust data is suspect as mentioned previously.

Report 13133-F-1

X,C, Performance Comparison (cont.)

Of all the injector configurations tested, only XDT1-A failed to achieve the above performance range. Only 2 tests were conducted with this unit. Further testing was discontinued due to a high injector pressure drop which exceeded the OME pressure schedule which prevailed at that time. In retrospect, the high ΔP may have resulted from inaccurate alignment of the platelet injector pattern to itself or relative to the injector manifold lands during bonding which might have resulted in partial element blockage and local mixture ratio maldistribution performance losses.

In the 12.8 in. length chamber, no difference was discernible between the XDT1 and XDT2-A injector patterns.

D. ANALYSIS AND EXTRAPOLATION TECHNIQUES

Analytical techniques have been used to extrapolate the test performance from its particular test configuration to a common OMS flight configuration. Statistical analysis techniques were also used to establish nominal performance values for a given test series and to derive influence coefficients for the effects of mixture ratio and chamber pressure on performance. A description of these techniques is included in the following paragraphs.

Analytical techniques used for the analysis and extrapolation of test performance are based on the simplified procedures first identified in the ICRPG Liquid Propellant Thrust Chamber Performance Evaluation Manual¹ and further developed by Powell². Briefly, these techniques utilize test data and estimated perfect injector performance for the hardware configuration and conditions tested to establish the injector energy release performance

¹ Pieper, J. L., ICRPG Liquid Propellant Thrust Chamber Performance Evaluation Manual, CPIA No. 178, September 1968

² Powell, W. B., Simplified Procedures for Correlation of Experimentally Measured and Predicted Thrust Chamber Performance, JPL TM-33-548, April 1, 1973

Report 13133-F-1

X, D, Analysis and Extrapolation Techniques (cont.)

efficiency. This energy release efficiency is then used together with an estimated perfect injector performance for the OMS flight configuration to provide the extrapolated flight configuration performance estimate. This procedure results in the estimate of energy release efficiency for all test conditions and compensates for the effects of various test configurations on specific impulse. As a result, it provides a common performance estimate for all test configuration nozzles (2:1 conical, 2.6:1 conical or 20:1 contoured nozzles) and combustion chambers (heat sink or regeneratively cooled) used during the test program.

Perfect injector performance is determined through an evaluation of the one-dimensional kinetic performance and an estimate of the boundary layer and divergence performance losses for the specific test configuration (area ratio, size and contour) and operating conditions (P_c , O/F , T_{prop}). Thus,

$$I_{sp \text{ Perfect Injector}} = I_{sp \text{ (ODK) @ Test Conditions}} - \Delta I_{sp \text{ B.L.}} - \Delta I_{sp \text{ Div}}$$

The energy release loss is then determined from the difference between the perfect injector and test calculated specific impulse, i.e.,

$$\Delta I_{sp \text{ ERL}} = I_{sp \text{ Perfect Injector}} - I_{sp \text{ Test}}$$

and energy release efficiency has been defined as,

$$ERE = \frac{I_{sp \text{ (ODE)}} - \Delta I_{sp \text{ ERL}}}{I_{sp \text{ (ODE)}}$$

Since the OME XDT injector energy release efficiency is primarily mixing-limited³, a simple energy release extrapolation was developed which would

³Injector Final Design Review, ALRC Report No. 6673:064, PDRD SE02B-10, pp 112-153, 15 August 1974

Report 13133-F-1

X, D, Analysis and Extrapolation Techniques (cont.)

reproduce the performance variations with area ratio which result from a mixing limited or mixture ratio maldistributed combustion process. Briefly, the energy release loss for any test condition is simulated by the mixture ratio distribution performance loss of a simple two zone stream tube distribution. A parameter, E_m (included in Table XIV), is selected such that the mass weighted ODK I_{sp} of a two zone distribution results in the test energy release loss. The mixture ratio and mass flow ratio in each stream tube are calculated as a function of EM and the test mixture ratio (O/F) as follows:

$$O/F \text{ Zone 1} = EM * O/F$$

$$O/F \text{ Zone 2} = O/F/EM$$

$$\text{Mass Fraction Zone 1} = (1.0 + O/F * E_m) / (1.0 + E_m) (1.0 + O/F)$$

$$\text{Mass Fraction Zone 2} = 1.0 - \text{Mass Fraction Zone 1}$$

The E_m selected in this manner is then used to calculate the energy release loss at the baseline nozzle area ratio ($\epsilon = 55$) using the same technique and the ODK I_{sp} for the $\epsilon = 55$ condition.

The boundary layer performance losses for the various test configurations were calculated from the Turbulent Boundary Layer⁴ and BLIMP⁵ Computer Programs. The boundary layer performance loss for the regeneratively cooled chambers was approximated by neglecting the heat flux from the boundary layer to the regenerative coolant (fuel flow) and using ODE and ODK specific impulse based on propellant tank temperatures. Generally, the performance loss resulting from the heat flux to the fuel coolant is approximately equal to the performance increase resulting from the increased fuel enthalpy. It is possible,

⁴Weingold, H. D., The ICRPG Turbulent Boundary Layer Reference Program, Pratt & Whitney Aircraft, July 1968.

⁵Evans, R. M., and Morse, H. L., Boundary Layer Integral Matrix Procedure Code Modifications and Verifications, Aerotherm Final Report 74-95, Contract NAS 8-29667, March 1974.

Report 13133-F-1

X, D, Analysis and Extrapolation Techniques (cont.)

however, that the injector performance is altered because of the increased fuel temperature (improved fuel vaporization, blowpart, etc.) and this effect is then justifiably included in the calculated energy release efficiency. For the heat-sink chamber configurations, the boundary layer loss includes the effects of the heat flux to the chamber walls. The effects of regenerative cooling are simulated by heating the fuel for the heat sink chamber tests and, in that case, the ODE and ODK specific impulse values are based on the injection propellant temperatures.

The divergence performance loss is calculated as follows:

$$\Delta I_{sp \text{ Div}} = I_{sp \text{ Test}} * \left[\frac{1.0}{ETAD} - 1.0 \right]$$

where ETAD is the nozzle divergence efficiency calculated from the TDK computer program using the ideal gas option. The following values of ETAD were calculated for each of the test configuration nozzles:

<u>Nozzle</u>	<u>Area Ratio</u>	<u>ETAD</u>
15° Conical	2:1	.9840
15° Conical	2.6:1	.9865
Rao Contoured Cut-Off	20:1	.9390
OMS	55:1	.9906

The techniques described above were used in the analysis of all test data. The nomenclature used in the performance summary is shown in Table XIII and the summary of the test-by-test data is presented on pages 218 through 242.

Statistical analysis techniques used to establish nominal performance values and parametric influence coefficients are based on a One-Way Multiple Covariance Analysis Computer Program. Standard multiple regression and covariance techniques are used and individual group, parallel plane, and single plane analyses are made. The analysis of covariance table, estimated components of

Report 13133-F-1

X, D, Analysis and Extrapolation Techniques (cont.)

variance, tests of hypotheses and adjusted dependent means are included in the program output. All average values and data correlations given in the previous section were determined using the Multiple Covariance Computer Program.

TABLE XIII
NOMENCLATURE USED IN PERFORMANCE SUMMARY

Test	Test series, sequence, number
Time	Data period end time (sec)
P_c	Chamber pressure (psia)
MRC	Core mixture ratio
MR	Overall mixture ratio
FFC	Fuel film cooling percentage (%)
CSTAR	Test characteristic velocity (ft/sec)
CSTART	ODE C^* at test condition (ft/sec)
% C^*	$(CSTAR/CSTART) \times 100$
ISPV	Test vacuum specific impulse (lbf-sec/lbm)
ISPT	ODE Isp at test condition (lbf-sec/lbm)
% Isp	$(Ispv/Ispt) \times 100$
KL	Kinetic loss (sec)
DL	Divergence loss (sec)
BL	Boundary layer loss (sec)
FCL	Film cooling loss (sec)
ERL	Energy release loss (sec)
ERE	Energy release efficiency (thrust based)
Isp-55	Extrapolated OMS configuration Isp
F_{vac}	Test vacuum thrust (lbf)
WO	Test oxidizer flowrate (lbm/sec)
WF	Test injector fuel flowrate (lbm/sec)
WFC	Test fuel film coolant flowrate (lbm/sec)
WT	Total flowrate (lbm/sec)
DPOJ	Oxidizer injector pressure drop (psid)
DPFJ	Fuel injector pressure drop (psid)
VOX	Oxidizer injection velocity based on DPOJ $(2 \Delta P/\rho)^{1/2}$
VF	Fuel injection velocity based on DPFJ $(2 \Delta P/\rho)^{1/2}$
KWO	Oxidizer injector admittance $WO/\sqrt{DPOJ \cdot Spgo}$
KWF	Fuel injector admittance $WF/\sqrt{DPFJ \cdot Spgf}$
TW	Gas-side wall temperature (°F)
TO	Oxidizer Inlet Temperature (°F)
TF	Fuel inlet temperature (°F)
TFJ	Fuel injector temperature (°F)
E_m	Energy release mixing limited factor
EREE	Energy release efficiency for OMS baseline configuration corresponding to E_m
ERC	Chamber pressure based energy release efficiency per MPL TM 33-548
MRE	Mixture ratio for extrapolated Isp
FFCE	Film cooling percentage for extrapolated Isp
ODE	One-dimensional equilibrium Isp for extrapolated condition
ODK	One-dimensional kinetic Isp for extrapolated condition
CFCL	C^* fuel film coolant loss (ft/sec)

PAGE 4

DATE 141675

2 100

9/11/75 10:10:40 F00117 000427581 000427

***** UMS ENGINE TEST DATA AND PERFORMANCE SUMMARY *****

Appendix to the Performance Section

PLATELET INJECTION PROGRAM XOT-1 INJECTOR

AREA MATIU 2 MUZZLE 13.5 IN. CHB. (13.9 IN. WITH FILM COOLANT RING)

PC BASED ON P(CAV) / 1.06

TEST	TIME	PC	MPC	MR	FFC	CSIAH	CSTART	XC*	ISPV	ISPT	XISP	KL	DL	BL	FCL	ERL	EWE	ISP-55
13	2.10	114.8	1.94	1.94	.0	5588.	5664.	98.6	246.6	260.5	94.7	1.69	4.01	2.55	.00	5.63	97.8	313.5
14	2.10	115.1	1.93	1.93	.0	5614.	5667.	99.1	247.2	260.5	94.9	1.67	4.02	2.54	.00	5.67	98.1	314.5
15	2.10	113.6	2.18	2.18	.0	5528.	5596.	98.6	243.9	257.5	94.7	1.64	3.97	2.53	.00	5.45	97.9	309.9
17	2.10	105.7	2.23	2.23	.0	5518.	5573.	94.0	244.1	256.6	95.1	1.75	3.97	2.56	.00	4.28	98.3	310.4
18	2.00	102.5	1.90	1.80	.0	5559.	5646.	97.7	246.4	261.3	94.4	1.68	4.01	2.61	.00	6.37	97.6	312.1
23	2.50	119.8	1.93	1.84	15.1	5495.	5698.	96.5	243.8	261.2	93.4	1.43	3.96	2.51	4.05	5.41	97.9	309.7
24	4.10	122.2	1.89	1.85	13.0	5524.	5700.	96.9	245.4	261.2	94.0	1.41	3.99	2.46	3.18	4.75	98.2	311.6
26	4.10	121.9	1.83	1.87	6.6	5553.	5702.	97.4	246.6	261.4	94.3	1.44	4.01	2.42	1.61	5.37	97.9	312.3

TEST	TIME	PC	MPC	MR	FFC	CSIAH	CSTART	XC*	ISPV	ISPT	XISP	KL	DL	BL	FCL	ERL	EWE	ISP-55
13	2.10	114.8	1.94	1.94	.0	5588.	5664.	98.6	246.6	260.5	94.7	1.69	4.01	2.55	.00	5.63	97.8	313.5
14	2.10	115.1	1.93	1.93	.0	5614.	5667.	99.1	247.2	260.5	94.9	1.67	4.02	2.54	.00	5.67	98.1	314.5
15	2.10	113.6	2.18	2.18	.0	5528.	5596.	98.6	243.9	257.5	94.7	1.64	3.97	2.53	.00	5.45	97.9	309.9
17	2.10	105.7	2.23	2.23	.0	5518.	5573.	94.0	244.1	256.6	95.1	1.75	3.97	2.56	.00	4.28	98.3	310.4
18	2.00	102.5	1.90	1.80	.0	5559.	5646.	97.7	246.4	261.3	94.4	1.68	4.01	2.61	.00	6.37	97.6	312.1
23	2.50	119.8	1.93	1.84	15.1	5495.	5698.	96.5	243.8	261.2	93.4	1.43	3.96	2.51	4.05	5.41	97.9	309.7
24	4.10	122.2	1.89	1.85	13.0	5524.	5700.	96.9	245.4	261.2	94.0	1.41	3.99	2.46	3.18	4.75	98.2	311.6
26	4.10	121.9	1.83	1.87	6.6	5553.	5702.	97.4	246.6	261.4	94.3	1.44	4.01	2.42	1.61	5.37	97.9	312.3

TEST	TIME	PC	MPC	MR	FFC	CSIAH	CSTART	XC*	ISPV	ISPT	XISP	KL	DL	BL	FCL	ERL	EWE	ISP-55
13	2.10	114.8	1.94	1.94	.0	5588.	5664.	98.6	246.6	260.5	94.7	1.69	4.01	2.55	.00	5.63	97.8	313.5
14	2.10	115.1	1.93	1.93	.0	5614.	5667.	99.1	247.2	260.5	94.9	1.67	4.02	2.54	.00	5.67	98.1	314.5
15	2.10	113.6	2.18	2.18	.0	5528.	5596.	98.6	243.9	257.5	94.7	1.64	3.97	2.53	.00	5.45	97.9	309.9
17	2.10	105.7	2.23	2.23	.0	5518.	5573.	94.0	244.1	256.6	95.1	1.75	3.97	2.56	.00	4.28	98.3	310.4
18	2.00	102.5	1.90	1.80	.0	5559.	5646.	97.7	246.4	261.3	94.4	1.68	4.01	2.61	.00	6.37	97.6	312.1
23	2.50	119.8	1.93	1.84	15.1	5495.	5698.	96.5	243.8	261.2	93.4	1.43	3.96	2.51	4.05	5.41	97.9	309.7
24	4.10	122.2	1.89	1.85	13.0	5524.	5700.	96.9	245.4	261.2	94.0	1.41	3.99	2.46	3.18	4.75	98.2	311.6
26	4.10	121.9	1.83	1.87	6.6	5553.	5702.	97.4	246.6	261.4	94.3	1.44	4.01	2.42	1.61	5.37	97.9	312.3

08/16/75 10:10:40 FD0117 000427581 000427 2 100 DATE 041675 PAGE 0

***** UMS ENGINE TEST DATA AND PERFORMANCE SUMMARY *****

PLATELET INJECTOR PROGRAM XDT-1 INJECTOR

AREA RATIO 2 NUZZLE 11.5 INCH CHAMBER

PC BASED ON P(CAV) / 1.06

TEST TIME	PC	MRC	MR	FFC	CSTAR	%C*	ISPV	ISPT	XISP	KL	DL	BL	FCL	ERL	ENE	ISP-55
19 2.10	114.2	1.94	1.94	.0	5500.	5607.	97.2	242.0	260.6	93.2	1.69	3.95	.00	9.74	96.3	306.5
20 2.10	115.4	2.20	2.20	.0	5486.	5589.	98.1	242.0	257.3	94.0	1.62	3.93	.00	7.47	97.1	304.9

Report 13133-F-1

TEST TIME	PC	FVAC	WD	WF	WFC	WT	DPOJ	DPFJ	VOX	VF	KMO	KMF	TM	TD	TF	TFJ
19 2.10	114.2	4304.0	11.850	6.120	.000	17.97	48.0	44.0	71.	90.	1.441	1.032	1160.	97.	207.	207.
20 2.10	115.4	4411.0	12.530	5.700	.000	18.23	53.4	38.1	75.	84.	1.446	1.033	1160.	90.	208.	208.

TEST PC	MR	MRC	EM	UREE	ERC	MRE	FFCE	UDE	ODK	KL	DL	BLL	ERL	FCL	CFCL	ISP-55
19 114.2	1.94	1.94	66.9	95.2	96.9	1.94	.0	340.6	331.4	9.25	2.90	5.69	16.28	.00	.0	306.5
20 115.4	2.20	2.20	68.8	95.4	98.0	2.20	.0	343.3	329.3	14.00	2.88	5.65	15.86	.00	.0	304.9

ORIGINAL PAGE IS
OF POOR QUALITY

***** * OPS ENGINE TEST DATA AND PERFORMANCE SUMMARY *****

PLATELET INJECTOR PROGRAM XDT-1 INJECTOR

12.9 IN. REGEN CHAMBER AREA RATIO 20:1 RAD CUT-OFF NOZZLE EXTENSION

J-4 ALTITUDE TESTING PC BASED ON P(CAV) / 1.06

TEST	TIME	PC	MHC	MR	FFC	CSTAR	CSTART	XC*	ISPV	ISPT	XISP	KL	DL	BL	FCL	ENL	ERE	TSP-55
30	5.00	120.0	1.69	1.74	8.1	5511.	5696.	96.7	287.7	322.6	89.2	5.45	18.69	3.57	1.74	5.45	98.3	314.4
31	5.00	118.3	1.69	1.72	8.7	5455.	5697.	95.7	284.7	322.3	88.3	5.37	18.50	3.53	1.98	8.21	97.5	311.1
31	10.00	117.3	1.43	1.75	9.0	5432.	5694.	95.4	283.4	322.8	87.8	5.67	18.41	3.53	2.17	9.71	97.0	309.8
31	15.00	116.4	1.48	1.74	9.2	5415.	5691.	95.2	282.5	323.2	87.4	5.91	18.35	3.53	2.32	10.58	96.7	309.0
32	5.00	119.6	1.70	1.63	9.3	5438.	5693.	95.5	283.0	320.3	88.3	4.63	18.38	3.47	1.82	5.16	97.2	309.0
32	10.00	119.2	1.61	1.64	8.4	5427.	5695.	95.3	282.2	320.7	88.0	4.76	18.33	3.48	1.92	10.02	96.9	308.2
32	15.00	118.9	1.82	1.65	9.2	5418.	5695.	95.1	281.7	320.9	87.8	4.83	18.30	3.47	1.92	10.70	96.7	307.8
33	5.00	105.7	1.75	1.60	8.9	5463.	5687.	96.1	283.3	319.7	88.6	4.68	18.40	3.57	1.61	8.12	97.5	309.0
33	10.00	105.3	1.76	1.61	4.5	5452.	5688.	95.9	282.8	319.9	88.4	4.74	18.37	3.56	1.53	8.91	97.2	308.2
33	15.00	104.9	1.78	1.62	8.7	5456.	5689.	95.9	282.9	320.2	88.4	4.87	18.38	3.58	1.60	8.86	97.2	308.4
34	5.00	121.9	1.61	1.61	.0	5517.	5693.	96.9	286.6	320.0	89.6	4.51	18.62	3.51	.00	6.77	97.9	312.4
34	10.00	120.5	1.64	1.64	.0	5443.	5694.	96.3	285.3	320.5	89.0	4.69	18.53	3.51	.00	8.46	97.4	311.1
34	15.00	120.5	1.65	1.65	.0	5442.	5696.	96.4	285.0	320.8	88.9	4.79	18.52	3.52	.00	8.92	97.2	310.9
35	5.00	120.7	1.74	1.74	.0	5521.	5697.	96.9	287.5	322.9	89.1	5.50	18.68	3.58	.00	7.59	97.7	313.8
35	10.00	120.4	1.75	1.75	.0	5518.	5696.	96.8	286.9	323.0	88.8	5.59	18.64	3.58	.00	8.31	97.4	313.1
35	15.00	105.2	1.79	1.79	.0	5511.	5687.	96.9	286.2	323.6	88.4	6.27	18.59	3.68	.00	8.89	97.3	312.0
37	5.00	105.0	1.75	1.75	.0	5525.	5691.	97.1	287.1	323.1	88.8	5.45	18.65	3.68	.00	7.79	97.6	312.6
37	10.00	104.9	1.77	1.77	.0	5516.	5690.	97.0	286.5	323.3	88.6	6.07	18.61	3.68	.00	8.40	97.4	312.2
37	15.00	104.3	1.77	1.77	.0	5521.	5686.	97.1	286.5	323.4	88.6	6.14	18.61	3.69	.00	8.51	97.4	312.2
38	5.00	120.9	1.77	1.77	.0	5519.	5695.	96.9	287.6	323.2	89.0	5.70	18.68	3.58	.00	7.67	97.6	313.9

Report 13133-F-1

ORIGINAL PAGE IN
OF POOR QUALITY

DATE 041675

2 100

04/16/75 10:10:40 FD0117 000427581 000427

***** UMS ENGINE TEST DATA AND PERFORMANCE SUMMARY *****

PLATELET INJECTOR PROGRAM XUT-1 INJECTOR

12.9 IN. WEGEN CHAMBER AREA RATIO 20:1 RAO CUT-OFF NOZZLE EXTENSION

J-4 ALTITUDE TESTING PC BASED ON P(CAV) / 1.06

TEST	TIME	PC	FVAC	NU	WF	WFC	WT	DPOJ	UPFJ	VDX	VF	KWD	KWF	TM	TO	TF	TFJ
30	5.00	120.0	5489.6	12.104	0.410	.563	19.08	51.4	50.4	73.	95.	1.410	.990	3460.	76.	76.	143.
31	5.00	116.3	5411.7	12.024	0.372	.610	19.01	50.5	61.1	72.	104.	1.414	.895	3460.	79.	76.	147.
31	10.00	117.3	5361.0	12.051	0.250	.619	16.92	50.6	68.0	72.	111.	1.414	.839	3460.	76.	71.	173.
31	15.00	116.4	5322.2	12.062	0.152	.625	16.84	50.7	71.6	72.	114.	1.413	.808	3460.	74.	66.	185.
32	5.00	119.4	5463.7	11.956	0.671	.681	19.31	49.4	75.1	72.	116.	1.422	.848	3460.	79.	84.	158.
32	10.00	119.2	5433.6	11.969	0.604	.682	19.25	49.6	76.5	72.	118.	1.419	.835	3460.	77.	82.	172.
32	15.00	116.9	5415.1	11.976	0.580	.670	19.23	49.5	76.8	72.	118.	1.421	.832	3460.	76.	78.	178.
33	5.00	105.7	4802.2	10.424	5.948	.578	16.95	36.8	51.0	62.	96.	1.437	.918	3460.	80.	88.	160.
33	10.00	105.3	4795.2	10.427	5.940	.555	16.92	36.8	50.3	62.	96.	1.436	.927	3460.	78.	88.	174.
33	15.00	104.9	4767.4	10.423	5.871	.556	16.85	36.8	49.7	62.	95.	1.434	.924	3460.	76.	83.	182.
34	5.00	121.9	5549.1	11.953	.408	.000	14.36	50.9	81.0	73.	122.	1.401	.913	3460.	81.	83.	181.
34	10.00	120.5	5443.6	11.950	7.360	.000	14.26	51.4	85.7	73.	126.	1.392	.885	3460.	78.	78.	215.
34	15.00	120.5	5478.8	11.972	7.252	.000	14.22	50.7	86.3	72.	127.	1.404	.877	3460.	77.	73.	218.
35	5.00	120.7	5510.7	12.182	6.984	.000	19.17	52.3	71.9	74.	115.	1.409	.916	3460.	81.	88.	193.
35	10.00	120.4	5486.9	12.162	6.944	.000	19.13	52.1	72.0	73.	116.	1.411	.919	3460.	79.	85.	217.
35	15.00	105.2	4766.9	10.727	5.964	.000	16.73	39.7	50.1	64.	96.	1.426	.943	3460.	84.	92.	194.
36	5.00	105.0	4781.2	10.610	6.046	.000	16.66	39.0	49.3	64.	95.	1.424	.960	3460.	85.	95.	199.
37	10.00	104.6	4762.3	10.612	6.009	.000	16.62	39.0	49.1	64.	96.	1.423	.966	3460.	83.	93.	224.
37	15.00	104.3	4744.2	10.590	5.972	.000	16.56	38.8	48.5	63.	96.	1.423	.968	3460.	82.	93.	231.
38	5.00	120.9	5522.5	12.265	6.939	.000	19.20	52.6	65.3	74.	109.	1.413	.955	3460.	78.	84.	187.

***** UNS ENGINE TEST DATA AND PERFORMANCE SUMMARY *****

PLATELET INJECTION PROGRAM XDI-1 INJECTOR

12.9 IN. GREEN CHAMBER AREA RATIO 20:1 RAD CUT-OFF NOZZLE EXTENSION

J-W ALTITUDE TESTING PC BASED ON P(CAV) / 1.06

TEST	PC	PM	PMG	EM	EMEF	EMC	MRE	FFCE	ONE	ODK	KL	DL	BLL	ERL	FCL	CFCL	ISP-55
30	120.6	1.74	1.69	77.8	98.4	97.2	1.74	8.1	336.8	330.2	6.64	2.97	5.56	5.50	1.74	37.6	314.4
31	118.3	1.72	1.69	73.1	97.5	96.3	1.72	8.7	336.5	329.9	6.59	2.94	5.53	6.37	1.98	43.1	311.1
31	117.3	1.75	1.93	71.6	97.1	96.0	1.75	7.0	337.2	330.3	6.91	2.93	5.51	9.84	2.16	45.8	309.8
31	116.4	1.74	1.96	70.6	96.6	95.4	1.74	9.2	337.7	330.5	7.20	2.92	5.50	10.84	2.33	47.8	309.0
32	114.8	1.63	1.79	70.3	97.3	96.0	1.63	9.3	334.0	328.1	5.84	2.92	5.44	8.94	1.60	42.7	309.0
32	114.2	1.64	1.81	69.4	97.0	95.9	1.64	9.4	334.4	328.5	5.97	2.92	5.48	9.91	1.91	44.6	308.2
32	112.9	1.65	1.62	68.8	96.4	95.7	1.65	9.2	334.7	328.6	6.04	2.91	5.48	10.55	1.92	44.4	307.8
33	105.7	1.60	1.75	71.6	97.7	96.5	1.60	8.9	333.1	327.0	6.10	2.92	5.66	7.82	1.61	38.0	309.0
33	105.3	1.61	1.75	70.3	97.4	96.3	1.61	8.5	333.3	327.1	6.18	2.92	5.65	8.82	1.53	36.0	308.2
33	104.9	1.62	1.74	70.6	97.3	96.4	1.62	8.7	333.8	327.5	6.32	2.92	5.66	8.85	1.61	37.6	308.4
34	121.9	1.61	1.61	73.7	97.9	96.7	1.61	.0	333.6	327.9	5.69	2.96	5.57	6.95	.00	.0	312.4
34	120.5	1.64	1.64	71.6	97.4	96.1	1.64	.0	334.2	328.3	5.88	2.94	5.54	8.72	.00	.0	311.1
34	120.5	1.65	1.65	71.1	97.2	96.2	1.65	.0	334.7	328.7	5.98	2.94	5.55	9.28	.00	.0	310.9
35	120.7	1.74	1.74	74.4	97.6	96.8	1.74	.0	337.0	330.3	6.68	2.97	5.58	8.01	.00	.0	313.8
35	120.4	1.75	1.75	73.4	97.4	96.7	1.75	.0	337.2	330.4	6.79	2.96	5.56	8.74	.00	.0	313.1
36	105.2	1.79	1.79	73.0	97.2	96.8	1.79	.0	337.9	330.1	7.80	2.95	5.73	9.36	.00	.0	312.0
37	105.0	1.75	1.75	74.2	97.5	97.0	1.75	.0	337.2	329.7	7.45	2.96	5.75	8.25	.00	.0	312.8
37	104.9	1.77	1.77	73.4	97.4	96.9	1.77	.0	337.4	329.8	7.58	2.95	5.74	8.88	.00	.0	312.2
37	104.3	1.77	1.77	73.4	97.4	97.0	1.77	.0	337.5	329.9	7.67	2.95	5.75	8.92	.00	.0	312.2
37	120.9	1.77	1.77	74.4	97.6	96.8	1.77	.0	337.5	330.6	6.89	2.97	5.58	8.18	.00	.0	313.9

Report 13133-F-1

ORIGINAL PAGE IS
OF POOR QUALITY

***** OMS ENGINE TEST DATA AND PERFORMANCE SUMMARY *****

PLATELET INJECTOR PROGRAM XDT-2AINJECTOR

AREA RATIO 2 NOZZLE 12.8 INCH CHAMBER

A-AREA TESTING PC BASED ON P-1 CORRECTED TO P(CAV)

TEST TIME	PC	MRC	MR	FPC	CSTAR	XCA	ISPV	ISPT	XISP	KL	DL	BL	FCL	ERL	ERE	ISP-55
125	1.80	134.2	2.10	2.10	5626.	99.7	245.7	250.6	94.9	1.48	3.99	2.47	.00	5.14	98.0	313.4
126	1.80	132.4	1.43	1.43	5656.	98.7	245.0	259.2	94.5	1.12	3.98	2.40	.00	6.76	97.4	307.5
127	1.80	105.1	1.85	1.85	5075.	99.0	246.1	261.3	94.2	1.71	4.00	2.59	.00	6.90	97.4	311.3
128	1.80	104.7	1.40	1.40	5556.	98.6	243.5	258.5	94.2	1.16	3.96	2.49	.00	7.46	97.1	304.4
129	1.80	119.3	1.62	1.62	5691.	98.9	246.8	261.2	94.5	1.40	4.01	2.51	.00	6.52	97.5	311.2
130	1.80	120.9	1.65	1.65	5694.	98.9	247.0	261.4	94.5	1.42	4.02	2.51	.00	6.48	97.5	311.7
131	1.80	115.9	1.54	1.54	5598.	98.5	245.6	260.6	94.2	1.33	3.99	2.49	.00	7.24	97.2	308.8
132	1.80	138.8	1.93	1.93	5674.	99.2	247.3	260.8	94.8	1.49	4.02	2.46	.00	5.58	97.9	314.9

Report 13133-F-1

TEST TIME	PC	WFO	WF	WFC	MT	DPOJ	DPFJ	VOX	VF	KMD	KMF	TW	ID	TF	TFJ
125	1.80	134.2	5095.0	14.053	6.687	.000	20.74	54.7	39.6	1.582	1.183	1110.	70.	211.	202.
126	1.80	132.4	5033.4	12.106	8.441	.000	20.55	41.2	63.2	1.569	1.168	1110.	69.	223.	209.
127	1.80	105.1	5089.0	10.530	5.681	.000	16.21	30.2	27.9	1.594	1.206	1110.	68.	224.	213.
128	1.80	104.7	3977.0	9.521	6.814	.000	16.34	24.9	40.5	1.586	1.202	1110.	67.	226.	217.
129	1.80	119.3	4533.8	11.368	7.002	.000	18.37	35.9	43.3	1.578	1.195	1110.	68.	228.	218.
130	1.80	120.9	4598.7	11.584	7.036	.000	18.62	37.4	43.7	1.575	1.197	1110.	67.	230.	220.
131	1.80	115.9	4408.9	10.897	7.056	.000	17.95	32.4	43.7	1.590	1.196	1110.	64.	232.	221.
132	1.80	138.8	5284.5	14.079	7.293	.000	21.37	54.9	46.5	1.578	1.203	1110.	64.	233.	221.

TEST PC	MR	MHC	EM	EMEE	ERC	MRE	FFCE	QUE	ODK	KL	DL	BLL	ERL	FCL	CFCL	ISP-55
125	134.2	2.10	74.4	97.2	99.5	2.10	.0	342.7	331.7	10.93	2.96	5.64	9.69	.00	.0	313.4
126	132.4	1.43	69.1	97.8	98.1	1.43	.0	327.8	323.1	4.61	2.91	5.62	7.10	.00	.0	307.5
127	105.1	1.85	72.2	96.9	98.6	1.85	.0	339.1	330.5	8.60	2.94	5.93	10.38	.00	.0	311.3
128	104.7	1.40	66.9	97.6	98.0	1.40	.0	326.2	321.1	5.15	2.68	5.65	7.94	.00	.0	304.4
129	119.3	1.62	72.2	97.6	98.5	1.62	.0	333.9	328.0	5.84	2.94	5.80	8.13	.00	.0	311.2
130	120.9	1.65	72.5	97.5	98.5	1.65	.0	334.5	328.6	5.94	2.95	5.78	8.22	.00	.0	311.7
131	115.9	1.54	70.0	97.4	98.1	1.54	.0	331.5	326.1	5.41	2.92	5.79	8.58	.00	.0	308.8
132	138.8	1.93	74.4	97.3	98.9	1.93	.0	340.7	332.7	8.02	2.98	5.62	9.13	.00	.0	314.9

***** UMS ENGINE TEST DATA AND PERFORMANCE SUMMARY *****

PLATELET INJECTOR PROGRAM XOT-2AINJECTOR

A AREA TESTS AREA RATIO 2 NOZZLE 10.4 IN. HEAT SINK CHAMBER

PCAVE=(1.046*PC-1 + 1.016*PC-2)/2

TEST	TIME	PC	MRC	MR	FFC	CSTAM	CSTANT	XC*	ISPV	ISPT	XISP	KL	DL	BL	FCL	ERL	ERE	ISP-55
133	2.45	138.2	1.90	1.90	.0	5717.	5660.	100.7	251.3	261.0	96.3	1.49	4.09	2.75	.00	1.45	99.4	321.3
134	2.45	138.3	1.90	1.90	.0	5720.	5680.	100.7	251.2	261.0	96.2	1.48	4.08	2.75	.00	1.48	99.4	321.1
135	2.45	138.8	1.43	1.43	.0	5641.	5654.	100.5	248.3	259.2	95.8	1.09	4.04	2.67	.00	3.06	98.8	311.4
136	2.45	139.1	1.49	1.49	.0	5712.	5669.	100.8	249.7	261.0	95.7	1.71	4.06	2.91	.00	2.67	99.0	317.8
137	2.45	137.7	1.49	1.49	.0	5678.	5668.	100.2	247.0	260.0	95.0	1.28	4.02	2.87	.00	4.66	98.1	310.0
138	2.45	127.2	1.70	1.70	.0	5737.	5697.	100.7	250.7	261.8	95.8	1.44	4.08	2.82	.00	2.69	99.0	317.7
139	3.45	126.5	1.71	1.71	.0	5737.	5697.	100.7	251.1	261.8	95.9	1.45	4.08	2.75	.00	2.45	99.1	318.1

Report 13133-F-1

ORIGINAL PAGE IS
OF POOR QUALITY

TEST	PC	MR	MRC	EM	EMEE	EMC	MHE	FFCE	ODE	ODK	KL	DL	BLL	ERL	FCL	CFCL	ISP-55
133	138.2	1.90	1.90	66.9	49.3	100.4	1.90	.0	340.2	332.5	7.65	3.04	5.77	2.39	.00	.0	321.3
134	138.3	1.90	1.90	66.2	49.2	100.4	1.90	.0	340.1	332.5	7.64	3.04	5.78	2.63	.00	.0	321.1
135	138.8	1.43	1.43	75.7	99.1	99.8	1.43	.0	327.6	323.1	4.53	2.94	5.74	3.04	.00	.0	311.4
136	139.1	1.49	1.49	82.5	98.8	100.6	1.69	.0	339.9	331.0	8.92	3.01	6.05	4.16	.00	.0	311.0
137	137.7	1.49	1.49	74.4	98.4	99.7	1.49	.0	329.7	324.4	5.32	2.93	6.02	5.41	.00	.0	317.7
138	127.2	1.70	1.70	81.9	99.0	100.3	1.70	.0	336.1	330.0	8.13	3.01	5.90	3.35	.00	.0	318.1
139	126.5	1.71	1.71	82.5	99.1	100.3	1.71	.0	336.3	330.1	6.22	3.01	5.90	3.12	.00	.0	318.1

TEST	TIME	PC	FVAC	WU	WF	WFC	WT	DMUJ	DPFJ	VOX	VF	KWO	KWF	TW	TU	TF	TFJ
133	2.45	138.2	5225.8	13.825	7.174	.000	20.80	52.1	44.7	73.	91.	1.568	1.196	1210.	65.	198.	198.
134	2.45	138.3	5226.0	13.825	7.177	.000	20.80	51.4	44.0	73.	90.	1.579	1.205	1210.	65.	197.	197.
135	2.45	138.8	5144.7	12.191	6.526	.000	20.72	40.7	62.4	65.	107.	1.587	1.203	1210.	64.	198.	198.
136	2.45	139.1	4100.4	10.744	5.677	.000	18.42	30.9	26.5	56.	70.	1.605	1.226	1160.	63.	191.	191.
137	2.45	137.7	4032.2	9.764	5.509	.000	16.32	25.4	36.0	51.	81.	1.608	1.216	1110.	63.	192.	192.
138	2.45	127.2	4782.1	12.020	7.052	.000	19.07	39.2	42.6	63.	89.	1.593	1.213	1160.	62.	216.	216.
139	3.45	126.5	4764.0	11.981	6.992	.000	16.97	38.8	42.1	63.	89.	1.596	1.212	1310.	62.	222.	222.

***** UMS ENGINE TEST DATA AND PERFORMANCE SUMMARY *****

PLATELET INJECTOR PROGRAM

XOTIA INJECTOR 16 IN, HEAT SINK CHAMBER 2:1 CONICAL NOZZLE

A-AREA TESTS PC BASED ON CAVITY PRESSURE MEASUREMENT

TEST TIME	PC	MHC	MR	FFC	CSTAR	CSTANT	XC*	ISPV	ISPT	XISP	KL	DL	BL	FCL	ERL	ERE	ISP-55
156 2.20	118.5	1.78	1.79	.0	5540.	5688.	97.5	247.0	261.6	94.4	1.56	4.02	2.73	.00	6.35	97.6	313.0
156 3.20	117.8	1.77	1.77	.0	5554.	5686.	97.6	247.4	261.7	94.5	1.56	4.02	2.66	.00	6.06	97.7	313.1
157 2.20	137.3	1.91	1.91	.0	5550.	5676.	97.8	247.6	261.0	94.9	1.50	4.03	2.64	.00	5.26	98.0	315.6
157 3.20	136.6	1.89	1.89	.0	5560.	5679.	97.9	248.0	261.2	95.0	1.49	4.03	2.50	.00	5.10	98.0	315.6

TEST TIME	PC	FVAC	WD	WF	MFC	WT	DPD	DPFJ	VOX	VF	KWD	KWF	TW	TO	TF	TFJ
156 2.20	118.5	4540.0	11.777	6.606	.000	18.38	54.2	58.6	74.	104.	1.319	.962	1210.	47.	203.	203.
156 3.20	117.8	4516.0	11.670	6.584	.000	18.25	51.6	58.4	72.	104.	1.336	.964	1360.	46.	209.	209.
157 2.20	137.3	5268.0	13.938	7.320	.000	21.28	74.5	72.6	87.	116.	1.333	.959	1260.	47.	201.	201.
157 3.20	136.6	5243.0	13.824	7.314	.000	21.14	72.2	72.2	85.	116.	1.341	.963	1560.	46.	208.	208.

TEST PC	MR	MRC	EM	ERE	ERC	MRE	FFCL	ODE	ODK	KL	DL	BL	ERL	FCL	CFCL	ISP-55
156 118.5	1.78	1.78	73.4	97.4	97.2	1.78	.0	337.8	330.7	7.14	2.96	5.74	8.95	.07	.0	313.0
156 117.8	1.77	1.77	73.7	97.4	97.3	1.77	.0	337.6	330.5	7.07	2.96	5.76	8.66	.00	.0	313.1
157 137.3	1.91	1.91	75.3	97.6	97.5	1.91	.0	340.3	332.5	7.78	2.99	5.58	8.31	.00	.0	315.6
157 136.6	1.89	1.89	75.6	97.6	97.6	1.89	.0	340.0	332.4	7.61	2.99	5.60	7.99	.00	.0	315.6

ORIGINAL PAGE IS
OF POOR QUALITY

04/16/75 10:10:40 FD0117 000427581 000427 2 100 DATE 041675 PAGE 35

***** DMS ENGINE TEST DATA AND PERFORMANCE SUMMARY *****

PLATELET INJECTOR PROGRAM

PLATELET INJECTOR 16 IN. HEAT SINK CHAMBER 2:1 CONICAL NOZZLE

A-JMEA TESTS PC BASED ON CAVITY PRESSURE MEASUREMENT

TEST	TIME	PC	MRC	MR	FFC	CSTAR	XC*	ISPV	ISPT	XISP	KL	DL	BL	FCL	ERL	EVE	ISP-55
158	3.20	122.0	1.64	1.64	.0	5634.	99.0	250.8	261.5	95.9	1.41	4.08	2.65	.00	2.52	99.0	316.8
159	3.20	123.0	1.86	1.86	.0	5588.	98.4	249.4	261.3	95.4	1.58	4.05	2.58	.00	3.72	98.6	317.1
160	3.20	122.3	1.49	1.49	.0	5582.	98.5	248.1	260.1	95.4	1.22	4.03	2.60	.00	4.21	98.4	311.6
161	2.80	147.8	1.88	1.88	.0	5615.	98.8	250.5	261.2	95.9	1.41	4.07	2.49	.00	2.75	98.9	319.8
162	2.90	145.8	1.46	1.46	.0	5626.	99.4	250.2	259.9	96.3	1.09	4.07	2.50	.00	2.06	99.2	313.6

TEST TIME	PC	FVAC	NO	WF	WFC	WT	DPOJ	DPFJ	VOX	VF	KWD	KWF	TW	TD	TF	TFJ
158 3.20	122.0	4671.8	11.582	7.044	.000	18.63	43.0	49.3	66.	96.	1.462	1.123	1410.	57.	210.	210.
159 3.20	123.0	4723.2	12.325	6.617	.000	18.94	46.7	43.2	68.	89.	1.484	1.123	1535.	42.	201.	201.
160 3.20	122.3	4674.2	11.269	7.574	.000	18.84	39.2	56.7	63.	102.	1.479	1.124	1385.	40.	204.	204.
161 2.80	147.8	5674.7	14.780	7.864	.000	22.65	66.0	62.6	83.	108.	1.474	1.113	1560.	40.	209.	209.
162 2.80	145.8	5570.5	13.236	9.068	.000	22.30	55.4	82.5	75.	124.	1.458	1.123	1432.	44.	222.	222.

TEST PC	MR	MRC	EM	EREE	ENC	MRE	FFCE	ODE	QOK	KL	DL	BLL	EHL	FCL	CFCL	ISP-55
158 122.0	1.64	1.64	81.9	94.1	98.5	1.64	.0	334.5	328.6	5.89	3.00	5.82	2.99	.00	.0	316.8
159 123.0	1.86	1.86	79.1	96.3	98.1	1.86	.0	339.4	331.6	7.84	3.00	5.75	5.72	.00	.0	317.1
160 122.3	1.49	1.49	76.2	98.7	97.9	1.49	.0	329.7	324.7	4.96	2.95	5.75	4.40	.00	.0	311.6
161 147.8	1.88	1.88	81.9	98.7	98.5	1.88	.0	332.8	332.8	7.09	3.02	5.57	4.40	.00	.0	319.8
162 145.8	1.46	1.46	82.5	94.3	98.7	1.46	.0	328.8	324.4	4.41	2.97	5.60	2.19	.00	.0	313.6

PAGE 39

DATE 041675

2 100

000427

04/16/75 10:10:40 F00117 000427581

***** UMS ENGINE TEST DATA AND PERFORMANCE SUMMARY *****

P L A T E L E T I N J E C T O R P R O G R A M

XD11B INJECTOR 16 IN. MEAT SINK CHAMBER 2:1 CONICAL NOZZLE

A-AREA TESTS PC BASED ON CAVITY PRESSURE MEASUREMENT

TEST	TIME	PC	MRC	MR	FFC	CSTAR	CSTART	XC*	ISPV	ISPT	XISP	KL	DL	BL	FCL	ERL	ERE	ISP-SS
163	2.80	99.5	1.85	1.85	.0	5510.	5070.	97.2	246.5	261.6	94.2	1.77	4.01	2.76	.00	6.62	97.5	311.5
164	2.80	98.8	1.53	1.53	.0	5491.	5671.	96.8	245.1	260.8	94.0	1.37	3.99	2.73	.00	7.57	97.1	307.1
165	2.80	75.5	1.65	1.65	.0	5483.	5678.	96.6	244.5	261.9	93.4	1.67	3.98	2.98	.00	8.55	96.7	306.3
166	2.80	65.6	1.69	1.69	.0	5399.	5675.	95.1	240.9	261.9	92.0	1.82	3.92	3.02	.00	12.24	95.3	301.1
167	2.80	65.3	1.44	1.44	.0	5425.	5645.	96.1	241.9	259.6	93.2	1.50	3.93	2.99	.00	9.52	96.3	301.2
173	2.80	123.5	1.71	1.71	.0	5615.	5695.	98.6	250.0	262.0	95.4	1.47	4.07	2.72	.00	3.86	98.6	316.5
174	1.90	100.8	1.91	1.91	.0	5639.	5690.	99.6	250.0	261.2	95.7	1.80	4.07	2.87	.00	2.38	99.1	317.4
175	1.90	145.6	1.48	1.48	.0	5601.	5670.	98.8	248.9	260.2	95.6	1.08	4.05	2.57	.00	3.66	98.6	312.7
176	1.90	149.9	1.93	1.93	.0	5625.	5677.	99.1	250.7	261.0	96.0	1.42	4.08	2.64	.00	2.25	99.1	320.7
177	1.90	149.3	1.93	1.93	.0	5615.	5676.	98.9	250.1	261.0	95.8	1.42	4.07	2.64	.00	2.73	99.0	319.8
178	1.90	101.1	1.54	1.54	.0	5582.	5675.	96.4	247.3	260.7	94.8	1.37	4.02	2.78	.00	5.28	98.0	310.3

TEST	TIME	PC	FVAC	MU	WF	WFC	WT	DPUIJ	DPFJ	VOX	VF	KMU	KMF	TW	TO	TF	TFJ
163	2.80	99.5	3808.4	10.032	5.419	.000	15.45	29.9	28.5	55.	73.	1.509	1.134	1330.	42.	208.	204.
164	2.80	98.8	3771.4	9.294	6.091	.000	15.38	25.8	36.1	51.	82.	1.506	1.132	1285.	43.	203.	203.
165	2.80	75.5	2878.1	7.327	4.446	.000	11.77	15.8	18.6	40.	59.	1.518	1.148	1140.	45.	197.	197.
166	2.80	65.6	2503.6	6.536	3.857	.000	10.39	12.1	13.9	35.	51.	1.549	1.156	1120.	43.	200.	200.
167	2.80	65.3	2491.6	6.076	4.225	.000	10.30	10.6	16.6	33.	55.	1.537	1.160	1120.	50.	204.	204.
173	2.80	123.5	4703.6	11.876	6.935	.000	18.81	44.4	50.3	67.	97.	1.476	1.094	1260.	57.	208.	208.
174	1.90	100.8	3821.4	10.034	5.249	.000	15.28	30.7	27.9	56.	72.	1.500	1.105	1240.	58.	193.	193.
175	1.90	149.6	5686.8	13.621	9.230	.000	22.85	58.8	87.4	77.	127.	1.471	1.104	1260.	58.	206.	206.
176	1.90	149.9	5714.0	15.019	7.777	.000	22.80	71.1	61.3	85.	106.	1.478	1.107	1260.	62.	198.	198.
177	1.90	149.3	5690.5	14.908	7.752	.000	22.75	70.4	60.9	85.	106.	1.481	1.105	1260.	59.	194.	194.
178	1.90	101.1	3832.2	9.385	6.112	.000	15.50	26.5	36.5	52.	82.	1.509	1.124	1260.	57.	185.	185.

TEST	PC	MR	MRC	EM	EREE	ERC	MRE	FFCE	ODE	ODK	KL	DL	BLL	ERL	FCL	CFCL	ISP-SS
163	99.5	1.85	1.85	72.8	97.1	97.0	1.85	.0	339.1	330.2	8.86	2.95	5.93	9.85	.00	.0	311.5
164	98.8	1.53	1.53	69.1	97.2	96.4	1.53	.0	330.9	325.1	5.80	2.90	5.92	9.20	.00	.0	307.1
165	75.5	1.65	1.65	66.4	96.6	96.3	1.65	.0	334.4	326.8	7.59	2.90	6.23	11.37	.00	.0	306.3
166	65.6	1.69	1.69	63.4	94.6	95.0	1.69	.0	335.6	327.2	8.44	2.85	6.29	16.96	.00	.0	301.1
167	65.3	1.44	1.44	64.4	96.5	95.7	1.44	.0	327.9	321.8	6.09	2.85	6.33	11.41	.00	.0	301.2
173	123.5	1.71	1.71	79.4	96.6	96.2	1.71	.0	336.3	330.0	6.32	2.99	5.81	4.68	.00	.0	316.5
174	100.8	1.91	1.91	83.1	98.8	99.4	1.91	.0	340.1	330.5	9.65	3.00	6.09	3.95	.00	.0	317.4
175	149.6	1.48	1.48	77.5	98.9	98.1	1.48	.0	329.4	325.0	4.40	2.96	5.58	3.69	.00	.0	320.7
176	149.9	1.93	1.93	83.7	98.9	98.8	1.93	.0	340.8	333.1	7.62	3.02	5.60	3.83	.00	.0	319.8
177	149.3	1.93	1.93	81.9	98.6	98.6	1.93	.0	340.8	333.1	7.68	3.02	5.60	4.71	.00	.0	319.8
178	101.1	1.54	1.54	74.1	98.1	97.9	1.54	.0	331.2	325.4	5.80	2.98	6.01	8.16	.00	.0	310.3

ORIGINAL PAGE IS
OF POOR QUALITY

Report 13133-F-1

PAGE 43

DATE 041675

2 100

000427

04/10/75 10:10:40 FD0117 000427581

***** UMS ENGINE TEST DATA AND PERFORMANCE SUMMARY *****

PLATELET INJECTOR PROGRAM

XD11B INJECTOR 16 IN. HEAT SINK CHAMBER 2:1 CONICAL NOZZLE

A-AREA TESTS MC BASED UN CAVITY PRESSURE MEASUREMENT

TEST TIME	PC	MRC	MP	FPC	CSTAR	CSTART	XC*	ISPV	ISPT	XISP	KL	DL	BL	FCL	ERL	ERE	ISP-SS
183	1.00	125.2	1.08	1.08	5519.	5694.	96.9	246.8	262.0	94.2	1.43	4.01	2.67	.00	7.12	97.3	311.5
184	1.00	126.0	1.73	1.73	5550.	5694.	97.5	247.9	262.1	94.6	1.48	4.03	2.69	.00	6.07	97.7	313.3
185	1.00	101.9	1.89	1.89	5560.	5665.	98.2	248.3	261.6	94.9	1.78	4.04	2.82	.00	4.64	98.2	314.4
187	1.00	125.8	1.08	1.08	5583.	5693.	98.1	249.1	262.1	95.0	1.43	4.05	2.70	.00	4.83	98.2	314.6
188	1.00	100.5	1.93	1.93	5563.	5654.	98.4	248.1	261.3	95.0	1.82	4.03	2.84	.00	4.49	98.3	314.2
189	1.00	126.2	1.74	1.74	5567.	5694.	97.8	248.4	262.2	94.7	1.49	4.04	2.70	.00	5.54	97.9	314.2
191	1.00	149.9	1.49	1.49	5558.	5671.	98.0	247.7	260.6	95.1	1.09	4.03	2.56	.00	5.16	98.0	311.5
192	1.00	125.4	1.73	1.73	5576.	5693.	97.9	249.0	262.1	95.0	1.48	4.05	2.71	.00	4.92	98.1	314.9
193	1.00	150.3	1.51	1.51	5568.	5676.	98.1	248.2	260.9	95.1	1.11	4.04	2.57	.00	4.96	98.1	312.2
194	1.00	149.0	1.50	1.50	5564.	5674.	98.1	248.0	260.8	95.1	1.11	4.03	2.57	.00	5.05	98.1	312.0

TEST TIME	PC	FVAC	MU	MF	MFC	WT	DPUJ	DPFJ	VOX	VF	KWO	KMF	TW	TU	TF	TFJ
183	1.00	125.2	4760.0	12.045	7.193	.000	19.29	43.7	51.0	97.	1.507	1.119	1260.	45.	191.	191.
184	1.00	126.0	4786.3	12.226	7.084	.000	19.31	45.2	49.4	95.	1.498	1.121	1260.	45.	193.	193.
185	1.00	101.9	3868.6	10.184	5.398	.000	15.58	31.0	28.5	72.	1.509	1.124	1260.	49.	187.	187.
187	1.00	125.8	4770.4	12.016	7.136	.000	19.15	44.3	50.5	96.	1.485	1.119	1260.	41.	197.	197.
188	1.00	100.5	3811.1	10.114	5.245	.000	15.36	30.4	27.0	70.	1.510	1.124	1260.	43.	196.	196.
192	1.00	126.2	4749.3	12.243	7.038	.000	19.24	45.2	49.1	95.	1.502	1.119	1260.	48.	197.	197.
191	1.00	149.9	5661.4	13.711	9.223	.000	22.93	56.7	84.2	125.	1.501	1.121	1260.	47.	201.	201.
192	1.00	125.4	4760.3	12.115	7.004	.000	19.12	44.3	48.6	94.	1.497	1.118	1260.	42.	195.	195.
193	1.00	150.3	5695.9	13.801	9.150	.000	22.95	57.4	82.9	124.	1.500	1.123	1260.	44.	204.	204.
194	1.00	149.0	5646.6	13.661	9.104	.000	22.76	56.4	82.2	124.	1.500	1.124	1260.	47.	208.	208.

TEST	PC	MR	MRC	EM	EHEE	ERC	MRE	FFCE	ODE	ODK	KL	DL	BLL	ERL	FCL	CFCL	ISP-SS
183	125.2	1.68	1.68	71.6	97.2	96.6	1.68	.0	335.5	329.5	6.04	2.95	5.71	9.33	.00	.0	311.5
184	126.0	1.73	1.73	73.7	97.5	97.2	1.73	.0	336.6	330.3	6.33	2.96	5.74	6.26	.00	.0	313.3
185	101.9	1.89	1.89	76.9	97.9	98.0	1.89	.0	339.7	330.5	9.22	2.97	6.01	7.10	.00	.0	314.4
187	125.8	1.08	1.08	76.2	96.1	97.7	1.68	.0	335.6	329.6	6.04	2.98	5.79	6.22	.00	.0	314.6
188	100.5	1.93	1.93	76.9	97.9	96.2	1.93	.0	340.4	330.5	9.92	2.97	6.03	7.27	.00	.0	314.2
190	126.2	1.74	1.74	75.0	97.8	97.5	1.74	.0	336.9	330.5	6.44	2.97	5.76	7.52	.00	.0	314.2
191	149.9	1.49	1.49	73.7	96.4	97.4	1.49	.0	329.7	325.3	4.43	2.95	5.56	5.32	.00	.0	311.5
192	125.4	1.73	1.73	76.2	98.0	97.6	1.73	.0	336.7	330.3	6.39	2.98	5.78	6.63	.00	.0	314.9
193	150.3	1.51	1.51	74.4	98.4	97.5	1.51	.0	330.5	326.0	4.50	2.95	5.57	5.24	.00	.0	312.2
194	149.0	1.50	1.50	74.4	98.4	97.5	1.50	.0	330.2	325.7	4.49	2.95	5.57	5.17	.00	.0	312.0

***** UMS ENGINE TEST DATA AND PERFORMANCE SUMMARY *****

PLA T E L E T I N J E C T O R P R O G R A M

XD11C INJECTOR 16 IN. MEAT SINK CHAMBER 2:1 CONICAL NOZZLE

206-210, PCAV VALID; 211-213 PCAV BASED ON PC-2(STATIC)

TEST	TIME	PC	MHC	MR	FFC	CSTAR	CSTART	XC*	ISPV	ISPT	XISP	KL	DL	BL	FCL	ERL	ERE	ISP-55
206	2.70	126.1	1.72	1.72	.0	5589.	5695.	98.1	249.8	262.3	95.2	1.46	4.06	2.61	.00	4.36	98.3	315.6
207	2.70	150.9	1.46	1.46	.0	5569.	5661.	98.4	248.6	260.2	95.5	1.05	4.04	2.44	.00	4.04	98.4	311.8
208	2.70	103.1	1.53	1.53	.0	5584.	5673.	98.1	247.5	261.2	94.8	1.36	4.02	2.69	.00	5.56	97.9	310.0
209	2.70	152.4	1.89	1.89	.0	5613.	5684.	98.8	250.9	261.7	95.9	1.40	4.08	2.52	.00	2.83	98.9	319.9
210	2.70	103.1	1.93	1.93	.0	5598.	5655.	99.0	249.1	261.3	95.3	1.79	4.05	2.77	.00	3.55	98.6	315.8
211	2.70	127.6	1.67	1.67	.0	5614.	5694.	98.6	249.9	262.1	95.4	1.40	4.06	2.66	.00	4.05	98.5	315.5
212	2.70	151.8	1.49	1.49	.0	5608.	5671.	98.9	249.2	260.6	95.6	1.08	4.05	2.43	.00	5.83	98.5	313.1
213	2.70	127.0	1.65	1.65	.0	5574.	5693.	97.9	249.6	261.7	95.4	1.39	4.06	2.64	.00	4.06	98.4	315.2

Report 13133-F-1

TEST	TIME	PC	FVAC	MD	WF	MFC	MT	DFUJ	DPFJ	VOX	VF	KWD	KWF	TM	TD	TF	TFJ
206	2.70	126.1	4794.1	12.123	7.067	.000	19.19	54.9	63.0	74.	109.	1.349	1.000	1460.	47.	218.	218.
207	2.70	150.9	5729.7	13.663	9.386	.000	23.05	71.5	110.4	85.	143.	1.332	.998	1480.	47.	205.	205.
208	2.70	103.1	3900.8	9.541	6.218	.000	15.76	33.2	47.6	58.	94.	1.363	1.009	1410.	44.	209.	209.
209	2.70	152.4	5790.7	15.085	7.995	.000	23.08	65.9	81.1	93.	123.	1.340	.993	1510.	44.	208.	208.
210	2.70	103.1	3901.5	10.518	5.344	.000	15.66	38.8	35.1	62.	80.	1.364	1.003	1410.	44.	192.	192.
211	2.70	127.6	4831.1	12.085	7.248	.000	19.33	54.1	65.4	74.	110.	1.353	1.001	1360.	45.	204.	204.
212	2.70	151.8	5730.1	13.772	9.253	.000	23.02	70.9	106.4	84.	140.	1.347	1.001	1560.	45.	202.	202.
213	2.70	127.0	4835.3	12.070	7.303	.000	19.37	54.6	65.7	74.	109.	1.347	.997	1360.	48.	173.	173.

TEST	PC	MHC	EM	EMEE	EMC	MRE	FFCE	ODE	ODK	KL	DL	BLL	ERL	FCL	CFCL	ISP-55
206	126.1	1.72	77.5	98.3	97.7	1.72	.0	336.4	330.1	6.25	2.99	5.79	5.75	.00	.0	315.6
207	150.9	1.46	76.2	98.8	97.6	1.46	.0	328.6	324.3	4.32	2.95	5.56	3.98	.00	.0	311.8
208	103.1	1.53	73.4	98.0	97.6	1.53	.0	331.2	325.5	5.73	2.93	6.00	6.48	.00	.0	310.0
209	152.4	1.89	81.9	98.7	98.4	1.89	.0	340.0	333.0	7.00	3.03	5.60	4.45	.00	.0	319.9
210	103.1	1.93	79.4	98.3	98.8	1.93	.0	340.5	330.7	9.80	2.99	6.04	5.84	.00	.0	315.8
211	127.6	1.67	78.1	98.5	98.1	1.67	.0	335.2	329.3	5.87	2.98	5.81	4.96	.00	.0	315.5
212	151.8	1.49	77.5	98.9	98.2	1.49	.0	329.8	325.4	4.40	2.96	5.60	3.74	.00	.0	313.1
213	127.0	1.65	77.6	98.5	97.4	1.65	.0	334.7	328.9	5.79	2.98	5.76	4.99	.00	.0	315.2

ORIGINAL PAGE IS
OF POOR QUALITY

Report 13133-F-1

PAGE

DATE 041675

2 100

000427

04/16/75 10:10:40 FD0117 000427581

***** OMS ENGINE TEST DATA AND PERFORMANCE SUMMARY *****

PLATELET INJECTOR PROGRAM

XOTIC INJECTOR 10 IN. HEAT SINK CHAMBER 211 CONICAL NOZZLE

PCAV BASED ON PC-2 (STATIC)

TEST	TIME	PC	MRC	MR	FFC	CSTAR	CSTART	XC*	ISPV	ISPT	XISP	KL	DL	DL	FCL	ERL	ERE	ISP-55
217	1.90	153.8	1.93	1.93	.0	5602.	5677.	98.7	250.7	261.5	95.9	1.39	4.08	2.54	.00	2.83	98.9	320.0
222	1.90	102.4	1.49	1.49	.0	5536.	5666.	97.7	248.1	260.8	95.2	1.30	4.03	2.71	.00	4.57	98.2	310.3
223	1.90	101.5	1.42	1.92	.0	5566.	5657.	98.4	249.9	261.5	95.5	1.60	4.06	2.74	.00	3.04	98.8	316.6
225	1.90	150.9	1.47	1.47	.0	5582.	5665.	98.5	248.4	260.4	95.4	1.06	4.04	2.44	.00	4.45	98.3	311.6
227	1.90	101.8	1.48	1.84	.0	5571.	5665.	98.3	249.1	261.9	95.1	1.79	4.05	2.76	.00	4.14	98.4	315.1
229	1.90	151.5	1.87	1.87	.0	5607.	5688.	98.6	251.0	262.0	95.8	1.41	4.08	2.52	.00	3.06	98.8	319.2
233	1.90	127.2	1.71	1.71	.0	5595.	5696.	98.2	250.4	262.4	95.5	1.46	4.07	2.61	.00	3.79	98.6	316.3
250	1.90	151.3	1.49	1.49	.0	5567.	5671.	98.2	248.8	260.7	95.4	1.09	4.05	2.49	.00	4.29	98.4	312.6
252	1.90	151.1	1.87	1.87	.0	5595.	5687.	98.4	250.5	261.9	95.7	1.40	4.07	2.58	.00	3.30	96.7	319.0
257	1.90	104.3	1.55	1.55	.0	5570.	5676.	98.1	248.2	261.3	95.0	1.37	4.04	2.78	.00	4.94	98.1	311.1
254	1.90	103.2	1.92	1.92	.0	5603.	5659.	99.0	249.6	261.5	95.4	1.79	4.06	2.80	.00	3.26	98.8	316.4

TEST	PC	MRC	EM	EM	EFEE	ERC	MRE	FFCE	ODE	UDK	KL	DL	BLL	ERL	FCL	CFCL	ISP-55
217	153.8	1.93	61.9	61.9	98.0	98.4	1.93	.0	340.7	333.3	7.41	3.03	5.61	4.68	.00	.0	320.0
222	102.4	1.49	75.3	75.3	98.5	97.3	1.49	.0	329.8	324.3	5.49	2.94	6.00	5.08	.00	.0	310.3
223	101.5	1.42	81.2	81.2	98.6	98.3	1.92	.0	340.3	330.5	9.78	2.99	6.06	4.86	.00	.0	316.6
225	150.9	1.47	75.0	75.0	98.6	97.9	1.47	.0	329.0	328.7	4.35	2.95	5.61	4.54	.00	.0	311.6
227	101.8	1.48	78.1	78.1	98.1	98.2	1.84	.0	339.7	339.5	9.20	2.98	6.06	6.34	.00	.0	315.1
229	151.5	1.87	60.6	60.6	98.6	98.3	1.87	.0	339.6	332.8	6.80	3.02	5.64	4.90	.00	.0	319.2
233	127.2	1.71	78.7	78.7	96.5	97.9	1.71	.0	336.2	330.1	6.18	2.99	5.82	4.99	.00	.0	316.3
250	151.3	1.49	75.9	75.9	96.7	97.6	1.49	.0	329.9	325.4	4.41	2.96	5.59	4.35	.00	.0	312.6
252	151.1	1.87	80.0	80.0	96.4	98.1	1.87	.0	339.8	332.9	6.84	3.02	5.61	5.29	.00	.0	319.0
257	104.3	1.55	75.0	75.0	96.3	97.8	1.55	.0	331.0	325.8	5.79	2.94	6.02	5.73	.00	.0	311.1
254	103.2	1.92	60.6	60.6	96.5	98.9	1.92	.0	340.3	330.7	9.62	2.99	6.09	5.16	.00	.0	316.4

ORIGINAL PAGE IS
OF POOR QUALITY

***** UMS ENGINE TEST DATA AND PERFORMANCE SUMMARY *****

PLATELET INJECTOR PROGRAM .6 XDT - SP INJECTOR

A AREA TESTS AREA RATIO 2 NOZZLE 16.7 IN. HEAT SINK CHAMBER

CHAMBER PRESSURE = 0.943* CAVITY PRESSURE

TEST	TIME	PC	MHC	MP	FPC	CSTAK	CSTART	XC*	ISPV	ISPI	XISP	KL	DL	BL	FCL	ERL	ERE	ISP-55
144	2.41	121.5	1.70	1.70	.0	5574.	5695.	97.9	248.5	259.9	95.6	1.46	4.04	2.81	.00	3.09	98.8	317.1
145	2.40	122.5	1.69	1.69	.0	5637.	5696.	99.0	250.9	261.0	93.1	1.44	4.08	2.84	.00	1.78	99.3	318.7
146	2.40	122.3	1.67	1.67	.0	5644.	5694.	99.1	251.1	260.9	96.3	1.43	4.08	2.85	.00	1.40	99.5	318.8
147	2.40	135.9	1.64	1.64	.0	5635.	5682.	99.2	251.1	260.5	96.4	1.47	4.08	2.74	.00	1.10	99.6	322.0
148	1.60	136.9	1.65	1.65	.0	5626.	5650.	99.4	248.9	259.0	96.1	1.12	4.05	2.82	.00	2.09	99.2	313.1
149	2.40	107.3	1.67	1.67	.0	5609.	5671.	98.9	249.5	260.6	95.8	1.69	4.06	2.92	.00	2.39	99.1	318.1
150	2.40	106.5	1.42	1.42	.0	5580.	5643.	98.9	247.3	258.3	95.7	1.18	4.02	2.87	.00	2.99	98.8	310.0

Report 13133-F-1

TEST	TIME	PC	FVAC	VU	MF	WFC	T	DPHJ	DPFJ	VOX	VF	KWD	KMF	TW	TU	TF	TFJ
144	2.40	121.5	4759.0	12.000	7.063	.000	9.07	36.5	40.1	61.	82.	1.647	1.192	1360.	59.	60.	60.
145	2.40	122.5	4770.7	11.935	7.082	.000	19.02	36.3	43.7	61.	90.	1.643	1.198	1360.	61.	206.	206.
146	2.40	122.3	4759.0	11.944	7.106	.000	18.95	35.7	44.4	60.	91.	1.638	1.190	1360.	53.	201.	201.
147	2.40	135.9	5299.1	13.769	7.334	.000	21.10	47.9	47.2	70.	93.	1.645	1.188	1490.	53.	195.	195.
148	1.60	136.9	5295.5	12.594	8.682	.000	21.28	40.0	65.4	64.	110.	1.649	1.198	1190.	57.	202.	202.
149	2.40	107.3	4174.2	10.969	5.821	.000	16.73	30.2	30.2	55.	75.	1.641	1.182	1360.	54.	202.	202.
150	2.40	106.5	4126.9	9.747	6.912	.000	16.70	24.4	41.2	50.	87.	1.637	1.200	1260.	53.	198.	198.

TEST	PC	MHC	EM	EMER	ERC	WHE	FACE	ODE	UDK	KL	DL	BLL	EPL	FCL	CFCL	ISP-55
144	121.5	1.70	86.6	96.4	97.9	1.70	.0	336.0	329.7	6.29	3.00	5.65	3.95	.00	.0	317.1
145	122.5	1.69	85.0	94.4	99.0	1.69	.0	335.6	329.5	6.15	3.01	5.72	2.01	.00	.0	318.7
146	122.3	1.67	86.2	94.5	99.2	1.67	.0	335.1	329.1	6.03	3.02	5.73	1.56	.00	.0	318.8
147	135.9	1.64	84.7	94.5	98.3	1.64	.0	334.6	332.3	7.48	3.05	5.60	1.65	.00	.0	322.0
148	136.9	1.45	82.5	94.3	99.4	1.45	.0	328.4	323.8	4.55	2.94	5.58	2.17	.00	.0	313.1
149	107.3	1.67	83.1	94.0	99.0	1.67	.0	334.5	330.8	6.76	3.01	5.84	3.78	.00	.0	316.1
150	106.5	1.42	74.7	90.0	96.0	1.42	.0	327.0	321.9	5.12	2.93	5.81	3.11	.00	.0	310.0

04/10/75 10:10:40 FD0117 000427501 000427 2 100 DATE 041675 PAGE 55

***** UMS ENGINE TEST DATA AND PERFORMANCE SUMMARY *****

PLATELET INJECTOR PROGRAM

MIXED ELEMENT INJECTOR 12 IN. HEAT SINK CHAMBER 2:1 CONICAL NOZZLE

***** PC BASED ON PCAV *****

TEST TIME	PC	MHC	MR	FFC	CSTAR	XC*	ISPV	ISPT	XISP	KL	DL	BL	FCL	ERL	ERE	ISP-55	
159 1.60	153.1	1.78	1.78	.0	5420.	5699.	95.2	244.1	261.9	93.2	1.35	3.97	2.37	.00	10.14	96.1	309.1
172 1.40	139.6	1.72	1.72	.0	5545.	5699.	97.3	249.2	262.0	95.1	1.38	4.05	2.54	.00	4.78	98.2	315.8

TEST TIME	PC	FVAC	MU	WF	KFC	WT	DPUJ	DPFJ	VOX	VF	KWO	KMF	TM	TO	TF	TFJ
159 1.60	153.1	5891.0	15.467	8.670	.000	24.14	55.3	65.8	75.	110.	1.717	1.194	1160.	51.	204.	204.
172 1.40	139.6	5308.0	13.630	7.909	.000	21.54	45.8	55.4	68.	101.	1.664	1.189	1010.	52.	208.	208.

Report 13133-F-1

TEST PC	MR	MHC	EM	ERE	ELC	MRE	FFCE	ODE	UDK	KL	DL	BLL	ERL	FCL	CFCL	ISP-55
159 153.1	1.78	1.78	66.6	95.7	94.8	1.79	.0	338.0	332.0	5.94	2.92	5.34	14.62	.00	.0	309.1
172 139.6	1.72	1.72	76.6	98.1	96.9	1.72	.0	336.6	330.7	5.88	2.99	5.59	6.30	.00	.0	315.8

04/10/75 10:10:40 FD0117 000427581 000427 2 100 DATE 041675 PAGE 59

***** OMS ENGINE TEST DATA AND PERFORMANCE SUMMARY *****

PLATELET INJECTOR PROGRAM

DAFFLED INJ. 16 IN. HEAT SINK CHAMBER 2:1 CONICAL NOZZLE

***** PC BASED ON PCAV *****

TEST	TIME	PC	MRC	MR	FFC	CSTAK	CSTART	XC*	ISPV	ISPT	XISP	KL	DL	BL	FCL	ERL	ERE	ISP-55
195	1.90	126.2	1.74	1.74	.0	5547.	5694.	97.4	249.3	262.1	95.1	1.49	4.05	2.72	.00	4.50	98.3	315.6
197	2.70	124.9	1.78	1.78	.0	5524.	5692.	97.0	248.8	262.2	94.9	1.53	4.04	2.57	.00	5.31	98.0	314.8
198	2.70	125.2	1.76	1.76	.0	5520.	5693.	97.0	248.4	262.1	94.8	1.52	4.04	2.57	.00	5.63	97.9	318.3
199	2.70	125.1	1.74	1.74	.0	5521.	5695.	96.9	248.2	262.2	94.7	1.50	4.04	2.56	.00	5.92	97.7	313.8
200	2.70	149.6	1.37	1.37	.0	5509.	5625.	97.9	247.3	258.5	95.7	.97	4.02	2.35	.00	3.80	94.5	308.8
202	2.70	126.4	1.76	1.76	.0	5560.	5694.	97.6	248.9	262.1	95.0	1.51	4.05	2.59	.00	4.99	98.1	315.2
204	2.70	126.4	1.82	1.82	.0	5565.	5688.	97.8	248.7	262.1	94.9	1.55	4.04	2.58	.00	5.25	98.0	315.0

TEST	TIME	PC	FWC	MO	WT	DPQJ	DPFJ	VOX	VF	KWO	KWF	TW	TD	TF	TFJ
195	1.90	126.2	4824.3	12.273	7.072	.000	19.35	65.1	67.4	81.	111.	1.256	.957	1200.	185.
197	2.70	124.9	4783.4	12.300	6.929	.000	19.23	65.8	64.2	82.	109.	1.254	.968	1480.	210.
198	2.70	125.2	4789.5	12.305	6.980	.000	19.28	66.1	64.3	82.	109.	1.252	.968	1475.	193.
199	2.70	125.1	4782.2	12.239	7.030	.000	19.27	65.3	65.4	81.	110.	1.254	.970	1500.	201.
200	2.70	149.6	5712.1	13.553	9.743	.000	23.10	78.5	125.5	89.	153.	1.249	.972	1544.	206.
202	2.70	126.4	4812.7	12.528	7.005	.000	19.33	66.4	64.7	82.	109.	1.253	.968	1470.	188.
204	2.70	126.4	4803.8	12.459	6.657	.000	19.32	67.5	63.0	83.	108.	1.253	.968	1510.	212.

TEST	PC	MRC	EM	EMEE	ERC	MRE	FFCE	UDE	ODK	KL	DL	BLL	ERL	FCL	CFCL	ISP-55
195	126.2	1.74	77.2	98.2	97.1	1.74	.0	336.8	330.4	6.41	2.99	5.74	6.09	.00	.0	315.6
197	124.9	1.78	75.6	97.8	96.8	1.78	.0	337.7	330.9	6.81	2.98	5.72	7.37	.00	.0	314.8
198	125.2	1.76	75.0	97.7	96.7	1.76	.0	337.4	330.7	6.68	2.97	5.71	7.70	.00	.0	314.3
199	125.1	1.74	74.4	97.6	96.7	1.74	.0	336.9	330.5	6.49	2.97	5.71	7.96	.00	.0	313.8
200	149.6	1.37	74.4	96.9	97.2	1.37	.0	325.2	320.6	4.39	2.92	5.50	3.63	.00	.0	308.8
202	126.4	1.76	76.2	94.0	97.4	1.76	.0	337.4	330.8	6.61	2.98	5.75	6.85	.00	.0	315.2
204	126.4	1.82	75.6	97.8	97.6	1.82	.0	336.5	331.4	7.18	2.98	5.76	7.60	.00	.0	315.0

PAGE 64

DATE 041675

2 100

000427

08/16/75 10:10:40 FD0117 000427581

***** UMS ENGINE TEST DATA AND PERFORMANCE SUMMARY *****

P L A T E L E T I N J E C T O R P R O G R A M

DEMU-1 INJECTOR 16 IN. HEAT SINK CHAMBER 2:1 CONICAL NOZZLE

A-AREA TESTS PC BASED ON CAVITY PRESSURE MEASUREMENT

TEST	TIME	PC	MRC	MR	FFC	CSTAK	CSTART	XC*	ISPV	ISPT	XISP	KL	DL	BL	FCL	ERL	EME	ISP-55
291	2.70	125.1	1.65	1.65	.0	5562.	5694.	97.7	248.6	261.9	94.9	1.40	4.04	2.62	.00	5.22	96.0	313.5
292	2.70	102.1	1.41	1.41	.0	5491.	5642.	97.3	244.7	259.2	94.4	1.18	3.98	2.63	.00	6.77	97.4	305.6
293	2.70	149.0	1.61	1.61	.0	5571.	5695.	97.8	249.6	261.6	95.4	1.22	4.06	2.53	.00	4.19	98.4	310.1
294	2.70	99.7	1.61	1.61	.0	5543.	5664.	97.5	247.2	261.7	94.5	1.48	4.02	2.70	.00	6.30	97.6	310.1
295	1.70	149.2	1.40	1.40	.0	5534.	5643.	98.2	246.9	259.1	95.3	1.00	4.01	2.46	.00	4.69	98.2	309.3
296	1.70	150.7	1.63	1.63	.0	5583.	5698.	98.0	249.2	261.6	95.3	1.23	4.05	2.56	.00	4.56	98.3	315.1
297	2.70	149.3	1.64	1.64	.0	5567.	5699.	97.7	249.4	261.7	95.3	1.25	4.06	2.53	.00	4.48	98.3	315.5
297	2.70	147.5	1.58	1.58	.0	5517.	5632.	98.0	246.8	258.7	95.4	.99	4.01	2.43	.00	4.45	98.3	308.7
300	1.70	150.8	1.43	1.43	.0	5546.	5653.	98.1	247.6	259.6	95.4	1.03	4.03	2.57	.00	4.22	98.4	310.7
307	2.70	67.1	1.67	1.67	.0	5500.	5679.	96.9	245.0	262.1	93.5	1.76	3.98	3.06	.00	8.27	96.8	306.5
308	2.70	102.9	1.93	1.93	.0	5548.	5658.	98.0	248.1	261.3	94.9	1.79	4.73	2.80	.00	4.63	98.2	314.4
309	1.70	151.9	1.98	1.98	.0	5561.	5668.	98.5	249.5	260.8	95.7	1.40	4.06	2.61	.00	3.26	98.8	318.9
310	1.70	129.6	1.87	1.87	.0	5590.	5681.	98.4	249.5	261.6	95.4	1.56	4.06	2.72	.00	3.80	98.5	317.2
313	2.70	151.1	1.42	1.42	.0	5541.	5645.	98.1	247.1	259.3	95.3	1.01	4.02	2.41	.00	4.78	98.2	303.7
314	2.70	153.3	1.96	1.86	.0	5579.	5649.	98.1	249.7	261.7	95.4	1.38	4.06	2.45	.00	4.09	98.4	318.1
315	1.60	103.7	1.41	1.41	.0	5531.	5640.	98.1	244.9	259.1	94.5	1.18	3.98	2.79	.00	6.27	97.6	306.1
316	1.90	104.2	1.91	1.91	.0	5545.	5661.	98.7	248.4	261.3	95.1	1.77	4.04	2.86	.00	4.20	98.4	315.1
317	1.90	103.1	1.87	1.87	.0	5545.	5670.	98.5	248.1	261.6	94.9	1.76	4.03	2.89	.00	4.74	98.2	314.3
318	1.90	152.4	1.92	1.92	.0	5592.	5678.	98.5	249.4	261.3	95.5	1.40	4.06	2.56	.00	3.86	98.5	318.4
319	1.90	150.8	1.41	1.41	.0	5540.	5645.	98.1	246.8	259.1	95.2	1.01	4.01	2.51	.00	4.85	98.1	309.6
320	1.90	152.6	1.94	1.84	.0	5577.	5674.	98.3	249.3	261.0	95.5	1.40	4.05	2.55	.00	3.72	98.6	318.4
321	1.90	106.3	1.91	1.91	.0	5542.	5661.	98.6	248.4	261.2	95.1	1.78	4.04	2.89	.00	4.11	98.4	315.2
322	1.90	106.3	1.41	1.41	.0	5520.	5641.	97.8	245.3	259.2	94.6	1.19	3.99	2.83	.00	5.96	97.7	306.5
323	2.20	101.4	1.67	1.67	.0	5545.	5640.	98.2	247.9	261.6	94.8	1.78	4.03	2.86	.00	5.04	98.1	313.8
323	3.20	101.3	1.67	1.67	.0	5557.	5668.	98.0	247.9	261.6	94.7	1.78	4.03	2.76	.00	5.20	98.0	313.3
324	1.90	151.2	1.41	1.41	.0	5541.	5644.	98.8	247.4	259.4	95.4	1.01	4.02	2.48	.00	4.47	98.3	309.0
325	1.90	152.3	1.68	1.68	.0	5624.	5686.	98.9	249.6	261.7	95.5	1.39	4.06	2.58	.00	3.76	98.6	318.3
326	1.90	102.7	1.80	1.60	.0	5527.	5642.	94.0	248.6	261.9	94.9	1.71	4.04	2.81	.00	4.77	98.2	314.2
327	1.90	103.8	1.44	1.44	.0	5577.	5644.	98.6	246.1	259.8	94.7	1.22	4.00	2.71	.00	5.81	97.8	307.4
328	1.90	104.3	1.26	1.26	.0	5525.	5557.	99.4	244.7	255.4	95.8	.77	3.98	2.36	.00	3.55	98.6	304.5
329	1.90	106.0	1.53	1.53	.0	5612.	5685.	98.7	249.7	261.0	95.4	1.05	4.05	2.48	.00	4.41	98.3	314.0
330	1.90	126.5	1.63	1.63	.0	5613.	5692.	98.6	248.8	261.8	95.0	1.37	4.05	2.64	.00	4.94	98.1	313.7
331	1.90	128.1	1.69	1.69	.0	5610.	5678.	98.6	249.2	261.8	95.3	1.37	4.05	2.64	.00	4.16	98.4	316.8
332	1.90	127.5	2.21	2.21	.0	5563.	5545.	94.6	247.4	257.8	96.0	1.51	4.02	2.55	.00	2.35	99.1	316.5
333	1.90	101.6	2.16	2.16	.0	5569.	5540.	94.6	247.2	258.6	95.6	1.82	4.02	2.65	.00	2.88	98.9	314.4
334	1.90	136.4	1.41	1.41	.0	5567.	5644.	98.6	246.7	259.3	95.1	1.06	4.01	2.53	.00	4.98	98.1	308.7
335	1.90	136.1	1.43	1.43	.0	5574.	5653.	98.6	247.3	259.7	95.2	1.08	4.02	2.53	.00	4.80	98.2	309.8
336	1.90	138.6	2.13	2.13	.0	5543.	5594.	94.6	247.6	259.0	95.6	1.98	4.03	2.75	.00	2.71	99.0	314.4

ORIGINAL PAGE IS
ON POOR QUALITY

Report 13133-F-1

***** UMS ENGINE TEST DATA AND PERFORMANCE SUMMARY *****

P L A T E L E T I N J E C T O R P R O G R A M

DEMU-1 INJECTOR 16 IN. HEAT SINK CHAMBER 2:1 CONICAL NOZZLE

A-AREA TESTS PC BASED ON CAVITY PRESSURE MEASUREMENT

TEST	TIME	PC	FVAC	NU	WF	WFC	WT	DPUJ	DPFJ	VOX	VF	KWO	KMF	TM	TO	TF	TFJ
291	2.70	125.1	4752.4	11.913	7.204	.000	19.12	40.4	48.5	64.	95.	1.553	1.157	1360.	59.	209.	206.
292	2.70	102.1	3866.3	9.252	6.549	.000	15.80	23.7	38.6	49.	84.	1.575	1.177	1360.	59.	202.	202.
293	2.70	149.0	5672.4	14.015	8.714	.000	22.73	56.4	68.1	76.	112.	1.546	1.179	1360.	59.	203.	203.
294	2.70	99.7	3779.8	9.429	5.863	.000	15.29	24.4	30.2	50.	76.	1.582	1.192	1410.	60.	217.	217.
295	1.70	149.2	5655.4	13.375	9.532	.000	22.94	50.6	81.0	72.	122.	1.557	1.183	1360.	62.	203.	203.
296	1.70	150.7	5716.1	14.218	8.723	.000	22.94	57.5	66.7	77.	110.	1.556	1.187	1310.	63.	185.	185.
297	2.70	149.3	5667.4	14.168	8.435	.000	22.80	57.5	66.0	77.	110.	1.549	1.184	1360.	60.	198.	198.
298	2.70	147.5	5610.0	13.192	9.541	.000	22.73	49.8	81.6	71.	123.	1.550	1.183	1410.	60.	210.	210.
304	1.70	150.8	5729.2	13.601	9.522	.000	23.12	53.1	85.5	73.	126.	1.540	1.153	1160.	58.	210.	210.
307	2.70	67.1	2501.6	6.449	3.845	.000	10.37	10.7	12.7	33.	49.	1.639	1.224	1130.	58.	222.	222.
308	2.70	102.9	3912.1	10.333	5.369	.000	15.77	29.5	26.2	55.	70.	1.585	1.179	1260.	61.	209.	209.
309	1.70	151.9	5771.6	15.354	7.776	.000	23.13	66.8	56.1	83.	102.	1.560	1.145	1260.	63.	201.	201.
310	1.70	126.6	4879.1	12.752	6.802	.000	19.55	45.6	44.0	68.	90.	1.569	1.148	1210.	65.	206.	206.
313	2.70	151.1	5729.0	13.584	9.594	.000	23.19	52.5	87.0	73.	127.	1.548	1.148	1460.	50.	201.	201.
315	2.70	153.3	5832.0	15.203	8.154	.000	23.36	65.6	62.3	81.	107.	1.549	1.153	1560.	49.	202.	202.
316	1.70	113.7	3941.0	9.310	6.604	.000	15.93	23.9	38.4	49.	84.	1.576	1.183	1110.	51.	183.	183.
319	1.70	144.2	5691.0	10.414	5.452	.000	15.87	24.3	26.2	54.	69.	1.589	1.184	1120.	51.	187.	187.
317	1.70	103.1	3604.0	10.220	5.473	.000	15.69	27.9	26.3	53.	69.	1.568	1.187	1110.	51.	188.	188.
318	1.70	152.4	5777.0	15.235	7.925	.000	23.16	65.2	57.6	81.	103.	1.557	1.168	1370.	49.	207.	207.
319	1.70	150.6	5708.0	13.543	9.589	.000	23.13	52.4	84.1	73.	121.	1.547	1.163	1260.	54.	189.	189.
320	1.70	152.6	5803.0	15.341	7.907	.000	23.27	66.5	57.2	82.	102.	1.557	1.162	1360.	53.	187.	187.
321	1.70	102.6	3690.0	10.242	5.377	.000	15.69	26.5	25.3	54.	69.	1.562	1.166	1110.	54.	187.	187.
322	1.70	100.3	3588.0	9.047	6.397	.000	15.44	22.3	36.6	48.	82.	1.585	1.177	1060.	55.	196.	196.
323	2.70	101.6	3454.0	10.131	5.414	.000	15.55	27.6	26.4	53.	70.	1.588	1.173	1160.	53.	190.	190.
325	3.20	101.3	3482.0	10.106	5.362	.000	15.50	27.8	26.5	53.	70.	1.584	1.170	1360.	52.	204.	204.
326	4.50	100.8	3621.0	10.050	5.364	.000	15.41	27.6	26.2	53.	70.	1.580	1.175	1560.	52.	213.	213.
324	1.70	151.2	5696.3	13.493	9.542	.000	23.04	51.8	84.4	73.	125.	1.555	1.164	1360.	62.	213.	213.
325	1.70	152.3	5750.5	15.021	7.993	.000	23.01	64.6	59.5	81.	105.	1.551	1.161	1360.	62.	212.	212.
324	1.70	152.7	5754.3	15.040	5.540	.000	15.52	26.7	27.8	52.	72.	1.603	1.171	1310.	63.	196.	196.
327	1.70	153.8	5811.6	15.339	6.475	.000	15.61	23.5	37.9	49.	84.	1.599	1.176	1310.	64.	206.	206.
328	1.70	104.3	3616.5	14.043	11.203	.000	25.29	57.1	116.7	76.	148.	1.545	1.164	1360.	60.	216.	216.
324	1.70	166.0	6260.5	15.199	9.646	.000	25.14	66.0	91.3	82.	130.	1.550	1.164	1360.	60.	207.	207.
330	1.70	126.5	4765.8	12.623	7.245	.000	19.16	30.0	48.7	63.	95.	1.575	1.169	1360.	60.	210.	210.
331	1.70	127.1	4837.6	12.697	6.722	.000	19.41	44.6	41.7	67.	86.	1.575	1.167	1410.	60.	213.	213.
332	1.70	127.5	4821.6	13.426	6.097	.000	19.49	49.6	34.3	71.	86.	1.577	1.162	1560.	60.	214.	214.
333	1.70	101.6	3434.5	11.500	4.917	.000	15.51	30.3	22.7	56.	65.	1.596	1.155	1610.	60.	212.	212.
334	1.70	156.4	5134.2	12.177	8.653	.000	23.63	41.2	66.8	65.	113.	1.574	1.171	1360.	62.	217.	217.
335	1.70	158.1	5200.0	12.502	8.671	.000	23.06	42.7	69.6	66.	114.	1.573	1.170	1360.	62.	224.	224.
336	1.70	158.6	5339.5	12.178	8.311	.000	13.49	22.1	17.6	48.	57.	1.621	1.152	1560.	63.	212.	212.

04/16/75 10:10:40 FD0117 000427

2 100

DATE 0416-5

PAGE

66

ORIGINAL PAGE IS
OF POOR QUALITY

Report 13133-F-1

***** UMS ENGINE TEST DATA AND PERFORMANCE SUMMARY *****

PLATELET INJECTOR PROGRAM

DEMU-1 INJECTOR 16 IN. HEAT SINK CHAMBER 2:1 CONICAL NOZZLE

A-AREA TESTS PL BASED ON CAVITY PRESSURE MEASUREMENT

TEST	PC	MR	MRC	EM	LRFE	ERC	MWE	FFCE	ODE	ODK	KL	DL	BLL	ERL	FCL	CFCL	ISP-55
291	125.1	1.65	1.65	75.0	98.0	97.3	1.65	.0	334.8	328.9	5.86	2.97	5.77	6.65	.00	.0	313.5
292	102.0	1.41	1.41	68.8	97.8	96.8	1.41	.0	326.9	321.7	5.22	2.89	5.92	7.26	.00	.0	305.6
293	149.0	1.61	1.61	77.2	98.6	97.3	1.61	.0	335.5	328.5	5.04	2.98	5.58	4.70	.00	.0	315.3
294	94.7	1.01	1.61	72.5	97.6	97.2	1.61	.0	333.4	327.0	6.41	2.93	6.01	7.91	.00	.0	310.1
295	149.2	1.40	1.40	73.1	98.6	97.4	1.40	.0	326.6	322.3	4.33	2.93	5.54	4.52	.00	.0	309.3
296	150.7	1.63	1.63	76.2	98.4	97.5	1.63	.0	334.2	329.1	5.12	2.98	5.58	5.40	.00	.0	315.1
297	149.3	1.64	1.64	76.9	98.5	97.2	1.64	.0	334.5	329.3	5.20	2.98	5.57	5.18	.00	.0	315.5
298	147.5	1.38	1.38	73.1	98.7	97.2	1.38	.0	325.7	321.3	4.39	2.92	5.53	4.21	.00	.0	308.7
306	150.6	1.43	1.43	75.0	98.7	97.4	1.43	.0	327.6	321.3	4.29	2.91	5.54	4.17	.00	.0	310.7
307	67.1	1.67	1.67	69.7	96.7	96.7	1.67	.0	335.0	326.9	8.12	2.90	6.45	11.00	.00	.0	306.5
308	102.4	1.93	1.93	76.9	97.0	97.8	1.93	.0	340.4	330.6	9.75	2.97	5.98	7.28	.00	.0	316.9
309	151.9	1.98	1.98	80.0	94.3	98.2	1.98	.0	339.7	331.9	7.75	3.02	5.57	5.79	.00	.0	317.2
310	124.6	1.87	1.87	78.7	98.2	98.1	1.87	.0	327.1	322.8	4.29	2.93	5.53	4.70	.00	.0	309.7
313	151.1	1.42	1.42	73.1	98.6	97.4	1.42	.0	339.6	321.7	5.18	2.90	5.95	6.24	.00	.0	318.1
314	153.3	1.46	1.46	78.1	98.2	97.7	1.46	.0	340.1	330.7	9.43	2.98	6.01	6.64	.00	.0	315.1
315	103.7	1.41	1.41	69.7	97.9	97.5	1.41	.0	339.4	330.5	8.89	2.97	6.03	7.22	.00	.0	314.3
316	104.2	1.91	1.91	77.8	94.0	98.4	1.91	.0	327.0	322.7	7.41	3.01	5.58	6.25	.00	.0	318.4
317	103.1	1.87	1.87	78.5	97.9	96.3	1.87	.0	340.6	333.2	7.41	3.01	5.53	4.65	.00	.0	309.6
318	152.4	1.92	1.92	78.7	98.2	98.2	1.92	.0	340.9	333.3	7.65	3.01	5.56	6.35	.00	.0	318.4
319	150.8	1.41	1.41	73.1	94.6	97.4	1.41	.0	340.2	330.6	9.54	2.98	6.02	6.46	.00	.0	315.2
320	152.8	1.94	1.94	78.7	94.1	98.0	1.94	.0	326.9	321.7	5.26	2.97	5.97	6.31	.00	.0	306.5
321	102.8	1.41	1.41	78.1	98.1	98.4	1.41	.0	334.4	330.4	6.99	2.97	6.01	7.64	.00	.0	313.8
322	100.3	1.41	1.41	70.5	98.1	98.4	1.41	.0	339.5	330.4	9.09	2.97	6.01	7.87	.00	.0	313.6
323	101.8	1.87	1.87	75.9	97.7	97.8	1.87	.0	334.5	330.4	9.10	2.96	6.02	8.08	.00	.0	313.3
323	100.9	1.67	1.87	75.6	97.6	97.8	1.87	.0	327.1	322.6	4.29	2.93	5.58	4.33	.00	.0	309.9
324	151.2	1.41	1.41	74.1	98.7	98.1	1.41	.0	330.9	332.9	6.92	3.01	5.62	5.98	.00	.0	318.3
325	152.3	1.88	1.88	74.7	98.2	98.6	1.88	.0	338.1	330.0	8.07	2.97	6.08	6.73	.00	.0	314.2
326	102.7	1.80	1.80	76.9	92.0	98.8	1.80	.0	328.0	322.8	5.24	2.91	6.01	6.43	.00	.0	307.4
327	103.8	1.44	1.44	71.2	99.1	98.4	1.44	.0	320.2	315.5	4.62	2.88	5.42	2.76	.00	.0	304.5
328	164.3	1.26	1.26	71.2	99.1	98.4	1.26	.0	331.2	326.9	4.29	2.97	5.51	4.39	.00	.0	314.0
329	168.0	1.53	1.53	75.2	94.7	98.1	1.53	.0	334.1	328.4	5.67	2.97	5.82	5.97	.00	.0	316.8
330	128.1	1.89	1.89	78.1	98.1	98.5	1.89	.0	339.9	332.0	13.56	2.99	5.75	4.68	.00	.0	316.5
331	128.1	2.21	2.21	81.2	98.6	99.4	2.21	.0	343.5	330.0	14.13	2.97	6.02	5.31	.00	.0	314.4
332	127.5	2.16	2.16	80.0	98.5	99.5	2.16	.0	342.9	328.7	4.54	2.92	5.68	4.87	.00	.0	308.7
333	101.8	1.41	1.41	72.5	98.5	97.0	1.41	.0	327.6	323.1	4.50	2.93	5.67	4.68	.00	.0	309.8
334	136.4	1.43	1.43	73.7	98.6	97.9	1.43	.0	342.5	328.1	14.36	2.97	6.21	4.55	.00	.0	314.4
335	138.1	2.13	2.13	81.2	96.7	99.7	2.13	.0									
336	88.6																

***** UMS ENGINE TEST DATA AND PERFORMANCE SUMMARY *****

P L A T E L E T I N J E C T O R P R O G R A M

0E40-2 INJECTOR 16 IN. HEAT SINK CHAMBER 2:1 CONICAL NOZZLE

A-AREA TESTS PC = P CAVITY TOFM NOMINAL, WD AND KWD QUESTIONABLE(3458)

TEST	TIME	PC	MHC	MR	FFC	CSTAR	CSTART	XC*	ISPV	ISPT	ZISP	KL	DL	BL	FCL	ERL	ERE	ISP-SS
337	2.70	126.3	1.57	1.57	.0	5587.	5687.	98.2	248.3	261.5	95.0	1.31	4.04	2.71	.00	5.14	98.0	312.5
338	2.70	102.5	1.36	1.36	.0	5508.	5617.	96.1	244.1	258.2	94.5	1.10	3.97	2.74	.00	6.32	97.6	304.1
339	2.70	147.6	1.36	1.36	.0	5546.	5621.	96.7	246.5	258.1	95.5	.96	4.01	2.51	.00	4.09	98.4	307.9
340	2.70	104.0	1.52	1.52	.0	5582.	5680.	98.3	247.8	261.9	94.6	1.71	4.03	2.83	.00	5.51	97.9	313.2
341	2.70	147.4	1.40	1.40	.0	5552.	5643.	98.4	246.9	254.1	95.3	1.01	4.02	2.50	.00	4.67	98.2	309.2
342	2.70	123.9	1.86	1.86	.0	5551.	5683.	97.7	249.0	262.0	95.0	1.58	4.05	2.64	.00	4.79	98.2	315.6
343	2.70	123.9	1.85	1.85	.0	5547.	5683.	97.6	249.0	261.9	95.1	1.58	4.05	2.63	.00	4.65	98.2	315.8
344	2.70	125.5	1.85	1.85	.0	5554.	5686.	97.5	249.9	261.8	95.1	1.40	4.05	2.63	.00	4.81	98.2	314.3
345	2.70	150.5	1.91	1.91	.0	5565.	5683.	97.9	250.0	261.6	95.6	1.41	4.07	2.49	.00	3.55	98.6	318.7
346	2.70	101.6	1.85	1.85	.0	5533.	5675.	97.5	247.9	262.0	94.6	1.75	4.03	2.78	.00	5.53	97.9	313.2

Report 13133-F-1

TEST	TIME	PC	FVAC	WD	WF	WFC	WT	DPOJ	DPFJ	VOX	VF	KWD	KWF	TW	TO	TF	TFJ
337	2.70	126.3	4773.2	11.753	7.467	.000	19.22	41.5	57.0	65.	104.	1.518	1.116	1185.	68.	229.	229.
338	2.70	102.5	3863.7	9.110	6.711	.000	15.83	24.1	46.1	50.	93.	1.545	1.117	1160.	68.	232.	232.
339	2.70	147.6	5576.1	13.037	9.594	.000	22.63	51.6	93.3	73.	131.	1.510	1.110	1260.	68.	205.	205.
340	2.70	104.0	3923.2	10.217	5.616	.000	15.83	30.2	32.2	56.	77.	1.546	1.103	1210.	68.	187.	187.
341	2.70	147.4	5571.1	13.170	9.391	.000	22.56	52.9	90.3	74.	130.	1.506	1.109	1310.	68.	216.	216.
342	2.70	123.9	4722.2	12.327	6.641	.000	18.97	47.7	43.7	70.	91.	1.485	1.139	1370.	68.	240.	240.
343	2.70	123.9	4726.6	12.332	6.649	.000	18.98	47.7	43.7	70.	91.	1.485	1.134	1375.	67.	227.	227.
344	2.70	125.5	4760.0	11.040	7.245	.000	19.20	45.0	51.6	68.	97.	1.484	1.123	1329.	69.	196.	196.
345	2.70	150.5	5740.7	15.078	7.905	.000	22.98	71.9	62.8	86.	109.	1.479	1.123	1484.	68.	224.	224.
346	2.70	101.6	3859.0	10.126	5.484	.000	15.61	32.1	28.9	57.	74.	1.487	1.149	1277.	69.	224.	224.

TEST	TIME	PC	MHC	EM	EREE	ERC	WKE	FFCE	ODE	ODK	KL	DL	BLL	ERL	FCL	CFCL	ISP-SS
337	126.3	1.57	1.57	74.7	96.2	97.6	1.57	.0	332.4	327.1	5.32	2.96	5.79	5.92	.00	.0	312.5
338	102.5	1.36	1.36	67.8	94.0	97.3	1.36	.0	324.6	319.4	5.20	2.88	5.93	6.44	.00	.0	304.1
339	147.6	1.36	1.36	73.1	96.8	97.7	1.36	.0	324.7	320.3	4.45	2.91	5.56	3.65	.00	.0	307.9
340	104.0	1.52	1.52	75.0	97.5	98.0	1.52	.0	338.5	330.2	8.22	2.96	6.01	8.06	.00	.0	313.2
341	147.4	1.40	1.40	73.1	95.6	97.5	1.40	.0	326.6	322.2	4.36	2.92	5.57	4.51	.00	.0	309.2
342	123.9	1.86	1.86	76.6	97.9	97.3	1.86	.0	339.3	331.6	7.73	2.99	5.77	7.18	.00	.0	315.6
343	123.9	1.85	1.85	76.6	97.9	97.3	1.85	.0	339.3	331.5	7.71	2.99	5.76	6.97	.00	.0	315.8
344	125.5	1.85	1.85	76.2	98.2	97.0	1.85	.0	334.7	328.9	5.83	2.97	5.75	5.86	.00	.0	314.3
345	150.5	1.91	1.91	79.4	98.3	97.6	1.91	.0	340.4	335.0	7.31	3.01	5.56	5.82	.00	.0	318.7
346	101.6	1.85	1.85	75.0	97.6	97.2	1.85	.0	330.0	330.3	6.69	2.96	5.98	6.19	.00	.0	313.2

04/16/75 10:10:40 FD0117 000427581

000427 2 100

DATE 041675

PAGE 72

ORIGINAL PAGE IS
OF POOR QUALITY

Report 13133-F-1

***** UMS ENGINE TEST DATA AND PERFORMANCE SUMMARY *****

P L A T E L E T I N J E C T O R P R O G R A M

DEMO-2 INJECTOR 12 IN. HEAT SINK CHAMBER 2:1 CONICAL NOZZLE

A-AREA TESTS PC = P CAVITY TOFM NUMINAL, MO AND KMO QUESTIONABLE

TEST	TIME	PC	MRC	MR	FFC	CSTAR	CSTART	XC*	ISPV	ISPT	XISP	KL	DL	BL	FCL	ERL	EML	ISP-55
342	2.70	119.3	1.37	1.37	.0	5389.	5627.	95.8	242.1	258.6	93.6	1.08	3.94	2.24	.00	9.29	96.4	302.0
343	2.70	119.7	1.58	1.58	.0	5453.	5687.	95.9	244.8	261.5	93.6	1.34	3.98	2.30	.00	9.11	96.5	307.1
344	2.70	122.9	1.80	1.80	.0	5477.	5690.	96.2	245.7	262.3	93.7	1.56	4.00	2.31	.00	8.66	96.7	310.1

TEST	TIME	PC	FVAC	MI	WF	MFC	WT	DPUJ	DPFJ	VOX	VF	KMO	KMF	TW	TF	TFJ
342	2.70	119.3	4557.1	10.895	7.924	.000	18.82	38.7	60.8	63.	107.	1.457	1.150	1180.	69.	234.
343	2.70	119.7	4567.8	11.424	7.238	.000	18.66	41.1	51.4	65.	98.	1.482	1.135	1213.	68.	221.
344	2.70	122.9	4688.6	12.264	6.810	.000	19.08	47.2	46.0	70.	94.	1.485	1.138	1246.	67.	241.

TEST	PC	MR	MRC	EM	EMLE	ERC	MRE	FFCE	ODE	UDK	KL	DL	BLL	ERL	FCL	CFCL	ISP-55
342	119.3	1.37	1.37	62.5	97.0	95.0	1.37	.0	325.3	320.4	4.88	2.86	5.61	9.91	.00	.0	302.0
343	119.7	1.58	1.58	66.9	96.6	95.3	1.58	.0	332.6	327.0	5.52	2.90	5.68	11.34	.00	.0	307.1
344	122.9	1.80	1.80	69.4	96.4	95.9	1.80	.0	338.2	331.1	7.15	2.93	5.68	12.33	.00	.0	310.1

***** OMS ENGINE TEST DATA AND PERFORMANCE SUMMARY *****

PLATELET INJECTOR PROGRAM

XDTIC INJECTOR HI CONTRACTION RATIO CHAMBER 2.6:1 NOZZLE

PC BASED ON PCAV/1.014 NOTE:OMS 55 ISP IS BASED ON PC=125.

TEST TIME	PC	MRC	MR	FFC	CSTAR	CSTART	XC*	ISPV	ISPT	XISP	KL	DL	BL	FCL	ERL	ERE	ISP-55
416 2.90	200.4	1.44	1.44	.0	5352.	5666.	94.5	255.8	268.3	95.3	.91	3.50	2.64	.00	5.29	98.0	306.9
417 2.90	195.6	1.90	1.90	.0	5405.	5701.	94.8	258.0	270.8	95.3	1.56	3.53	2.98	.00	4.77	98.2	314.6
418 2.30	245.3	1.75	1.75	.0	5450.	5732.	95.1	258.8	271.2	95.4	1.20	3.54	2.98	.00	4.71	98.3	316.3
419 2.30	205.0	1.43	1.43	.0	5444.	5668.	96.0	257.0	268.0	95.9	.05	3.52	2.79	.00	4.72	98.2	310.2
420 2.10	249.3	1.85	1.85	.0	5444.	5745.	95.7	258.8	271.0	95.5	1.26	3.54	2.98	.00	4.49	98.3	320.1
421 2.10	142.7	1.64	1.64	.0	5426.	5700.	95.2	255.4	270.6	94.4	1.52	3.50	3.53	.00	6.62	97.6	307.4

Report 13133-F-1

TEST TIME	PC	FVAC	WU	WF	WFC	WT	DPUJ	OPFJ	VOX	VF	KWO	KMF	TM	TO	TF	TFJ
416 2.90	200.4	4062.0	9.378	6.501	.000	15.88	34.1	51.6	59.	99.	1.338	1.019	1660.	71.	225.	225.
417 2.90	195.6	3959.0	10.058	5.289	.000	15.35	38.2	33.2	63.	79.	1.356	1.032	1660.	72.	220.	220.
418 2.30	245.3	4940.0	12.145	6.946	.000	19.09	55.6	59.0	76.	105.	1.357	1.016	1460.	72.	218.	218.
419 2.30	295.0	5906.0	13.513	9.471	.000	22.98	71.0	114.5	85.	147.	1.336	.998	1460.	72.	227.	227.
420 2.10	299.3	5975.0	14.467	8.103	.000	23.09	84.9	81.6	94.	124.	1.356	1.007	1310.	73.	217.	217.
421 2.10	142.7	2850.0	6.937	4.221	.000	11.16	18.0	20.2	43.	61.	1.364	1.050	1060.	75.	207.	207.

TEST PC	MR	MPC	EM	EHEE	ERC	MRE	FFCE	QOE	UDK	KL	DL	BLL	ERL	FCL	CFCL	ISP-55
416 200.4	1.44	1.44	72.5	94.5	93.6	1.44	.0	328.4	324.9	3.42	2.90	10.05	5.05	.00	.0	306.9
417 195.6	1.90	1.90	76.9	97.9	94.4	1.90	.0	340.5	335.0	5.48	2.98	10.21	7.21	.00	.0	314.6
418 245.3	1.75	1.75	77.2	98.3	94.5	1.75	.0	337.5	334.8	2.76	2.99	9.86	5.59	.00	.0	316.3
419 295.0	1.43	1.43	74.1	98.8	94.9	1.43	.0	328.1	326.4	1.75	2.93	9.49	3.78	.00	.0	310.2
420 299.3	1.85	1.85	77.8	98.2	95.1	1.85	.0	340.0	338.8	1.17	3.03	9.58	6.11	.00	.0	320.1
421 142.7	1.64	1.64	72.5	97.6	94.7	1.64	.0	334.5	329.2	5.34	2.91	10.93	7.98	.00	.0	307.4

04/16/75 10:10:40 FD0117 000427581

000427

2

100

DATE 041675

PAGE 80

***** OMS ENGINE TEST DATA AND PERFORMANCE SUMMARY *****

PLATELET INJECTOR PROGRAM

LOW P XDT INJECTOR 16 IN. HEAT SINK CHAMBER 2:1 CONICAL NOZZLE

A-AREA TESTS PC BASED ON CAVITY PRESSURE MEASUREMENT

TEST TIME	PC	MRC	MR	FPC	CSTAR	XC*	ISPV	ISPT	XISP	KL	DL	BL	FCL	ERL	ERE	ISP-SS	
424 1.50	127.7	1.67	1.67	.0	5613.	5701.	98.4	250.2	262.1	95.5	1.40	4.07	2.85	.00	3.57	98.6	316.2
424 1.70	126.8	1.66	1.66	.0	5558.	5700.	97.5	248.3	262.2	94.7	1.40	4.04	2.75	.00	5.65	97.8	313.3

TEST TIME	PC	FVAC	WO	WF	WFC	WT	DPOJ	DPEJ	VOX	VF	KWD	KWF	TW	TO	TF	TFJ
424 1.50	127.7	4823.0	12.055	7.218	.000	19.27	32.2	32.2	58.	77.	1.784	1.416	960.	90.	195.	195.
424 1.70	126.6	4798.0	12.064	7.256	.000	19.32	32.7	32.5	58.	78.	1.769	1.422	1110.	86.	204.	204.

TEST PC	MR	MRC	EM	EREE	ERC	MKE	FFCE	UDE	ODK	KL	DL	BLL	ERL	FCL	CFCL	ISP-SS
424 127.7	1.67	1.67	79.4	98.7	98.1	1.67	.0	335.2	329.3	5.88	2.99	5.83	4.33	.00	.0	316.2
424 126.8	1.66	1.66	74.4	97.9	97.1	1.66	.0	335.0	329.2	5.86	2.96	5.77	7.15	.00	.0	313.3

Report 13133-F-1

ORIGINAL PAGE IS
OF POOR QUALITY

04/16/75 10:10:40 F00117 000427501 000427 2 100 DATE 041675 PAGE 84

***** UMS ENGINE TEST DATA AND PERFORMANCE SUMMARY *****

LIKE DOUBLET INJECTOR N204/MMH TESTS

A-AREA TEST SERIES 6K-28- 16 IN. HEAT SINK CHAMBER

AREA RATIO 2 NOZZLE STABILITY TESTS PC BASED ON PC-1 AND PC-2

TEST	TIME	PC	MRC	MR	FFC	CSTAR	%C*	ISPV	ISPT	XISP	KL	DL	BL	FCL	ERL	ERE	ISP-55
272	1.90	155.5	1.44	1.44	.0	5555.	98.2	248.6	260.2	95.5	1.01	4.04	2.58	.00	3.98	98.5	311.4
273	1.90	105.2	1.41	1.41	.0	5531.	98.0	247.4	259.8	95.2	1.17	4.02	2.77	.00	4.39	98.3	308.2
274	1.90	156.6	1.81	1.81	.0	5582.	98.0	250.4	262.5	95.4	1.37	4.07	2.65	.00	4.02	98.5	318.0
275	1.90	105.7	1.80	1.80	.0	5574.	98.1	249.7	262.5	95.1	1.71	4.06	2.86	.00	4.13	98.4	315.2
280	1.90	154.4	1.80	1.80	.0	5582.	97.9	250.1	262.6	95.2	1.58	4.07	2.66	.00	4.38	98.3	317.4
281	1.90	103.8	1.40	1.40	.0	5525.	98.1	246.8	259.4	95.1	1.15	4.01	2.77	.00	4.66	98.2	307.3
282	1.90	154.6	1.41	1.41	.0	5545.	98.2	248.0	259.8	95.5	.99	4.03	2.57	.00	4.22	98.4	310.3
283	1.90	102.6	1.84	1.84	.0	5554.	97.9	249.2	262.4	95.0	1.76	4.05	2.87	.00	4.56	98.3	314.4

TEST	TIME	PC	FVAC	WQ	WF	WFC	WT	OPOJ	DPFJ	VDX	VF	KWD	KWF	TW	TF	TFJ
272	1.90	155.5	5848.0	13.870	9.658	.000	23.53	87.1	93.9	94.	131.	1.230	1.109	1160.	56.	190.
273	1.90	105.2	3956.0	9.359	6.630	.000	15.99	39.2	44.6	63.	91.	1.238	1.107	1160.	57.	200.
274	1.90	156.6	5907.0	15.203	8.385	.000	23.59	104.4	71.3	103.	115.	1.231	1.108	1160.	56.	201.
275	1.90	105.7	3960.0	10.247	5.689	.000	15.94	46.7	32.8	69.	73.	1.241	1.104	1160.	57.	192.
280	1.90	154.4	5818.0	14.946	8.314	.000	23.26	101.0	70.1	101.	114.	1.230	1.109	1160.	55.	204.
281	1.90	103.8	3897.0	9.201	6.589	.000	15.79	37.5	43.5	62.	89.	1.243	1.112	1160.	55.	194.
282	1.90	154.6	5813.0	13.726	9.718	.000	23.44	85.6	94.6	93.	132.	1.227	1.113	1160.	55.	196.
283	1.90	102.6	3871.0	10.059	5.477	.000	15.54	45.0	29.9	68.	74.	1.241	1.115	1160.	56.	196.

TEST	PC	MR	MRC	EM	EMEE	ERC	MRE	FFCE	ODE	ODK	KL	DL	BLL	ERL	FCL	CFCL	ISP-55
272	155.5	1.44	1.44	76.2	98.8	97.6	1.44	.0	327.9	323.7	4.21	2.95	5.58	3.80	.00	.0	311.4
273	105.2	1.41	1.41	74.4	94.6	97.5	1.41	.0	326.8	321.7	5.15	2.92	6.00	4.52	.00	.0	308.2
274	156.6	1.81	1.81	78.1	94.3	97.6	1.81	.0	338.6	332.5	6.08	3.01	5.60	5.89	.00	.0	318.0
275	105.7	1.80	1.80	76.1	94.2	97.6	1.80	.0	338.1	330.2	7.92	2.98	6.05	5.94	.00	.0	315.2
280	154.4	1.80	1.80	77.5	98.2	97.6	1.80	.0	338.3	332.2	6.01	3.00	5.62	6.10	.00	.0	317.4
281	103.8	1.40	1.40	73.1	96.5	97.5	1.40	.0	326.2	321.0	5.17	2.91	6.01	4.79	.00	.0	307.3
282	154.6	1.41	1.41	75.0	98.8	97.5	1.41	.0	327.0	322.8	4.23	2.93	5.57	3.97	.00	.0	310.3
283	102.6	1.84	1.84	76.9	98.0	97.7	1.84	.0	338.8	330.3	8.51	2.97	6.06	6.88	.00	.0	314.4

ORIGINAL PAGE IS
OF POOR QUALITY

XI. FULL SCALE HEAT TRANSFER

XI. FULL SCALE HEAT TRANSFER

A. INTRODUCTION

This section discusses the heat transfer analysis of the full scale tests at ALRC. Since most of the testing was done with uncooled combustion chambers, the typical result of the analysis is an axial profile of heat flux or heat transfer correlating coefficient values. These parameters are determined from the transient response of thermocouples located on the gas-side wall. The response is used as a boundary condition in a one-dimensional radial finite difference conduction network; this analytical technique has proven useful in the past and was confirmed in the present case by means of a two-dimensional model that accounted for axial conduction effects. Agreement between the one- and two-dimensional models was excellent.

In addition to the results of the chamber heat transfer analysis, there will also be a discussion of the mini-skirt data, inferred cavity environment, injector face temperature levels, and the baffle heating experienced in the integral baffle injector tests. A comprehensive analysis of regenerative chamber heat transfer as determined in WSTF testing has been presented previously,^{1,2}.

B. CHAMBER HEAT FLUXES

1. XDT-1 Injector

Heat fluxes have been inferred from thermocouple responses on six heat sink tests run with the full-scale XDT-1 injector, three with film cooling and three without. These results are shown in Figure 89 which also indicates the characteristics of the XDT subscale unit and a conventional unlike-doublet IR&D injector. Significant differences are noted between the subscale and full scale XDT injectors with no film cooling. The subscale unit provided

1 WSTF Test Report, ALRC Report 13133-S-1, 12 December 1973
2 1974 WSTF Test Report, ALRC Report 13133-S-3, 1 April 1975

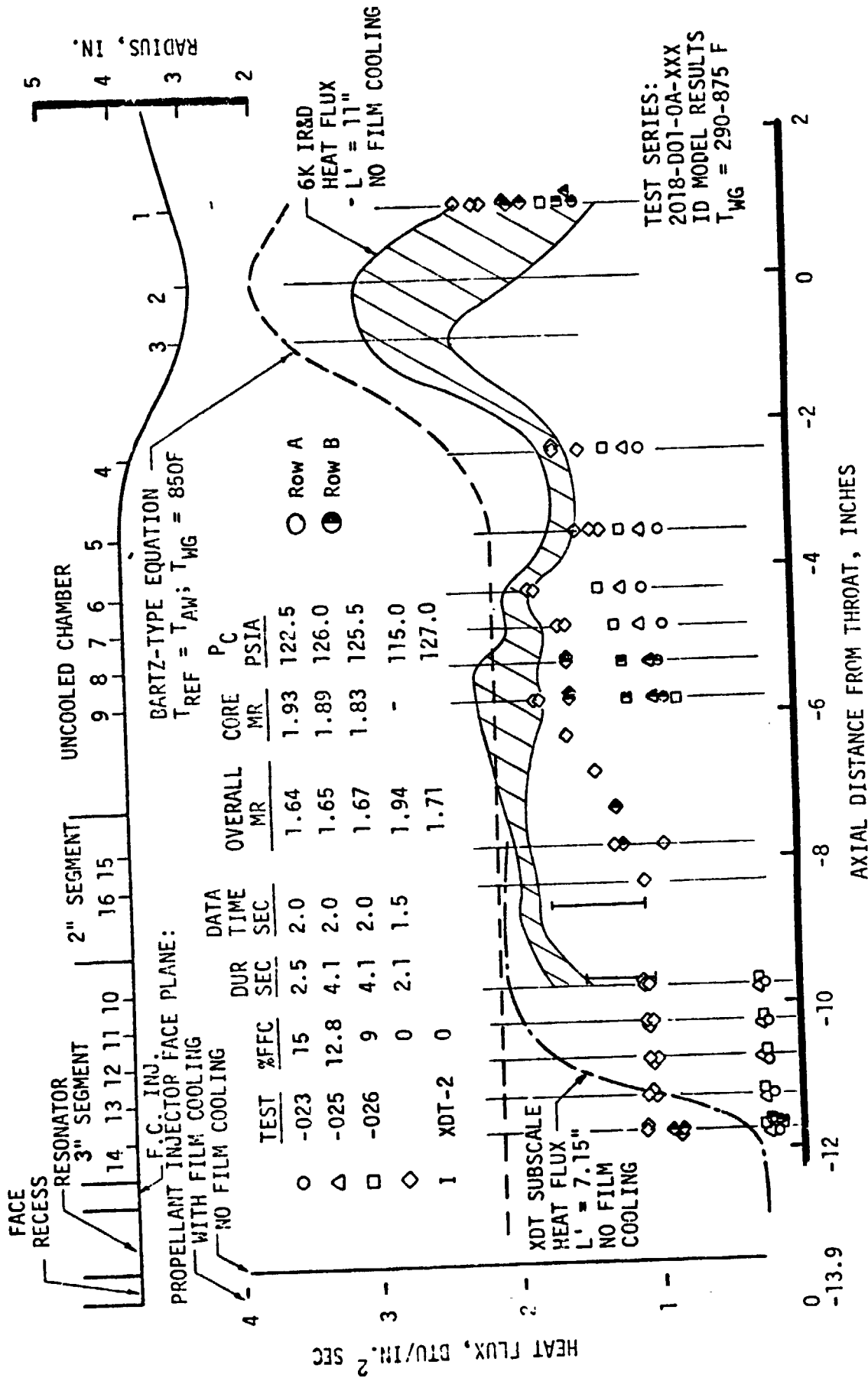


Figure 89. Heat Flux Data for the XDT-1 Injector

XI,B, Chamber Heat Fluxes (cont.)

a liquid fuel film for about 1.6 in., followed by a transition (mixing) region in which the heat flux increased to about $2.0 \text{ Btu/in}^2 \text{ sec}$, a typical cylindrical section value for a number of injector types. Although the full scale data do not indicate the presence of a liquid film, no thermocouples were located within 1.6 in. of the injector face. However, a low mixture ratio region is seen to persist for at least five inches with the full scale unit; in this region the heat flux never exceeds $1.1 \text{ Btu/in}^2 \text{ sec}$. It is followed by a mixing region in which the flux increases to $1.6 - 1.8 \text{ Btu/in}^2 \text{ sec}$. Applying a non-reactive heat transfer coefficient correlation inferred downstream of this mixing region, the low heat flux data indicate the wall mixture ratio in the initial five inch region is about 0.6. After about seven inches, mixing is complete and the XDT-1 data in the remainder of the cylindrical section and in the convergent section agree with the lower end of the IR&D data range. Throat thermocouples were inoperative on these tests, but downstream of the throat the XDT-1 and IR&D data ranges are similar.

Three tests with fuel film cooling are included in Figure 89. with the coolant flow ranging from 9-15 percent of the fuel flow. A liquid film length of at least 2.5 in. is observed in each case. Downstream of the liquid film significant reductions in heat flux compared to no film cooling are noted; these reductions extend into the expansion section.

2. XDT-2 Injector

Chamber heat fluxes for the XDT-2 injector are shown on Figure 90 as a function of circumferential location at axial distances of 3.9 and 4.9 in. from the injector face. All data were obtained on a 4-inch L^* section, since other thermocouples were inoperative. A good comparison with XDT-1 heat flux data is not possible since the latter were obtained at only two circumferential locations. At these locations, the XDT-1 heat fluxes were independent of axial position for a distance of at least 5 in; these fluxes are shown on Figure 90 for comparison with the XDT-2 data. It is

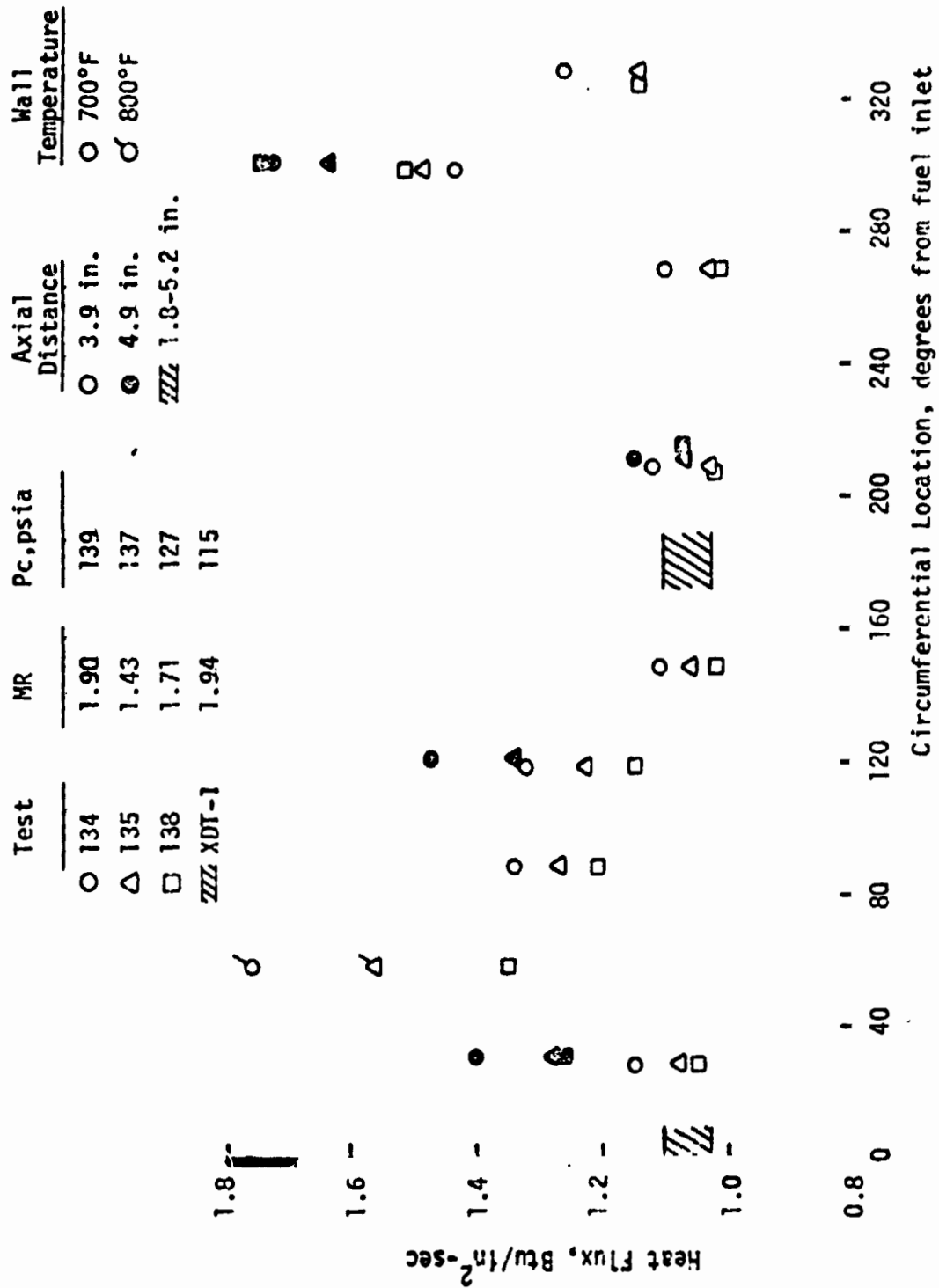


Figure 90. Heat Flux Data for the XDT-2 Injector

XI,B, Chamber Heat Fluxes (cont.)

noted that the low flux XDT-2 data at 30, 150, 210 and 270 degrees from the fuel inlet agree with the XDT-1 results. However, significant hot streaks are observed at 60° and 300°, with smaller flux increases at 90, 120 and 330 degrees. All four locations at which both axial positions were instrumented indicate an increase in flux at the downstream position. Therefore, the low mixture ratio zone established at the wall does not persist as far downstream with XDT-2 as it did with XDT-1. The XDT-2 data ranges for Test 138 are shown on Figure 89 at the appropriate distances from the injector face to provide further comparison with XDT-1.

3. Mixed Element Injector

Figure 91 shows the heat flux results for five tests with the mixed element injector. The large spread in the data is caused by the wide range of operating conditions covered by these tests and by the instability associated with Test 151. Also shown in Figure 91 are the data ranges for the X-doublet injectors and two IR&D conventional doublet injectors. Figure 92 provides a more meaningful comparison of injector effects by shifting the injector faces to a common location; Figure 91 should be used to compare results in the convergent section and throat region. Mixed element heat fluxes are in general agreement with the conventional doublets throughout the chamber. X-doublet fluxes are initially lower due to the low O/F zone noted previously, but Figure 92 indicates that all injectors are similar after about 7-8 inches.

Of particular interest is the comparison of the mixed element injector with the X-doublet units. The operating conditions of Test 152 on Figure 91 correspond closely with those for the XDT-1 data. Figure 93 compares the data from this test with the XDT-1 data range from Figure 89; the latter have been shifted in the injector-affected zone to provide a common injector face location. Also shown in Figure 93 are the mixed-element throat data from Test 149 and the heat flux range which matched nominal regen chamber throat wall temperatures with the XDT-2 injector. The mixed-element fluxes are

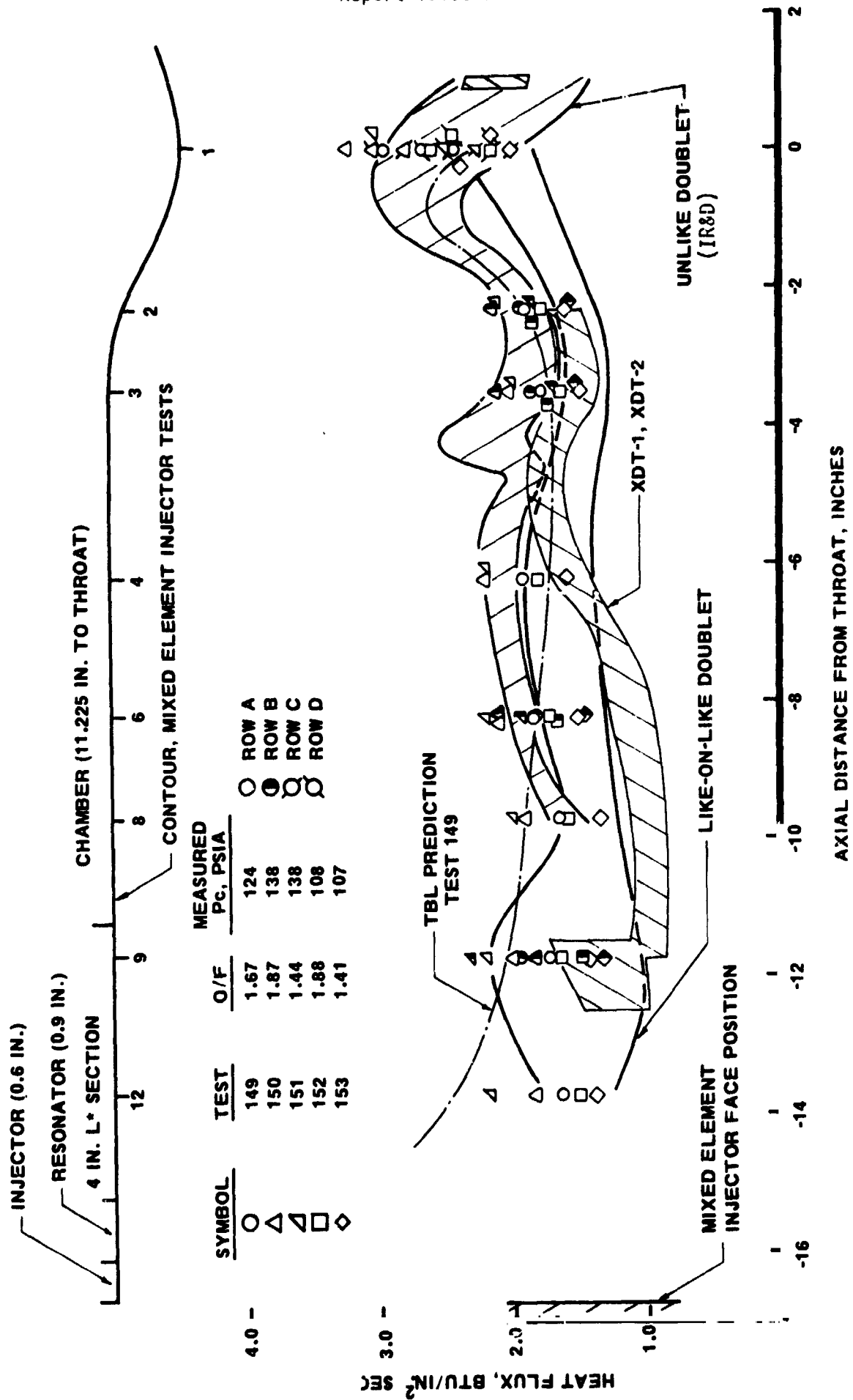


Figure 91. Mixed Element Injector Heat Flux Results

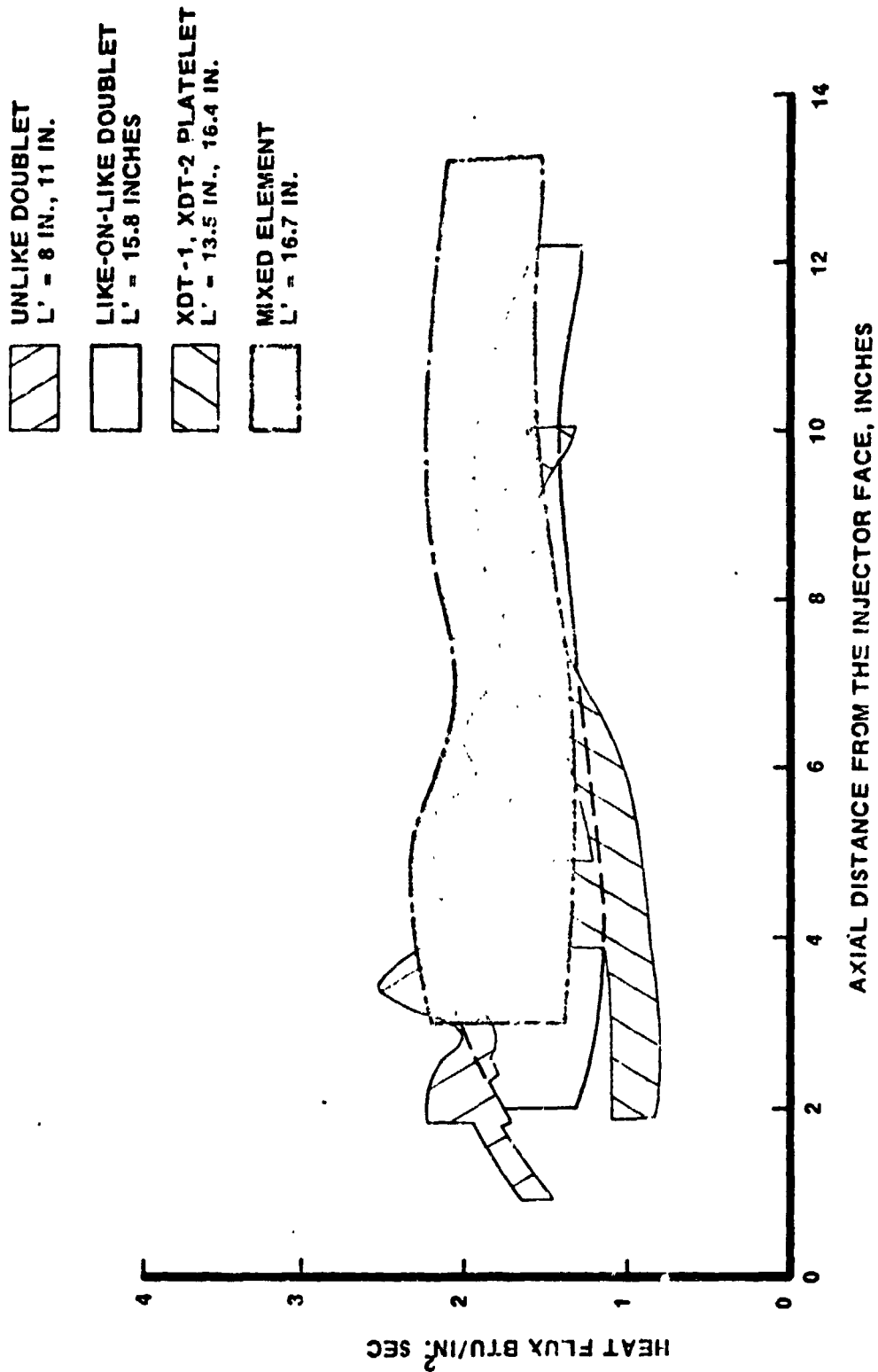


Figure 92. Heat Flux Results for the Cylindrical Combustion Chamber

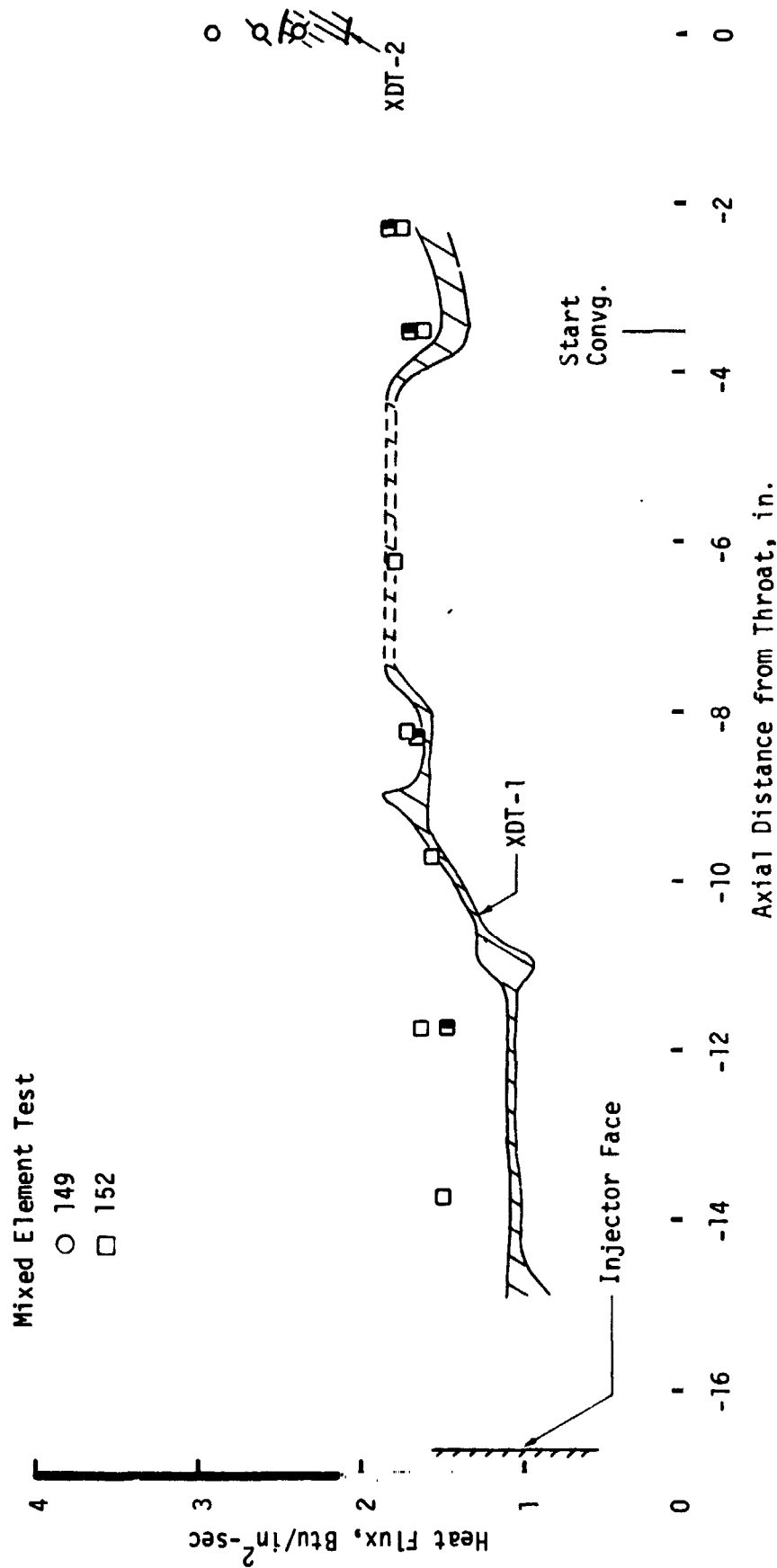


Figure 93. Comparison of the Mixed Element and XDT Injectors

XI,B, Chamber Heat Fluxes (cont.)

initially about 40 percent higher than those for XDT-1, but after about seven inches the cylindrical section data are in good agreement. At the start of the convergent section, mixed element fluxes are slightly higher than XDT-1 values; they are also a little higher in the throat than the XDT-2 fluxes inferred from regenerative chamber data.

Figure 91 also includes a heat flux prediction for Test 149 using the Turbulent Boundary Layer Computer Program. This prediction is in reasonable agreement with the data after about 8 inches, although it is slightly low in the throat.

4. DXDT1-1 Injector

Figure 94 shows the axial distribution of heat flux for the demo injector DXDT1-1; the trends shown are generally consistent with the above XDT-1 data. A low flux region is evident within four inches of the injector face. Flux levels in this region are similar to XDT-1, but show a rapid increase with axial distance compared to the relatively uniform flux of XDT-1. This perturbation may have been caused by the acoustic cavity overlap ring, which created a discontinuity in the chamber inside diameter. The transition to the high flux region is much more gradual in Figure 94 than for XDT-1, although the ultimate flux levels are consistent. For DXDT1-1 this transition occurs over a 5-6 in. length, compared to about 2.5 in. for XDT-1. In both cases a reduction in flux is observed at the end of the cylindrical section, with the DXDT1-1 reduction being somewhat smaller.

Figure 94 clearly shows the increases in heat flux associated with increases in chamber pressure and mixture ratio. These variations are exhibited by all the demo injector data and are consistent with the gas-side wall temperature variations observed at WSTF with XDT-2 injector on the regen chamber.

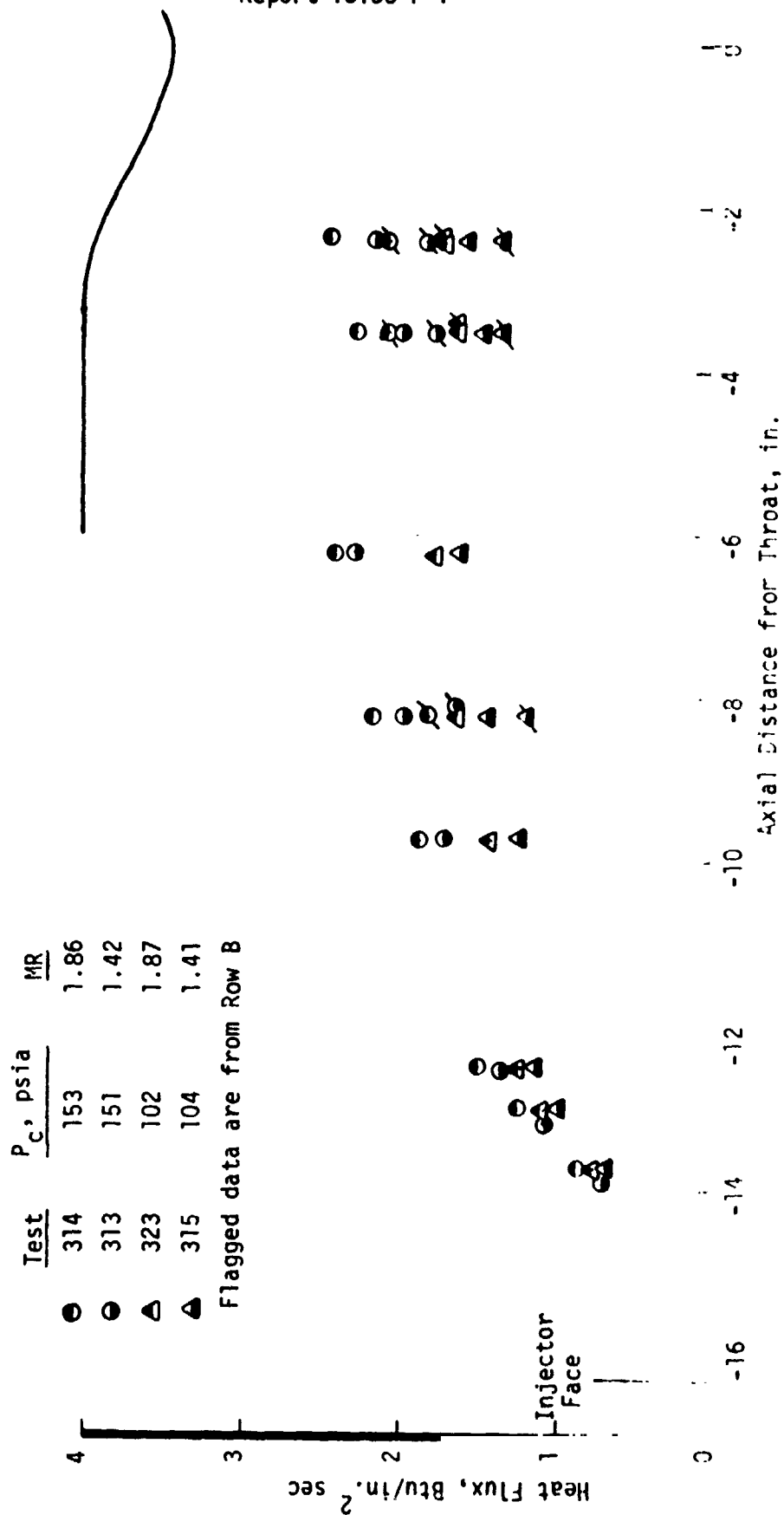


Figure 94. Heat Flux Data for the DXDT-1 Injector

XI,B, Chamber Heat Fluxes (cont.)

Figure 95 gives the circumferential heat flux variation obtained from the special L* section with XDT1-2. Similar data which were obtained at approximately the same axial location were presented in Figure 90 for the XDT-2 pattern. The present data are much more uniform, although a streak is observed in the 60-80° region. The thermocouple at 260° is probably in error, since such low fluxes have never been observed at this axial position with either the present or previous data. Differences between the two rows of thermocouples are evident on Figure 94; these differences appear to be consistent with the scatter in Figure 95.

5. DXDT1-2 Injector

The axial variation in heat flux for DXDT1-2 is shown in Figure 96; data ranges from Figure 95 are included for common test conditions. Comparison of Figures 94 and 95 reveal the same trends for both injectors. This is shown in detail in Figure 97, which includes data from both injectors at common test conditions. Good agreement is noted between the circumferential data on DXDT1-2 and the data obtained just upstream with the -1 injector. In the transition and high flux regions the -2 injector gives slightly lower fluxes than the -1 unit.

6. High Contraction Ratio Chamber

Heat fluxes inferred from the high contraction ratio chamber, i.e., Tests 417-420, are shown on Figure 98. Comparison of the four tests indicates heat flux increases with chamber pressure and mixture ratio consistent with previous data. B-row fluxes are readily lower than A-row in the cylindrical section; however, at the start of the convergent section, B-row values are higher. Approaching the start of the convergent section, A-row heat fluxes decrease consistent with most previous data. However, B-row fluxes increase; in one previous case (XDT-1B), heat fluxes were unchanged, but this is the only time an increase in heat flux has been observed at

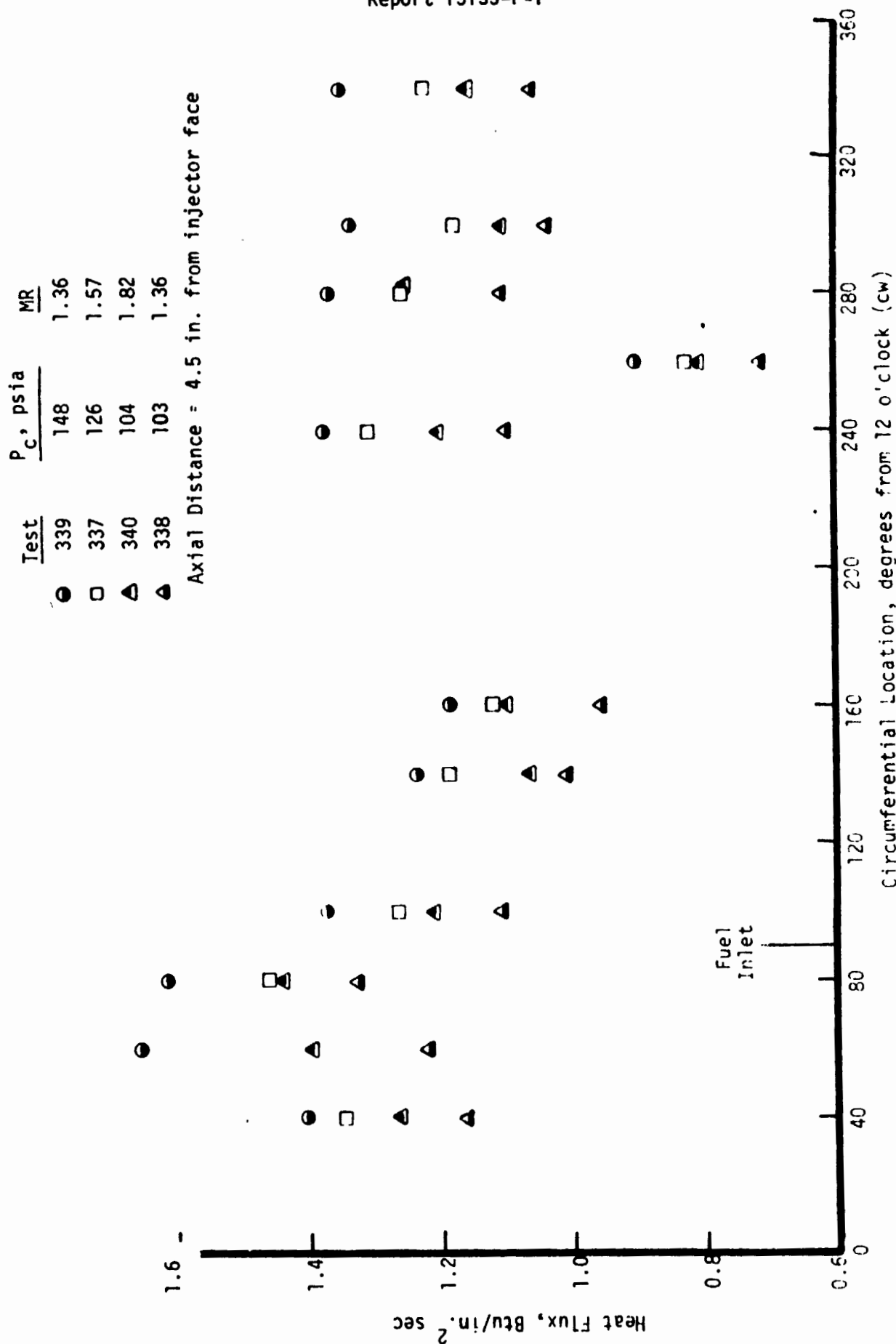


Figure 95. Circumferential Heat Flux Data for DXDT1-2

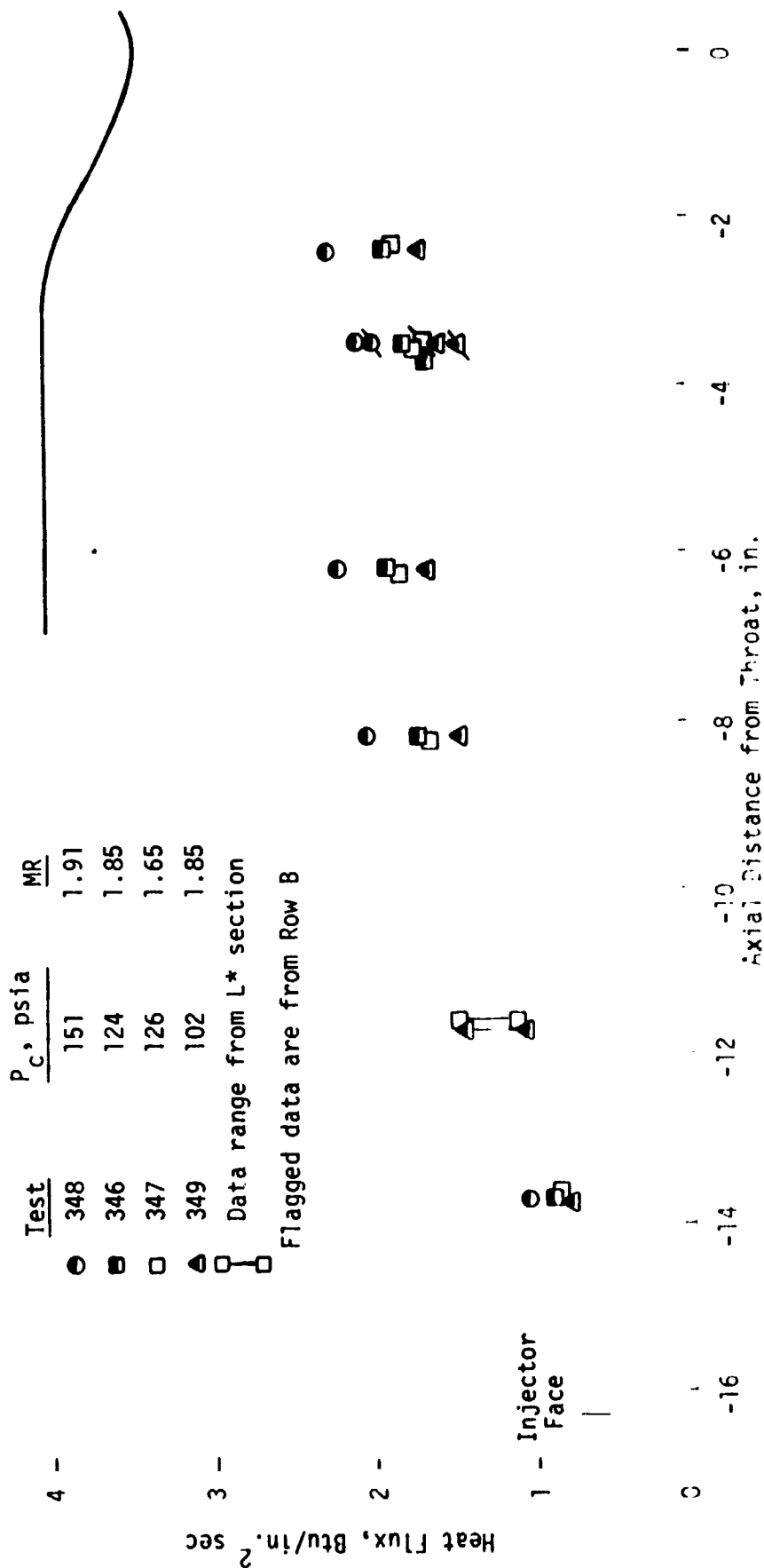


Figure 96. Heat Flux Data for the DXDT1-2 Injector

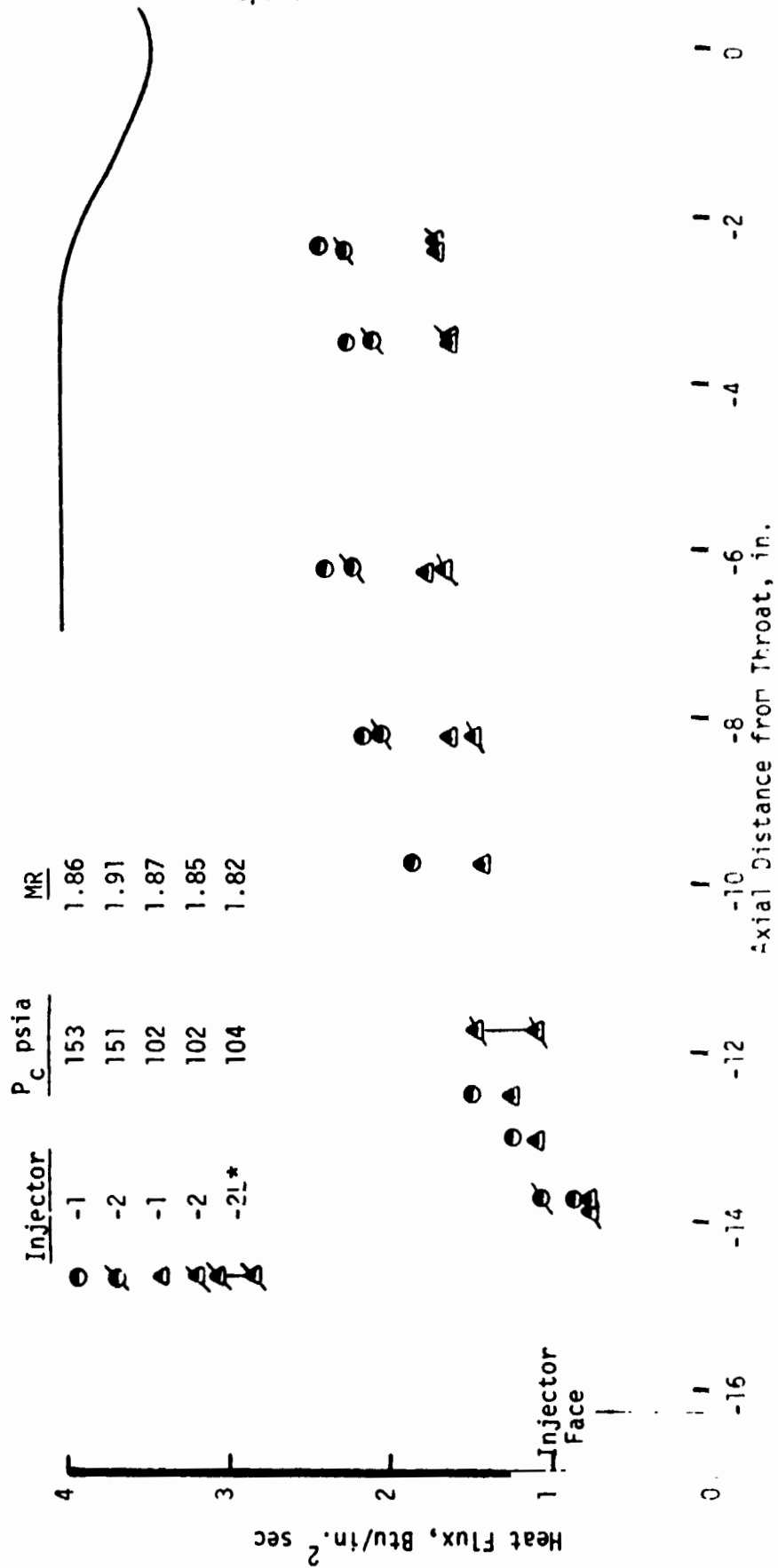


Figure 97. Comparison of Demonstration Injector Heat Fluxes

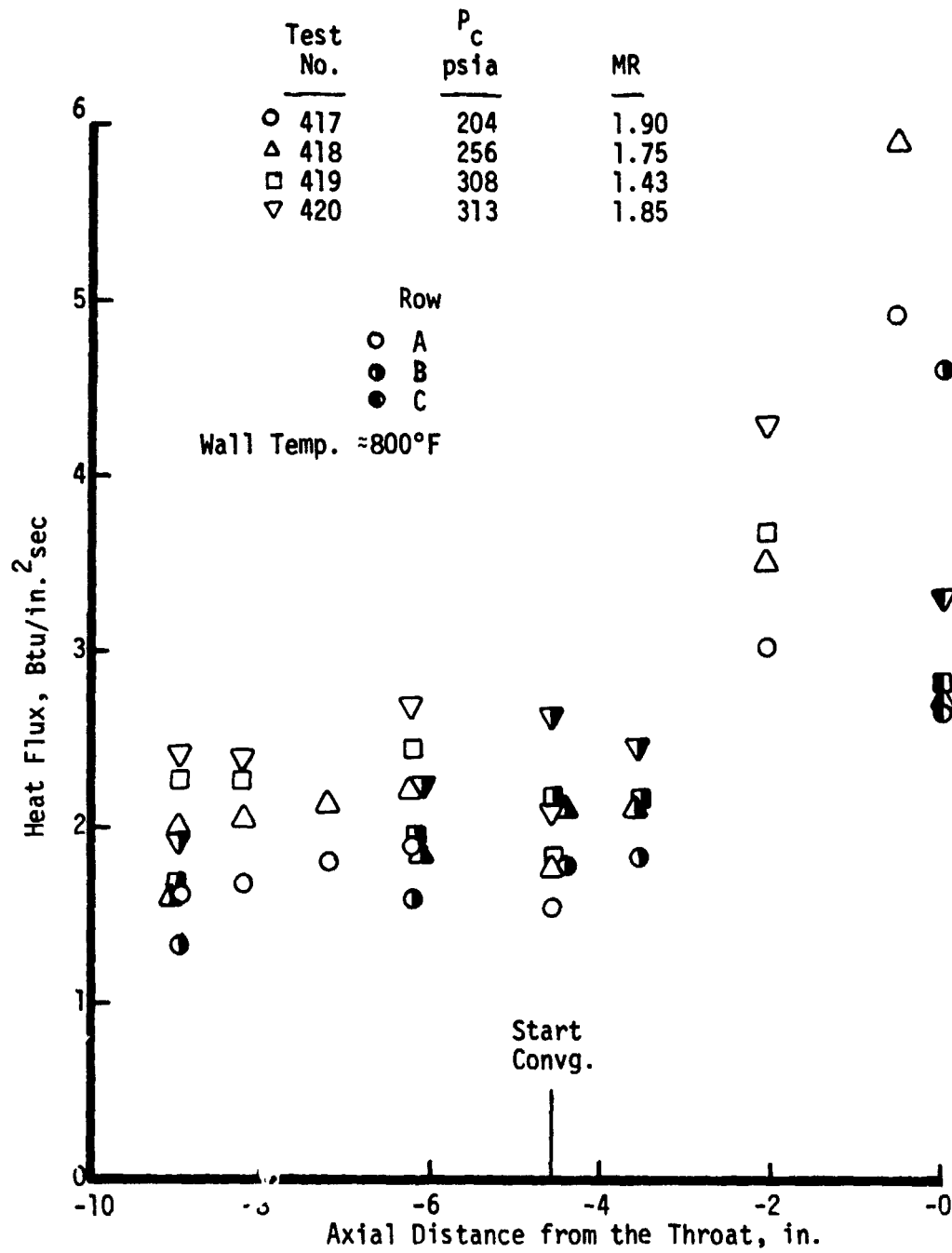


Figure 98. Heat Flux Data for the High Contraction Ratio Chamber

XI,B, Chamber Heat Fluxes (cont.)

the start of convergence. The C location at the throat indicates much lower fluxes than corresponding or adjacent A- and B-row data.

Test 418 approximates the total flow rate of previous tests at 125 psia chamber pressure, so that the cylindrical section experiences the same mass velocity as previous nominal tests. Comparison of these data shows that the high-pressure heat fluxes are slightly higher.

C. CHAMBER HEAT TRANSFER CORRELATING COEFFICIENT

1. XDT-1 and XDT-2 Injectors

Heat transfer correlation coefficients have been inferred from the heat flux data of Figures 90 and 91 using the following reactive models:

$$\phi = 0.026 C_g \rho_f u_e Re_f^{-0.2} Pr_f^{-0.6} (H_{aw} - H_w)$$

where ϕ is the heat flux, C_g the correlating coefficient, ρ the density, u_e the free stream velocity, Re the Reynolds Number, Pr the Prandtl Number, and H the enthalpy, with all film properties (subscript f) evaluated at 0.5 $(T_{aw} + T_w)$. All properties were evaluated at the overall mixture ratio; thus, the low mixture ratio region near the injector is represented by an artificial reduction in correlation coefficient. Figures 99 and 100 show the range of C_g results obtained. Initial results are those for the XDT injectors; unlike-doublet results are shown in the throat region. Since the heat sink testing was conducted with a conical nozzle, correlation coefficients inferred from the regenerative chamber wall temperature data are shown downstream of the throat; these results are consistent with the heat sink data in the throat region. The C_g reduction observed in the convergent section is typical and results from flow acceleration effects in the boundary layer. Figure 99 also shows the XDT-2 correlation coefficient curve which satisfactorily predicts regen chamber characteristics for nominal operating conditions. In the first part

$$\phi = 0.026 C_g \rho_f u_e Re_f^{-0.2} Pr_f^{-0.6} (H_{aw} - H_w)$$

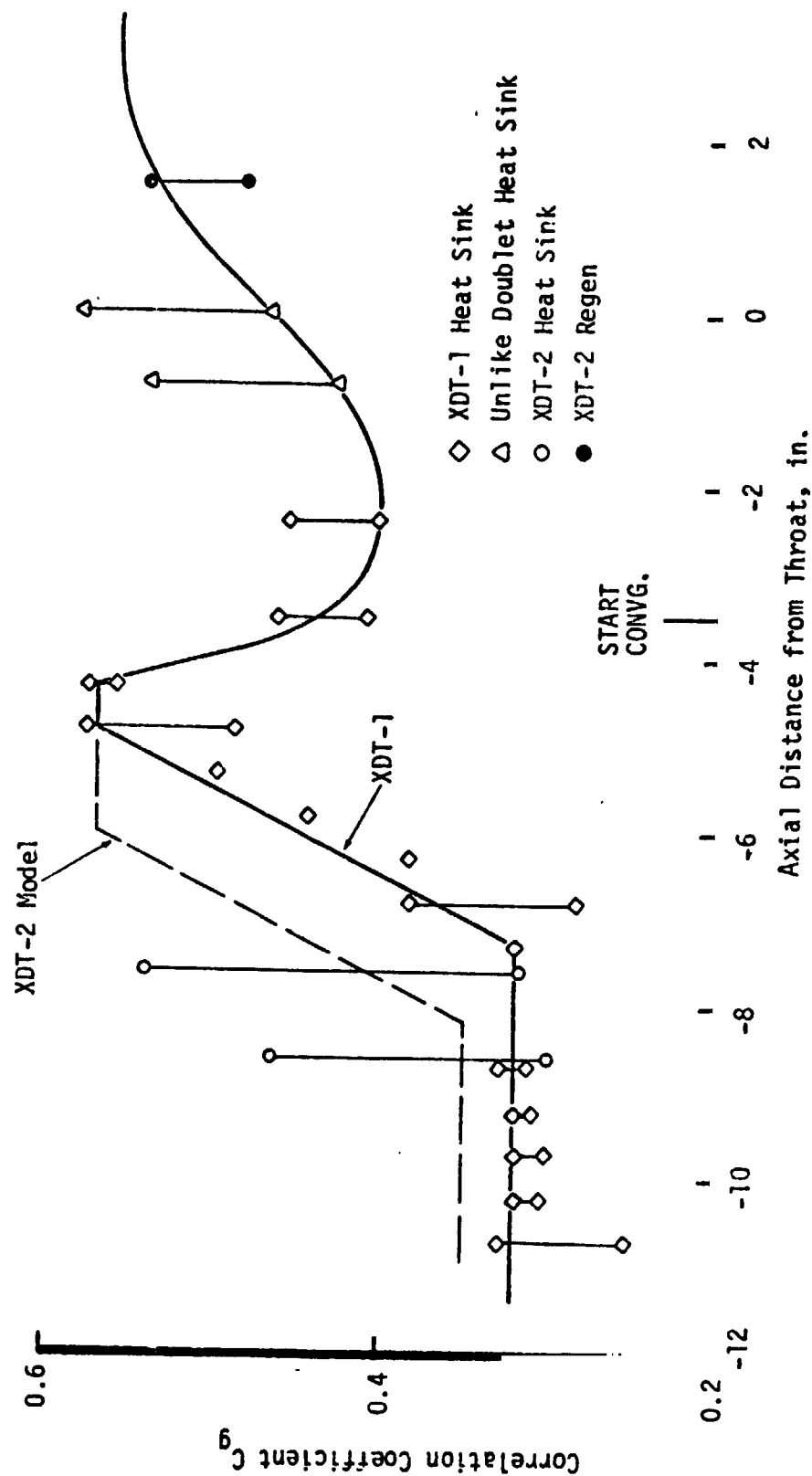


Figure 99. Heat Transfer Correlation Coefficients - Reactive

XI,C, Chamber Heat Transfer Correlating Coefficient (cont.)

of the cylindrical section this curve was developed from the shape of the XDT-1 data and circumferential integration of the XDT-2 data.

Figure 100 shows the correlation coefficients for the corresponding nonreactive model:

$$\phi = 0.026 C_g' \rho_f u_e Re_f^{-0.2} Pr_f^{-0.6} C_{p_f} (T_{aw} - T_w)$$

The tighter correlation of the data that results from the reactive model is apparent.

2. DXDT1-1 and DXDT1-2 Injectors

The correlating coefficient profiles for the demo injectors, as determined in regeneratively cooled chamber tests at WSTF, are shown in Figure 101.

D. MINI-SKIRT HEAT FLUXES

Heat fluxes were inferred from mini-skirt thermocouple responses on six ALRC tests, both with and without film cooling. Figure 102 shows these results for a wall temperature of 600°F as a function of axial position; an additional thermocouple location at the start of the flange was not utilized due to the uncertainties associated with predicting conduction into the flange region. A small reduction in heat flux due to film cooling is noted.

Heat transfer correlation coefficients have been determined from the nominal test with no film cooling using the nonreactive model with all film properties evaluated at $0.5 (T_{aw} + T_w)$. Use of this reference temperature provides good correlation of the effect of wall temperature on heat flux. This is especially important since the present skirt data must be extrapolated to considerably higher wall temperatures for design application. Figure 103

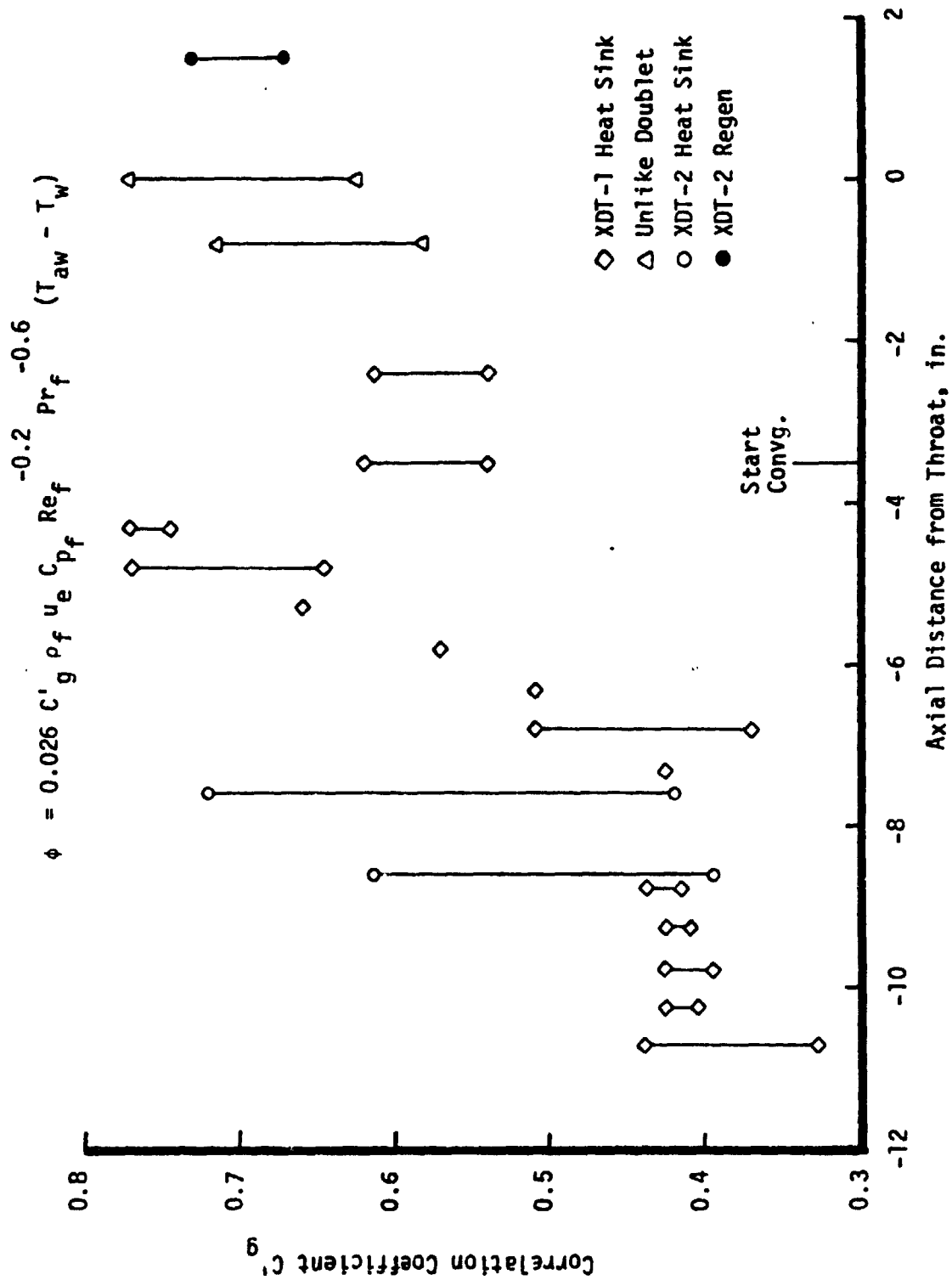


Figure 100. Heat Transfer Correlation Coefficients - Non-Reactive

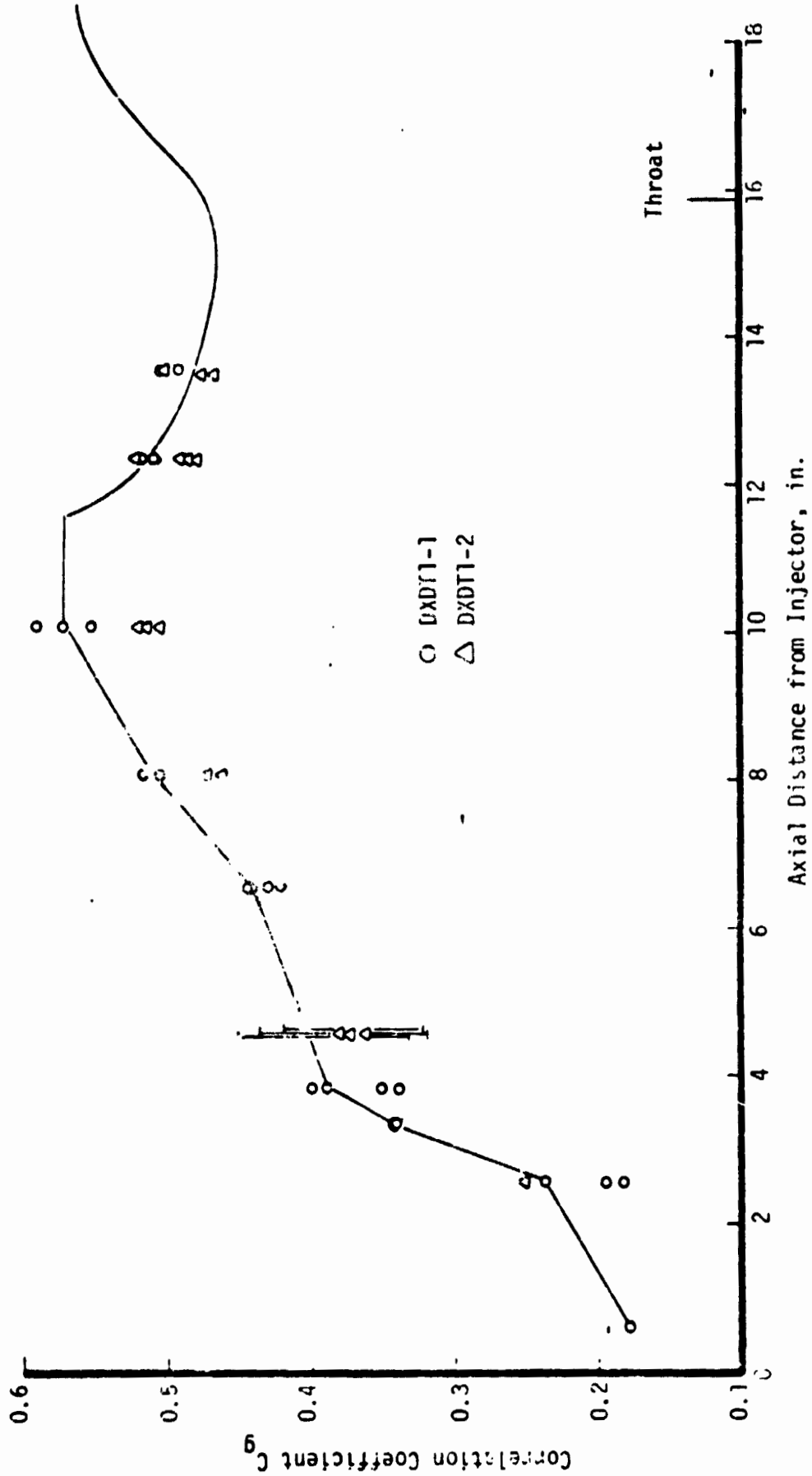


Figure 101. Gas-Side Heat Transfer Correlation, DXDT1 Injectors

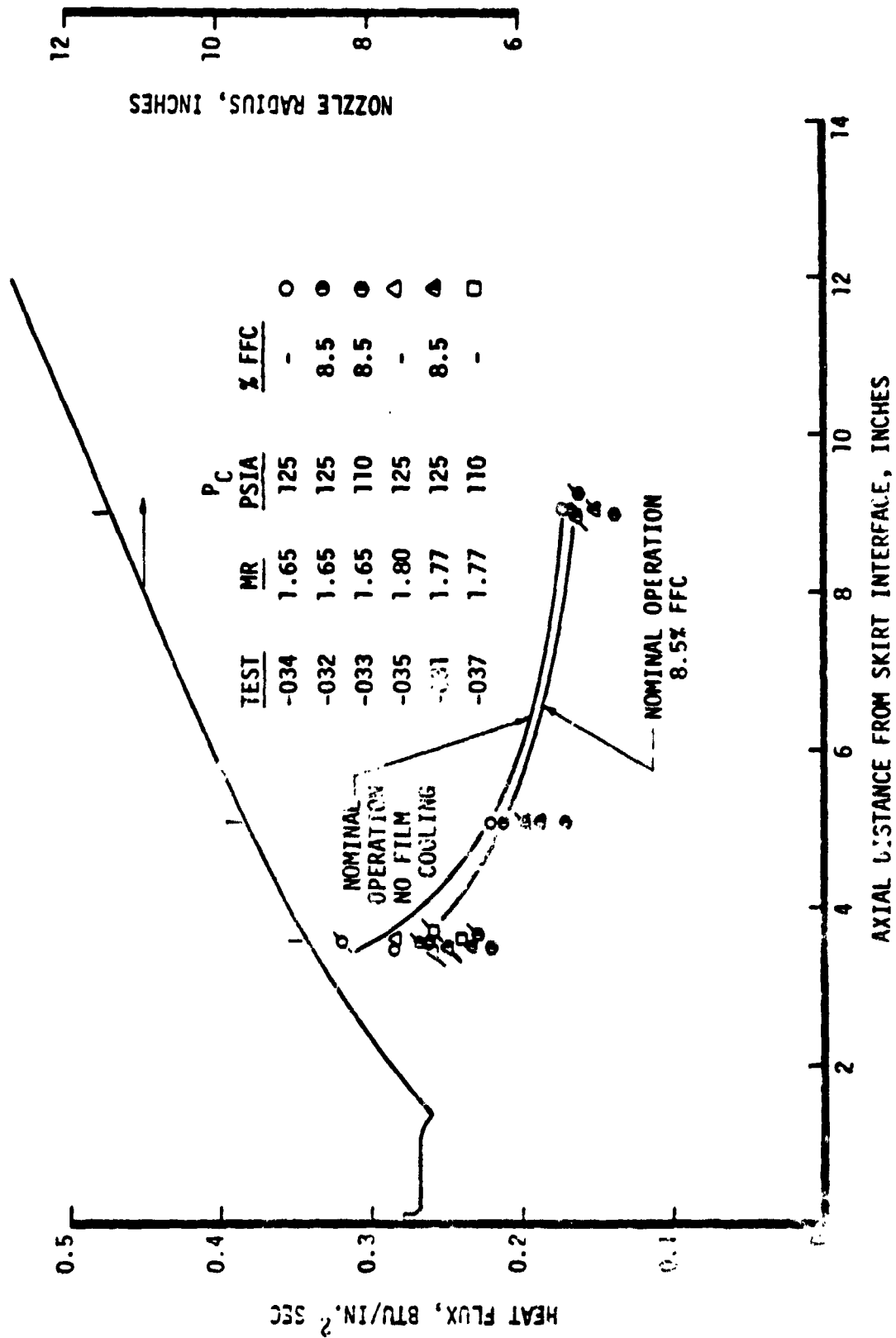


Figure 10. Mini-Skirt Heat Flux Data

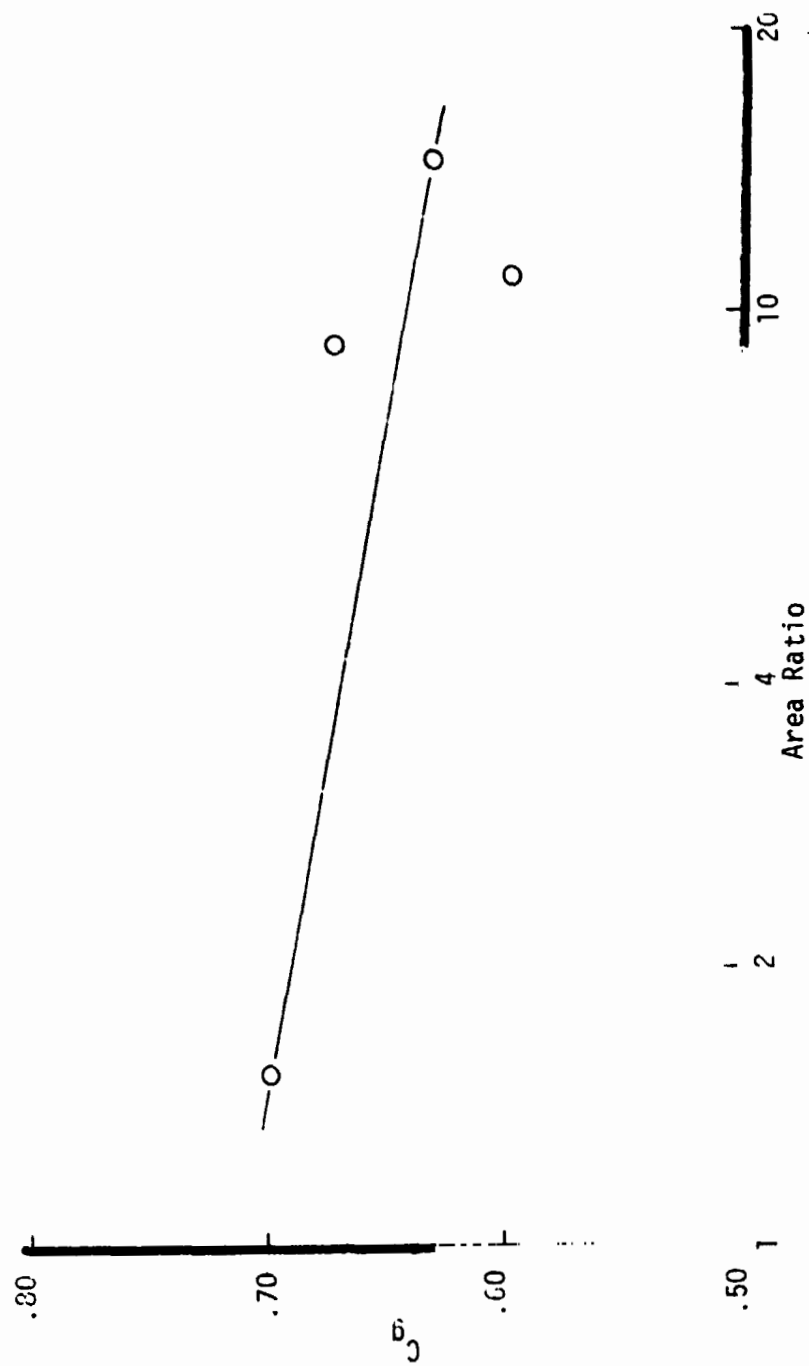


Figure 103. Non-Reactive Nozzle Heat Transfer Correlation Coefficients

XI, C, Chamber Heat Transfer Correlation Coefficient (cont.)

shows the resulting correlation coefficients as a function of area ratio and includes a point at area ratio 1.54 inferred from regen chamber wall temperature measurements. The latter point is consistent with the mini-skirt data; a slight reduction in C_g with increasing area ratio is observed.

E. CAVITY ENVIRONMENT

Cavity gas temperature values are not easily generalized, partly because of the wide variation of measured values with operating point and inlet condition, partly because of the large and rapid fluctuations that were experienced even within a single firing, and partly because of the unreliability of the indicated thermocouple responses. Nevertheless, the cavity gas temperatures measured with the XDT-1 pattern injectors were typically in the range of 800 to 1400°F, with numerous indications of fuel saturation temperature, i.e., 300 to 400°F, being evident. The XDT-2 pattern injectors typically produced much higher cavity temperatures, usually in the range of 1800 to 2200°F. No fuel saturation temperatures were experienced. No doubt the lower temperatures measured with the XDT-1 pattern are due to the orientation of the outer row of fuel elements, which causes the edge of the fuel fan to splash directly into the cavity.

More important from the standpoint of hardware design is the actual heat flux level. Based on gas-side thermocouple responses taken around the cavity, the corresponding heat fluxes have been inferred by means of a two-dimensional axially symmetric conduction model. Figure 104 shows the flux levels determined for the XDT-2 pattern, which produced the higher cavity gas temperatures, based on 1973 WSTF results. All fluxes indicated in the figures have the units of $\text{Btu/in}^2\text{sec}$. The flux on the side of the cavity partition, which is not shown, is estimated to be 0.07, half the value of the top surface of the partition.

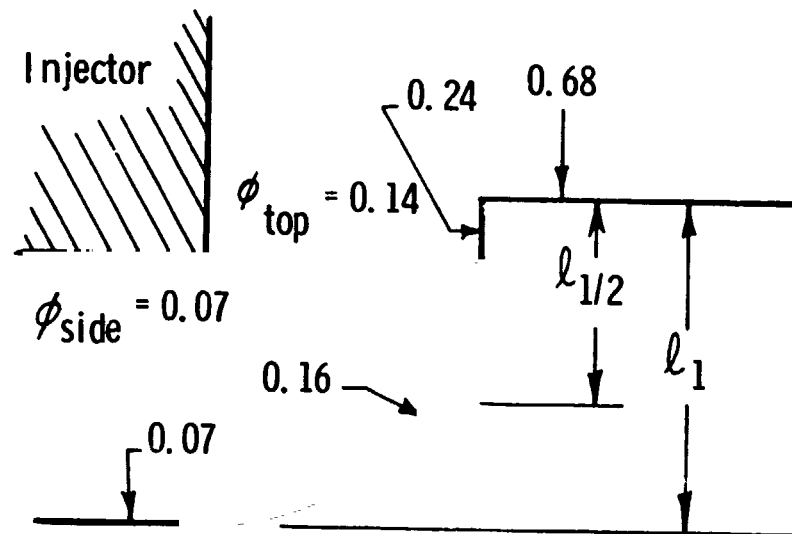


Figure 104. Cavity Heat Flux

XI, Full Scale Heat Transfer(cont.)

F. INJECTOR FACE ENVIRONMENT

Injector face temperatures were measured by as many as four thermocouples on various units tested. Typical face temperatures were running from 500 to 750°F, depending on exact location, propellant temperature and operating point. Figure 105 displays the maximum face temperatures measured with the XDT-1 injector as a function of mixture ratio.

A three-dimensional conduction model of a very local region of the injector face and ring manifold wall was created to allow some interpretation of these data, that is, to determine face flux levels. Typical calculated fluxes ranged from 1.5 to 2.0 Btu/in²sec. A reasonably good correlation of calculated flux versus mixture ratio and chamber pressure was achieved. This is shown in Figure 106.

G. BAFFLE HEAT TRANSFER

The mixed element-integral baffle injector had only a few test points that were not unstable; consequently, the amount of meaningful baffle heat transfer data is somewhat limited. The baffle had a significantly higher pressure drop for the oxidizer coolant than was predicted, 115 psid as compared to 48 psid. This was due to weld penetration in each of the baffle legs.

Valid heat transfer data were obtained in only three tests: two at nominal conditions, the other one at high P_c and low O/F. Steady-state baffle outlet temperatures were achieved in 1.3 sec, with a nominal bulk temperature rise of 12°F. The predicted rise was 18°F, indicating that the thermal environment was less severe than anticipated. Total heat pickup is given in Figure 107 for the three points. The average heat flux corresponding to these points is about 1.0 to 1.4 Btu/in²sec, based on the entire baffle area.

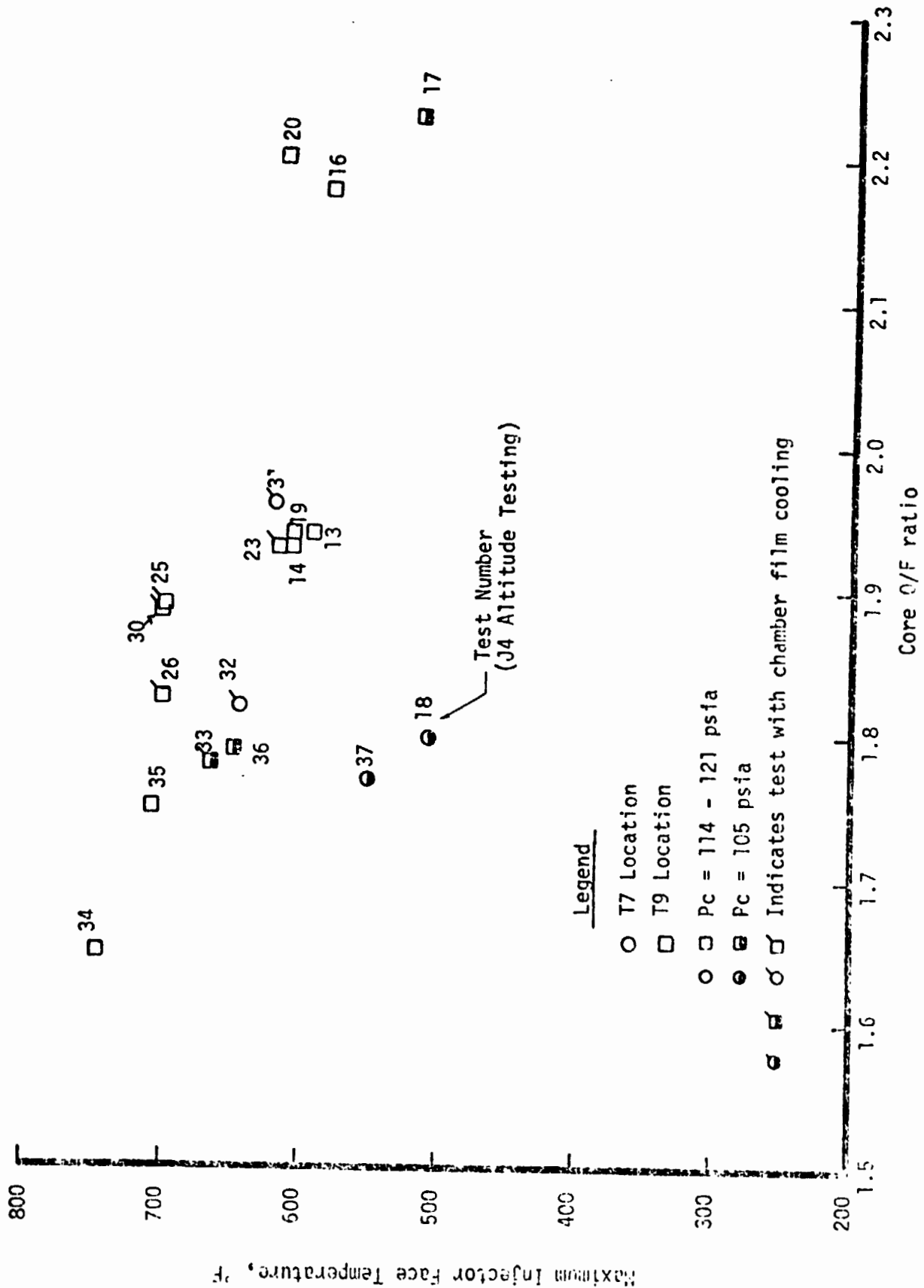


Figure 105. Maximum Face Temperature vs O/F Ratio

ϕ_{\max} = Maximum Heat Flux, Btu/in²-sec
 P_c = Chamber Pressure, psia

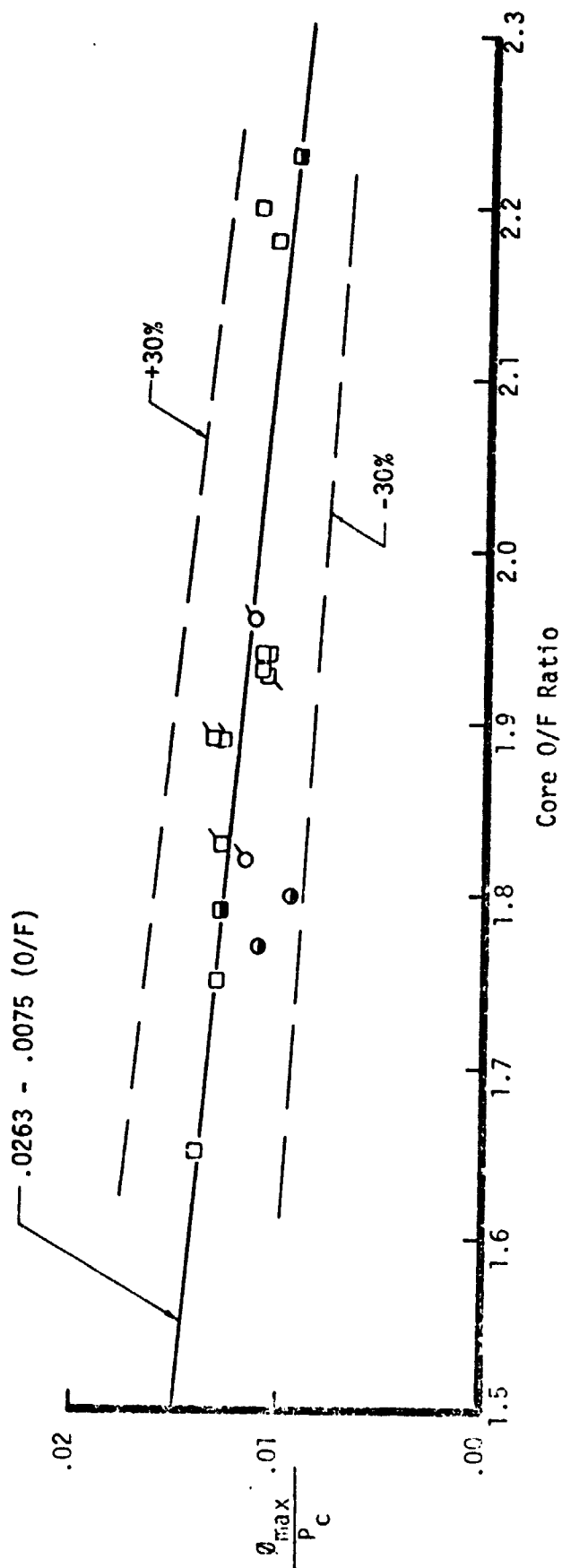


Figure 106. Injector Face Heat Flux Correlation

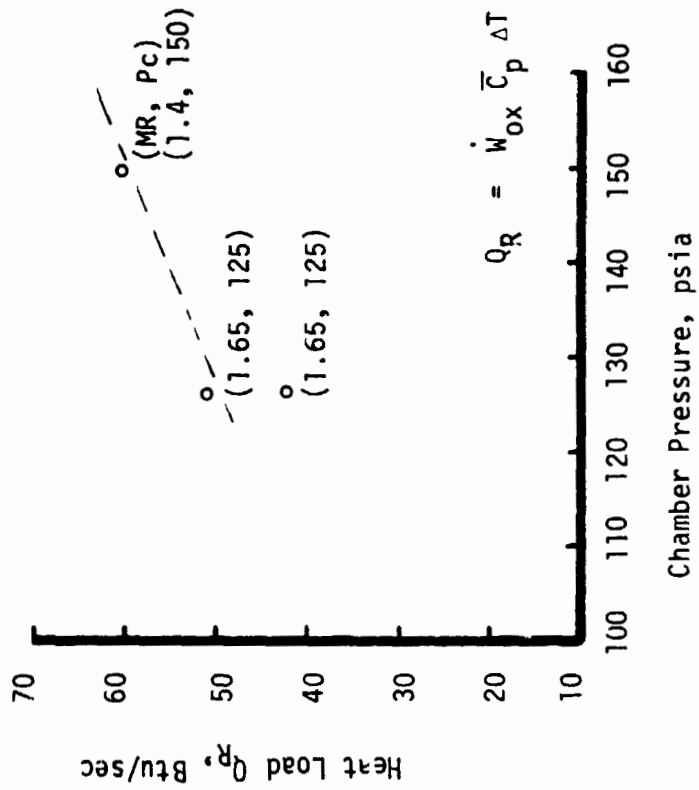


Figure 107. Total Baffle Heat Load, Integral Baffle Injector

ORIGINAL PAGE IS
OF POOR QUALITY

XII. FULL SCALE COMBUSTION STABILITY

XII. FULL SCALE COMBUSTION STABILITY

A. INTRODUCTION

A significant part of the program effort involved the evaluation of combustion stability characteristics of the full scale hardware. For the most part, this work focused on the X-doublet pattern injectors. Although the demo (DXDT1) injector configuration was entirely stable over the range of operating conditions tested, instabilities could be induced by seemingly minor changes in cavity configuration. Two basically different types of instabilities were typically encountered. The first of these, termed "resurging", was unique to the X-doublets; the second type encompassed the classical acoustic modes commonly experienced in rocket firings.

Resurging is characterized by periodic bursts of high frequency modes. The bulk of what follows addresses the resurging phenomenon.

The classical acoustic modes and their nominal frequencies for the full scale chamber are:

<u>Chamber Acoustic Mode</u>	<u>Frequency (Hz)</u>
First longitudinal (1-L)	1400
First tangential (1-T)	3100
Second tangential (2-T)	5200
First radial (1-R)	6500
Third tangential (3-T)	7100
Fourth tangential (4-T)	9000
First tangential and first radial (1-T + 1-R)	9100

The introduction of acoustic cavities into the chamber distorts these classical modes. This has been demonstrated for OMS-type hardware in acoustic tests conducted under Contracts NAS9-14232 and NAS9-12802. With the baseline acoustic cavity described in Section IX, the distorted or suppressed 1-T mode has a calculated frequency of 2600 Hz. This value was corroborated experimentally:

XII, A, Introduction (cont.)

the measured 1-T frequencies were generally in the range of 2600 Hz rather than 3100 Hz. Thus, in the following discussion, reference to the 1-T mode implies the distorted mode at 2600 Hz rather than the 3100 Hz undistorted mode. Discussion of the classical modes will be limited in what follows to the interaction thereof with the resurging-type instabilities.

Stability investigations were also made of mixed element patterns containing X-doublet and splash plate elements in both a baffled and an unbaffled configuration. The mixed element injector was bomb tested 17 times; eleven of these tests showed high frequency instabilities, predominantly the second tangential mode. The inclusion of a radial resonator tuned to the second tangential frequency stabilized the injector. The integral baffle mixed element injector was tested 12 times; the initial tests exhibited the expressed first tangential mode indicating the ineffectiveness of the three-bladed baffle. Additional damping for this mode was provided by returning the acoustic cavity; improved stability resulted for the majority of the remaining tests.

Also, considerable emphasis was placed in WSTF testing on chugging behavior at low pressure operation, and on the occurrence of short duration pops early in a firing. These subjects are fully described elsewhere¹ and will not be considered further. What follows then is primarily a description of the resurge phenomenon, what influences it, and what causes it.

B. HARDWARE DESCRIPTION

There were three basic injector patterns employed during the full scale testing portion of this program: the X-doublet pattern, the flat faced mixed element pattern, and the integrally baffled mixed element pattern. Detailed descriptions of these injectors are given in Section IX. The stability bomb tests were all conducted in heat sink chambers described in the same section. The instrumentation used during the stability tests normally consisted of low frequency pressure instrumentation in the combustion chamber and both the injector manifold

¹1974 WSTF Test Report, NAS 9-13133, April 1, 1975

XII, B, Hardware Description (cont.)

circuits and high frequency pressure transducers in the combustion chamber and one or more of the acoustic cavities. In addition, temperature measurements were made in the acoustic cavities using chromel-alumel thermocouple probes. The life of these probes was rather short and the probe could not be changed frequently; cavity temperature data were not obtained on all tests.

In general, the tests were conducted with ambient temperature oxidizer and heated fuel. The nominal fuel temperature when heated was 200°F.

C. X-DOUBLET INJECTORS

Ten different injector face assemblies were used in obtaining the X-doublet stability data. These injector face assemblies and the cores on which they were mounted are listed in Table XIV.

TABLE XIV

X-DOUBLET INJECTORS

<u>Core</u>	<u>Face Assembly</u>
Workhorse S/N 1 (Predam)*	XDT1
Workhorse S/N 1 (Postdam)*	XDT1-A XDT1-B XDT1-C
Workhorse S/N 2 (Predam)*	XDT2
Workhorse S/N 2 (Postdam)*	XDT2-A LDP XDT
Demonstration S/N 1	DXDT1-1
Demonstration S/N 2	DXDT2-2 DXDT2-1

*"Predam" is without face ring dams installed, "postdam" is following installation of face ring dams.

D. X-DOUBLET TESTING

The stability testing on the X-doublet injectors can be divided into three phases, each phase having its own objectives. These are summarized below.

XII,D, X-Doublet Testing (cont.)

1. Phase I - Elimination of Resurging Instability

Resurging instability was initially encountered in the first full scale test series conducted at the ALRC J-4 facility. The XDT1 injector was used in these tests. Subsequent testing -- at J-4, WSTF, and the ALRC A-5 facility -- were directed toward eliminating the resurge. This was accomplished by the installation of the face ring dams.

2. Phase II - Evaluation of Cavity Entrance Geometry Effects

X-doublet injector stability was observed to be quite sensitive to the acoustic cavity inlet geometry. The relative stability of various cavity inlet configurations was evaluated over Tests 173 through 369, although other types of tests were also conducted during this period. The XDT1-B, XDT1-C, and DXDT1-1 injectors were used for this testing, which established the stability of the baseline configuration and the sensitivity of this configuration to various geometric changes.

3. Phase III - Stability Margin Testing

The intent of this phase was to determine the stability design margin of the baseline cavity in terms of cavity area and tune. This was accomplished by systematically reducing the cavity area, by increasing the rib thickness, and varying the tune to determine the minimum area configuration. Stability margin testing was conducted in Tests 376 to 423. The XDT1-C injector was utilized. In these tests, the baseline cavity was determined to have an 80% design margin in terms of cavity area, i.e., the baseline cavities have an entrance area approximately 80% greater than the minimum required for stable operation.

E. DESCRIPTION OF RESURGING

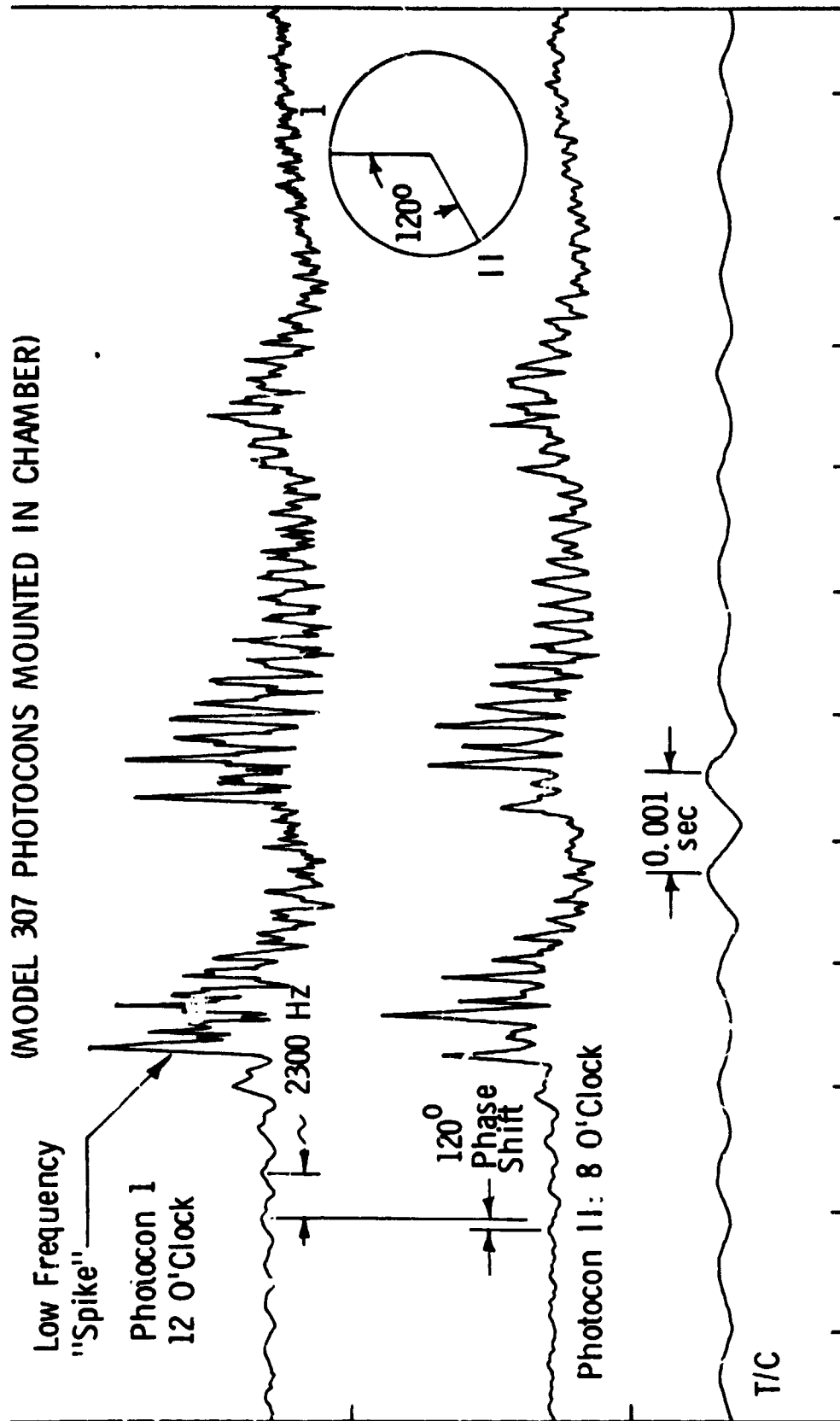
Resurging is illustrated by the high frequency oscillograph trace

XII,E, Description of Resurging (cont.)

reproduced in Figure 108. It is seen to consist of periodic bursts of high frequency instability and gives the appearance of being a combination of a low frequency chug, about 400 Hz, and one or more high frequency modes with frequencies ranging from 2000 Hz to 7000 Hz. Resurging has occurred both spontaneously and as a result of stability bombs; the number of resurges has varied from a single event to continuous resurging which lasts until engine shutdown.

A detailed examination of a number of both spontaneous and bomb-induced resurges showed that they have a common, readily identifiable characteristic. This is that the resurge can be broken into three phases, as shown in Figure 109. Each resurge starts, in the first phase, with a spinning 1-T mode which rapidly increases in amplitude and undergoes a slight increase in frequency. As a high amplitude wave, this spinning 1-T mode will only make a single revolution of the chamber. It then decays to much smaller amplitude. During the period of rapid 1-T growth, the mean chamber pressure rises, indicating the rate of gas generation within the chamber exceeds the steady state value and some burn-off of accumulated propellant is occurring. The high amplitude wave is a detonation wave which atomizes and consumes essentially all the unburned propellant in the chamber. It subsides due to a lack of propellant available to fuel it. If the resurging is spontaneous, the time required for the spinning 1-T mode to build up from zero amplitude is 0.003 to 0.004 seconds. However, once resurging is established, each new resurge grows out of the noise level existing in the chamber from the previous resurge. In this case, the time for the 1-T buildup to occur is on the order of 0.0004 sec.

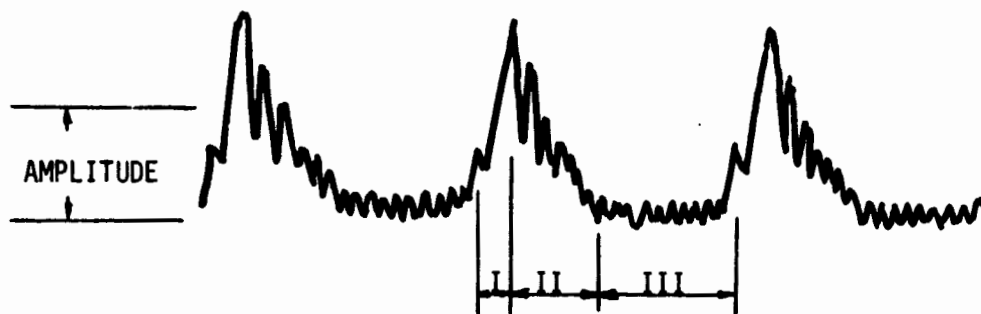
The second phase of resurging begins after the spinning 1-T wave has peaked in amplitude. This second phase is characterized by a decay in chamber pressure to less than the steady-state value. During the decay, a number of lower amplitude, high frequency modes are present in the chamber with the 1-T, 2-T, 3-T and 1-R modes all having been noted during this phase. Apparently, the



COMMENTS:

1. "Spikes" always result from divergent 2300 Hz wave going non-linear not SPS type "pops"
2. Phase relationship shows divergent wave is a "spinning" mode.

Figure 108. Mixed Mode Characteristics



- I BURNOFF
- II BLOWDOWN
- III ACCUMULATION

Figure 109. Three Phases of Resurge Instability

h-4

XII,E, Description of Resurging (cont.)

rate of combustion drops off considerably during this phase because of the previous consumption of propellant by the detonation wave in addition to the reduction of propellant injection during the high pressure period. The chamber pressure decay reflects the fact more gas is leaving the chamber than is being generated. This second phase of resurging lasts about 0.0006 to 0.0008 seconds.

The third phase consists of a leveling-off and slow rise in the chamber pressure. There can still be a significant amount of high frequency ringing or noise in the chamber during this time. The chamber pressure rise indicates the combustion rate or gas generation rate has returned to essentially its steady-state value and any gross disturbances of the injection flow rate have apparently died out. This reestablishment of the near-steady-state condition is seemingly the requirement for the next resurge. The duration of this third phase is not sharply defined but ranges between 0.0010 to 0.0015 seconds.

As noted previously, resurging frequently stops by itself and stable steady-state combustion resumes. A careful review of test records was made to see to what differences, if any, exist between the final resurge and preceding resurges, to determine what causes the resurging to cease. In no case was it possible to distinguish between the final resurge and its predecessors. The conclusion reached was that the trigger for each resurge lies hidden in the high frequency noise resulting from the previous resurge. Although in the spontaneously unstable tests the trigger for the first resurge has been clearly identified as a spinning 1-T mode, this is not necessarily the case for subsequent resurges. There may not be a single triggering event which can be identified as causing all resurges. The test data have indicated that certain cavity configurations and operating conditions are more susceptible to resurging than others. This implies some tests require larger resurging triggers than others and possibly even a different mechanism. For those instances in which the resurging just stops by itself, it can only be assumed that the chamber noise produced by the previous resurge did not contain the proper combination of frequency, amplitude, and phase relationship to trigger the next resurge.

XII, Full Scale Combustion Stability (cont.)

F.. FACTORS INFLUENCING RESURGING

A number of factors were experimentally investigated to determine their influence on resurging characteristics. Some of these were found to be of considerable impact while others had negligible effect. The more significant of these are discussed below.

1. Acoustic Communication within the Face Ring Manifolds

The two initial full scale X-doublet injectors (XDT1 and XDT2) were fabricated with the face ring manifold grooves completely unobstructed circumferentially, as shown in Figure 110. They were used in this configuration in Tests 1 through 38 in the ALRC J-4 testing, in Tests I-I-1, 5, 6, 7, and 8 at WSTF, and Tests 101 through 123 in the ALRC A-5 testing. Approximately half of these tests exhibited resurging instability. Following Test 123, the face was machined off the XDT2 injector and dams were installed at the three null points in each of the outer twelve face rings. A new face was bonded to the injector body and the unit was designated as XDT2-A. It was retested (Tests 124 through 138) and found to be stable under operating conditions which had previously been unstable. All subsequent injectors incorporated the face ring dams. The installation of the dams had a more pronounced effect on resurging instability than any other single factor.

2. Fuel Temperature

It was determined very early in testing that high fuel temperatures had a destabilizing effect on the X-doublet injectors. This was noted on units both with and without face ring dams. During Tests 101 through 123 with injector XDT2, a number of configurations which were bomb-stable with ambient or warm fuel (70° to 120°F) were unstable with hot (180° to 220°F) fuel. This fuel temperature sensitivity is probably also the reason the first tests at

ORIGINAL PAGE IS
OF POOR QUALITY

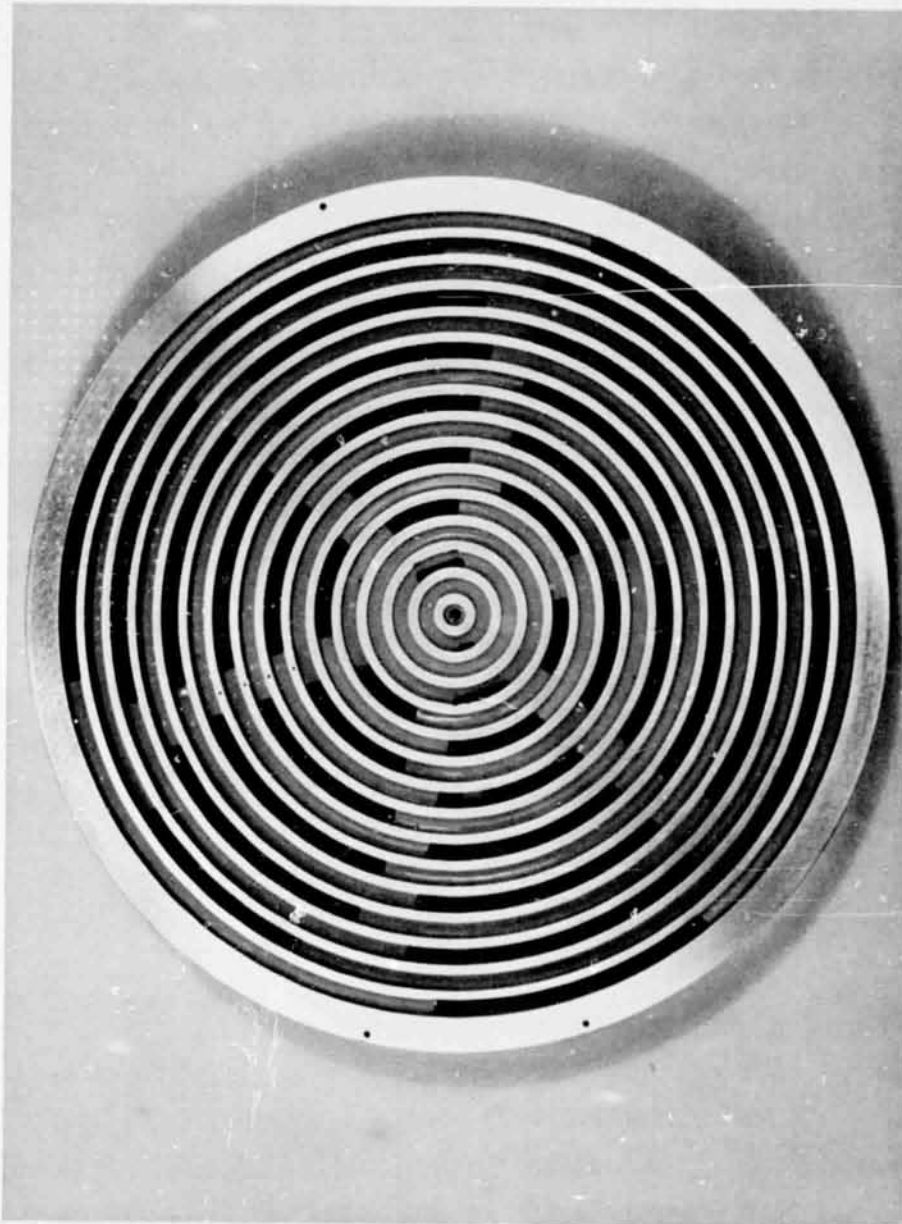


Figure 110. Injector Core

XII,F, Factors Influencing Resurging (cont.)

WSTF with the XDT1 injector and no ring dams were stable initially and then went unstable in resurging. The stable operation occurred while cool fuel flowed into the injector. After the regenerative chamber and the fuel reached steady-state conditions, the resurging began.

3. Acoustic Cavity Area

One of the more significant influences on resurging instability was acoustic cavity area. In general, the instability would change from resurging to pure high frequency modes as high frequency damping, i.e., cavity area, was reduced. This was demonstrated twice. First, on Tests 289 and 290, the XDT1-C injector was run with the acoustic cavities completely blocked off. In both tests the injector was bombed unstable in what appeared to be the 2T mode (5200 Hz), with the 1R mode also present (6500 Hz). There was no resurging. Second, in the cavity margin testing, which employed the same injector, the cavity area and tune were altered to determine the minimum area required for stable operation. With decreasing area, the injector showed more of the acoustic mode instabilities and less resurging (Tests 383 through 414). The 1-T mode was the predominant one encountered in these tests.

4. Injector Pressure Drop

During the program, injectors with several different pressure drops were tested. These ranged from DXDT2-1 with 23 psid on the oxidizer side and 37 psid on the fuel side, to XDT1 which when partially obstructed by wax in the fuel circuit had pressure drops of 50 psid on the oxidizer circuit and 81 psid on the fuel circuit (Test 34, ALRC J-4 testing). In addition, inlet orifices were installed on the XDT2 injector to provide an additional 65 psid drop in each circuit; these were used in the first 23 tests. Earlier, 50 psid orifices were installed in both circuits of the XDT1 injector following its resurging instability in Test I-I-5 at WSTF. None of the above increases in pressure drop had any significant effect on resurging instability. The resurges prior to

XII,F, Factors Influencing Resurging (cont.)

and after the insertion of the added pressure drop were very similar. It was recognized that the additional pressure drop, to have its maximum effectiveness, would have to be located at a velocity antinode and that this could be done by placing the pressure drop as close to the injector face as possible. An attempt was made to achieve a high pressure drop close to the face in the fuel circuit of the XDT2 injector following Test 109. This was done by inserting a ring in the fuel circuit torus as shown in Figure 111. This ring partially obstructed the 1/4 in. holes coming from the outer fuel torus and introduced an additional 35 psid pressure drop at that point. This ring also contained three null point dams which prevented communication from one fuel pie to another via the small torus downstream. In this configuration there was no change in resurge behavior from what had been demonstrated previously.

5. Feed System Acoustics

When resurging was first encountered, the low frequency (400 Hz) portion of the instability was thought to be the result of feed system coupling with the combustion process. In an effort to uncouple the feed system, a liquid accumulator or "can" was installed in both the fuel line and the oxidizer line. This was done during testing of XDT2 at ALRC. The fuel can was installed prior to Test 110 and the oxidizer can prior to Test 121. The effect which these cans had on isolating the feed lines is shown in Figure 112, which shows the low frequency trace of the feed line pressures prior to and after installation of the cans. It can be seen that although both feed circuits upstream of the cans were effectively uncoupled from the combustion chamber, the resurging continued virtually unchanged. This indicated that the feed system was simply responding to the pressure oscillations in the combustion chamber rather than being a contributing element in a feedback loop.

6. Cavity Entrance Geometry

The acoustic cavity geometry was altered considerably in the

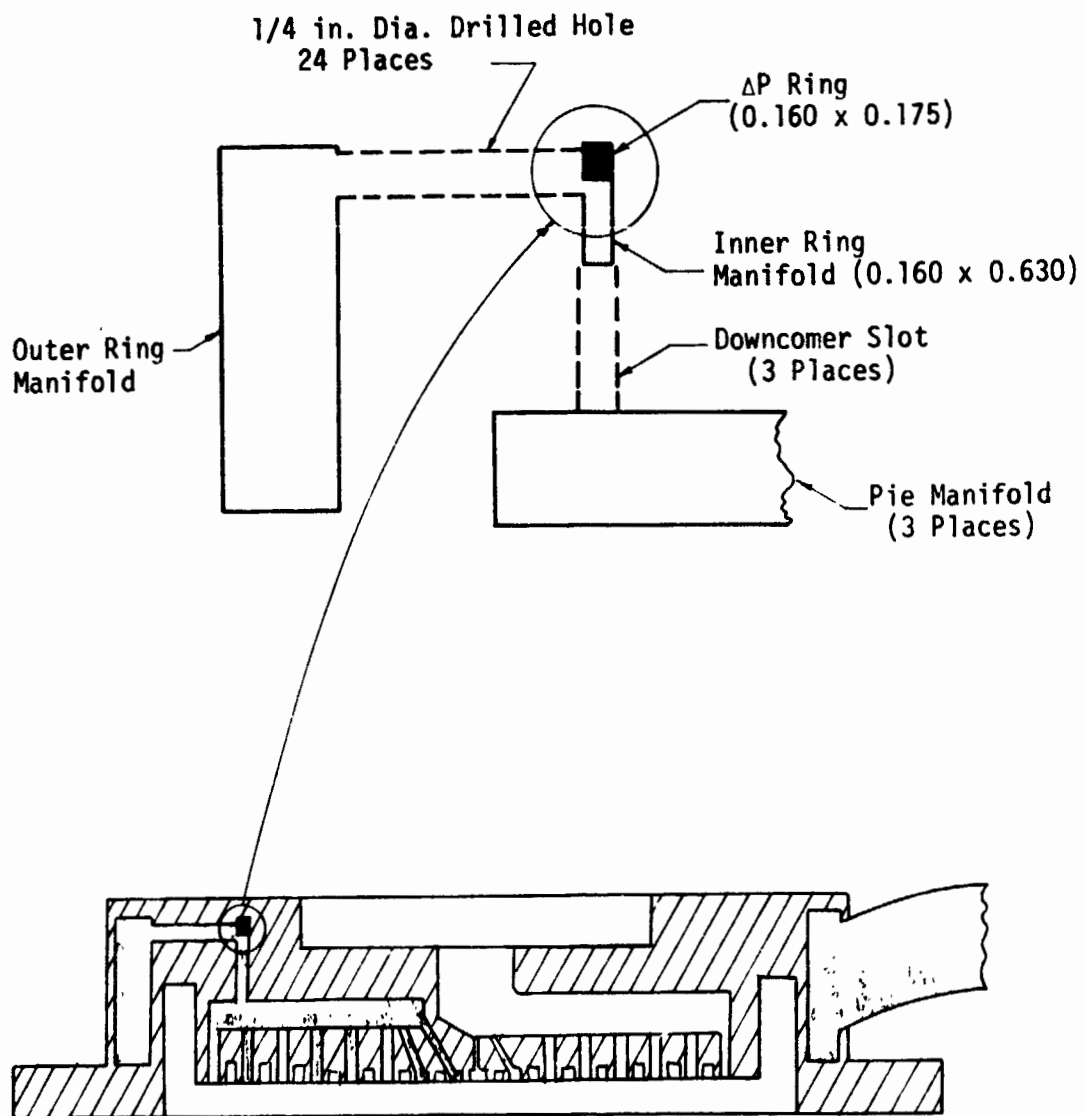
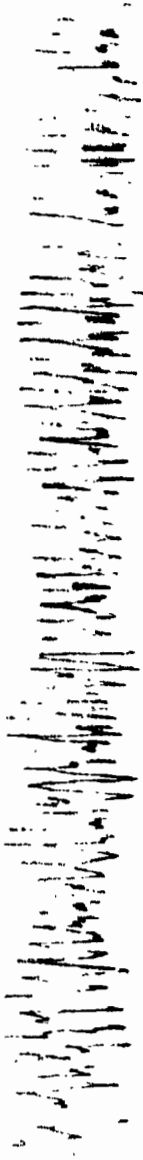


Figure 111. Fuel Circuit Pressure Drop Ring

ORIGINAL PAGE 14
OF POOR QUALITY

BEFORE INSTALLATION
OF CAN



AFTER INSTALLATION
OF CAN

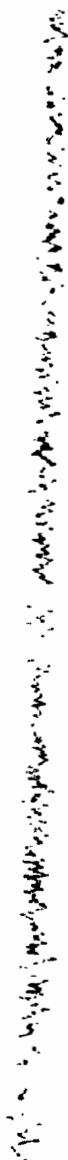


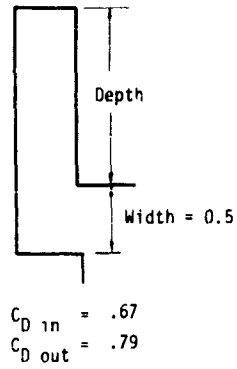
Figure 112. Fuel Circuit Pressure Responses During Instability

XII,F, Factors Influencing Resurging (cont.)

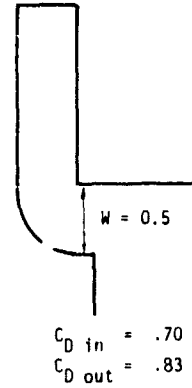
course of the test program. Early in the testing, Tests 158 - 167, a rectangular workhorse or baseline cavity configuration was demonstrated to be stable. This configuration is shown in Figure 113. Following this testing, the fully contoured configuration, also shown in Figure 113, was found to be unstable. This sensitivity to inlet configuration precipitated the evaluation of a variety of configurations as described in Section IX. The results, which are summarized in Figure 114, indicated that combustion stability is strongly influenced by the cavity lip geometry and by overlap. Overlap, as illustrated in Figure 115, is the distance the downstream edge of the cavity projects inward beyond the outer diameter of the injector core.

Two series of tests were conducted to evaluate the effect of overlap on stability (Tests 306 - 336 and 350 - 368). The results of these tests are summarized in Figure 115. With both injectors tested, it was found that increased overlap improved combustion stability. The effect of cavity entrance geometry on stability, which was summarized in Figure 114, is consistent with these results: namely, the inlet configuration which placed the downstream edge of the cavity close to the injector face was more stable than those configurations which did not. The fully contoured entrance was unstable while those with the sharp-edged entrances were stable. The radiused edge cavities produced greater stability than the fully contoured entrances but less stability than the sharp-edged cavities. One test series (Tests 351 - 369) was conducted to determine whether it was the sharp edge of the cavity or the overlap which was stabilizing. In this series the overlap was increased from the nominal 0.125 in. to 0.25 in. at the same time a 0.125 in. radius was placed on the edge, as shown in Figure 116. These tests served to determine whether the destabilizing effect of a radiused cavity entrance was caused by increased entrance flow coefficient or decreased effective overlap. By placing the radius on the high overlap lip, the combination of high flow coefficient and high overlap could be tested. This was found to be a basically stable configuration, thereby indicating that the stability was the result of overlap and not the result of low flow coefficient from the sharp-edged lip.

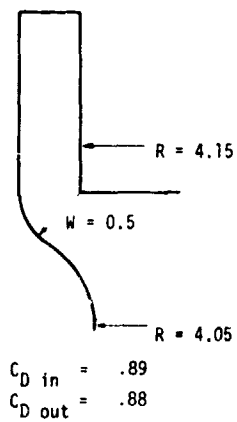
Baseline



Partial Contour



Contoured



Restricted Inlet Contour

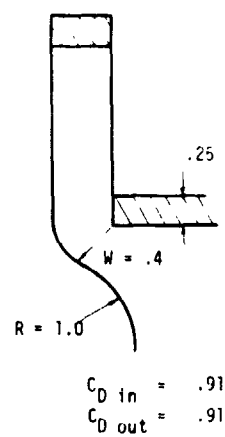


Figure 113. Resonator Inlet Configurations

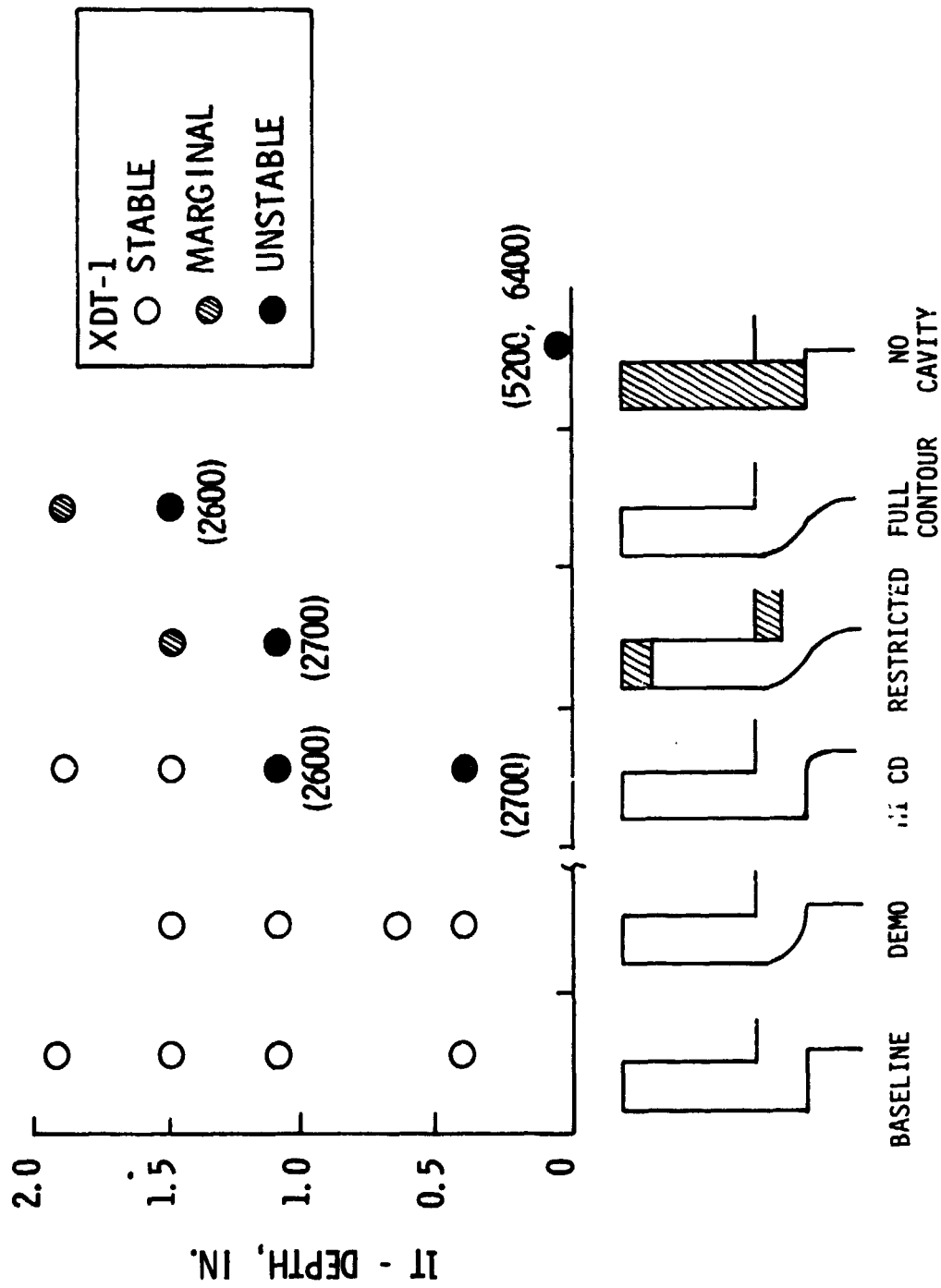


Figure 114. Cavity Inlet Effect

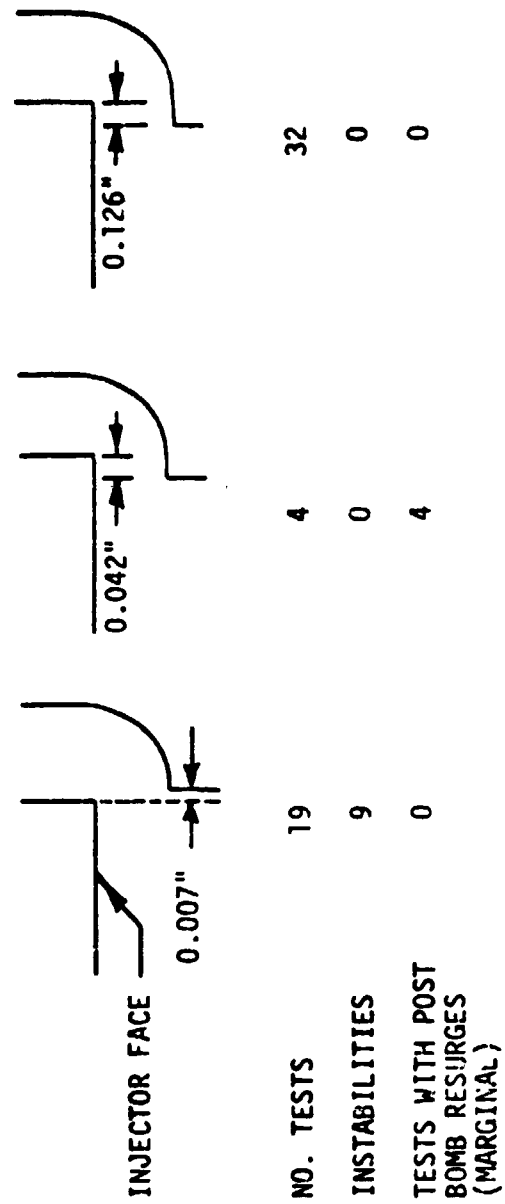


Figure 115. Cavity Overlap Results

OME PLATELET INJECTOR PROGRAM

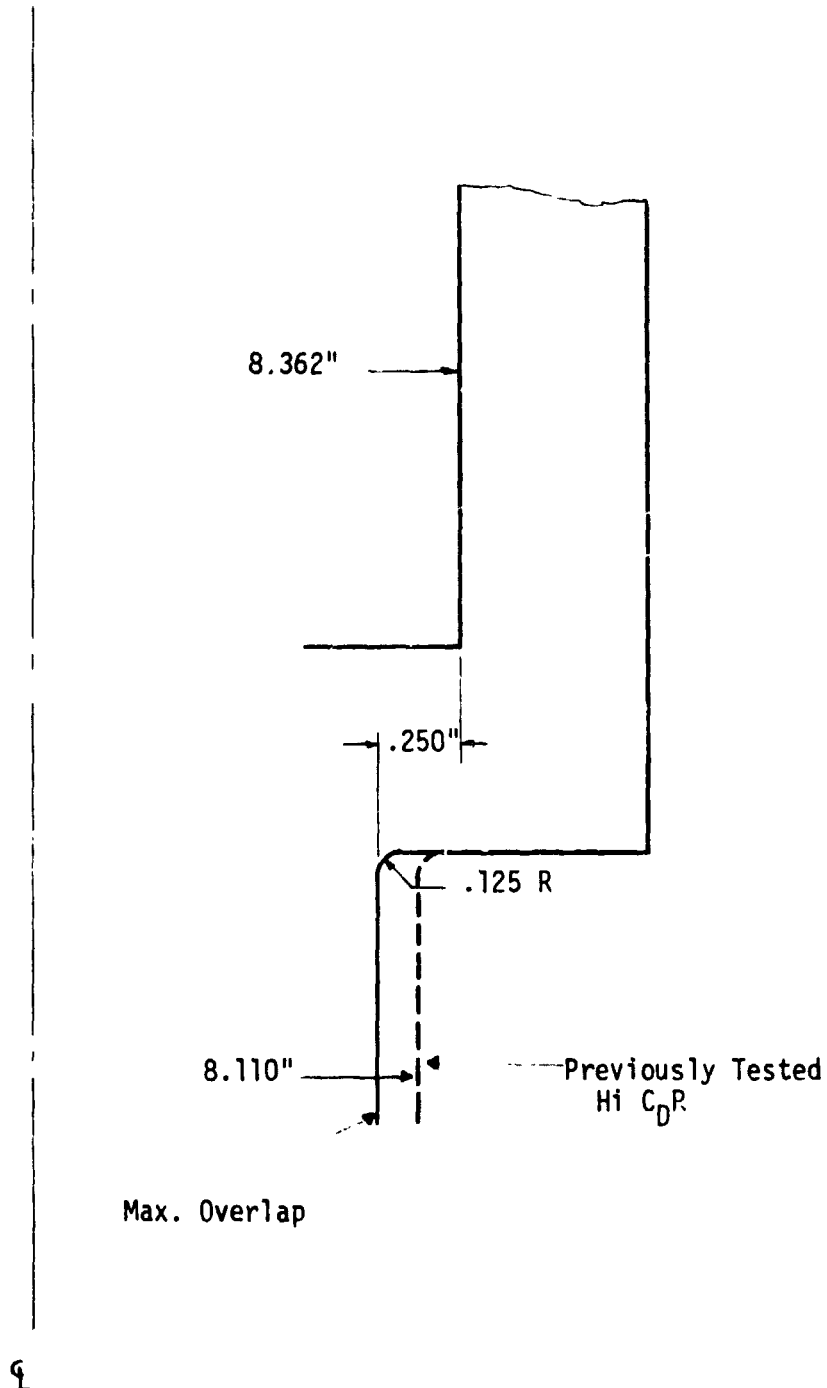


Figure 116 Maximum Overlap - High C_D Resonator Inlet Configuration.

Report 13133-F-1

XII,F, Factors Influencing Resurging (cont.)

Extensive variations in cavity depth were made during two test series. While testing the various inlet geometries, it was standard test procedure to alter the cavity depth over a relatively wide range, in order to rate the stability of the various inlet geometries. Those inlet geometries which would not show resurging with the widest range of l-T tuning were considered more stable than those which could only tolerate a small depth change. The results of this testing were given in Figure 114. In these tests, the l-T cavity depth was varied from 0.4 inches to 1.9 inches, giving an acoustic range of 1.0 inches to 2.5 inches. If the nominal l-T cavity tune is taken as approximately 3000 Hz, this depth variation represents a range of l-T cavity tuning of from 2500 to 6300 Hz. These tests showed quite clearly that resurging instability was definitely effected by cavity tune and that deep cavities were required to eliminate resurging with a poor entrance geometry. With the baseline entrance, however, the resurging instability was absent over the entire range of cavity tunes tested.

The second test series in which cavity depth was varied was the stability margin series. As noted earlier, these tests were intended to establish the minimum cavity area required to stabilize the injector. The approach employed was to systematically reduce the cavity area and vary the cavity tune at each reduced area until the stable range of cavity tune at each area could be established. The results of these tests are presented in Figure 117. These tests showed that at the minimum area the optimum l-T depth was 1.1 inches, which is considerably removed from the 1.5 to 1.9 inch depth which was apparently optimum at the full (18%) l-T area. Also, as the cavity area and tune decreased, the character of the instabilities began to change with more l-T and less resurging becoming evident. An oscillograph trace illustrating this is given in Figure 118. As noted previously, it appeared possible to go from a resurge instability to a pure acoustic mode instability at will, simply by reducing the amount of acoustic mode damping present in the chamber.

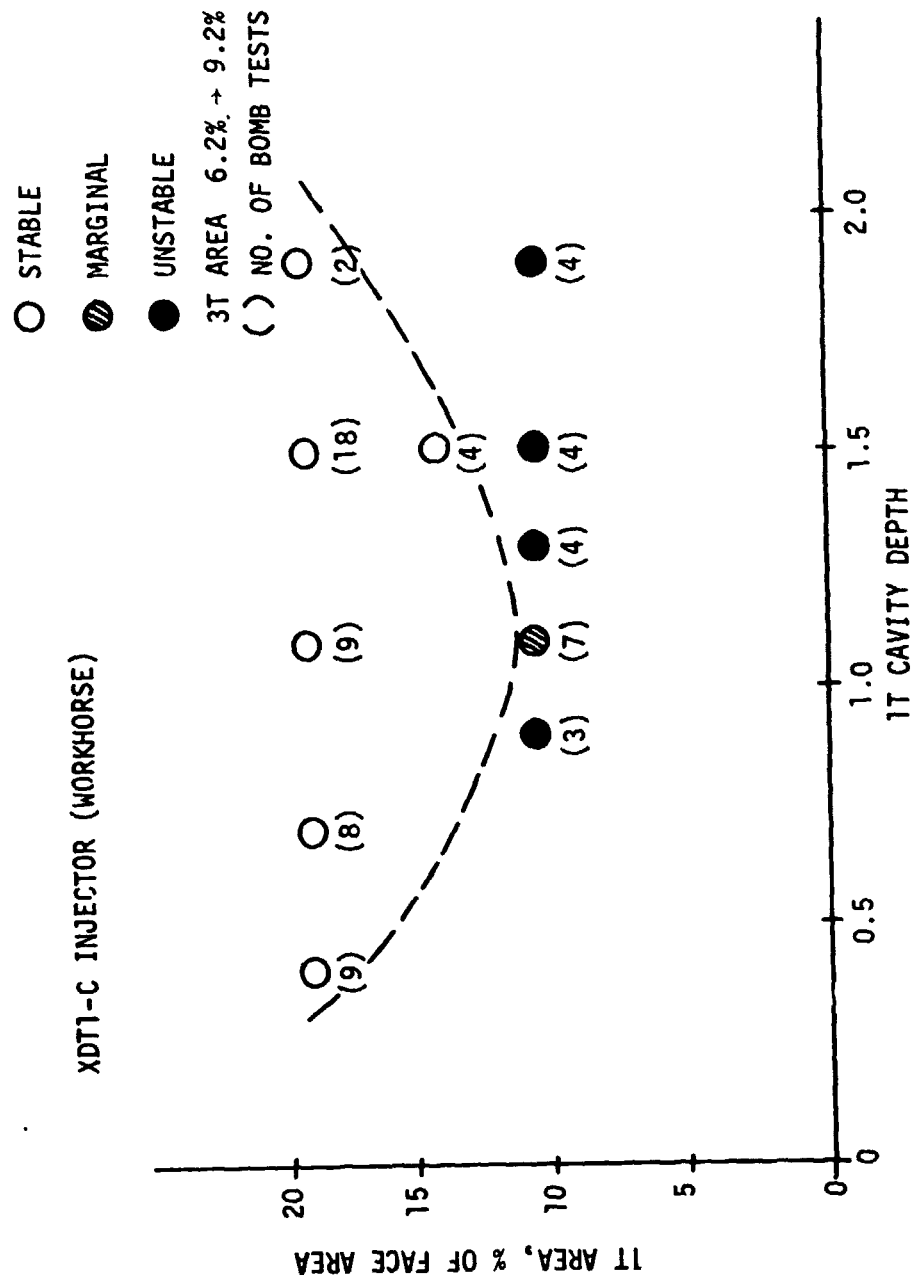


Figure 117. Stability Margin Testing

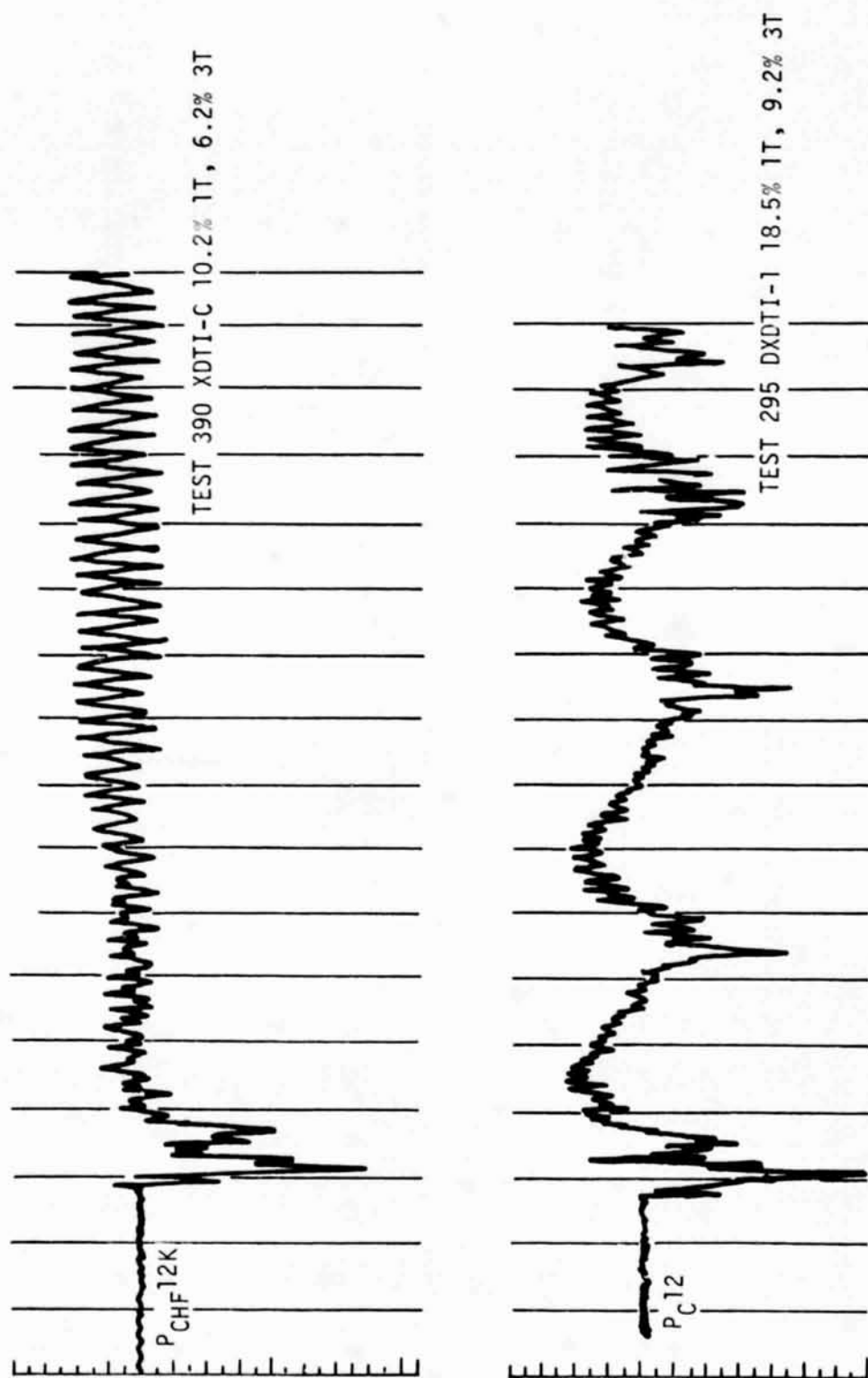


Figure 118. Effect of Cavity Area on Wave Form

XII,F, Factors Influencing Resurging (cont.)

One other cavity configuration, the partial contour also shown on Figure 113, was evaluated. The back corner of this configuration was radiused, although the inlet had a sharp, rectangular corner. This is essentially the flight hardware configuration as is necessitated by wall cooling and fabrication considerations. There was no observable difference in the operating characteristics with this configuration.

7. Cavity Tune

The tune frequency of the acoustic cavities is dependent upon the acoustic or effective length of the cavities, and the temperature and molecular weight of the gas in the cavity. Of these three factors, only the cavity depth can be accurately controlled. The sensitivity of cavity operation or injector stability to shifts in the cavity tune is of considerable importance. For this reason, a significant number of tests were conducted in which cavity depth was varied and cavity temperatures were measured. No attempts were made to sample the cavity gas to determine its molecular weight, however.

a. Cavity Depth

The baseline cavity depths (measured from the injector face) were 1.5 inches for the 1-T cavities and 0.4 inches for the 3-T cavities. The cavity entrance added an effective length of approximately 0.6 inches to each of these cavities, giving acoustic lengths of approximately 1.0 and 2.1 inches for the 3-T and 1-T cavities, respectively. The effective entrance length was established in acoustic tests conducted under Contract NAS 9-14232. The cavity depths were varied by adding or removing filler blocks in the individual cavities.

XII, F, Factors Influencing Resurging (cont.)

b. Cavity Temperature

Cavity temperatures were measured in a number of tests by inserting chromel-alumel thermocouple probes into the acoustic cavity. In most instances a single .020 in. diameter sheathed probe was used, but in a number of tests a four-probe rake was inserted to determine the temperature profile along the length of the cavity. Typical temperature responses obtained with the rake are given in Figure 119. These data, obtained during a test with heat sink hardware, extrapolate to a steady-state cavity temperature of approximately 1700 to 1800°F. Plots showing the effect of location and mixture ratio on cavity temperature are given in Figures 120 and 121. These figures show that the temperature in the cavity is nearly uniform and that mixture ratio has no significant influence on cavity temperature.

The temperatures shown on Figures 120 and 121 were taken 1.5 seconds into the tests and are not steady-state values. The indicated pressure dependence in the figures simply reflects the fact that the thermocouples approach steady-state more rapidly at high pressure than at low pressure and is not indicative of increased cavity temperature with increasing pressure.

The effect of cavity depth on cavity temperature is given in Figure 120. The cavity temperature is measured at the plane of the injector face. No dependence of cavity temperature on cavity depth is apparent. In no case was any correlation ever noted between cavity temperature and the occurrence of resurging.

A final set of cavity temperature data was obtained with the two demonstration X-doublet injectors. These injectors were unique in that when operating with the 0.126 inch overlap the downstream edge of the cavity projects into the spray from the outer fuel elements and deflected some of the fuel spray into the cavity. The result was a very wide spread in measured cavity temperatures as given in Figure 122. The temperatures ranged from the fuel saturation temperature up to 1600°F and showed no mixture ratio dependence. Even though this represented a wide range in cavity tune, it did not have any observable effect on the occurrence of resurging instability.

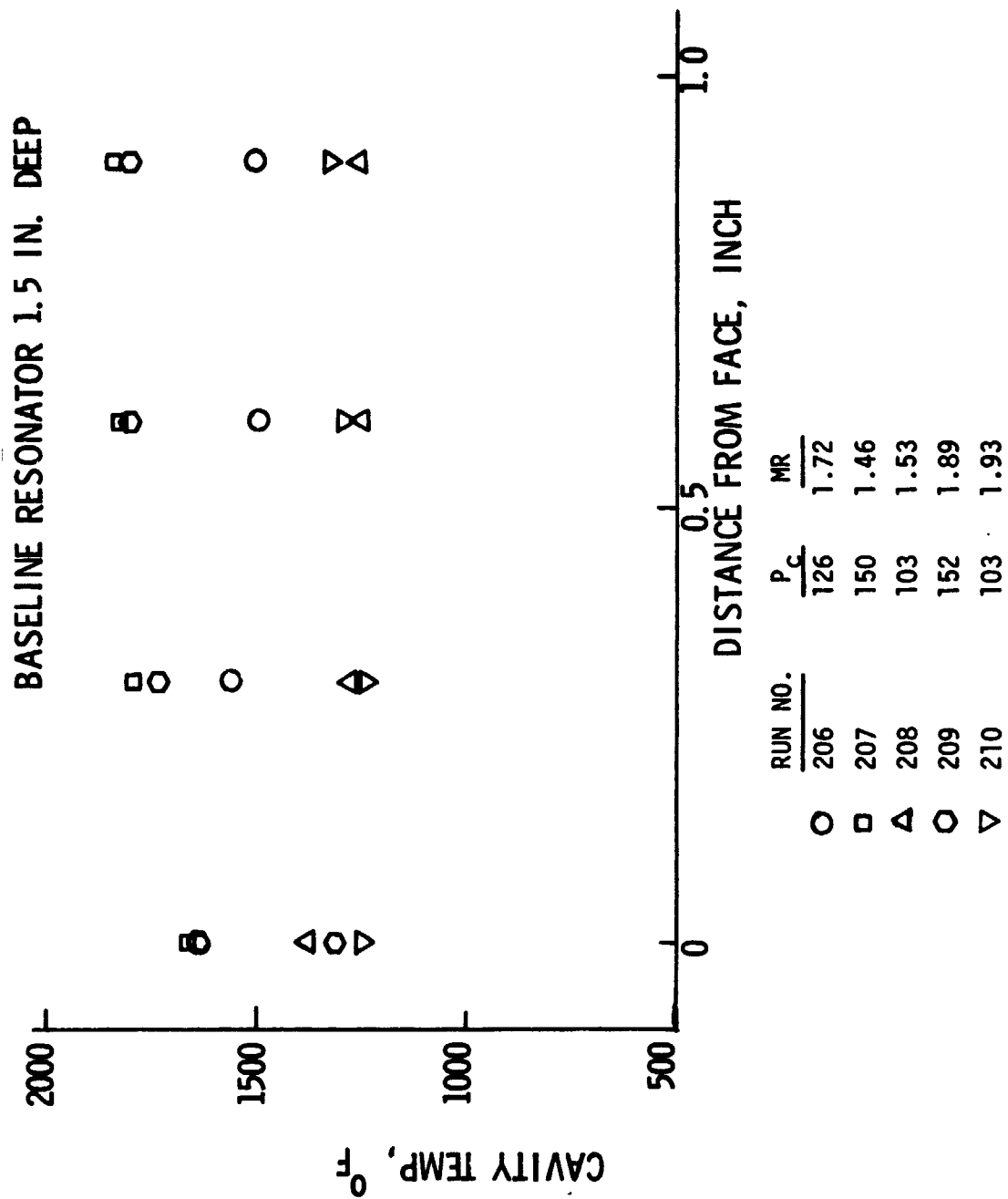


Figure 119. Cavity Temperature at Shutdown

Note: Av. Cavity Temperature Based on Average of Four Operating Points (Shown Below)

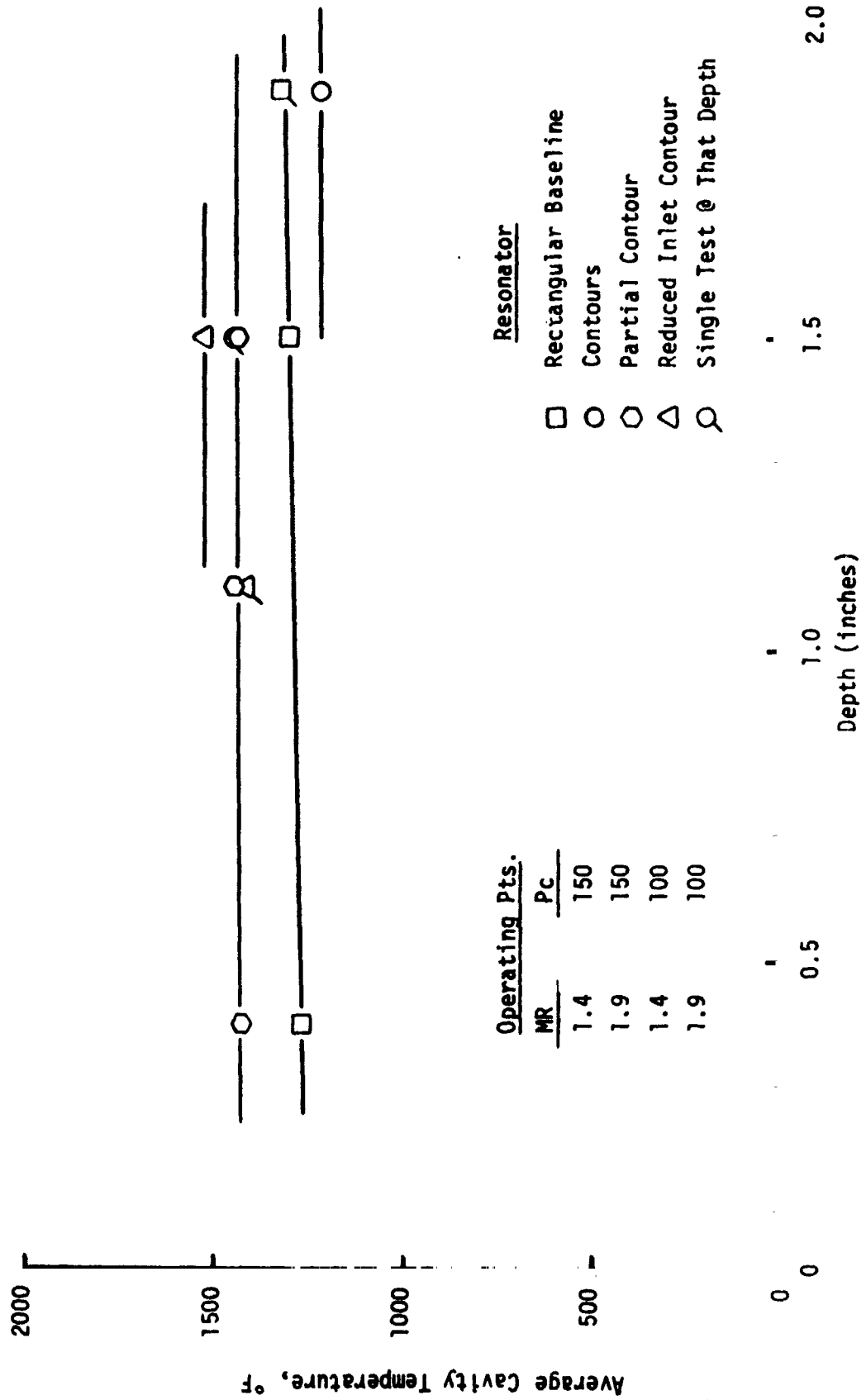


Figure 120. 1T Resonator Temperature Data Summary

(Prior to Shutdown)
Baseline Resonator
1.5 in. Deep

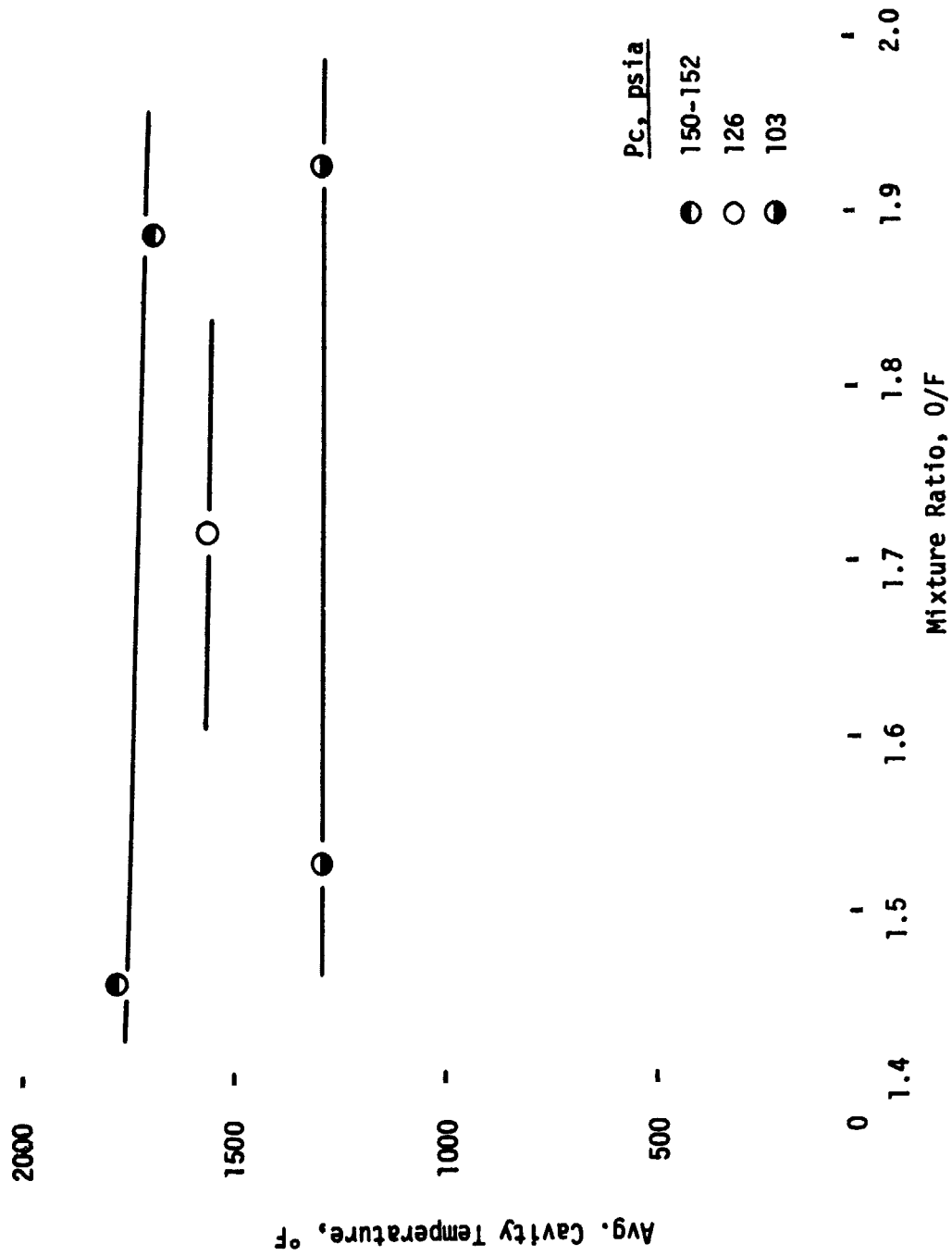


Figure 121. Cavity Temperature vs Mixture Ratio

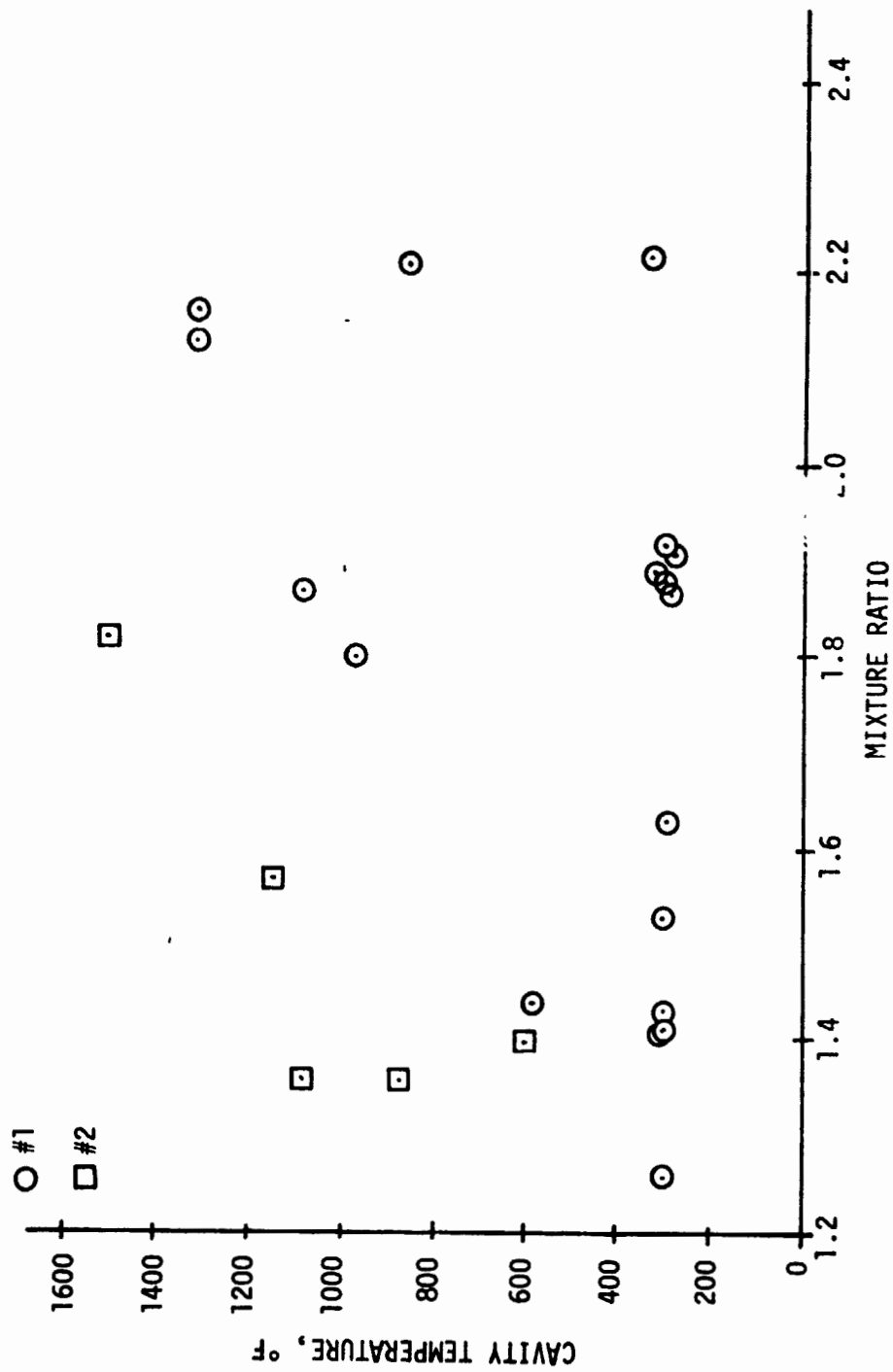


Figure 122. Demonstration Injector Cavity Temperatures

XII, Full Scale Combustion Stability (cont.)

G. MECHANISM OF RESURGING

Resurging instability manifests itself as periodic low frequency (~400 Hz) bursts of high frequency (2200-2700 Hz) instability. Because resurging has both a well defined low frequency and high frequency characteristic, attempts have been made to analyze and eliminate it from both low and high frequency points of view. This is evidenced by the number of feed system and acoustic cavity modifications that were evaluated in the course of the program. Although no single low or high frequency damping device was found to eliminate resurging, the effects of the various changes did provide sufficient insight to allow a phenomenological model of resurging to be constructed. This model explains essentially all the experimentally observed characteristics of resurging.

Resurging is considered to be an element- and pattern-related phenomenon. The X-doublet element can be characterized as a good atomizing, poor mixing element. When it is used with the concentric ring manifold pattern, a spray of concentric rings of well atomized fuel and oxidizer exists which extends some distance downstream from the injector face. This is evidenced not only by the mixing test results but also by hot fire heat transfer data which indicate the existence of a low heat flux region for several inches downstream of the injector.

The resurge begins with a low amplitude spinning I-T wave. This wave is supported by the induced mixing of the edges of the fuel and oxidizer fans very close to the face and quite possibly by a monopropellant decomposition of the fuel droplets. The possibility of a monopropellant fuel reaction supporting the I-T wave is based on the great sensitivity to fuel temperature, and is substantiated by the photographic work done under Contract NAS 9-14186. The combustion photographs show that with the X-doublet element there is a significant monopropellant fuel reaction before the unlike fans impinge and the bipropellant reaction begins.

XII, G, Mechanism of Resurging (cont.)

00

The spinning 1-T wave also can couple with the flow out the injector elements. The X-doublet element is a low inertance element and is calculated to have a break frequency of about 6200 Hz on the fuel side. The break frequency is that frequency at which the ability of the element to respond to perturbations begins to fall off rapidly. Since the spinning 1-T wave is in the 2000 to 3000 Hz frequency range, the perturbations are readily fed back into the face ring channels. The calculated fuel ring resonant frequencies are also in this range so that a coupling between the combustion and the propellant in the face ring channels could readily occur. The fact the insertion of the three face ring dams in each ring had a very pronounced stabilizing effect indicates that such coupling was occurring. However, the occurrence of resurging after the installation of the face dams implies other sources of damping are required in addition to the face ring dams.

Once the spinning 1-T wave begins it rapidly grows in amplitude and frequency until it becomes a detonation wave. The increasing wave strength can come from several sources. The radial and circumferential motion induced by the spinning wave promotes mixing of the atomized but unmixed propellants. Also, as the wave increases in strength it produces droplet shattering and mono-propellant fuel reaction. At this time the wave is gaining strength from the combustion of the unburned propellants accumulated downstream of the injector, raising the gas generation rate above its steady-state value and causing the chamber pressure to rise. All the high frequency records reviewed indicate that the detonation wave makes only one circuit of the chamber before it decays. As a high amplitude wave it consumes almost all the unburned propellant available so that there is very little left to support it in the next cycle. The subsequent decay can be compounded by the decrease in the propellant injection rate brought about by the higher chamber pressure.

XII, G, Mechanism of Resurging (cont.)

Third, the cavity entrance may be distorting the peripheral flow of injected propellant. Visual cold flow tests have shown that the outer edge of the fuel spray impinges on the cavity lip and is deflected by it. The cavity lip acts as a splash plate, deflecting the outer fuel inboard into the oxidizer. This produces early mixing and combustion of the injected propellants around the periphery of the injector, depleting that area of the downstream unburned propellant. Since the area immediately adjacent to the wall is most important in supporting the spinning l-T wave, this effect would be expected to be stabilizing. Improved stability did in fact result from increased overlap. This implies that the source of the resurging is largely the low mixing of the outer X-doublet pattern and that the elimination of resurging could be accomplished by a pattern modification in that area.

H. SUMMARY

The demo (DXDT1) injector pattern was entirely stable over the range of operating conditions tested in conjunction with the OMS baseline cavity configuration. Other configurations were frequently unstable in a hybrid mode termed resurging, however. Resurging is characterized by repetitive bursts of high frequency mode instabilities.

Resurging seems to be unique to the X-doublet injection element. It is attributed to the accumulation of unburned propellant within the chamber which is consumed by a detonation wave that originates as a spinning l-T wave. The detonation wave makes only one circuit of the chamber, following which the pressure decays. Acoustic cavities do not damp out the resurge and in effect may be fostering it by virtue of damping out the high frequency modes which normally would promote mixing and combustion of unburned propellant.

Report 13133-F-1

XII, H, Summary (cont.)

After the peak amplitude is reached, it takes a period of time for the flow and steady-state combustion to be re-established. This is also a period in which the unburned propellant cloud downstream of the injector is re-established. A significant amount of high frequency activity at several different acoustic modes can exist during this time period as the chamber is ringing down from the detonation wave. The spinning 1-T does not begin again until the unburned propellant is accumulated, since it receives most of its energy from this source. However, once the propellant is there the whole process repeats, with the spinning 1-T arising from the ringdown noise in the chamber.

When 1-T damping is removed from the system, the resurging disappears and a normal 1-T or 2-T acoustically coupled mode appears. Resurging disappears because the acoustic mode aids the mixing process and prevents the accumulation of unburned propellant. Thus, there is no burn-off and accumulation process since the propellant burns as rapidly as it is injected into the chamber. In effect, the addition of acoustic mode damping suppresses the normal acoustic modes, allows unburned propellant to accumulate, and thereby makes resurging possible.

The sensitivity of the resurging instability to cavity entrance geometry and overlap is probably the result of three separate effects. First, a rounded entrance on the cavity reduces the viscous energy dissipation of the oscillating gas jet at the cavity entrance. Although this effect is real, it may not be significant. Second, if the jet of gas exiting from the cavity induces mixing and combustion in the reacting propellants, it will have a stabilizing effect by virtue of adding energy out of phase with the acoustic mode in the chamber. Changing the cavity lip and overlap can result in a redirection of the jet from an area of high induced mixing to low induced mixing or vice versa and thereby change the effectiveness of the cavity. The importance of this effect is unknown at this time.

Report 13133-F-1

XII, H, Summary (cont.)

Among the factors that influence the resurge behavior are (1) acoustic communication within the face ring manifolds, (2) fuel temperature, (3) acoustic cavity depth, (4) cavity open area, and (5) cavity entrance configuration. Resurging is considered to be an element- and pattern-related phenomenon, apparently originating with the peripheral row of injection elements. Elimination of resurging may be possible by pattern modification of the peripheral row.

ORIGINAL PAGE IS
OF POOR QUALITY

BIBLIOGRAPHY

BIBLIOGRAPHY

The following bibliography summarizes the contents of all the monthly progress reports (M-1 through M-32) and WSTF test reports (S-1, -2, -3), Test Plans and Oral Reviews.

Monthly Reports

- 13133-M-1, covering October 1972: plexiglas element models, concept selection evaluation, spray tests, unelement chamber design and injector details.
- 13133-M-2, covering November 1972: unelement fab and testing, flow calibration spray comparisons, mixing evaluation, hot firings.
- 13133-M-3, covering December 1972: unelement mixing results, energy release and specific impulse from hot firings, conclusions regarding unelement configurations and test program.
- 13133-M-4, covering January 1973: unelement data analysis, mixing patterns of candidate elements, hot firing results, subscale injector and chamber designs.
- 13133-M-5, covering February 1973: expanded unelement testing, hydraulic and hot fire test results.
- 13133-M-6, covering March 1973: hydraulic, mixing, and hot fire test results with subscale hardware (SP1 and XDT injectors) including bomb stability tests.
- 13133-M-7, covering April 1973: hot fire results from XDT, XDI and SP2 subscale configurations, including bomb tests.
- 13133-M-8, covering May 1973: subscale stability comparison of XD and SP injectors; thermal analyses, flat face and baffled full scale injector designs, bonding experiments.
- 13133-M-9, covering June 1973: subscale mixed element performance, full scale injector hydraulics.
- 13133-M-10, covering July 1973: initial full scale sea level altitude uncooled and regen cooled tests at ALRC including performance, heat transfer, stability.
- 13133-M-11, covering August 1973: additional altitude regen testing at ALRC; initial WSTF tests.
- 13133-M-12, covering September 1973: sea level stability tests at ALRC and altitude tests at WSTF to remedy stability problem, stabilization with manifold dams.

Bibliography cont.

- 13133-M-13, covering October 1973: subscale thermal cycle tests, ALRC testing of XDT2 injector performance and heat transfer.
- 13133-M-14, covering November 1973: full scale mixed element injector heat transfer and performance results at ALRC, injector hydraulics.
- 13133-M-15, covering December 1973: full scale mixed element testing A-50, XDT-1A testing, A-2 chamber design and fabrication details, stress and thermal/hydraulic analysis of A-2 chamber.
- 13133-M-16, covering January 1974: full scale XDT-1B and mixed element testing, baffled injector, test plan for proposed WSTF testing, heat transfer analysis of bubble ingestion and chugging.
- 13133-M-17, covering February 1974: full scale baffled injector tests, XDT-1B tests, resonator inlet evaluation, XDT-1B heat flux data, test matrices for proposed WSTF testing.
- 13133-M-18, covering March 1974: additional unielement concepts, full scale large thrust per element injector, high contraction ratio chamber, resonator inlet evaluation, undamped testing of XDT-1B and like-doublet injectors, XDT-1B rework.
- 13133-M-19, covering April 1974: full scale DXDT1-1 stability tests at ALRC, resonator differences in A-1 and A-2 chambers.
- 13133-M-20, covering May 1974: full scale DXDT1-2 stability testing at ALRC, heat flux data from DXDT1-1 and -2, XDT-1C testing, DXDT1-2 mixing tests.
- 13133-M-21, covering June 1974: additional unielement design details and spray test results: full scale XDT-1C injector testing at ALRC, high contraction ratio chamber test, low pressure drop injector, cavity inlet thermal analysis, cavity temperatures, like-doublet testing at WSTF, DXDT1-2 injector testing at WSTF.
- 13133-M-22, covering July 1974: full scale high contraction ratio chamber stability and thermal analyses, fuel circuit helium bubble tests at WSTF, postfire inspection of DXDT1-2 injector, XDT-1C tests at ALRC, pop analysis, postfire thermal effects and propellant evacuation.
- 13133-M-23, covering August 1974: full scale A-2 chamber checkout tests at WSTF, DXDT2-1 instabilities at high O/F and during hot restart.
- 13133-M-24, covering September 1974: full scale hot and cold engine restarts with DXDT2-1 at WSTF, repeat with DXDT1-1R injector, A-2 chamber failure.

Bibliography cont

- 13133-M-25, covering October 1974: primary activity consisted of WSTF test data analysis and documentation.
- 13133-M-26, covering November 1974: primary activity consisted of analysis and documentation of WSTF tests, hardware and test summary of WSTF testing; stability tests of XDT-1C injector at ALRC.
- 13133-M-27, covering December 1974: primary activity consisted of analyzing WSTF data: stability tests at XDT-1D and XDT-1E at ALRC.
- 13133-M-28, covering January 1975: primary activity consisted of analyzing WSTF data and preparing WSTF Final Report; stability tests of XDT-1F at ALRC.
- 13133-M-29, covering February 1975: primary activity consisted of preparing WSTF Final Report.
- 13133-M-30, covering March 1975: primary activity consisted of preparing the program final report.
- 13133-M-31, covering April 1975: primary activity consisted of preparing the program final report.
- 13133-M-32, covering May 1975: primary activity consisted of preparing the program final report.

Special Reports

- S-1 WSTF Test Report, covering 1973 WSTF testing: summary of tests, hardware, measurements, results and conclusions: analysis of performance, heat transfer, hydraulics, and dynamics; test plan, data summaries, computer program for calculating performance, analog data.
- S-2 Test Summary Report Summarizing ALRC Testing at WSTF (1974): summary of hardware and test facility, description of test series, summary of individual tests, contents included in S-3 below.
- S-3 1974 WSTF Test Report: technical analysis of 1974 WSTF testing in areas of performance, heat transfer, stability, start and shutdown transients, evacuation and soakout characteristics of purged and unpurged engine, nickel compatibility tests; results, conclusions, recommendations, compliance with OMS specification; includes S-2 above.

Program Plans

Program Plan - 10/20/72 - Defines program logic task description and schedule.

Task IA Test Plan - 10/30/72 - Unielement cold flow and hot test plans, hardware and test system description.

Task II Test Plan - 1/23/73 - Subscale cold flow and hot test plan, hardware and test system description.

Task VI Test Plan - 5/11/73 - Full scale altitude and sea level test plan, operating procedures, requirements, data analysis, hardware and test system description.

Task VII Test Plan - 8/17/73 - 1973 WSTF test program, operating procedures and requirements, data analysis, hardware and test system description.

Task VII Test Plan - 2/1/74 - 1974 WSTF test program, operating procedures and requirements, hardware and test system description.

Program Oral Reviews

10/30/72 - NASA/JSC - Program plan, logic, task description and schedule

1/5/73 - NASA/JSC - Unielement test results, subscale design

1/16/73 - RI/Downey - Unielement test results

3/20/73 - NASA/JSC - Subscale test results, expanded unielement test results, full scale design review

4/17/73 - NASA/JSC - Subscale program review, full scale injector selection

4/26/73 - RI/Downey - Full scale design review, subscale test program results

6/31/73 - NASA/JSC - Overall program review, preliminary full scale test results

8/17/73 - RI/Downey - Full scale test program results, WSTF test program plan

9/25/73 - NASA/JSC - Stability results from full scale test program

Program Oral Reviews cont.

10/19/73 - RI/@ ALRC WSTF test results review, full scale design selection analysis

10/30/73 - NASA/JSC - WSTF test program results and full scale design selection

12/12/73 - NASA/JSC - Mixed element injector results, diffusion bonding, demo injector design

3/12/74 - NASA/JSC - Acoustic cavity operation, stability results, demo injector test plan

5/7/74 - NASA/JSC - General stability review

6/30/74 - NASA/JSC - Overall program review, stability results summary

11/12/74 - NASA/JSC - Stability review

11/13/74 - NASA/JSC - 1974 WSTF test program results summary